



# LEAD ACID BATTERIES IN EXTREME CONDITIONS: ACCELERATED CHARGE, MAINTAINING THE CHARGE WITH IMPOSED LOW CURRENT, POLARITY INVERSIONS INTRODUCING NON-CONVENTIONAL CHARGE METHODS

Thi Minh Phuong Nguyen

## ► To cite this version:

Thi Minh Phuong Nguyen. LEAD ACID BATTERIES IN EXTREME CONDITIONS: ACCELERATED CHARGE, MAINTAINING THE CHARGE WITH IMPOSED LOW CURRENT, POLARITY INVERSIONS INTRODUCING NON-CONVENTIONAL CHARGE METHODS. Other. Université Montpellier II - Sciences et Techniques du Languedoc, 2009. English. NNT : . tel-00443615

**HAL Id: tel-00443615**

**<https://theses.hal.science/tel-00443615>**

Submitted on 31 Dec 2009

**HAL** is a multi-disciplinary open access archive for the deposit and dissemination of scientific research documents, whether they are published or not. The documents may come from teaching and research institutions in France or abroad, or from public or private research centers.

L'archive ouverte pluridisciplinaire **HAL**, est destinée au dépôt et à la diffusion de documents scientifiques de niveau recherche, publiés ou non, émanant des établissements d'enseignement et de recherche français ou étrangers, des laboratoires publics ou privés.

**UNIVERSITY MONTPELLIER II**  
– SCIENCES AND TECHNOLOGIES OF LANGUEDOC –

**THESIS**

A dissertation submitted to the graduate faculty  
in partial fulfillment of the requirements for the degree of

**Doctor of University Montpellier II**

*Discipline: ELECTRONIC, OPTRONIC and SYSTEMS*  
*Doctoral Formation: Electronic: Components and Systems*  
*Doctoral School: Information, Structures and Systems*

Presented and defended  
by

**NGUYEN Thi Minh Phuong**

the 5<sup>th</sup> June 2009

---

LEAD ACID BATTERIES IN EXTREME CONDITIONS:  
ACCELERATED CHARGE, MAINTAINING THE CHARGE WITH  
IMPOSED LOW CURRENT, POLARITY INVERSIONS

INTRODUCING NON-CONVENTIONAL CHARGE METHODS

---

JURY

M. Jean ALZIEU  
M. Didier DEVILLIERS  
M. Guy FRIEDRICH  
M. Christian GLAIZE  
M. Jack ROBERT

Examiner  
Reporter  
President - Reporter  
PhD Supervisor  
Examiner

*For my parents*

*For GC & PC*

*The work presented in this thesis was done at the Research and Development facilities of Electricité de France (EDF R&D), in the Battery and Energy Management Group of the Electrical Equipment Laboratory, in cooperation with Université Montpellier II and Institut Electronique du Sud (IES). It was financially supported by Association Nationale de la Recherche Technique – ANRT France.*

*This thesis would not have been possible without the help and support of a number of people, and I would like to express my gratitude to all of them.*

*I wish to express my sincere appreciation and gratitude to Jean ALZIEU, Senior Researcher at EDF R&D, the father of this thesis.*

*I gratefully thank to my supervisor, Professor Christian GLAIZE at Université Montpellier II.*

*I sincerely thank to the members of my thesis defense jury, Professor Didier DEVILLIERS, Professor Guy FRIEDRICH and Professor Jack ROBERT.*

*I warmly thank all of my colleagues of EDF R&D - Battery and Energy Management Group and of IES - Materials and Energy Management Group: Stéphane LASCAUD, Laurent TORCHEUX, Luc GOMBERT, Vincent TOUREN, Philippe BERCKMANS, Guy SCHWEITZ, Philippe STEVENS, Guillaume DILLENSEGER, Kelli MAMADOU...*

*I wish to express my warmest thank to France country, where I was well come and met my French lovely friends Fanny STORCK, Marie Christine LENOIR, Stephanie HONGOIS and Gwenaëlle TOUSSAINT.*

*I owe my deepest gratitude to my country Vietnam, my parents Van Ky NGUYEN and Thi Nguyet MAI, my sister Thi Kieu Giang NGUYEN and my brother in law Hoai Quang HOANG NGOC, my nephew Nguyen HOANG NGOC, my best friends Thi Minh Hue NGUYEN and Ngoc Ha DINH.*

*My special thank is due to my Italian Jacopo TESTA.*

*Thank you all my family, all my friends!*

## TABLE OF CONTENTS

<b>INTRODUCTION.....</b>	<b>5</b>
<b>CHAPTER 1 - LEAD ACID BATTERIES [1-10] .....</b>	<b>6</b>
1.1 LEAD ACID BATTERY CONSTITUTION, TECHNOLOGIES AND MARKET [1-6] .....	6
1.1.1 Positive electrode .....	6
1.1.1.1 Flat plate .....	6
1.1.1.2 Tubular plate .....	8
1.1.2 Negative electrode.....	8
1.1.3 Grid [1, 8] .....	8
1.1.4 Separator.....	9
1.1.5 Electrolyte .....	10
1.1.5.1 Liquid electrolyte .....	10
1.1.5.2 Immobilized electrolyte.....	10
1.1.6 Lead acid battery families .....	11
1.1.6.1 Flooded batteries .....	12
1.1.6.2 VRLA batteries .....	12
1.1.7 Lead acid battery market [13] .....	12
1.2 OPERATION OF LEAD ACID CELL [14] .....	14
1.2.1 Electrochemical cell.....	14
1.2.1.1 Relative electrode potential and cell voltage.....	14
1.2.1.2 Electrode polarity .....	15
1.2.2 Galvanic & electrolytic cells: lead acid cell.....	15
1.2.2.1 Galvanic cell.....	15
1.2.2.2 Electrolytic cell .....	16
1.2.2.3 Lead acid cell or lead acid accumulator .....	16
1.3 PRINCIPAL & SECONDARY REACTIONS IN LEAD ACID CELL.....	17
1.3.1 Pourbaix diagram .....	17
1.3.2 Main reactions (discharge-charge of active materials).....	18
1.3.2.1 Discharge.....	18
1.3.2.2 Charge .....	19
1.3.3 Side reactions .....	19
1.3.3.1 Water electrolysis .....	19
1.3.3.2 Internal gas cycle.....	19
1.3.3.3 Corrosion.....	20
1.3.3.4 Oxido-reduction of unwanted ions .....	22
1.4 CHARACTERISTIC OF LEAD ACID CELL WHEN NO EXTERNAL CURRENT FLOWS .....	23
1.4.1 Thermodynamic laws [1] .....	23
1.4.2 Equilibrium potential notion [21] .....	24
1.4.2.1 Influencing factor on the equilibrium values: electrolyte density – Nernst equation .....	25
1.4.2.2 Influencing factor on the equilibrium values: temperature .....	27
1.5 CHARACTERISTICS OF LEAD ACID CELL WHEN EXTERNAL CURRENT FLOWS .....	27
1.5.1 Current conduction in lead acid cell [23].....	27
1.5.1.1 Current conduction in the electrolyte volume .....	28
1.5.1.2 Phenomena at interface of electrode/electrolyte .....	28
1.5.2 Faraday phenomenon.....	30
1.5.2.1 Faradic and capacitive current.....	30
1.5.2.2 Anodic and cathodic current .....	30

1.5.2.3	Faraday' Law of Electrolysis .....	31
1.5.2.4	Faraday efficiency .....	32
1.5.3	<i>Principal steps of an electrochemical reaction [1, 18].....</i>	33
1.5.3.1	Charge transfer (Electron transfer).....	33
1.5.3.2	Reactant transport (mass transport): diffusion and migration.....	34
1.5.3.3	Chemical reactions, forming reactions: nucleation and crystal growth .....	36
1.5.4	<i>Electrode kinetics - Polarization, overvoltage notions [21] .....</i>	37
1.5.4.1	Electrode kinetics .....	37
1.5.4.2	Polarization and overvoltage notions .....	37
1.5.4.3	Activation overvoltage (or charge transfer overvoltage) $\eta_a$ .....	38
1.5.4.4	Diffusion overvoltage $\eta_d$ .....	40
1.5.4.5	Reaction overvoltage $\eta_r$ .....	42
1.5.4.6	Crystallization overvoltage $\eta_{cr}$ .....	43
1.5.4.7	Ohm overvoltage or resistance overvoltage $\eta_\Omega$ .....	43
1.5.5	<i>Voltage at the terminals of an electrochemical cell.....</i>	44
1.5.6	<i>Current-related heat effects (the Joule effect) [1] .....</i>	45
1.6	CAPACITY OF LEAD ACID BATTERY [1, 25] .....	46
1.6.1	Capacity .....	46
1.6.2	State of charge.....	47
1.6.3	State of health.....	47

## **CHAPTER 2 - CHARGE OF LEAD ACID BATTERIES: FROM TRADITIONAL CHARGE TO ACCELERATED CHARGE WITH EARLY DESTRATIFICATION .. 50**

2.1	CHARGE OF LEAD ACID BATTERY .....	50
2.1.1	<i>Reminder of reactions during charging .....</i>	50
2.1.2	<i>Charge acceptance .....</i>	52
2.1.2.1	Definitions .....	52
2.1.2.2	Charge acceptance profile .....	53
2.1.3	<i>Electrolyte stratification.....</i>	57
2.1.3.1	Phenomenon .....	57
2.1.3.2	Consequences .....	58
2.1.3.3	Destratification by gassing .....	59
2.1.4	<i>Charge definitions [51].....</i>	60
2.1.4.1	Full charge.....	60
2.1.4.2	Normal charges .....	60
2.1.4.3	Accelerated and fast charges .....	61
2.1.5	<i>Charge acceptance and gassing current variations during a IUi typical charge process of lead acid batteries.....</i>	61
2.1.5.1	Gassing Voltage .....	63
2.1.6	<i>Control of Destratification phase.....</i>	64
2.2	CHARGE ACCEPTANCE MEASUREMENTS .....	66
2.2.1	<i>Current ramps .....</i>	66
2.2.1.1	Principle .....	66
2.2.1.2	Experimental .....	67
2.2.1.3	Results and discussion.....	68
2.2.1.4	Conclusions of current ramp method .....	72
2.2.2	<i>Voltage squares.....</i>	72
2.2.2.1	Principle .....	72
2.2.2.2	Experimental .....	73
2.2.2.3	Results and discussion.....	74
2.2.2.4	Conclusions of voltage square method.....	77

2.3	NEW CHARGE ALGORITHM WITH EARLY DESTRATIFICATION FOR ACCELERATED CHARGES .....	77
2.3.1	<i>Objectives</i> .....	77
2.3.2	<i>Principle</i> .....	78
2.3.3	<i>Experimental</i> .....	79
2.3.4	<i>Results and discussion</i> .....	80
2.3.5	<i>Conclusions</i> .....	82
<b>CHAPTER 3 - DISCHARGE OF LEAD ACID BATTERY – POLARITY INVERSION 85</b>		
3.1	THEORY ABOUT THE DISCHARGE OF LEAD ACID BATTERY AND POLARITY INVERSIONS 85	
3.1.1	<i>Reminder of discharge reactions</i> .....	85
3.1.2	<i>Discharge cell voltage and end-of-discharge criterion</i> .....	86
3.1.3	<i>Diffusion of sulfate ions</i> .....	87
3.1.4	<i>Proposed mechanisms of polarity inversion</i> .....	87
3.2	EXPERIMENTAL .....	90
3.2.1	<i>Initial objective</i> .....	90
3.2.2	<i>Tools</i> .....	90
3.2.3	<i>Electrode potential measurement using reference electrodes</i> .....	91
3.3	POLARITY INVERSION OF FLAT-PLATE BATTERY .....	93
3.3.1	<i>Experimental</i> .....	93
3.3.2	<i>Results and discussion</i> .....	94
3.4	POLARITY INVERSION OF TUBULAR PLATE BATTERY .....	99
3.4.1	<i>Experimental</i> .....	99
3.4.2	<i>Results and discussion</i> .....	99
3.5	ANALYZING A DEFECTIVE BATTERY BY USING POLARITY INVERSION DISCHARGE... 105	
3.5.1	<i>Experimental</i> .....	105
3.5.2	<i>Results and discussion</i> .....	105
3.6	ANALYZING EVOLUTION OF SEPARATED STATES OF CHARGE OF NEGATIVE AND POSITIVE ELECTRODES USING POLARITY INVERSION DISCHARGE .....	108
3.6.1	<i>Experimental</i> .....	108
3.6.2	<i>Results and discussion</i> .....	109
3.6.2.1	B105 – DCH(1) with B101 – DCH(1) .....	109
3.6.2.2	B101 – DCH(2) with B103 – DCH(2) .....	110
3.6.2.3	B103 – DCH(2) with B103 – DCH(3) .....	111
3.7	CONCLUSIONS OF POLARITY INVERSION .....	111
<b>CHAPTER 4 - NEW METHOD OF MAINTAINING THE CHARGE OF STATIONARY LEAD ACID BATTERIES..... 115</b>		
4.1	LEAD ACID BATTERIES IN STATIONARY APPLICATIONS .....	115
4.1.1	<i>Secondary reactions as causes of self-discharge</i> .....	115
4.1.1.1	Self-discharge reactions at the negative electrode .....	116
4.1.1.2	Self-discharge reactions at the positive electrode .....	116
4.1.1.3	Self-discharge rate [1] .....	117
4.1.2	<i>Traditional method of maintaining the charge: float charge - a trade-off between state of charge and state of health</i> .....	118
4.1.2.1	Bimodal float voltage distribution between the negative and positive electrodes – difference between vented and VRLA batteries. ....	119
4.1.2.2	Cells in series configuration – scattering problem .....	121
4.1.3	<i>Secondary reactions as causes of failure modes</i> .....	122
4.1.3.1	Corrosion .....	122
4.1.3.2	Water loss .....	124

4.2	NEW METHOD OF MAINTAINING THE CHARGE - LOW CURRENT METHOD .....	126
4.2.1	<i>New method of maintaining the charge</i> .....	126
4.2.1.1	Heritage of intermittent charges .....	126
4.2.1.2	Benefit of corrosion minimum .....	127
4.2.1.3	Principle of the new maintaining charge method.....	127
4.2.2	<i>Experimental</i> .....	128
4.2.2.1	Lead sulfate content measurement [6] .....	129
4.2.2.2	Capacity measurement by discharge test .....	130
4.2.3	<i>Sulfate content measurement – results &amp; discussion</i> .....	131
4.2.3.1	Lead sulfate content at open-circuit .....	131
4.2.3.2	Lead sulfate content at low currents.....	132
4.2.4	<i>Capacity measurement – results &amp; discussion</i> .....	137
4.2.4.1	Exide 110 Ah/12 V, SLI heavy truck batteries, 1.6%Sb grid alloys.....	137
4.2.4.2	EnerSys 400 Ah/2V VRLA AGM batteries, new .....	140
4.2.4.3	EnerSys 400 Ah/ 2V AGM VRLA batteries, old.....	141
4.2.5	<i>Conclusion</i> .....	142
4.3	NEW MANAGEMENT SYSTEM FOR ANTIMONY-FREE STANDBY BATTERY .....	143
<b>GENERAL CONCLUSION .....</b>		<b>148</b>
<b>REFERENCES .....</b>		<b>151</b>
<b>RESUME EN FRANÇAIS.....</b>		<b>I</b>
INTRODUCTION .....		II
CHAPITRE 1 – BATTERIES AU PLOMB .....		III
CHAPITRE 2 – CHARGE DE BATTERIES AU PLOMB : DE LA CHARGE TRADITIONNELLE A LA CHARGE RAPIDE.....		IV
CHAPITRE 3 – DECHARGE DE BATTERIES AU PLOMB : INVERSION DE POLARITE .....		VII
CHAPITRE 4 - NOUVELLE METHODE DE MAINTIEN EN CHARGE DE BATTERIES STATIONNAIRES X CONCLUSION ET PERPECTIVE INDUSTRIELLES .....		XV



## INTRODUCTION

Invented in 1859 by French physicist Gaston Planté, lead acid batteries represent the oldest design and are the most commonly used rechargeable batteries today. Despite having modest energy-to-weight ratio and energy-to-volume ratio, their ability to supply high surge currents means that the cells maintain a relatively large power-to-weight ratio. These features, along with their low cost, their high recycling ratio, 97%, and their technological maturity make them attractive for several applications. Three main applications of lead acid batteries are: starting, lighting and ignition batteries (SLI batteries), motive batteries and stationary batteries.

Increasing attention to the global climate change and the sustainable development open new applications for energy storage using lead acid batteries: electric transport, renewable energies such as photovoltaic and wind, grid storage, quality and emergency supplies. In some cases, new applications need new charge algorithms. One should not forget either, the economic factor that requires a deep understanding of phenomena inside the battery in order to improve its lifetime.

This has driven Electricité de France (EDF) in collaboration with Université de Montpellier II to do research on lead acid batteries and their applications. It includes the PhD works of H. Smimite (on fast charge of valve regulated lead acid batteries for electric car, 1997), of P. Izzo (on battery management for photovoltaic applications, 2002) and of G. Dillenseger (on methods of maintaining the charge for stationary lead acid batteries, 2004). In continuity of these works, this thesis investigates the behaviors of lead acid batteries in extreme conditions related to three main topics. The first is accelerated charges of flooded batteries used in electric buses, in grid-connected inverter combined with energy storage for production optimization. The second is deep discharges with polarity inversion. The last topic is maintaining the charge of stationary batteries with imposed low current. First of all, this work consists in studying and analyzing the state of the art in this field throughout the existing results. Then, new charge methods are investigated. Finally, these new charge methods are tested with laboratory tools as well as with commercial chargers.

This thesis begins with a chapter about the generality of lead acid batteries, especially intended to non-electro-chemist colleagues. It introduces how lead acid batteries work as well as their behaviors during several conditions that will be detailed in the next chapters. The second chapter deals with the charge of lead acid batteries: from the traditional charge to accelerated and fast charges. A new charge method for accelerated and fast charges of flooded lead acid batteries is developed and tested. The discharge of lead acid batteries is discussed in the third chapter, where batteries are subjected to very deep discharge to evaluate capacities of both negative and positive electrodes. The polarity inversion phenomenon is discussed here in detail through experiments on different types of lead acid batteries. The last chapter deals with maintaining the charge of stationary lead acid batteries. A new method of maintaining the charge with imposed low currents and periodical charges is tested and compared to the case of open circuit (without maintaining the charge) and traditional float charges. This method is applied in a new management system for standby lead acid batteries at EDF. The thesis ends with a long abstract in French.

## CHAPTER 1 - LEAD ACID BATTERIES [1-10]

### Introduction

This chapter has been written especially for my electrical engineer colleagues, who are not familiar with electrochemical matters as I was when I began this thesis work. It presents lead acid battery as a complex electrochemical system from constitution to functional principle and basic laws of thermodynamic and kinetic that govern the whole system in six main parts. The first part deals with elements that set up a lead acid battery as well as their technologies and application fields. The second part explains the function of a lead acid cell in converting chemical energy to electrical energy and vice versa. The third part presents reactions of a lead acid cell consisting of main reactions (charge and discharge of active materials) and side reactions (water electrolysis, oxygen recombination, corrosion...). The fourth and fifth parts describe the thermodynamic and kinetic laws that govern the function of a lead acid cell when it is at open circuit as well as when an external current flows. The final party defines characteristic parameters of a lead acid cell: capacity, state of charge, state of health.

### 1.1 LEAD ACID BATTERY CONSTITUTION, TECHNOLOGIES AND MARKET [1-6]

A lead acid battery consists of several cells, also called accumulators. The nominal voltage of a cell is 2 Volt. These cells are connected in series configuration to obtain the expected voltage for applications.

The 2 Volt cell is the basic unit of a lead acid battery. It consists of an alternately gathered group of positive plates (whose active material is  $\text{PbO}_2$ ) and negative plates (Pb). The number of plates of each polarity and their dimensions are the main parameters, which define the cell capacity. In order to avoid short-circuits between the different polarity plates, an insulating micro-porous separator is placed between these plates during assembly. Positive plates are put together in pack as well as negative plates. The positive and negative packs are then grouped together and finally put in a container filled with an electrolyte. All of this, i.e. packs of negative and positive plates, electrolyte and container, form a cell (cf. Figure 1). The electrolyte is a solution of sulfuric acid and distilled water. The container is generally made of polystyrene or ABS<sup>1</sup>. The container has to keep the acid within the cell and at the same time provide mechanical support to the battery. It is designed in a variety of ways to prevent leakage and dry-out while allowing accumulated gases to escape. The two terminals made of lead metal connected with the pack of each polarity allow the connection to an external circuit.

#### 1.1.1 Positive electrode

There are two kinds of positive plate: flat plate and tubular plate.

##### *1.1.1.1 Flat plate*

The “Faure flat plate” consists of a lead grid alloy that assures both the mechanic support of the plate and the current collector (cf. Figure 2). This grid is filled with a paste prepared from sulfuric acid and a powder consisting of a combination of lead oxide and lead metal. Cells are then subjected to the equivalent of a prolonged charge called “formation”. During this

---

<sup>1</sup> Acrylonitrile-Butadiene-Styrene (plastic – ISO 1043)

formation phase, the initial mixing of oxide is oxidized to lead dioxide ( $\text{PbO}_2$ ) at the positive plate.

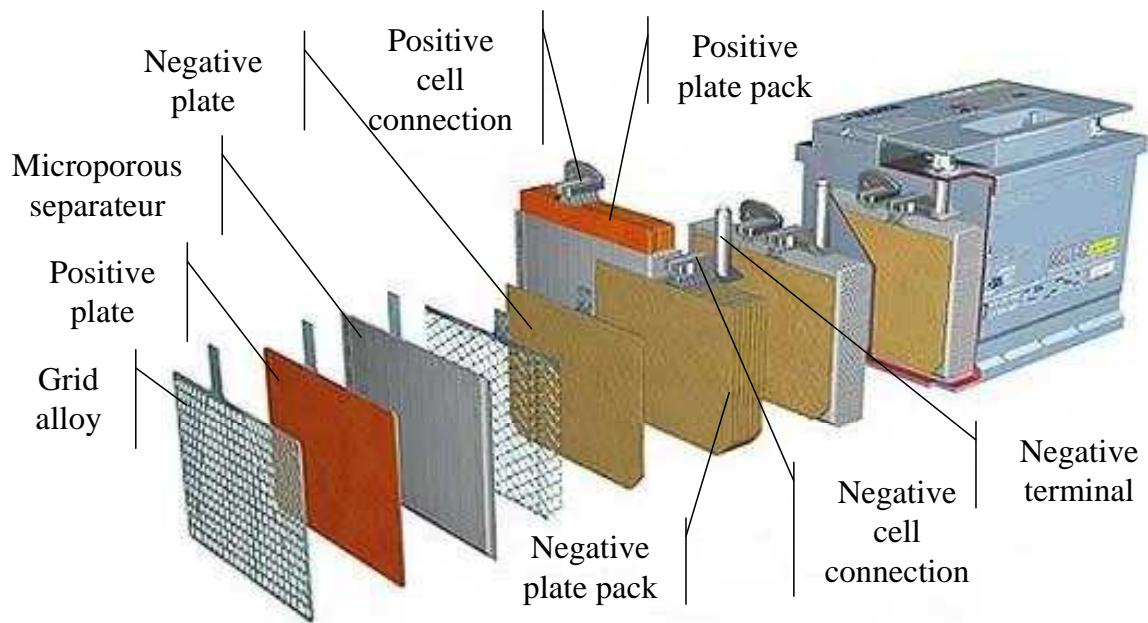


Figure 1: Schematic representation of a flooded lead acid battery [7]

The grading of the powder is important because it determines the active material specific surface, which is the reactive surface: the pore size is of the order of the micron. For the positive plate, the reactive surface is about  $2 \text{ m}^2/\text{g}$ .

The “flat plate” technology is the cheapest (because it contains a minimum of material and its manufacturing process is simple), the most fragile and is the technology able to reach the best mass performances. It is mainly (100 % in United State) used in SLI batteries (Starting, Lighting, Ignition).

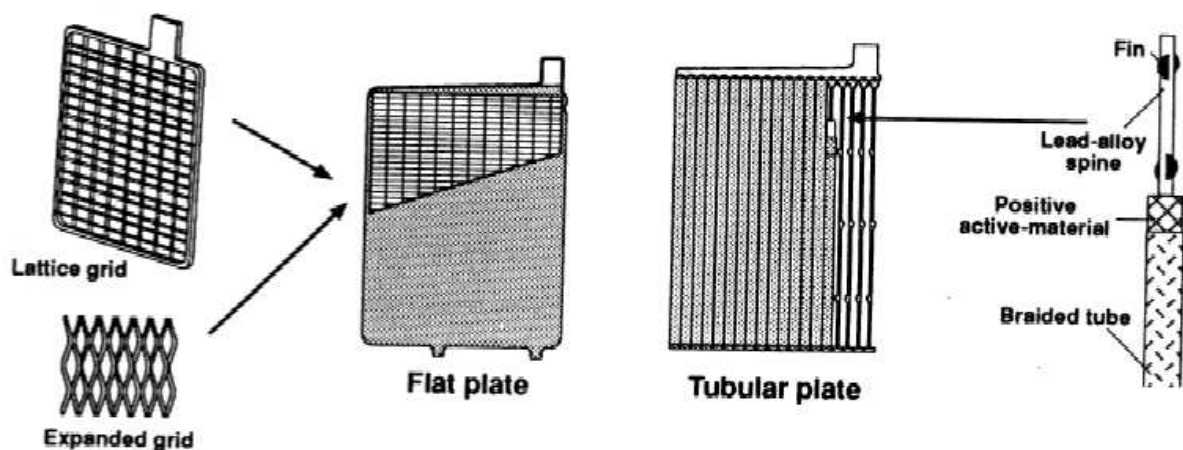


Figure 2: Lead acid battery plates: flat plate and tubular plate [8]

### *1.1.1.2 Tubular plate*

The tubular plate consists of lead alloy spines (charge collector) slipped into a porous tube that contains the active material in the free space between the spine and the braided tube (cf. Figure 2). The positive electrode is thus made up of series of vertical cylindrical tubes one next to the other. The cylindrical shape allows the dilatation and the contraction of the active material during charge-discharge cycles while keeping almost an excellent cohesion and a good electric contact with the central conductor. This is the reason why the electrode life span is found to be improved.

This robust technology is used in applications that require high endurance in cycles and long service life: heavy traction, stationary (emergency supply and photovoltaic), submarines.

### **1.1.2 Negative electrode**

The negative plate is always designed according to the “flat plate” technologies. As explained before for the positive electrode, it consists of a grid filled with active material paste. The active material is made of spongy lead, which is prepared from sulfuric acid and a powder consisting of a combination of lead oxide and lead metal. During the formation phase, this combination is reduced to spongy lead metal (Pb) at the negative plate. In order to make the active material porosity deteriorate less rapidly, another products, called expanders, are added in a small quantity. Additives that are usually added to negative active material are barium sulfate ( $\text{BaSO}_4$ ) and carbon (C). The reactive surface of negative material is about  $0.2 - 0.4 \text{ m}^2/\text{g}$ .

### **1.1.3 Grid [1, 8]**

The grids (and the spines), fundamental elements of the battery, consist of lead alloys. They are used at the same time to collect the current and to mechanically hold the active material. Many researches have been done to improve the grid alloy because the grid corrosion is one of the most frequent causes that limit the battery life time [9, 10]. Several studies have also been done to reduce the high self-discharge rate of the negative electrode in batteries with antimony positive grid alloys.

The choice of metals for the grid remains limited. The lead is almost the only metal that does not constitute a poison for the battery while resisting to the corrosive conditions of the electrolyte. Since the pure lead is too soft to be directly used, other metals (like tin, antimony, calcium, silver) are inserted into the grid composition in order to improve the toughness as well as the resistance against corrosion.

Conventional grid alloys are based on lead / antimony alloys containing up to 8% Sb. The role of the Sb is to strengthen and harden the Pb through the formation of a finely dispersed eutectic phase at the grain boundaries. The tensile strength, yield strength and creep resistance of the alloy all increase with Sb content [11]. In addition, the alloying agent improves castability and the adherence of the paste to the plate. Unfortunately, the addition of antimony has also some disadvantages. During battery charge, the Sb dissolves (corrodes) progressively from the positive grid, diffuses through the electrolyte and deposits on the negative electrode where it reduces the overvoltage (cf. 1.5.4.2) for hydrogen evolution. This results in greater gassing rates, the water loss as well as the self-discharge rates and in the need for more frequent maintenance. This is called “antimony effect”.

In order to overcome this problem, a range of low-Sb alloys has been developed. Early attempts to use low-Sb alloys led to cracking on casting, but this was overcome by the addition of grain refining agents such as As, Cu, Se, S and Te. These enhance the stiffness, the tensile strength and the corrosion resistance of the grid alloys. Castability is improved by the addition of 0.1 wt.% Sn that increases the fluidity of lead alloys. Low-Sb alloys, as used in “low-maintenance” automotive batteries, contain 2 wt.% Sb.

Many automotive batteries today are of the so-called “maintenance-free” variety in which the grids are constructed of Pb/Ca alloy (up to 0.1 wt.% Ca), sometimes with the addition of Sn or Sr. On quenching the grids during manufacture, a dispersion of  $Pb_3Ca$  forms around the pure lead grains resulting in precipitation hardening. These alloys exhibit higher hydrogen overvoltage than antimony types and water loss during charging is largely eliminated, provided that the top-of-charge voltage is controlled. They have improved electrical conductivity, but are substantially weaker than their Pb/Sb counterparts. Batteries with Pb/Ca grids are normally used in “float” conditions (e.g. automotive or stand-by applications). They are unsuited to regular deep discharge as the cycle life under these conditions is strictly limited. Explanations advanced for this are complex, involving the build-up and cracking of corrosion layers on the Pb/Ca plate and structural changes in the porous active material.

*Table 1: Grid alloys for lead acid batteries, their characteristics and fields of applications [1],*

Kind of alloy	Advantage	Disadvantage	Field of applications
Standard antimony 4-11% Sb As, Sn, Cu (Ag)	Strong grids, stability for active material in positive electrode, improvement of cycle performance	Increase of water decomposition rate with service life	Traction
Low antimony 0.5 – 3.5% Sb Se, Te, S, Cu <sup>1</sup> , As, Sn, (Al)	Decrease of Sb contamination at negative electrode	Stability of capacity during float charge, preservation of cycle performance	Low maintenance (stationary, traction), SLI batteries
Standard calcium 0.06 – 0.12% Ca 0 to 3 % Sn, (Al)	No Sb contamination at negative electrode	Grid growth, reduced stability of capacity	Stationary, vented and VRLA batteries, SLI batteries
Pure lead	Improvement of deep-discharge performance	Softness	Planté plates, BELL system round cell (BELL Linage 2000)
Antimony/cadmium 1.5% Sb, 1.5 Cd	Low antimony release	Toxicity of cadmium	VRLA batteries

#### 1.1.4 Separator

In general, the separator must have at least the following properties:

- Electronic isolation
- Ionic conduction by providing open pores that are filled with acid. The ionic transfer between both electrodes has to be easy so that the internal resistance of the lead acid cell is minimized
- High porosity for a good ionic conductivity but also a low displacement of acid
- Appreciated mechanic resistance in order to suffer the variation of active material volume during discharge-charge cycles
- Suitable chemical resistance to withstand the strong corrosive electrolyte.

The separators are usually manufactured in polymer (mainly in polyethylene) or glass fibres.

### 1.1.5 Electrolyte

According to the types of batteries, the electrolyte can be liquid, gelled or absorbent. Inside lead acid accumulator, the electrolyte plays two roles: it assures the electric transport in ionic conduction (but not electric conduction as this would cause internal short-circuit) and it participates, like a reactant, at discharge-charge reactions. In the electrolyte, the ionic movement is due to many phenomena:

- Migration: electric field effect on charged particles
- Diffusion: concentration gradient effect
- Convection: density gradient effect due to, for example, the thermal effects in the accumulator

#### 1.1.5.1 Liquid electrolyte

The electrolyte is a solution whose solvent is distilled water and the solute is sulfuric acid. The composition ratio defines the concentration, which is linked, for a given temperature to the electrolyte density. An electrolyte having 33% (in mass) of sulfuric acid has a density of about 1.25.

At liquid state, the water molecule disassociates into ions  $\text{H}_3\text{O}^+$  and  $\text{OH}^-$ . The  $\text{H}^+$  ion only does not exist, it associates always with a water molecule to form an  $\text{H}_3\text{O}^+$  ion.

In water, the sulfuric acid molecules disassociate by a majority to  $\text{H}^+$  (which become ions  $\text{H}_3\text{O}^+$ ) and  $\text{HSO}_4^-$ . It is present also in a low proportion the sulfate ions  $\text{SO}_4^{2-}$ .

#### 1.1.5.2 Immobilized electrolyte

The electrolyte is immobilized in order to provide open space for the fast transport of oxygen as a gas. Otherwise, the internal oxygen cycle (cf. 1.3.3.2) is hindered by the too slow diffusion rate of the dissolved oxygen. In lead acid battery two ways are used for electrolyte immobilization: absorption of the sulfuric acid by a glass felt, or gelled acid by addition of  $\text{SiO}_2$ .

One characteristic of both methods of electrolyte immobilization is that, during service, the (very small quantity) water loss leads to an increase of the gas channels. The transport of oxygen from the positive to the negative electrode is therefore made easier. The result of this is a slight increase in float-charge current during the operational life of the batteries due to reduced polarization of the negative electrode (cf. 4.1.3.2).

#### Absorption of the electrolyte by a glass mat (AGM)

The electrolyte is absorbed into fine fibres of glass felts (diameters in the  $\mu\text{m}$  range) forming a pore system. Such glass felts simultaneously fulfill a double function:

- They act as a conventional separator that insulates the electrodes of different polarities from one another and prevents short-circuits between the electrodes, since lead dendrites do not grow from the negative to the positive electrode through the fine pore system of glass felt.
- They immobilize the electrolyte by effective absorption that fills most of their pores.

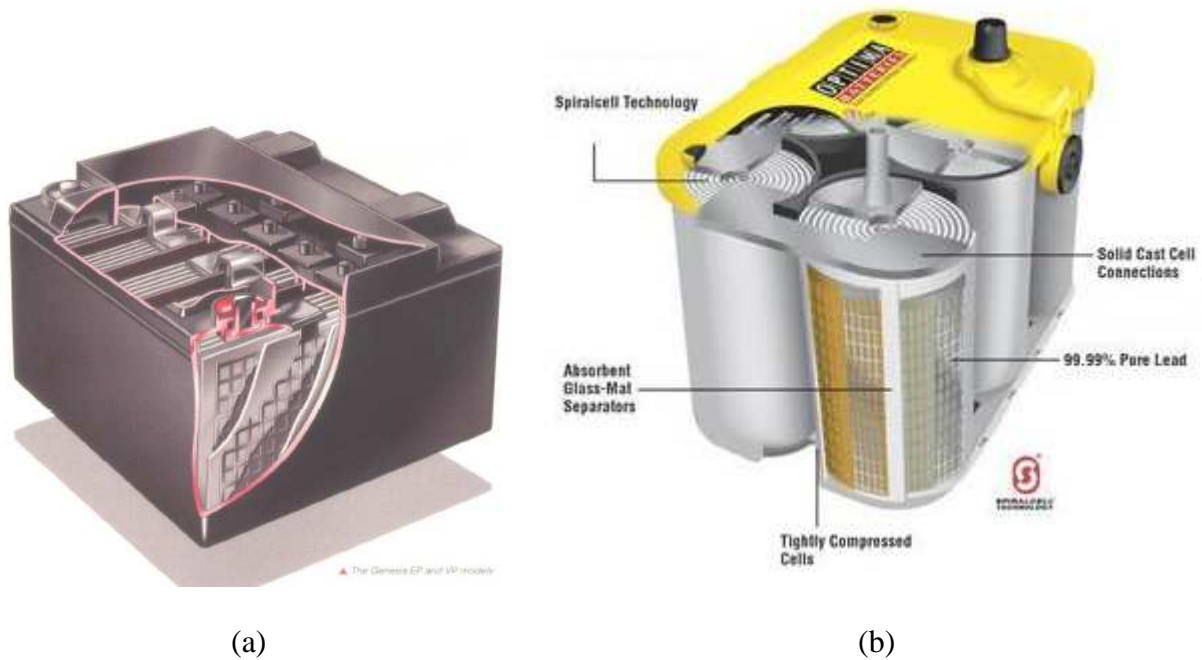


Figure 3: (a) Shattered view of a VRLA AGM battery, EnerSys GENESIS. (b) VRLA battery in spiral wound design [12]

In a battery, the dosage of the electrolyte must be kept low enough that the absorbent mat separator is not completely saturated with electrolyte, so the required gas channels are formed in the felt. Otherwise, the battery acts at least partially, like a vented one, until water loss has sufficiently reduced the amount of water.

#### Gelled electrolyte by addition of $\text{SiO}_2$

Sulfuric acid, in the concentrations usually applied in batteries, forms a solid gel when about 6%  $\text{SiO}_2$  are added. It is a thixotropic gel that can be kept highly liquid by intensive agitation, which is an advantage for filling the battery. Shrinkage during solidification squeezes electrolyte out of the gel and forms cracks that run through the solid electrolyte and allow fast transport of gaseous oxygen. Real pores, as in a felt, cannot be observed in the gelled electrolyte. But the gelled sulfuric acid behaves in the same way as in a felt, with a pore structure one order of magnitude finer than that of the usual microglass-mat separator.

Gelled electrolyte cannot fulfill the function of a separator, since it does not suppress penetration of lead dendrites.

The electrolyte volume and its density are defined by manufacturers according to battery types and utilizations. It is a trade-off between the wanted capacity, the lifetime, the provided current intensity and the expected behavior at low temperatures (the temperature affects the viscosity and therefore the electrolyte conductivity).

### **1.1.6 Lead acid battery families**

In this thesis work, two principal families of lead acid battery are presented: flooded (vented) batteries and VRLA (Valve-Regulated Lead Acid Battery) batteries. They differ from each other in the state of their electrolytes: liquid electrolyte for flooded batteries and immobilized electrolyte for VRLA batteries.

### 1.1.6.1 Flooded batteries

The *flooded or vented battery* is the first used-technology of lead acid battery, created by Planté in 1859. The word “flooded” means that the electrodes are immersed in a solution of sulfuric acid, and the word “vented” relates to the gas productions almost not recombining and venting out of the battery. The combination between hydrogen and ambient air can be potentially explosive as soon as wt.4% of hydrogen in volume.

Some flooded batteries produced actually are considered to be “maintenance free”. This associates to the fact that the electrolyte consummation is weak and the initial electrolyte reservation is sufficient to assure a good function of the battery during its lifetime service. Their grid alloys consist of low-antimony or calcium grids which lead to strong polarizations of oxygen and hydrogen

### 1.1.6.2 VRLA batteries

The first VRLA batteries of the SONNENSCHNEIN society appeared in the battery market at the end of 1950. Different names are in use for this kind of lead acid battery such as “sealed lead acid battery”, “sealed maintenance free lead acid battery”, “sealed valve-regulated lead acid battery” and “valve-regulated lead acid battery”. The words “sealed” and “valve-regulated” relate to the fact that in this technology of battery, thanks to the immobilized electrolyte, the oxygen can be fast enough transported from positive to negative electrodes and reduce into water, the gas production is therefore strongly reduced; a regulated valve is sufficient to escape gas. In fact, the term “sealed” is not really exact because the generation of hydrogen can never be avoided completely, therefore there is always a small amounts gas escaping. Moreover, the term “valve” comprises already the term “sealed” as a valve can operate only when the battery itself is sealed. Hence, the term now mostly used is “Valve-Regulated Lead Acid battery” or its abbreviation “VRLA battery”. Two main characteristics of the VRLA battery which differ from the flooded battery are the following:

- There is not a continuous gas exchange between the interior of the battery and the surrounding atmosphere.
- The battery is not completely sealed but equipped with a valve that opens even during normal operation from time to time to let the gas escape

In VRLA batteries, only antimony free grid alloys, Pb/Ca alloys, are used.

*Table 2: Principal comparisons of two lead acid battery families: flooded and VRLA batteries [6]*

Battery family	Flooded (vented)	VRLA
Electrolyte	Liquid	Gelled or AGM
Positive grid alloy	All kinds of grid alloys	Pb/Ca and pure Pb grid alloys
Advantage	Longer lifetime The cheapest technology	Maintenance free Security (very weak gas escape)
Disadvantage	Water consumption Specific installation (gas escape)	Short service life, low reliability Temperature effect

### 1.1.7 Lead acid battery market [13]

Lead acid battery market is divided into three major segments:

- Starting, lighting and ignition lead acid batteries (SLI)



- Motive lead acid batteries (MLA)
- Stationary lead acid batteries (SLA)

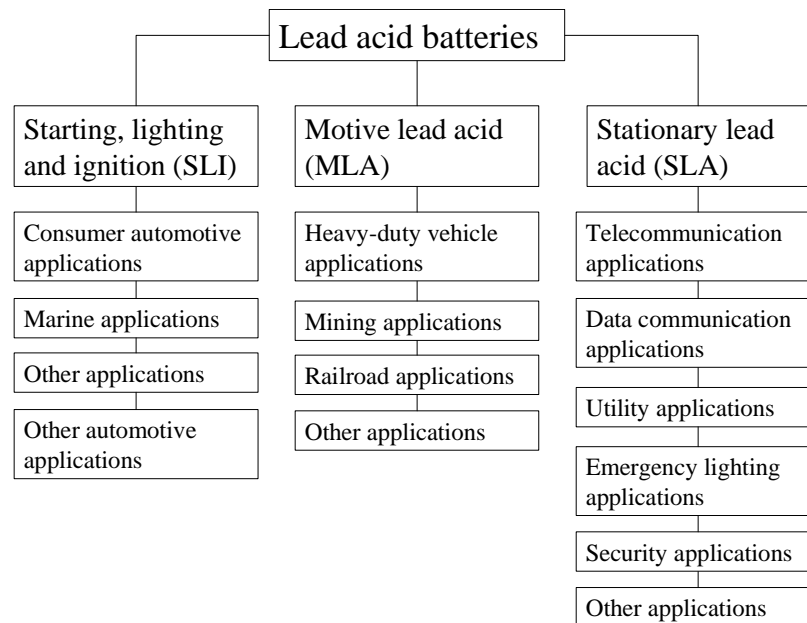


Figure 4: Lead acid battery market: market segmentation (World), 2001. Source: Frost & Sullivan [13]

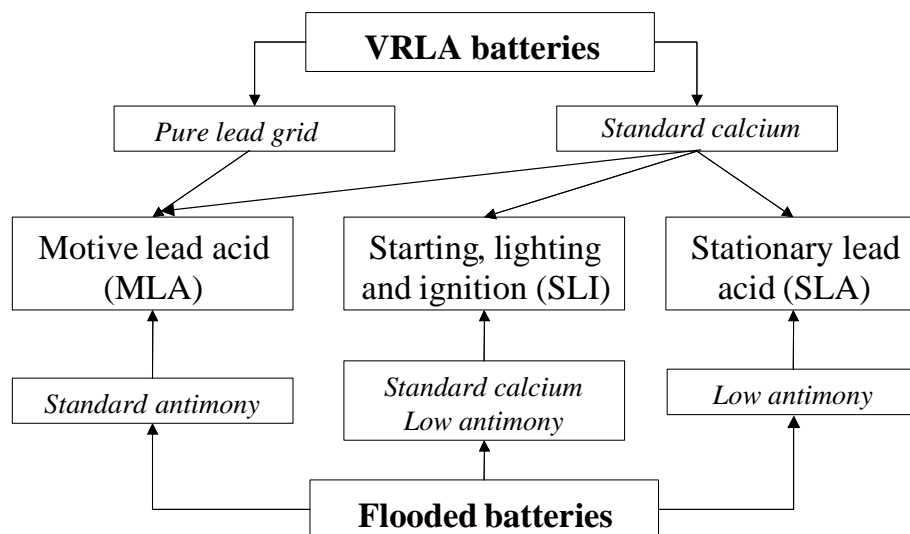


Figure 5: Lead acid battery families of flooded and VRLA batteries, their kinds of grid alloys and their application fields

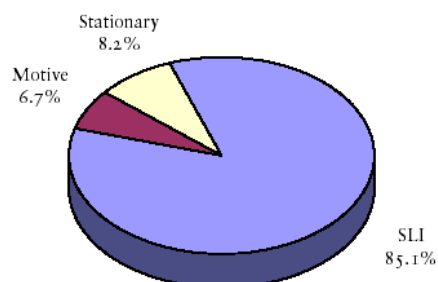


Figure 6: Lead acid battery revenue breakdown by product type (world), 1998-2008. All figures are rounded; the base year is 2001. Source: Frost & Sullivan [13]

In 2001, the world lead acid battery market generated approximately \$29.28 billion, growing approximately 2.9 % compounded annually.

## 1.2 OPERATION OF LEAD ACID CELL [14]

Lead acid cell is able to supply electrical energy from chemical energy to a load and is able to re-establish its energy reserve thanks to a generator. This section explains how this system works.

### 1.2.1 Electrochemical cell

The potential difference between the electrode (Pb or PbO<sub>2</sub>) and the electrolyte (sulfuric acid solution) is called the “electrode potential”. The “absolute electrode potential” is not measurable, however the “relative electrode potential” can be measured in associating two electrode/electrolyte interfaces. This is also the schema of an electrochemical cell.

An electrochemical cell consists of two electrode/electrolyte interfaces as shown in Figure 7. In the case of two different electrolytes, they are linked together by an electrolytic junction (ionic bridge), which allows ions flow.

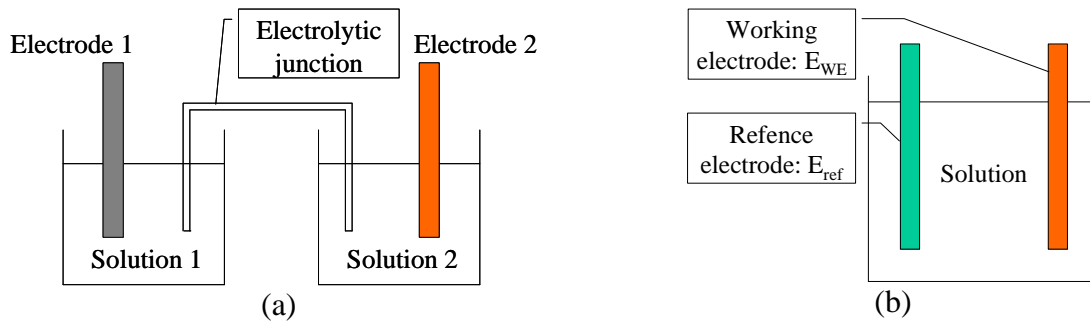


Figure 7: (a) Presentation of an Electrochemical cell. (b) Electrode Potential measurement by a reference electrode. The principle is the same: two electrodes with one electrolyte or with two electrolytes linked together by electrolyte bridge.

#### 1.2.1.1 Relative electrode potential and cell voltage

As mentioned above, the absolute potential cannot be measured, since a potential difference can only be measured between two electronic conductors. Thus the electrode potential has to be related to a “reference electrode” having a stable and well-known potential, like the Standard Hydrogen Electrode (SHE), which is now universally used (cf. Figure 7).

The potential difference between the working electrode and the reference electrode is called the electrode potential related to the reference:

$$E_{WE/ref} = E_{WE} - E_{ref} \quad (1)$$

The potential difference between two electrodes of a cell is the “cell voltage”. E is called cell voltage at open circuit; another name is “electromotive force” (emf).

$$E = E_2 - E_1 \quad (2)$$

### 1.2.1.2 Electrode polarity

The “electrode polarity” is defined according to the sign of the cell voltage. For instance, if the cell voltage  $E$  is positive, the electrode 2, whose potential is  $E_2$ , is said to have a positive polarity and the electrode 1,  $E_1$ , a negative polarity and vice versa.

In addition, when an external current flows through the cell, one of two electrodes becomes “anode” (gives electrons) and other becomes “cathode” (receives electrons). There is not a relation between the electrode polarity and its role of anode or cathode. In contrast of the anode and cathode notions, the electrode polarity is defined even though there is no external current flow.

## 1.2.2 Galvanic & electrolytic cells: lead acid cell

When an external current flows through an electrochemical cell, it becomes *galvanic* or *electrolytic cell*.

### 1.2.2.1 Galvanic cell

When an electrochemical cell whose voltage is  $V$  (different zero) is connected to an external resistance  $R$  (not infinite), a current flow is observed  $i = V/R$ .

Galvanic cell mechanism (Figure 8): a reduction is observed at the side whose potential is higher (reduction of the oxidant 2 -  $Ox_2$ , better oxidant than the oxidant 1 -  $Ox_1$ ) and an oxidation is observed at the side whose potential is weaker (oxidation of the reducer 1 -  $Red_1$ , better reductive than the reducer 2 -  $Red_2$ ). In addition, electrode 1 gives away electrons and electrode 2 obtains electrons, the circulation between two electrodes is assured by an external circuit. Chemical energy is converted to electric energy.

Conventionally, the electrodes at which take place reduction and oxidation are called cathode and anode respectively. In the case of a galvanic cell, the positive electrode plays the role of cathode and the negative electrode the role of anode.

Finally, the closed circuit demands the ion passage through the electrolytic junction in order to maintain electro-neutrality in the solution.

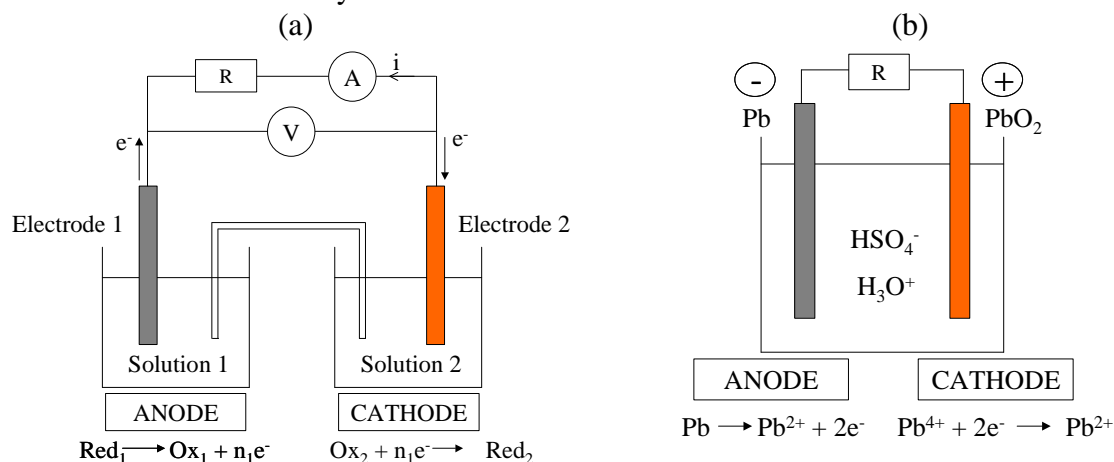


Figure 8: Representation of a galvanic cell associated to  $Ox_1/Red_1$  and  $Ox_2/Red_2$  couples of electrode potentials  $E_1$  and  $E_2$  respectively with  $E_1 < E_2$ . Representation of lead acid cell as a galvanic cell.

## 1.2.2.2 Electrolytic cell

In this type of cell, the direction of reactions at electrodes is opposite to the one in the galvanic cell.

Thanks to the external generator, the direction of the electron flow is imposed to enable the reduction of the less oxidant ( $Ox_1$ ) and the oxidation of the less reductive ( $Red_2$ ). Electric energy is converted to chemical energy. Theoretically, to create electrolysis one needs to apply between two terminals of the cell a voltage  $V$  higher than the potential difference  $E$  between two electrodes. Practically, electrode polarizations and Joule loss due to the cell internal resistance have to be taken into account (cf. 1.5.4), so  $V$  is always higher than  $E$  for a electrolytic cell (in the same way, for a galvanic cell,  $V$  is always smaller than  $E$ ).

In this case, the electrodes play the opposite roles compared to the case of the galvanic cell: the anode for the positive electrode and the cathode for the negative electrode.

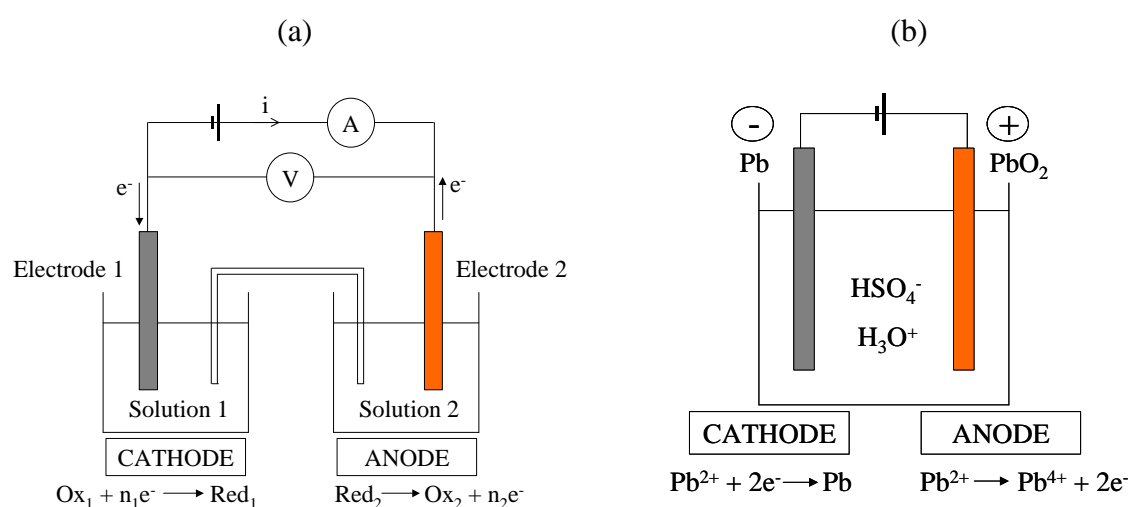
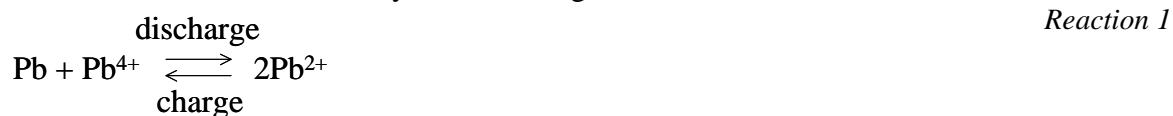


Figure 9: Representation of an electrolytic cell associated to  $Ox_1/Red_1$  and  $Ox_2/Red_2$  couples whose electrode potentials are  $E_1$  and  $E_2$  respectively (with  $E_1 < E_2$ ). Representation of lead acid cell as an electrolytic cell.

## 1.2.2.3 Lead acid cell or lead acid accumulator

A lead acid accumulator (or a lead acid cell) is an electrochemical cell, which can work either as a galvanic cell (during discharging) or as an electrolytic cell (during charging).

It has three redox states  $\text{Pb}^0$ ,  $\text{Pb}^{2+}$  and  $\text{Pb}^{4+}$ .  $\text{Pb}^0$  is spongy metal lead; it constitutes the negative active material.  $\text{Pb}^{2+}$  is associated to  $\text{SO}_4^{2-}$  to form insoluble  $\text{PbSO}_4$ , the discharge product.  $\text{Pb}^{4+}$  is associated to  $\text{O}^{2-}$  ions to form lead dioxide ( $\text{PbO}_2$ ), which is the positive active material. These three redox states form two pairs  $\text{Pb}/\text{Pb}^{2+}$  (or  $\text{Pb}/\text{PbSO}_4$ ) and  $\text{Pb}^{2+}/\text{Pb}^{4+}$  (or  $\text{PbSO}_4/\text{PbO}_2$ ) for which electronic exchange is reversible. The global operation of the lead acid cell can be schematized by the following reaction:



During discharging, the cell works like a galvanic cell and supply electric energy to the load. During charging the cell works like an electrolytic cell to regenerate the active materials Pb and PbO<sub>2</sub> at each electrode.

### 1.3 PRINCIPAL & SECONDARY REACTIONS IN LEAD ACID CELL

When producing electrical energy or storing chemical energy, chemical and electrochemical reactions occur inside the cell. Even when the cell is at open circuit, there are also some reactions happening. This section presents the main and the side reactions that can take place in the lead acid cell.

#### 1.3.1 Pourbaix diagram

Pourbaix diagrams are used to represent the influence of pH (acid or base solutions) on the thermodynamic equilibrium state of the system (Nernst equations, cf. 1.4.2.1) where many redox pairs take place. Furthermore, it is particularly interesting to anticipate the thermodynamical behaviors of the system whose redox pairs depend in different ways on the pH. In the case of lead acid cell, besides the principal redox pairs of Pb/Pb<sup>2+</sup> and Pb<sup>2+</sup>/Pb<sup>4+</sup> there are also the secondary pairs of H<sub>2</sub>O/O<sub>2</sub> and H<sub>2</sub>/H<sub>2</sub>O (H<sub>2</sub>/H<sub>3</sub>O<sup>+</sup> and OH<sup>-</sup>/O<sub>2</sub>) as the water is always present in lead acid cell electrolyte. Moreover, the Pb metal of the grid alloy is not stable in the potential zone of the positive electrode. Thanks to Pourbaix diagrams, we will see how these redox pairs stay together. The pH of the lead acid cell electrolyte is between -1 and 0.

In the literatures, it exists the potential/pH diagrams of the Pb/H<sub>2</sub>O system and of the Pb/H<sub>2</sub>SO<sub>4</sub> system [15]. In this thesis, the Pourbaix diagram of the Pb/H<sub>2</sub>O system (cf. Figure 10) is used to describe redox pairs of a lead acid cell and not the Pourbaix diagram of the Pb/H<sub>2</sub>SO<sub>4</sub> system, as H<sub>2</sub>SO<sub>4</sub> is, in general, not present at the interface of the grid/active material during the battery service life (cf. 1.3.3.3).

The observations of Pourbaix diagrams of the Pb/ H<sub>2</sub>O system are the following:

- Potential equilibrium values are about 1.68V and -0.34V (cf. 1.4.2) for the pairs Pb<sup>2+</sup>/Pb<sup>4+</sup> and Pb<sup>0</sup>/Pb<sup>2+</sup> respectively. The cell voltage at equilibrium is around 2V.
- When the cell voltage is under 2V, the reactions take place in the sense to produced Pb<sup>2+</sup>; the cell is discharged. In contrast, when the cell voltage is above 2V, Pb and PbO<sub>2</sub> are produced; the cell is recharged.
- Potential equilibrium values are about 1.23 V and 0 V (cf. 1.4.2) for the pairs H<sub>2</sub>O/O<sub>2</sub> and H<sub>2</sub>/H<sub>2</sub>O respectively. Water electrolysis takes place as soon as a voltage is above 1.23V. Between 0 and 1.23V, recombination of H<sub>2</sub> and O<sub>2</sub> can occur to reform H<sub>2</sub>O (cf. 1.3.3.2).
- In the potential zone of positive electrode (around 1.68V) the Pb metal is not stable; it will be oxidized to Pb<sup>2+</sup> and then to Pb<sup>4+</sup>. This is the corrosion phenomenon at the grid of the positive electrode.

We keep in mind that in a lead acid cell there are not only the principal reactions of discharge-charge but also the secondary reactions. They are water electrolysis, water recombination and corrosion of positive electrode grid. The secondary reactions take place always in the lead acid cell and take place simultaneously with the principal reactions.

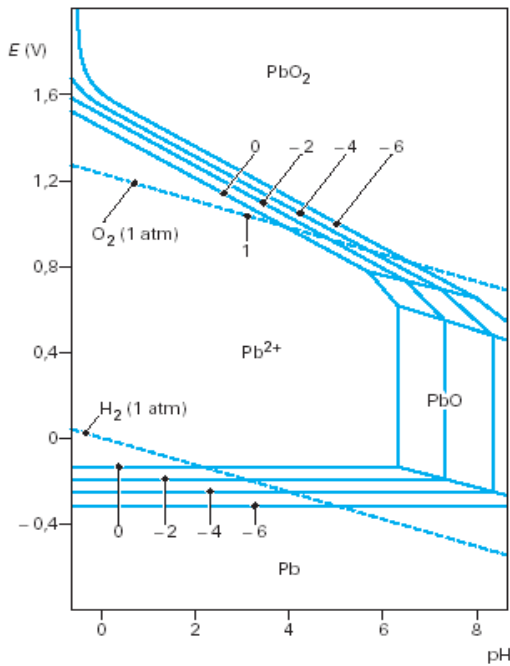


Figure 10: Pourbaix diagram [16]

The lines noted 0, -2, -4, -6 correspond to the concentration of  $Pb^{2+}$  ions, which equals to 1,  $10^{-2}$ ,  $10^{-4}$ ,  $10^{-6}$  mol/l.

### 1.3.2 Main reactions (discharge-charge of active materials)

#### 1.3.2.1 Discharge

During discharging, the lead acid cell, which behaves as a galvanic cell, supplies electricity to the load; chemical energy is converted to electrical energy. The operation of a cell during discharging is shown schematically in Figure 11 (a). When the cell is connected to an external load, the electrons flow from the negative electrode (Pb), which is oxidized (become  $Pb^{2+}$ ), through the external load to the positive electrode ( $PbO_2$ ), where they are accepted and the positive material reduced (become also  $Pb^{2+}$ ). The electric circuit is closed in the electrolyte by the positive ion flows ( $H_3O^+$ ) from the negative to the positive electrodes.

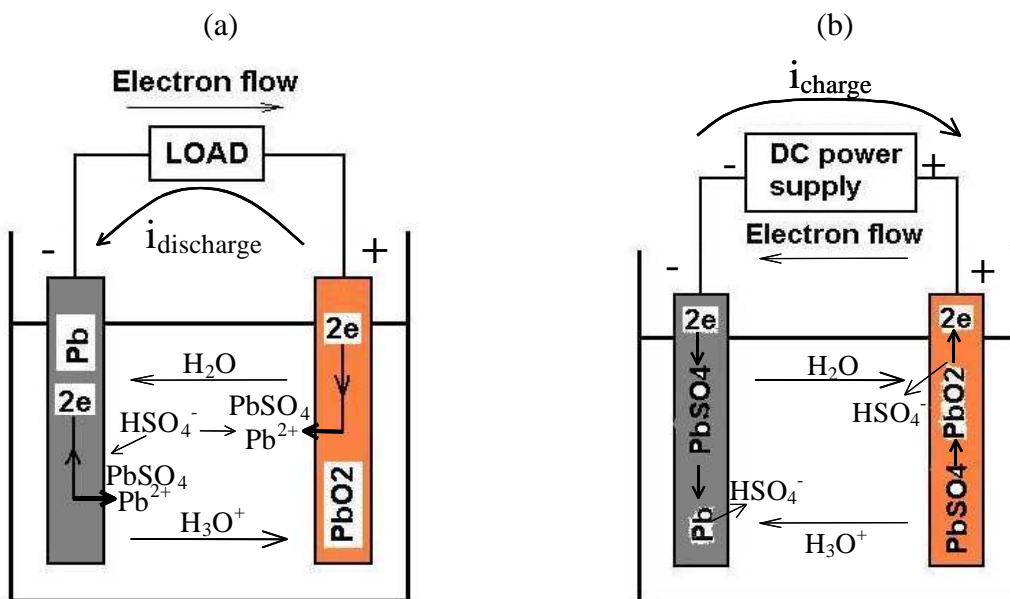
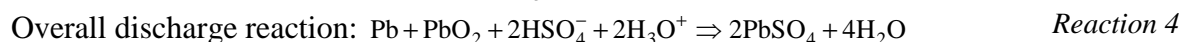
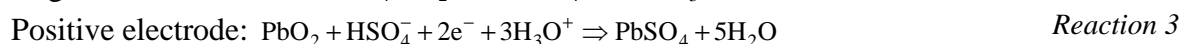
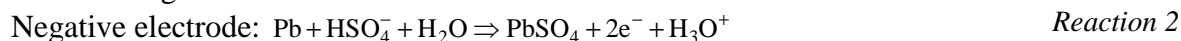


Figure 11: Products and reactants of a lead acid cell producing during (a) discharging and (b) charging.

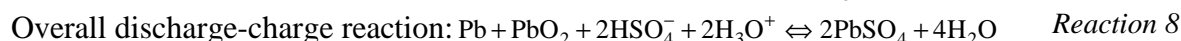
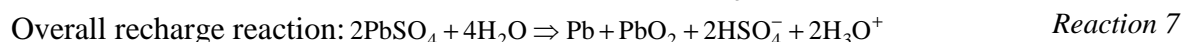
The discharge reactions can be written as follows:



### 1.3.2.2 Charge

During charging, lead acid cell behaves as an electrolytic cell: it receives electricity from the DC power supply to reform its active materials; electrical energy is converted to chemical energy. Oxidation takes place at the positive electrode and reduction at the negative electrode, as shown in Figure 11 (b).

The charge reactions can be written:



As a small portion of  $\text{SO}_4^{2-}$  ions is present in the electrolyte, another overall discharge-charge reaction can be written:



## 1.3.3 Side reactions

### 1.3.3.1 Water electrolysis

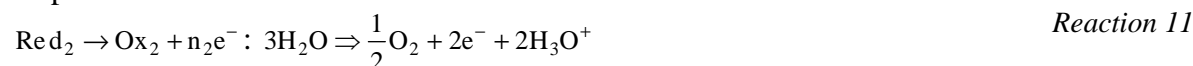
According to the Pourbaix diagram of the lead acid cell, the water electrolytic reaction occurs always in the lead acid cell, at open circuit as well as during discharging and charging, as the cell voltage (around 2 V) exceeds the water redox pair voltage (about 1.23 V).

Applying the electrolytic cell schema to the redox pairs  $\text{H}_2\text{O}/\text{O}_2$  ( $\text{OH}^-/\text{O}_2$ ) and  $\text{H}_2/\text{H}_2\text{O}$  ( $\text{H}_2/\text{H}_3\text{O}^+$ ), water electrolytic reactions at electrodes are the following:

At negative electrode:



At positive electrode:



Overall reaction:



### 1.3.3.2 Internal gas cycle

Water electrolytic reactions (Reaction 10 and Reaction 11), which generate hydrogen and oxygen gas, always take place in lead acid cell and the reversed reactions (water recombination) are also possible in favorable conditions. This is called internal gas cycle.

Applying the galvanic cell schema for the redox pairs  $\text{H}_2\text{O}/\text{O}_2$  ( $\text{OH}^-/\text{O}_2$ ) and  $\text{H}_2/\text{H}_2\text{O}$  ( $\text{H}_2/\text{H}_3\text{O}^+$ ), water recombination reactions at electrodes are the following:

At positive electrode:



At negative electrode:



We have to note that  $\text{H}_2$  that is generated at the negative electrode has to be consumed at the positive electrode whose potential is favorable for the reaction to take place. In fact, Reaction 13 occurs only when the potential exceeds 0 V (cf. Figure 10) and, at the positive electrode, it is around 1.68 V, which satisfies this condition. In the same way, the  $\text{O}_2$  that is produced at the positive electrode recombines at the negative electrode.

The condition for establishing internal gas cycles is that the rates of Reaction 13 and Reaction 14 have to be high enough otherwise the gases escape the battery. This is the reason why the internal hydrogen cycle is almost negligible due to the fact that the rate of Reaction 13 is too low. The internal oxygen cycle is possible because the rate of Reaction 14 is quite high and the oxygen can reach the negative electrode fast enough thanks to the immobilized electrolyte.

### 1.3.3.3 Corrosion

#### Definitions:

- “Corrosion” means, in chemistry, the breaking down of essential properties of a material due to chemical reaction with its surroundings. This means an oxidation, i.e. a loss of electrons of a metal reacting with its surroundings [17].
- “Corrosion area” is the potential area in a Pourbaix diagram (cf. Figure 12) where ion species are stable [14].
- “Non-corrosion area”: is the potential area where insoluble species are stable. Two non-corrosion regions may be distinguished: one region where the solid stable form is the metal itself (area of “immunity”, or of “cathodic protection”), and one region where the solid stable form is an oxide (area of “passivation”). In the area of passivation, the metal tends to become coated with its oxide, which can, according to the circumstances, form on the metal either a nonporous film practically preventing all direct contact between the metal itself and the solution (in this case protection is perfect), or a porous deposit which only partially prevents this contact (in this case protection is imperfect and pitting occurs) [18].

Figure 10 showing Pourbaix diagrams for lead acid cell can be simplified as shown in Figure 12, which describes the theoretical conditions of corrosion, immunity and passivation of lead in an aqueous solution.

We can observe that:



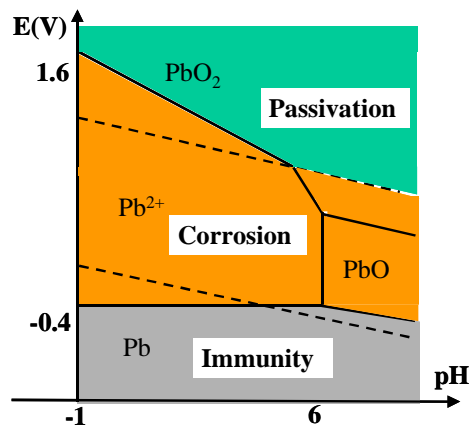
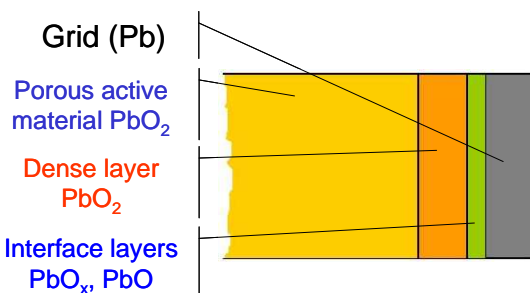


Figure 12: Theoretical conditions of corrosion, immunity and passivation of lead, at 25°C in the absence of substances forming insoluble salts

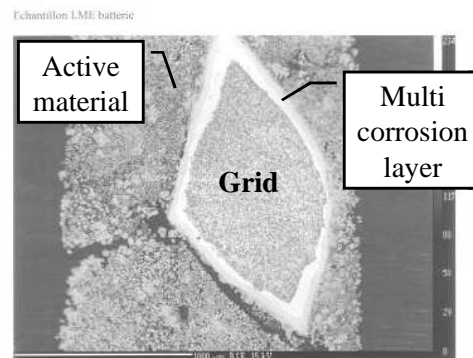
- At the negative electrode, during discharging or at open circuit, lead metal of the grid can be corroded to form lead oxide. However, it can be re-reduced to lead during charging, since the electrode potential corresponds to the immunity area. In this region, lead remains stable.
- At the positive electrode, whose potential is never less than  $-0.34\text{V}$ , grid corrosion occurs in permanence. During discharging and at open circuit ( $E_+ \leq 1.68\text{V}$ ), lead is oxidized to lead oxide ( $\text{PbO}$  then  $\text{PbO}_x$ ). During charging ( $E_+ > 1.68\text{V}$ ), these oxides will be oxidized to  $\text{PbO}_2$ ; the oxidation of  $\text{Pb}$  to  $\text{PbO}$  and  $\text{PbO}_x$  continues.

As the results of the corrosion phenomenon between the positive grid and the active material there are multi corrosion layers of lead oxides as illustrated in Figure 13.

The process of corrosion occurs in the following way: the metallic lead grid is progressively transformed into lead oxide; this oxidation is performed in two steps; each step corresponds to a loss of two electrons.



[1]



(source: EDF)

Figure 13: Structure of the corrosion layer at the positive grid surface

These electrons are evacuated by conduction. The remaining positive ions,  $\text{Pb}^{2+}$  and  $\text{Pb}^{4+}$  have to be in equilibrium with other negative species. Two types of anions are available in the heart of a positive electrode:  $\text{O}^{2-}$  and  $\text{HSO}_4^-$ .

- The  $\text{O}^{2-}$  ions are present in a solid phase in the lead oxides  $\text{PbO}$  and  $\text{PbO}_2$  (i.e.  $\text{Pb}^{2+}$  and  $2\text{O}^{2-}$ ). This dioxide is a non-stoichiometric compound<sup>1</sup>. Its closed composition is

<sup>1</sup> **Non-stoichiometric compounds** are chemical compounds with an elemental composition that cannot be represented by a ratio of well-defined natural numbers, and therefore violate the law of definite proportions.

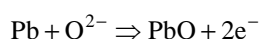
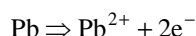
$\text{PbO}_{1.95}$ . It means, in the middle of crystals there are blanks that enable  $\text{O}^{2-}$  ions to move by jumping. This diffusion in the solid phase creates the intermediate zone consisting of  $\text{PbO}_x$  between the initial layer of  $\text{PbO}$  and the reservoir of  $\text{O}^{2-}$  ions, which is the positive active material. Once the  $\text{PbO}_2$  active material loses  $\text{O}^{2-}$  for corrosion, it will pick up  $\text{O}^{2-}$  ions of  $\text{H}_2\text{O}$  (i.e.  $2\text{H}_3\text{O}^+$  and  $\text{O}^{2-}$ ) of the electrolyte to neutralize its charge.

- The  $\text{HSO}_4^-$  ions are available in the electrolyte solution. They can reach the  $\text{Pb}^{2+}$  ions by following the path created by cracks inside multi-layers of  $\text{PbO}$  and  $\text{PbO}_x$  and form  $\text{PbSO}_4$ . Such anion contribution (diffusion in the liquid phase) provokes then a quicker corrosion compared to the solid phase of  $\text{O}^{2-}$  ions.

If the battery is frequently at charge, the  $\text{PbO}$  layer can stay thin as  $\text{PbO}$  is oxidized to  $\text{PbO}_2$ . The dense  $\text{PbO}_2$  layer plays the role of preventing the contact between  $\text{PbO}$  and sulfuric acid  $\text{H}_2\text{SO}_4$  in the solution. Otherwise, when the  $\text{PbO}$  layer exceeds a certain volume, it causes the formation of crevices or cracks at the dense  $\text{PbO}_2$  layer.  $\text{H}_2\text{O}$  can reach the grid faster via these cracks and  $\text{H}_2\text{SO}_4$  can pass through the  $\text{PbO}_2$  layer and act with  $\text{PbO}$  to form lead sulfate  $\text{PbSO}_4$ . Excessive formation of  $\text{PbSO}_4$  can destroy the  $\text{PbO}_2$  layer and severe grid corrosion can thus occur. This is usually the case when the battery stands for prolonged periods without any charge.

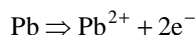
The reactions are the following.

When lead oxides supply the  $\text{O}^{2-}$  ions:



*Reaction 15*

When the grid is in contact with the electrolyte:



*Reaction 16*

During charging, in addition of Reaction 15 and Reaction 16 above, there is also:



*Reaction 17*

Reaction 17 shows also that corrosion causes water consumption.

#### 1.3.3.4 Oxido-reduction of unwanted ions

When the electrolyte contains impurities such as Fe, HCl, As... and when the electrode potential values are favorable the oxido-reduction reactions of these impurities can take place [19, 20]. Let's take the case of  $\text{Fe}^{2+}$  and  $\text{Fe}^{3+}$  ions for example.

$\text{Fe}^{2+}$  can be oxidized at the anode to give  $\text{Fe}^{3+}$  in the electrolyte with the presence of  $\text{PbO}_2$ . And then this  $\text{Fe}^{3+}$  can diffuse to the negative electrode Pb, where it can react with the latter to form  $\text{Fe}^{2+}$ . At its turn,  $\text{Fe}^{2+}$  diffuses to the positive electrode and returns to its initial state of

---

Often, they are solids that contain crystallographic point defects that result in the excess or deficiency of an element [wikipedia].

$\text{Fe}^{3+}$  at the contact with  $\text{PbO}_2$ . The role of Fe is to transport electrons from the positive to the negative electrode. These parasite reactions can take place indefinitely and cause the discharge of the cell.

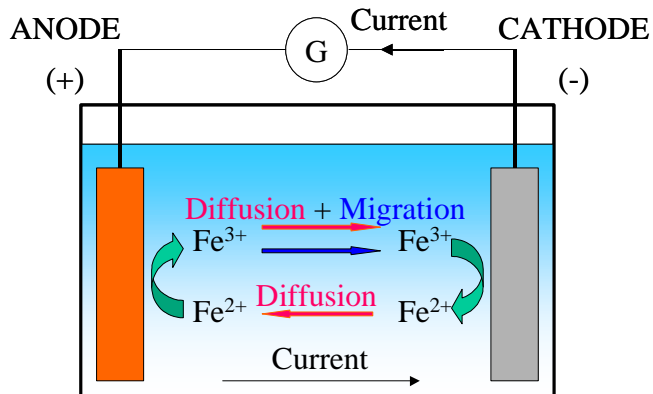
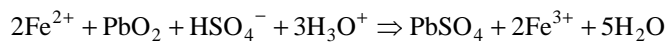
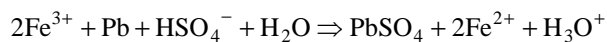


Figure 14: Representation of redox reactions of ions  $\text{Fe}^{2+}$  and  $\text{Fe}^{3+}$  in a lead acid cell during charging [20]



Reaction 18



Reaction 19

#### 1.4 CHARACTERISTIC OF LEAD ACID CELL WHEN NO EXTERNAL CURRENT FLOWS

What is the condition for a charge or a discharge reaction to happen? As explained in the section 1.3.1, this condition is met when the voltage is different or shifted from the equilibrium value of the cell. What is equilibrium voltage of the lead acid cell and which factors influence it? What is the relation between the equilibrium voltage of the cell and its ability to supply energy?

##### 1.4.1 Thermodynamic laws [1]

A chemical or electrochemical reaction can occur only when the thermodynamic conditions are possible and favorable. The thermodynamic laws apply generally to the equilibrium state, which means all reactions are balanced. In the electrochemical cell, these data can be measured only when there is no current flowing through the cell or its electrodes. On account of this balance, the thermodynamic parameters do not depend on the reaction path; they consider only on different energy levels between final and initial components (products and reactants of the electrochemical reaction). It describes therefore the maximum performance that can be expected from the electrochemical system.

The energy exchange, connected with electrochemical reactions, is described by three thermodynamic functions: “enthalpy  $H$ ”, “free enthalpy  $G$ ” (or “Gibbs free energy”) and “entropy  $S$ ”.

Because these thermodynamic functions, concerning an electrochemical reaction, describe the energy differences before the reaction started and after it was completed, they are usually written with a “ $\Delta$ ” and called as follows:

- Enthalpy of reaction ( $\Delta H$ ): the total amount of energy released or absorbed by the reaction.

- Free enthalpy of reaction or Gibbs free energy change ( $\Delta G$ ): the maximum amount of chemical energy that can be converted into electrical energy and vice versa during reaction (charge or discharge).
- Entropy of reaction ( $\Delta S$ ): describes the energy loss or gain connected with the reaction. When there is no current flows through the cell, the “product  $T\Delta S$ ”, called “reversible heat effect” ( $Q_{rev}$ ) represents the heat exchange with the surroundings.

These functions can be negative or positive. In the first case, the system losses energy, in the other case, it gains energy. For example, during discharging, the sign of  $\Delta G$  is negative because the electrochemical system delivers energy; when the cell is recharged, it is positive.

The relations of these three functions are:

$$\Delta G = \Delta H - T.\Delta S \text{ or } \Delta H = \Delta G + T.\Delta S \quad (3)$$

$T$  : temperature (K)

Reversible heat effect  $T.\Delta S = Q_{rev}$  expresses the difference between  $\Delta H$  and  $\Delta G$

### 1.4.2 Equilibrium potential notion [21]

A difference of electrical potential usually forms at a boundary between two phases such as, in a lead acid cell, between the active material (Pb or  $PbO_2$ ) and the electrolyte (sulfuric acid solution). The development of such an electrochemical potential difference requires the transport of electrically charged particles, ions or electrons, in either direction. When the equilibrium potential is reached, this reaction apparently ceases macroscopically. However, from the kinetic viewpoint, the forward reaction rate does not become zero when the equilibrium potential is reached, but is compensated by a reverse reaction of identical rate. From the molecules point of view there is a constant exchange of charge in both directions, even though the reaction has macroscopically come to a complete standstill at the equilibrium potential. In practice, it is supposed that equilibrium potential exists when no external current is passing through the phase boundary.

The equilibrium potential between two electrodes, called difference of potential, can be calculated thermodynamically from the Gibbs free energy change  $\Delta G$  of reaction. During the electrochemical cell operation, chemical energy is converted into electrical energy and it is mathematically described as the product of the cell difference potential and the electric charges, which are transferred through the cell:

$$\text{Electrical energy} = \Delta E_0.Q \quad (4)$$

$\Delta E_0$  : potential difference at equilibrium (zero external current) [V]

$Q$  : integral of current in time [coulombs C].  $Q$  can be calculated as  $n.F$

$n$  : number of exchanged mole of electrons in the reaction

$F$  : Faraday constant, which is the electric quantity in one mole of electrons, equivalent to 96485 As/mol.

The potential difference at zero current is the possible maximum potential. The maximum energy obtained from a chemical reaction can be calculated. It is referenced to the electric work and described by Eq. (4) where the work is defined to be positive for the system (e.g. charge).

$$W_{\max} = W_{\text{electric}} = -nF\Delta E_0 \quad (5)$$

As Gibbs free energy change  $\Delta G$  is defined as the maximum energy delivered by the system (cf. 1.4.1), it can be written:

$$\Delta G = -nF\Delta E_0 \quad (6)$$

Eq. (6) can be rewritten as follows, which is also known as the formula of the cell equilibrium voltage:

$$\Delta E_0 = -\frac{\Delta G}{nF} \quad (7)$$

One observation is that a positive cell potential leads to a negative change of the free energy. It is a simple question of conversion: what is given by the system is what the system loses and so is negatively counted.

Eq. (3) can be written also according to Gibbs-Helmholtz at constant pressure:

$$\Delta H = \Delta G - T \left[ \frac{\partial(\Delta G)}{\partial T} \right]_p \quad (8)$$

Electrochemical function data of different particles and ions are present in [15, 22]

From Eqs. (3) and (6), we can write:

$$\Delta H = -nF \left[ \Delta E_0 - T \left( \frac{\partial \Delta E_0}{\partial T} \right)_p \right] \quad (9)$$

Eq. (9) represents released or absorbed energies of reactions in function of the difference potential ( $E$ ). The first term defines the part of electric energy ( $-nF\Delta E$ ) and the second term is the heat ( $nFT(\partial \Delta E / \partial T)_p$ ).

#### 1.4.2.1 Influencing factor on the equilibrium values: electrolyte density – Nernst equation

The electrode potential at different concentrations is given by the Nernst equation as follow:

$$E_0 = E_{0,\text{standard}} + \frac{RT}{nF} \ln \left( \frac{[\text{Ox}]}{[\text{Red}]} \right) \quad (10)$$

$E_0$  : equilibrium electrode potential related to reference electrode.

$E_{0,\text{standard}}$  : standard electrode potential related to reference electrode, it means when all activities of oxidant and reducer are equal the unity (equal to 1).

$R$  : molar gas constant,  $8.3145 \text{ J.mol}^{-1}.\text{K}^{-1}$

$n$  : total mole number(s) of exchanged electron

$F$  : Faraday constant, which is the electric quantity in one mole of electron, equivalent to 96485 As.

$[Ox]$  : activity of oxidant

$[Red]$  : activity of reducer

In which, it is known that: activity = activity coefficient x concentration.

In battery practice, numerical approximation of the dependence of the equilibrium potential on the acid concentration can be obtained using the electrolyte density:

$$\text{Equilibrium cell voltage} = \text{acid density} + 0.84 \quad (11)$$

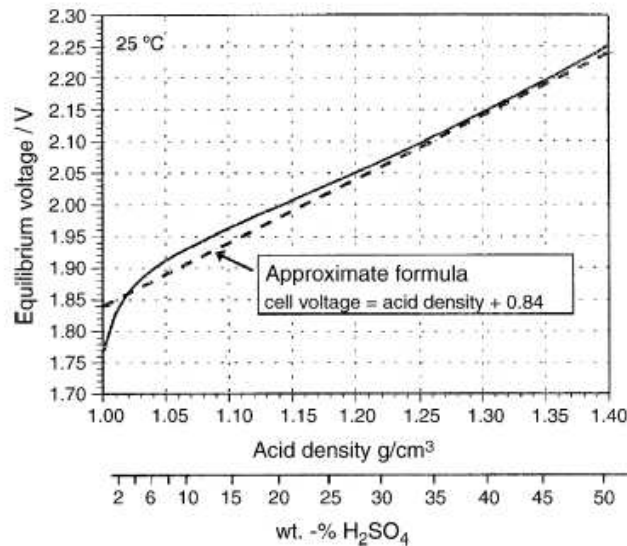


Figure 15: Equilibrium cell voltage of the lead-acid cell referred to acid density and acid concentration in wt.%  $\text{H}_2\text{SO}_4$ , the dashed line represents the approximate formula of Eq. (11) [1].

Applying the data of thermodynamic functions from [15] into Eqs. (3) and (7), the potential differences at equilibrium of the discharge-charge reactions are shown in the table following:

Reaction	Equilibrium potentials (V)
$\text{PbO}_2 + \text{HSO}_4^- + 3\text{H}_3\text{O}^+ + 2\text{e}^- \rightleftharpoons \text{PbSO}_4 + 5\text{H}_2\text{O}$	$E_{0,\text{PbSO}_4/\text{PbO}_2} = 1.631$
$\text{PbO}_2 + \text{SO}_4^{2-} + 2\text{e}^- + 4\text{H}_3\text{O}^+ \rightleftharpoons \text{PbSO}_4 + 6\text{H}_2\text{O}$	$E_{0,\text{PbSO}_4/\text{PbO}_2} = 1.690$
$\text{Pb} + \text{HSO}_4^- + \text{H}_2\text{O} \rightleftharpoons \text{PbSO}_4 + \text{H}_3\text{O}^+ + 2\text{e}^-$	$E_{0,\text{Pb}/\text{PbSO}_4} = -0.299$
$\text{Pb} + \text{SO}_4^{2-} \rightleftharpoons \text{PbSO}_4 + 2\text{e}^-$	$E_{0,\text{Pb}/\text{PbSO}_4} = -0.359$

Applying the Nernst equation of the equilibrium voltage for lead-acid cell:

$$\text{For Reaction 8: } \Delta E_0 = 1.931 + 0.0592 \log \frac{a_{H^+} a_{HSO_4^-}}{a_{H_2O}} \quad (12)$$

$$\text{For Reaction 9: } \Delta E_0 = 2.049 + 0.0592 \log \frac{a_{H^+}^2 a_{SO_4^{2-}}}{a_{H_2O}} \quad (13)$$

#### 1.4.2.2 Influencing factor on the equilibrium values: temperature

The Nernst's equation shows that the temperature can have an influence on the potential in two ways:

- Directly, via the term  $RT/F$ : the influence is however quite weak because if the ambient temperature increase to  $100^\circ\text{C}$ , this factor is modified just a rate of  $373/298 = 1.25$
- Indirectly, via the equilibrium potential difference: according to Eq. (7), we have

$$\frac{\partial \Delta E_0}{\partial T} = -\frac{1}{nF} \frac{\partial(\Delta G)}{\partial T} = \frac{\Delta S}{nF} \quad (14)$$

Temperature coefficient  $\frac{\partial \Delta E_0}{\partial T}$  and equilibrium potential  $\Delta E_0$  are often listed for the usual temperature of  $25^\circ\text{C}$  ( $= 298\text{K}$ ) [18]. The temperature coefficient of the equilibrium potential of Reaction 8 can be calculated according to Eq. (3) and Eq. (14).

We have the thermodynamic data below:  $\Delta G = -372.6 \text{ kJ.mol}^{-1}$ ,  $\Delta H = -359.4 \text{ kJ.mol}^{-1}$  so  $T.\Delta S = 13.2 \text{ kJ.mol}^{-1}$ .

Division by temperature gives:  $\Delta S = 45 \text{ J.K}^{-1}$  per multiple of cell reaction ( $T = 298\text{K}$ )

Inserting this value into Eq. (14) we have:  $\frac{\partial \Delta E_0}{\partial T} = 0.23 \text{ mV / K}$

The equilibrium potential difference at any temperature is:

$$\Delta E_0(T) = \Delta E_0(298) + \left( \frac{\partial \Delta E_0}{\partial T} \right) (T - 298) \quad (15)$$

## 1.5 CHARACTERISTICS OF LEAD ACID CELL WHEN EXTERNAL CURRENT FLOWS

In this section, we will see how a current flows inside a lead acid cell and the principal phenomena occur due to this current flow: the Faraday phenomenon, the individual steps of an overall reaction and the Joule effect. Electrochemical kinetic laws are used to describe the rate of an overall reaction by expression of electrode polarization or overvoltage.

### 1.5.1 Current conduction in lead acid cell [23]

As introduced in 1.1.7, the electric circuit of discharge-charge is completed by the charge transport (ions) in the electrolyte from negative to positive electrodes and vice versa. This part describes the current flow in the volume of different conductive mediums as well as through different interfaces of the system.

### 1.5.1.1 Current conduction in the electrolyte volume

The charge transport in the electrolyte volume occurs usually in three ways:

**Migration:** movement of ions under the influence of an electric field. It is generally characterized by the concentration of charge carriers.

**Diffusion:** movement of ions under the influence of a concentration gradient (or activity gradient). Reactants move by diffusion from the most concentrated zone toward the less concentrated zone. The diffusion is characterized by the diffusion coefficient of charge carriers.

**Convection:** movement of the medium, which is a fluid (liquid or gaseous). This movement, characterized by a speed ( $\text{m.s}^{-1}$ ), will carry along the specie  $i$ , whose concentration is  $c$  ( $\text{mol.m}^{-3}$ ). It can be the natural convection caused by density gradients, or forced convection caused by agitation.

In different experimental conditions, there are some zones where diffusion phenomenon is negligible compared to other phenomena of migration and convection. For instance, the Nernst model is adopted for the charge transport phenomena in the electrolyte of lead acid cell when a mechanical agitation device is used to homogenize the electrolyte (forced convection).

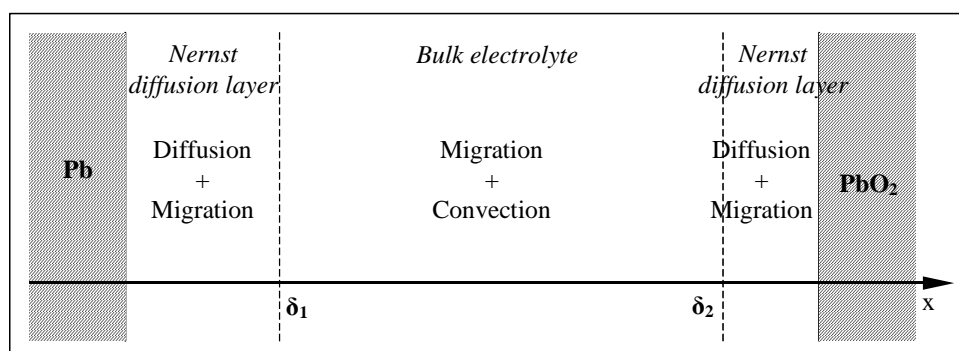


Figure 16: Nernst conduction model in electrolyte of lead acid cell when a mechanical agitation device is used or during the gassing phase to homogenize the electrolyte.

Figure 16 sums up the conduction modes according to the Nernst model in the forced convection condition. In the two diffusion layers near the electrodes, the convection phenomenon can be negligible, while outside these layers the convection presence allows to ignore the diffusion phenomenon.

### 1.5.1.2 Phenomena at interface of electrode/electrolyte

In lead acid cell, the current conduction has to be assured at the interfaces between the solid active material (Pb or  $\text{PbO}_2$ ) and the solution ( $\text{H}_2\text{SO}_4$  and  $\text{H}_2\text{O}$ ).

#### Reactive phenomenon

The free electrons, which assure the current conduction in the active materials, are not present in the electrolyte solution. So there are other mechanisms that allow the current transmission to ion carriers. One of them is an electrochemical reaction. As shown in Figure 17, it is the electrodeposited reaction of  $\text{Pb}^{2+}$  to Pb by reduction at the negative electrode during charging,



where the Pb formed stays at the surface. Reactive interfaces are the interfaces, where there is at least one chemical reaction.

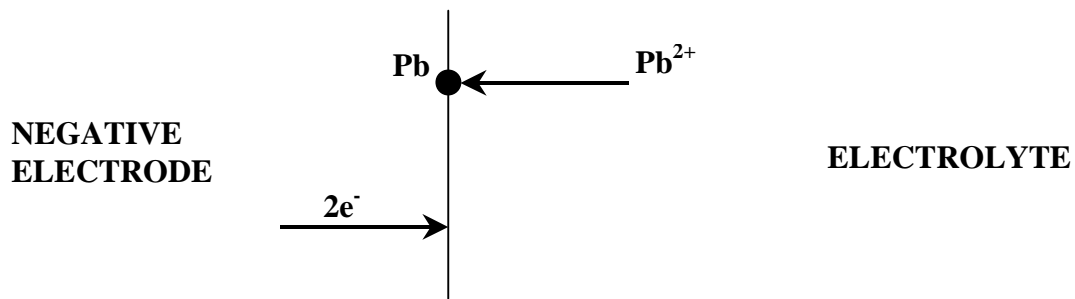


Figure 17: Reduction of an ion  $\text{Pb}^{2+}$  at the interface of negative electrode (Pb)/electrolyte during charging: electrode position of Pb.

#### Exchange phenomenon

When two sides of the interface present the same mobile species but in different states (solid and liquid), the exchange between these two phases can take place. It is the case at interface of lead acid cell where  $\text{Pb}^{2+}$  reacts with  $\text{SO}_4^{2-}$  to form  $\text{PbSO}_4$  crystals.

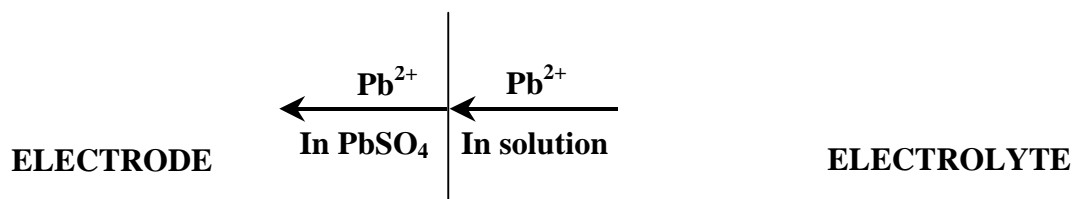


Figure 18: Exchange schema of  $\text{Pb}^{2+}$  ion at the interface electrode/electrolyte during discharging

#### Accumulation phenomenon – Electrical double layer

One of the accumulation phenomena in lead acid cell is the formation of *electrical double layer* at its interfaces. Here, two models of double layers of Helmholtz and Stern are presented (cf. Figure 19).

The first model of the double layer was proposed by Helmholtz in 1850s. In this model, Helmholtz suggested that there was no charge transfer and the solution consisted only of electrolyte. The interactions between the ions in the solution and the electrode surface take place in a way that assures the electrostatic nature (overall charges equals zero). The electrode surface has a charge density  $q^m$ , which is the result of excess or insufficiency of electrons at the electrode surface. For the interface to be neutral at charge, the charge present at the electrode surface would be in equilibrium with the redistribution of ions near the electrode surface.

The attracted ions, which come close to the electrode surface forming a layer, are in equilibrium with the electrode charge. The overall results are two layers of charge (double layer) and a voltage drop in this area called *Outer Helmholtz Plane (OHP)*. This result is absolutely similar to an electric capacitor which has two plates separated by a certain distance (d) with a linear voltage between these two plates.

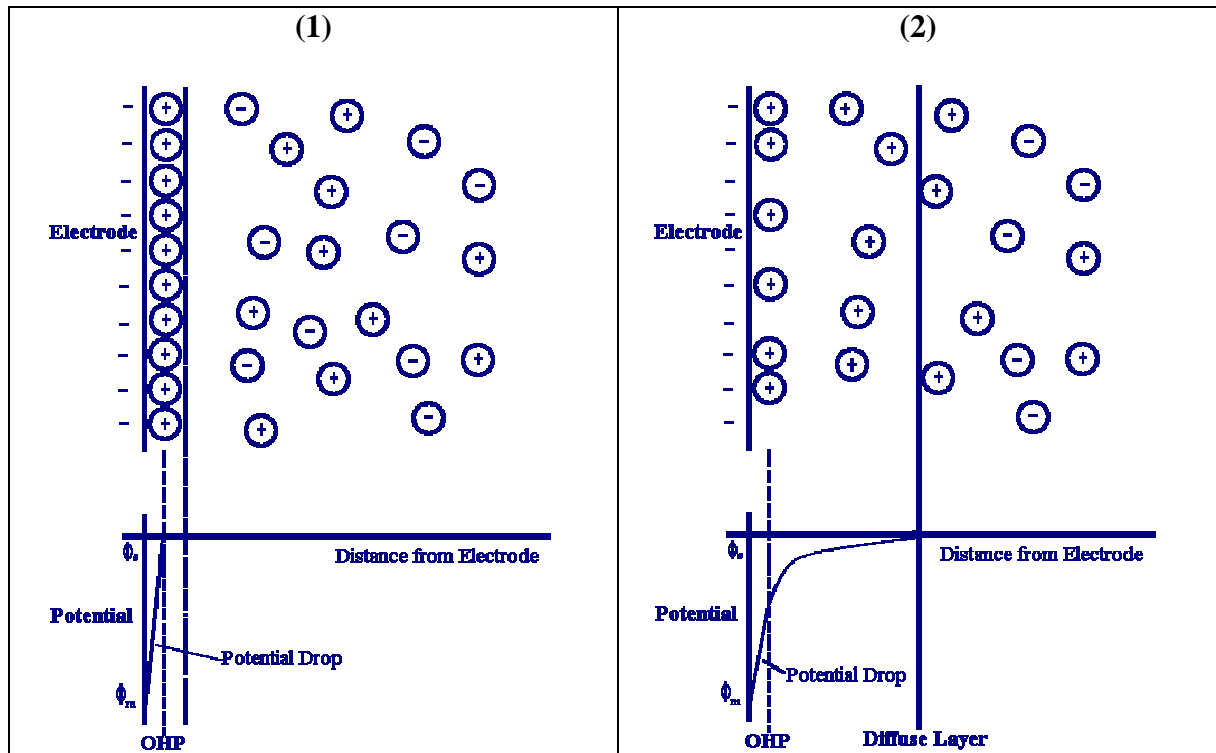


Figure 19: Helmholtz (1) and Stern (2) models of electrical double layer [24]

Stern proposed another model of double layer, which differs from the Helmholtz model in the fact that the ions can move in the solution and that the electrostatic interactions are in concurrence with the Brownian motion<sup>1</sup>. The result is always a charge layer at the vicinity of the electrode surface ( $100 \times 10^{-10}$  m) but in this case the voltage drop occurs in a larger area called the *diffuse layer*.

## 1.5.2 Faraday phenomenon

### 1.5.2.1 Faradic and capacitive current

In general, the current flow corresponds to the reactive phenomenon, exchange and accumulation phenomena. The current has two contributions:

- The faradic current (because this component verifies the Faraday law), which relates to the reactive phenomenon (and eventually the exchange phenomenon) of the consumed and produced species.
- The capacitive current (simple schema of a plate capacitor), which relates to the accumulation phenomenon at the double layer capacitance.

### 1.5.2.2 Anodic and cathodic current

A current (faradic part) flowing through a cell is described by both its magnitude  $I$  and by its direction. When positive current flows from the electrode to the electrolyte, the electrode acts as an anode and the current is called anodic. A cathodic current is the one that flows in the opposite direction. In this case, the electrode acts as the cathode. Figure 20 shows the

<sup>1</sup> **Brownian motion** (named in honor of the botanist Robert Brown) is the random movement of particles suspended in a liquid or gas or the mathematical model used to describe such random movements, often called a particle theory [wiki]

direction of the flow of current through the phase boundary. Thus, with a cathodic current, positive charges flow from the electrolyte to the electrode, or negative charges pass the phase boundary in the opposite direction. An anodic current causes an anodic electrode reaction while a cathodic current causes a cathodic one.

When a current flows in a cell, one electrode becomes the anode and other one the cathode. Thus, anodic and cathodic electrode reactions take place simultaneously in the cell.

By definition, the anodic current (in Ampere) and the anodic current density (in Ampere/cm<sup>2</sup>) are positive while the cathodic current and cathodic current density are negative.

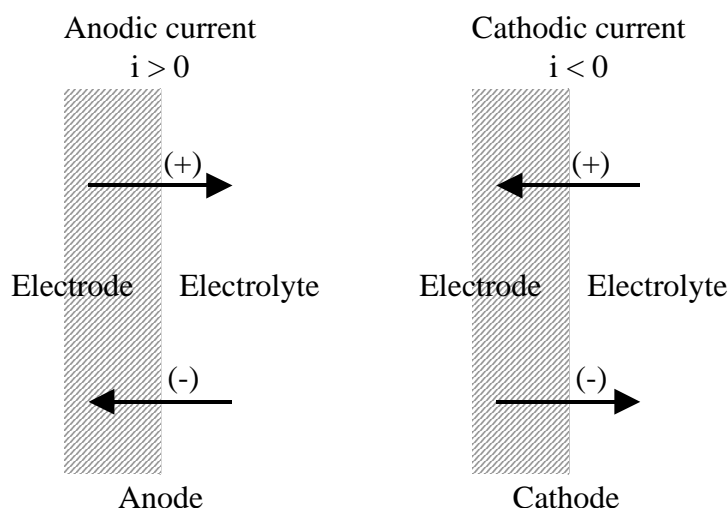


Figure 20: Definition of anodic and cathodic currents with indication of their sign [21]

### 1.5.2.3 Faraday' Law of Electrolysis

The part of the current that follows the Faraday's law corresponds to the reaction rate of system evolution compared to the initial state: it characterizes the material quantity that is transformed.

Faraday's Law [21]: (1) the amount of chemical change produced by electrolysis (any reaction that involves the charge transfer across an electrode interface) is proportional to the total amount of charge passed through the cell; (2) the amount of chemical change produced is proportional to the equivalent weight of the substance undergoing chemical change. In other words, the amount of substance consumed or produced at one of the electrodes in an electrolytic cell is directly proportional to the amount of electricity that passes through the cell.

If the reaction is at the electrode surface (cf. Figure 17), the amount of chemical change is usually expressed as weight of the deposit, and Faraday's Law may conveniently be summarized by the following formula:

$$m = \frac{M.I.t}{n.F} \quad (16)$$

$m$  : weight of the deposit [g]

$M$  : atomic weight of the substance, which is being electrodeposited [g.mol<sup>-1</sup>]

$I$  : current [A]

$t$  : elapsed time [s]

$n$  : number of charges involved in the reaction

It is thus the total charge passed and  $M/n$  is the equivalent weight.

$F$  : Faraday constant. Inspection of Eq. (16) shows that  $F$  must be equal to the charge contained in one equivalent weight,  $F = 96,500$  coulombs<sup>1</sup>/equivalent weight (based on the chemical scale of atomic weights<sup>2</sup>).

The equation  $F = N_L e_0$  describes the relationship between the Avogadro number  $N_L$ , the elementary charge  $e_0$ , and one Faraday. Thus, one faraday is the total charge of “one mole of elementary charges” [21].

Applying the Faraday’ law, each discharged Ah (equivalent to a quantity of 3600 Coulombs) consumes 3.660g of  $H_2SO_4$ , 3.865g of Pb and 4.462g of  $PbO_2$  [15]. During charging, it is inversed (3.660g of  $H_2SO_4$  is consumed) except beyond the moment where the charge is finished; such a case concerns the *overcharge*.

#### 1.5.2.4 Faraday efficiency

When the Faraday’s law is tested experimentally, apparent deviations are frequently found. *Faraday efficiency* is defined as the percent of the total charge, which is effective in carrying out the desired reaction.

$$r_{\text{Faraday}} = \frac{m_{\text{real}}}{m_{\text{Faraday}}} \quad (17)$$

$r_{\text{Faraday}}$  : faraday efficiency

$m_{\text{real}}$  : real experimental weight obtained

$m_{\text{Faraday}}$ : calculated weight obtained by Faraday’s law

A common cause to explain efficiencies less than 100% is the occurrence of side reactions during the electrolysis. For instance, in the lead acid cell, as shown in Pourbaix diagram (cf. 1.3.1), the water electrolysis (which produces oxygen and hydrogen) occurs simultaneously with the discharge-charge reaction.

Other causes that bring to lower efficiencies are the recombination of the product of electrolysis, the dissolution of the electrodes and reactions of the primary products of electrolysis with the solvent, electrodes, or environment.

All of these effects tend to lower the amount of the desired product and thus lower the efficiency from 100%. In this thesis, we deal only with the occurrence of water electrolysis and oxygen recombination.

---

<sup>1</sup> 1 Coulombs = 1 A.s

<sup>2</sup> Since 1961, the unified atomic mass unit is equal to one-twelfth of the mass of a carbon-12 atom.

The definition of the faradic efficiency related to the weight is difficult to use because the weight of the products cannot always be measured. Generally, this definition is rewritten in terms of electrical quantities. The electrical efficiency is defined as the ratio between the electrical quantity involved in productive reactions (active material charge) ( $Q_{CH}$ ) and the total electrical quantity that is supplied ( $Q_{CHsup}$ ).

$$r_{Faraday} = \frac{Q_{CH}}{Q_{CHsup}} \quad (18)$$

In practice, the faraday efficiency of a charge/discharge cycle can be defined as the ratio of the electrical quantity given by lead acid cell during a discharge ( $Q_{DCH}$ ) and the electrical quantity provided to the cell during a charge ( $Q_{CHsup}$ ).

$$r_{Faraday} = \frac{Q_{DCH}}{Q_{CHsup}} \quad (19)$$

### 1.5.3 Principal steps of an electrochemical reaction [1, 18]

Reactions which occur at electrodes includes:

- The deposition of metals:  $Pb^{2+} + 2e^- \rightarrow Pb$
- The evolution of gases:  $2H^+ + 2e^- \rightarrow H_2$   
 $2O^{2-} \rightarrow O_2 + 4e^-$
- The deposition of solid salts:  $Pb + SO_4^{2-} \rightarrow PbSO_4 + 2e^-$
- Electron transfer reactions:  $Pb^{4+} + 2e^- \rightarrow Pb^{2+}$
- Oxidation-reduction reactions:  $Pb + PbO_2 + 2HSO_4^- + 2H_3O^+ \rightleftharpoons 2PbSO_4 + 4H_2O$

Electrode reactions may take place in a number of steps, which include the follows:

- Charge transfer
- Mass transport: diffusion and migration
- Chemical reaction
- Crystallization

#### 1.5.3.1 Charge transfer (Electron transfer)

At the charge transfer reaction, charge is transferred across the interface (across the electrical double layer).

At a redox electrode (e.g. the negative electrode of lead acid cell), electrons are simultaneously accepted and donated by the Pb at the same surface, as illustrated by the arrows in Figure 21. The lengths of the arrows represent the magnitude of the charge crossing the phase boundary in either direction per unit area and unit time. Hence, the lengths of the arrows correspond to the densities of the two currents flowing in opposite directions, i.e. the anodic partial current density  $i_+$  and the cathodic partial current density  $i_-$ . Since the anodic and cathodic current densities  $i_+$  and  $i_-$  are positive and negative quantities (cf. 1.5.2.2) respectively, the total current density through the double layer is:

$$i = i_+ + i_- \quad (20)$$

In the charge transfer reaction, taking place on the negative electrode, the reduced Pb species is oxidized into  $\text{Pb}^{2+}$  species by donating two electrons to the inert electrode metal ( $\text{Pb} \rightarrow \text{Pb}^{2+} + 2\text{e}^-$ , anodic direction). Conversely, the charge transfer reaction in a cathodic direction involves transfer of two electrons from the metal to the oxidized species  $\text{Pb}^{2+}$ , which is reduced to Pb ( $\text{Pb}^{2+} + 2\text{e}^- \rightarrow \text{Pb}$ ).

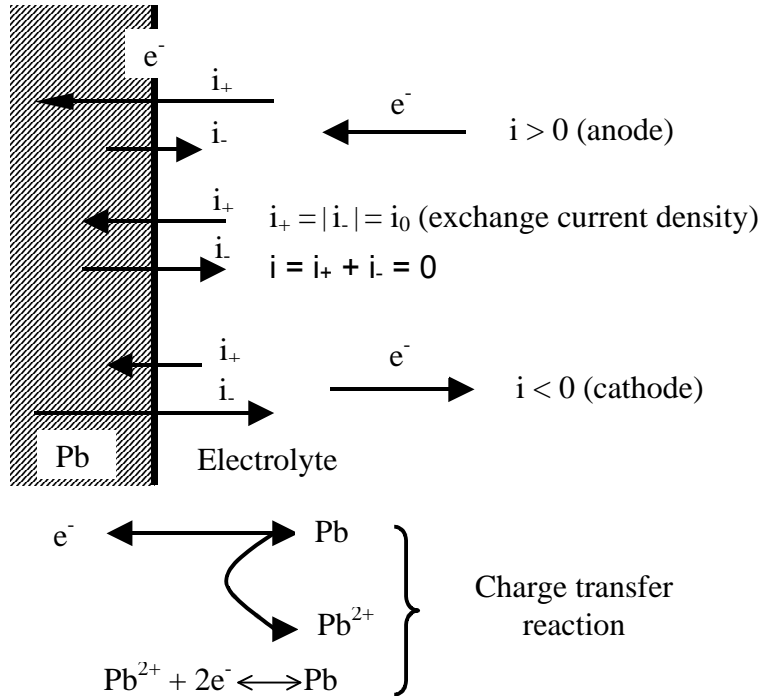


Figure 21:

Charge transfer reactions at negative electrode [21]

The charge transfer reaction is of fundamental importance in electrochemical kinetics, since it is the only reaction directly affected by the electrode potential. The effect of other variables on the potential is only indirect because these variables can influence the charge transfer reaction.

#### 1.5.3.2 Reactant transport (mass transport): diffusion and migration

The transport of reactants to and from the interface occurs in two ways: diffusion thanks to concentration gradient and migration, which is the movement of ions under the electric field. The following equation represents the mass transfer:

$$N_j = \frac{i_j}{nF} = -D_j \frac{\partial c_j}{\partial \xi} + \frac{i_j t_j}{z_j F} \quad (21)$$

$N_j$  : flux of species j [mol.cm<sup>-2</sup>.s<sup>-1</sup>]

$i_j/nF$  : current equivalent

$\partial c_j / \partial \xi$  : concentration gradient [mol.cm<sup>-4</sup>]

$D$  : diffusion coefficient [cm<sup>2</sup>.s<sup>-1</sup>]

$t_j$  : transference number

$z_j$  : valence number (charges par ion j)

$\xi$  : diffusion direction [cm]

In Eq. (21), the first addend  $\left(-D_j \frac{\partial c_j}{\partial \xi}\right)$  relates to the reactant transfer by diffusion and the second  $\left(\frac{i_{t,j}}{z_j \cdot F}\right)$  by migration.

### **Diffusion**

The first law of Fick describes the basic relation for one-dimensional diffusion:

$$dn = -D \cdot f \cdot \frac{dc}{dx} dt \quad (22)$$

$n$  : number of moles, which are transferred

$f$  : section where the reactants pass through by diffusion [cm<sup>2</sup>]

$dc/dx$  : concentration gradient [mole/cm<sup>3</sup> par cm]

$dt$  : period of time [s]

The diffusion depends on the concentration gradient. In the first addend of Eq. (21), the diffusion corresponds to an equivalent current and we can write:

$$\frac{i_{j,D}}{nF} = D_j \frac{c_j - c_{j,o}}{d} \text{ or } i_{j,D} = \frac{nFD_j}{d} (c_j - c_{j,o}) \quad (23)$$

$c_j - c_{j,o}$  : (negative) concentration gradient of species j

$d$  : thickness of the diffusion layer

### **Migration**

The second addend in Eq. (21) relates to the movement of ions under the electric field influence. This transport corresponds to an electric current, called *migration*, which creates concentration gradients.

The transference number in Eq. (21) announces the share of the total current that is carried by the corresponding ionic species. In a binary electrolyte, dissociated into A<sup>+</sup> and B<sup>-</sup>, the transference number are connected by the relation:

$$t_+ + t_- = 1 \quad (24)$$

The transference number depends on the ion concentration and on the temperature. For sulfuric acid in diluted solutions as well as electrolytes used in lead acid batteries, the transference numbers are:

$$t_+ = t_{H^+} = 0.9$$

$$t_- = t_{HSO_4^-} = 0.1$$

Therefore, in this sulfuric acid solution, 90% of the ionic current is carried by protons ( $H^+$ ) and only 10% by negative ions ( $HSO_4^-$ ).

### 1.5.3.3 Chemical reactions, forming reactions: nucleation and crystal growth

Chemical reactions, where the ions of opposite signs get together to form new products, precede or follow the charge transfer reaction. They may occur in the bulk of the electrolyte or at the interface only.

The crystal or nucleation reaction is the reaction in which metal atoms, deposited on the surface during the course of the charge transfer reaction, are included or released into or from the ordered lattice of the solid metal electrode.

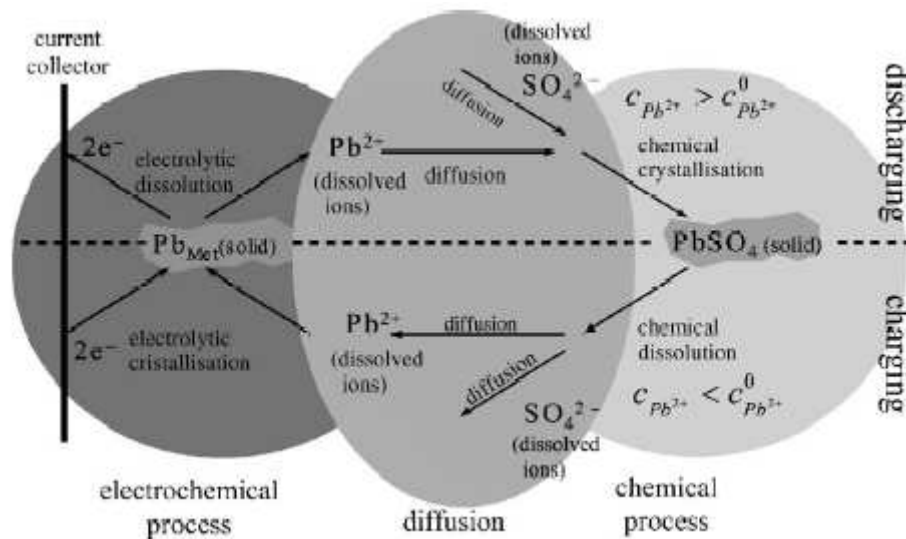


Figure 22: Schematic presentation of discharge-charge process in lead acid battery using negative electrode as example: charge transfer, mass transport (diffusion), chemical reaction, crystallization and dissolution. [2]

Figure 22 results schematically the electrochemical reaction, diffusion and chemical reaction during discharge-charge process of the lead acid negative electrode.

During discharging, the Pb metal dissolves and gives two electrons to the grid and becoming a  $Pb^{2+}$  ion (dissolution, charge transfer). As the concentration of  $Pb^{2+}$  ions increases gradually at the grid surface, they move therefore toward the electrolyte bulk and meet the  $SO_4^{2-}$  ions, which are at the same time attracted from the electrolyte bulk toward the electrode porous volumes where their concentration is weaker (diffusion). These ions of opposite signs react to form  $PbSO_4$  crystals (chemical reactions, crystallization).

During charging, the process is the same but in the opposite direction.



## 1.5.4 Electrode kinetics - Polarization, overvoltage notions [21]

### 1.5.4.1 Electrode kinetics

One task of electrode kinetics is to explain the sequence of partial reactions constituting the overall electrode reaction, which can be determined by chemical analysis. Another task is to determine rates of electrode reaction, which according to Faraday's law are proportional to the current density  $i$ . The dependence of the current density, or of the reaction rate on the electrode potential  $E$ , on the concentrations  $c_j$  of reactants  $S_j$  and on other variables (like the temperature) must be determined in order to solve the two foregoing problems.

Valuable information about partial reactions can be obtained especially from the dependence of the total current density  $I$  on electrode potential  $E$  and concentration  $c_j$ . The total current density  $i$  is the sum of the positive anodic partial current density  $i_+$  ( $> 0$ ) and the negative cathodic partial current density  $i_-$  ( $< 0$ ). Dependence of the current on potential and concentration is primarily governed by the coefficient  $\alpha$ , the electrochemical reaction orders  $z_{0,j}$ ,  $z_{r,j}$ , limiting diffusion current densities  $i_d$ , limiting reaction current densities  $I_r$ , the stoichiometric factors  $\nu_j$ , the electrode reaction valence  $n$ , and the transfer valence  $z$ .

In electrode kinetics, as in chemical reaction kinetics, the slowest partial reaction is the rate-determining of the total reaction. The magnitudes and type of overvoltage is therefore governed by the slowest partial reaction.

### 1.5.4.2 Polarization and overvoltage notions

When current flows through an electrode, its potential  $E(i)$  assumes a value different from that in the absence of current  $E(0)$ . As introduced in 1.4.2, the zero current potential  $E(0)$ , will be the  $E_0$ . However, in the case of lead acid electrode, besides the discharge-charge reactions, there are always secondary or parasite reactions (cf. 1.3). The zero current potential of lead acid electrode does not correspond exactly to the equilibrium potential  $E_0$  of only the charge-discharge reaction, but it is a mixed potential of principal discharge-charge reactions and secondary reactions. Therefore, there are two definition of the deviation of the electrode potential  $E(i)$  from the potential in absence of the current flow ( $E(0)$ )

- The deviation of the electrode potential  $E(i)$  at the current  $i$  from the equilibrium potential of the discharge-charge reaction  $E_0$  is called *overvoltage*
- The deviation of the electrode potential  $E(i)$  at the current  $i$  from the zero current potential of lead acid electrode,  $E(0)$ , is called *polarization*.

$$\eta = E(i) - E_0 = \text{overvoltage} \quad (25)$$

$$\eta = E(i) - E(0) = \text{polarization} \quad (26)$$

Since an overall electrochemical reaction consists of many steps (cf.1.5.3), different types of correspondent overvoltage/polarization are defined: charge transfer or activation overvoltage  $\eta_a$  for charge transfer reaction, diffusion overvoltage  $\eta_d$  for mass transport by diffusion reaction, reaction overvoltage  $\eta_r$  for chemical reaction, crystallization overvoltage  $\eta_{cr}$  for forming reaction. Furthermore the ohm drop causes also an overvoltage, called resistance overvoltage  $\eta_\Omega$ .

The overall overvoltage is the sum of all overvoltages above:

$$\eta = \eta_a + \eta_c + \eta_r + \eta_{cr} + \eta_{\Omega} \quad (27)$$

According to the four types of overvoltage (not including resistance overvoltage), there are four possible types of rate-control or rate-determining.

#### 1.5.4.3 Activation overvoltage (or charge transfer overvoltage) $\eta_a$

Hindrance of the charge transfer reaction across the electrical double layer causes the formation of charge transfer overvoltage  $\eta_a$ .

The electrical double layer, which forms on the surface of the electrode, acts somewhat as a capacitor, and, before the electrochemical reaction can start, some energy is needed to overcome this energy barrier, known as the activation energy  $\Delta G_A$ .

According to Eq. (6), a change of the electrode potential,  $E$ , results in a change of the free energy of reaction by  $nFE$  per mole of reactants. Thus the free energy of the cathodic reaction is changed by  $\alpha nFE$ , while that for the anodic reaction is changed by  $(1-\alpha)nFE$ , where  $\alpha$  is a fraction, called *transfer coefficient* of the cathodic charge. The transfer coefficient  $\alpha$  denotes how “symmetrically” the reaction and its reversal depend on electrode potential (usually  $\alpha$  is about 0.5).

The rate constant of a reaction,  $k$ , is proportional to  $\exp(-\Delta G_A/RT)$  according to Arrhenius equation [1] so that:

The rate constant of anodic reaction is  $k_+ \exp(\alpha nFE/RT)$ .

The rate constant of cathodic reaction is  $k_- \exp[-(1-\alpha)nFE/RT]$ .

The rate of the reverse reaction is:

$$i = i_+ + i_- = k_+ c_{\text{red}} \exp\left(\frac{\alpha nFE}{RT}\right) - k_- c_{\text{ox}} \exp\left(-\frac{(1-\alpha)nFE}{RT}\right) \quad (28)$$

$i, i_+, i_-$  : currents per unit area of the electrode (anodic and cathodic electrodes)

$c_{\text{red}}, c_{\text{ox}}$  : concentrations of the reactants at the electrode surface (reducer and oxidant)

$k, k_+, k_-$  : rate constants at the potential from which  $E$  is measured.

To avoid the term  $k$  that depends on some potential from which  $E$  is measured, it is useful to use the value of the equilibrium potential  $E_0$ . Although there is no net reaction ( $i = 0$ ), the equilibrium is of course dynamic, the rate of the anodic and cathodic reactions being equal (cf. 1.4.2). The equal rates are expressed by the exchange current. At equilibrium  $E = E_0$ , the reactant concentrations are equal to those in the bulk of solution, the currents in both directions are equal:  $i_+(0) = -i_-(0) = i_0$ , so we can write:

$$i_+ = k_+ c_{\text{red}} \exp\left(\frac{\alpha nF}{RT} E\right), i_- = -k_- c_{\text{ox}} \exp\left(-\frac{(1-\alpha)nF}{RT} E\right) \quad (29)$$

$$i_0 = i_+(0) = k_+ c_{\text{red}} \exp\left(\frac{\alpha nF}{RT} E_0\right), -i_0 = i_-(0) = -k_- c_{\text{ox}} \exp\left(-\frac{(1-\alpha)nF}{RT} E_0\right) \quad (30)$$

Where  $i_0$  is called *exchange current density* that characterizes the dynamic equilibrium. It is an important kinetic parameter. High exchange current density means that the equilibrium potential is rather stable, while low exchange current density indicates that the electrode potential will be polarized even when a quite small current flows through the electrode. In lead acid electrode, the exchange current density of the charge reaction is in the order of  $10^{-5} \text{ A.cm}^{-2}$ , while the exchange current density for hydrogen evolution is in the order of  $10^{-13} \text{ A.cm}^{-2}$ .

Combining Eq. (29) and Eq. (30), the *Butler-Volmer* equations are obtained:

$$i = i_0 \left[ \exp\left(\frac{\alpha n F}{RT} (E - E^0)\right) - \exp\left(-\frac{(1-\alpha) n F}{RT} (E - E^0)\right) \right] \text{ or} \quad (31)$$

$$i = i_0 \left[ \exp\left(\frac{\alpha n F}{RT} \eta_a\right) - \exp\left(-\frac{(1-\alpha) n F}{RT} \eta_a\right) \right]$$

Eq. (31) describes the current/voltage curve (cf. [1], p. 239).

The voltage deviation from equilibrium  $E - E_0 = \eta_a$  is *activation overvoltage*.

This double exponential form of the current-voltage reaction Eq. (31) is characteristic of simple electrochemical reactions. It has two useful limiting forms:

- When  $|i| \gg i_0$  (or  $|\eta_a| \gg RT/nF$ ), one of the exponential may be neglected depending on the sign of the current and the overvoltage is proportional to  $\log|i|$ . This was observed experimentally by Tafel in 1905 and the plot of  $\eta_a$  against  $\log|i|$  is called *Tafel line*. The following expressions are obtained for the anodic and cathodic current densities:

$$i = i_0 \exp\left(\frac{\alpha n F}{RT} \eta_a\right) \text{ and } \eta_a = -\frac{RT}{\alpha n F} \ln i_0 + \frac{RT}{\alpha n F} \ln i = a + b \log i \text{ or} \quad (32)$$

$$i = -i_0 \exp\left(-\frac{(1-\alpha) n F}{RT} \eta_a\right) \text{ and } \eta_a = \frac{RT}{(1-\alpha) n F} \ln i_0 - \frac{RT}{(1-\alpha) n F} \ln |i| = a + b \log |i|$$

Thus, at high overvoltage, a linear relationship exists between the charge-transfer overvoltage and the logarithm of the current density  $\ln|i|$  or  $\log|i|$ . Eqs. (32) are known as *Tafel equations*. By extending the Tafel lines to the equilibrium potential  $\eta_a = 0$ , one obtains the exchange current density  $i_0$ . The value of the transfer coefficient  $\alpha$  is obtained from the slope of the line, which corresponds to the value  $b$  in Eqs. (32).

- When  $|i| \leq i_0$  the exponentials may be expanded and terms is higher than the second which is neglected:  $i = i_0 n F \eta / RT$ . Since the current is now a linear function of the overvoltage, the electrode behaves as a simple or “ohm” resistance.

At constant temperature and current density, the value of the activation overvoltage is small for most solid electrode systems, but accounts for the small drop in voltage immediately when the current is switched on (*coup de fouet* phenomenon [25]).

#### 1.5.4.4 Diffusion overvoltage $\eta_d$

Diffusion overvoltage appears when the supply of reactants at the electrode or the removal of the reaction products is rate-determining of the reaction. The condition for the appearance of pure diffusion overvoltage is that all chemical processes, including the crystallization processes and also the charge transfer reaction are in equilibrium. It indicates that in this case the calculation of the potential of an electrode with a flow of current is possible with the aid of the Nernst equation for equilibrium potential. However, the concentrations of the components directly at the surface must be used and not those in the interior of the electrolyte.

Therefore, the diffusion overvoltage  $\eta_d$  is equal to the difference between the equilibrium potential  $E_0$  in absence of current flow and the equilibrium potential  $E_0(i)$  which form during current flow as a result of the changed concentration  $c_j$  of the component  $S_j$  directly adjacent to the surface, in accordance with the Nernst equation (cf. Eq.(10)).

$$\eta_d = E_0(i) - E_0 = E_{0, \text{standard}} + \frac{RT}{nF} \ln(c_j) - E_{0, \text{standard}} - \frac{RT}{nF} \ln(c_j^0)$$

$$\eta_d = \frac{RT}{nF} \ln \left( \frac{c_j}{c_j^0} \right) \quad (33)$$

$c_j^0$  : concentration of the component  $S_j$  at equilibrium, which is a function of the temperature and the concentration of sulfuric acid.

$c_j$  : actual concentration of the component  $S_j$

Diffusion can limit the reaction rate when the mass transport precedes the charge transfer step. Within a very strong current, the concentration  $c_j$  tends to zero at the electrode surface, meaning that all ions and molecules arriving by diffusion are charged or discharged immediately and thus lose their charges. Eq. (33) assumes that  $\eta_d$  has to be close to  $-\infty$  so that the exponential can be neglected. It is thus not possible to increase the current in increasing the voltage. As a result, the current cannot exceed a certain value, called limiting diffusion current  $i_{lim}$ , which is obtained from Eq. (23) at  $c_j = 0$ .

$$i_{lim,j} = -\frac{nFD_j}{d} c_{j0} = k c_{j0} \quad (34)$$

As  $k$  is a constant, the limiting diffusion current does not depend on applied voltage and the Ohm law does not apply anymore.

Combining Eq. (23) and Eq. (34) results in:

$$\frac{i}{i_{lim}} = -\frac{c - c_0}{c_0} = 1 - \frac{c}{c_0} \quad \text{or} \quad \frac{c}{c_0} = 1 - \frac{i}{i_{lim}} \quad (35)$$

$$\eta_d = \frac{RT}{nF} \ln\left(\frac{c}{c_0}\right) = \frac{RT}{nF} \ln\left(1 - \frac{i}{i_{\text{lim}}}\right)$$

$$\eta_d = \frac{RT}{nF} \ln\left(\frac{kc_0 - i}{kc_0}\right) \quad (36)$$

Eq. (36) shows that at a given current value, the diffusion polarization can be observed when the concentration at equilibrium  $c_0$  is weak and it is lower when there is an increase of  $c_0$ . The diffusion polarization can be diminished as well by increasing the constant  $k = -nFD/d$  ( $i = \frac{nFD}{d}(c - c_0)$ , cf. Eq. (23)), so decreasing  $d$  (vigorous agitation) or by increasing the electrode cross-section  $q$  ( $i = I/q$ ). Like the diffusion current, the diffusion polarization does not depend on the potential.

The definition of the diffusion overvoltage is equivalent to that of the concentration overvoltage, which relates to all types of concentration changes. Thus the concentration overvoltage is the sum of the diffusion and the reaction overvoltage.

Figure 23 and Figure 24 illustrate schematically how concentration polarization operates during the discharge of the lead acid electrode (cf. Reaction 2).

As soon as the charge transfer reaction starts, the concentration of ions reacting with the electrode falls rapidly at a rate dependent on the current in its immediate vicinity and decreases less as the distance increases. The electrode potential falls by an amount defined by the Nernst equation. Migration and diffusion processes operate to reduce the concentration gradients by mass transport of the reactants.

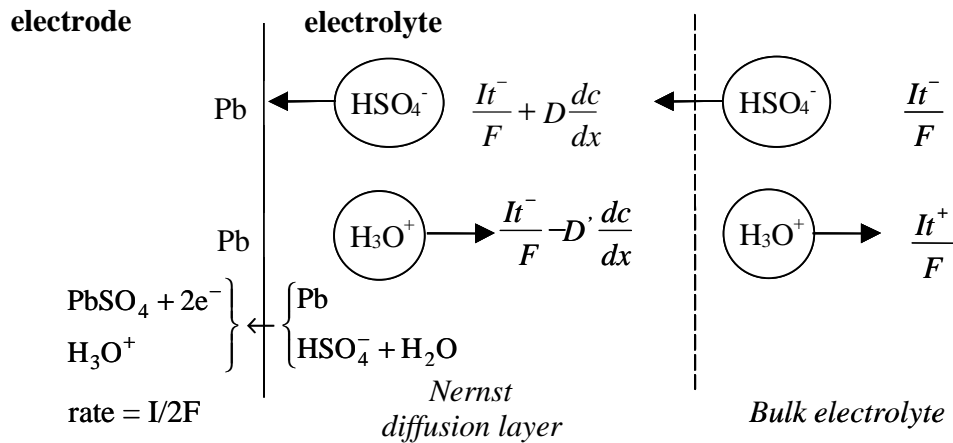


Figure 23: Concentration polarization during discharging at negative electrode [26]

$\text{HSO}_4^-$  ions are removed at the electrode surface at a rate equal to  $I/2F$  moles/s and replenished from the bulk electrolyte at  $It^-/F$  moles/s while protons in form of  $\text{H}_3\text{O}^+$  move into the bulk electrolyte at a rate  $It^+/F$  moles/s (cf. 2<sup>o</sup> term of Eq. (21): migration).  $t^+$  and  $t^-$  are the transport numbers of  $\text{HSO}_4^-$  and  $\text{H}_3\text{O}^+$  ions respectively.

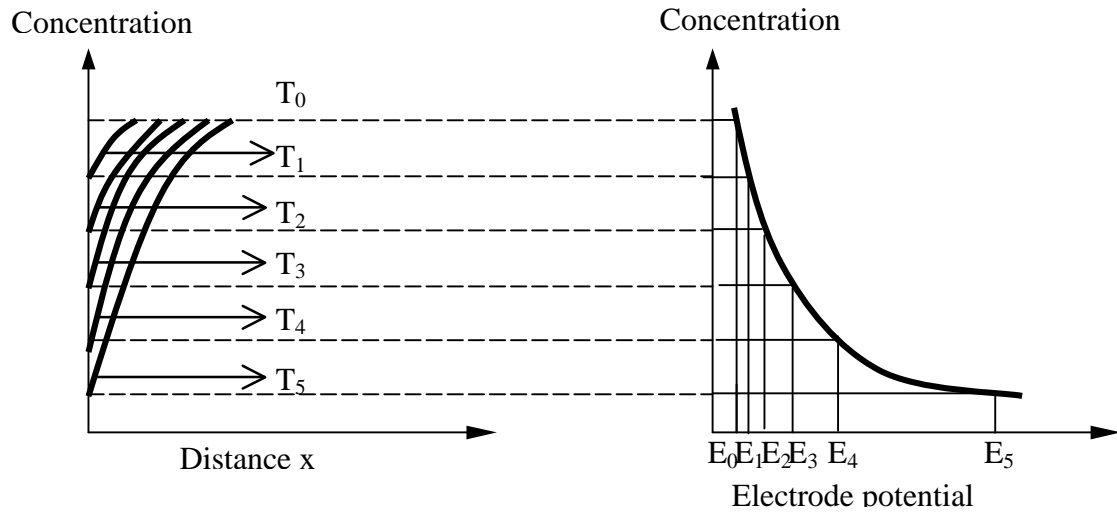


Figure 24: Electrode potentials ( $E_0$  to  $E_5$ ) with corresponding times ( $T_0$  to  $T_5$ ) vs. concentration [26]

The concentration gradients in the diffusion layer accelerate the diffusion of  $\text{HSO}_4^-$  ions by amounts equal to  $D \cdot dc/dx$  but retard the diffusion of  $\text{H}_3\text{O}^+$  ions by amounts equal to  $D' \cdot dc/dx$ , where  $D$  and  $D'$  are the diffusion constants and  $dc/dx$  is the evolution of the concentration  $c$  at a distance  $x$  from the surface (cf. 1<sup>st</sup> term of Eq. (21): diffusion). Figure 24 shows how changes in the concentration (which occur in the vicinity of the electrode at time  $T_0$  to  $T_5$  from the outset of the discharge) affect the electrode potential, as defined by the expression

$$E = E_0 - \frac{RT}{nF} \ln c.$$

A similar model can be drawn for the  $\text{PbO}_2$  positive electrode, although this is more complex. In this case, the formation of  $\text{H}_2\text{O}$ , as indicated by Reaction 3, causes further dilution of the electrolyte in the diffusion layer.

#### 1.5.4.5 Reaction overvoltage $\eta_r$

The reaction overvoltage  $\eta_r$  is a phenomenon resulting from the existence of a slow (rate-determining) chemical step on the overall electrode reaction.  $\eta_r$  appears separately when the other component steps of the overall reaction, such as the charge transfer and diffusion of the substances, are not the rate-determining. By definition, this chemical step is a reaction whose rate constant does not depend on the electrode potential.

If only the reaction overvoltage occurs, the charge transfer equilibrium for the transfer of the charge carriers through the double layer must remain undisturbed during the flow of current, even though an electrochemical reaction takes place. The charge transfer equilibrium remains undisturbed during the flow of current only when the exchange current density  $i_0$  is infinitely high or the external current density  $i$  is very small compared to  $i_0$  ( $i \ll i_0$ ), so the deviations of the charge transfer equilibrium are negligibly small (cf. 1.5.4.3).

According to Vetter [21], from the general definition of overvoltage, the reaction overvoltage can be defined by:

$$\eta_r = v \frac{RT}{nF} \ln \left( \frac{a(i)}{a^0} \right) \quad (37)$$

In which:

$v$  : stoichiometric factor of the substance  $S$  in the partial electrode reaction, which is positive when  $S$  is an oxidized component of the partial electrode reaction and negative when  $S$  is a reduced component of the reaction

$n$  : electrode reaction valence (mole number of charges involved in the reaction).

$a(i)$  : activity of the substance  $S$ , which is a function of the current density because of the slow rate-determining chemical step.

$a^0$  : activity of the substance  $S$  at equilibrium.

#### 1.5.4.6 Crystallization overvoltage $\eta_{cr}$

With metal/metal ion electrodes, overvoltage is observed and it is due not only to transport and to reaction, but also to crystallization. According to Stranski's theory of crystal growth, each metallic ion deposited must first find its way to a suitable site at the edge of a lattice plane before it can be accepted into the lattice. Crystallization overvoltage is caused by a hindrance in the inclusion or the release of the "ad-atoms" into and from, respectively, the ordered lattice of the solid metal electrode. The ad-atoms on the metal surface in the state of metallic bond are metal ions in the state in which they are deposited on the surface during the course of cathodic charge transfer reaction. The ad-atoms are the reduced species  $S_M$  of the charge transfer reaction at the surface concentration  $c_M$  (or activity  $a_M$ ) (cf. 1.5.4.3).

The crystallization overvoltage is defined so that it occurs alone only when all other processes, such as charge transfer, diffusion and chemical reaction in the electrolyte are in thermodynamic equilibrium<sup>1</sup> even during the current flow. Hence, for the calculation of the overvoltage, the Nernst equation can be applied to the activities of the ad-atoms, in the case of equilibrium,  $a_M^0$ , and during the flow of current,  $a_M$ . In accordance with the general definition of overvoltage, the crystallization overvoltage  $\eta_{cr}$  equals the difference between the two potentials:

$$E - E^0 = \eta_{cr} = - \frac{RT}{nF} \ln \left( \frac{a_M}{a_M^0} \right) \quad (38)$$

$v_M$  : = -1 for ad-atom ( $S_M$  is a reduced specie)

$n$  : ion metal valence

#### 1.5.4.7 Ohm overvoltage or resistance overvoltage $\eta_\Omega$

Resistance polarization was studied in detail by Vetter in [21]. In brief, resistance polarization or ohm polarization drop consists of three factors:

- Resistance polarization due to electrolyte resistance

---

<sup>1</sup> The necessary deviation from equilibrium during the flow of current will be assumed to be so small that this influence cannot be observed experimentally.

- Resistance polarization of surface films
- Resistance polarization as a result of the current-dependent resistance of the diffusion layer.

Barak [26] explained these phenomena in the galvanic lead acid cell as follows:

During discharging, the concentration of the electrolyte falls steadily with a corresponding increase in electrical resistance. As show in Table 3, this amounts to over 60% for a fall in SG from 1.250 to 1.070. The high resistance of  $\text{PbSO}_4$  puts it almost in the category of a non-conductor and the combined effect of these two factors adds another vector to the polarization of the cell. It is interesting to note that the resistivity of massive  $\text{PbO}_2$  is ten times higher than that of metallic lead, but less than that of storage battery electrolyte by a factor of  $10^4$ .

Problems of mass transport, caused by restricted diffusion, are mainly responsible for the low coefficients of use of both positive and negative active materials. To limit the polarization, these materials are prepared in a highly porous state. The average pore size is, however, small and the channels for circulation of the electrolyte are tortuous, presenting additional obstacles to diffusion. For this reason, plate thicknesses are kept as low as possible, particularly where discharges at high rates are often needed.

As the discharge proceeds, the particles of active material become isolated from one another and also from the current-collecting grids by films of lead sulfate. The molecular volume of the  $\text{PbSO}_4$  is appreciably higher than that of either the  $\text{PbO}_2$  or the Pb, from which it is formed and the porosity of the active material falls steadily during the discharge. There is, however, a practical limit to the porosity of the active materials, which must retain electrical contact between particles and sufficient mechanical strength to prevent disruption by dimensional changes, leading to premature shedding and loss of capacity.

Table 3: Specific resistivity and density at 20°C [26]

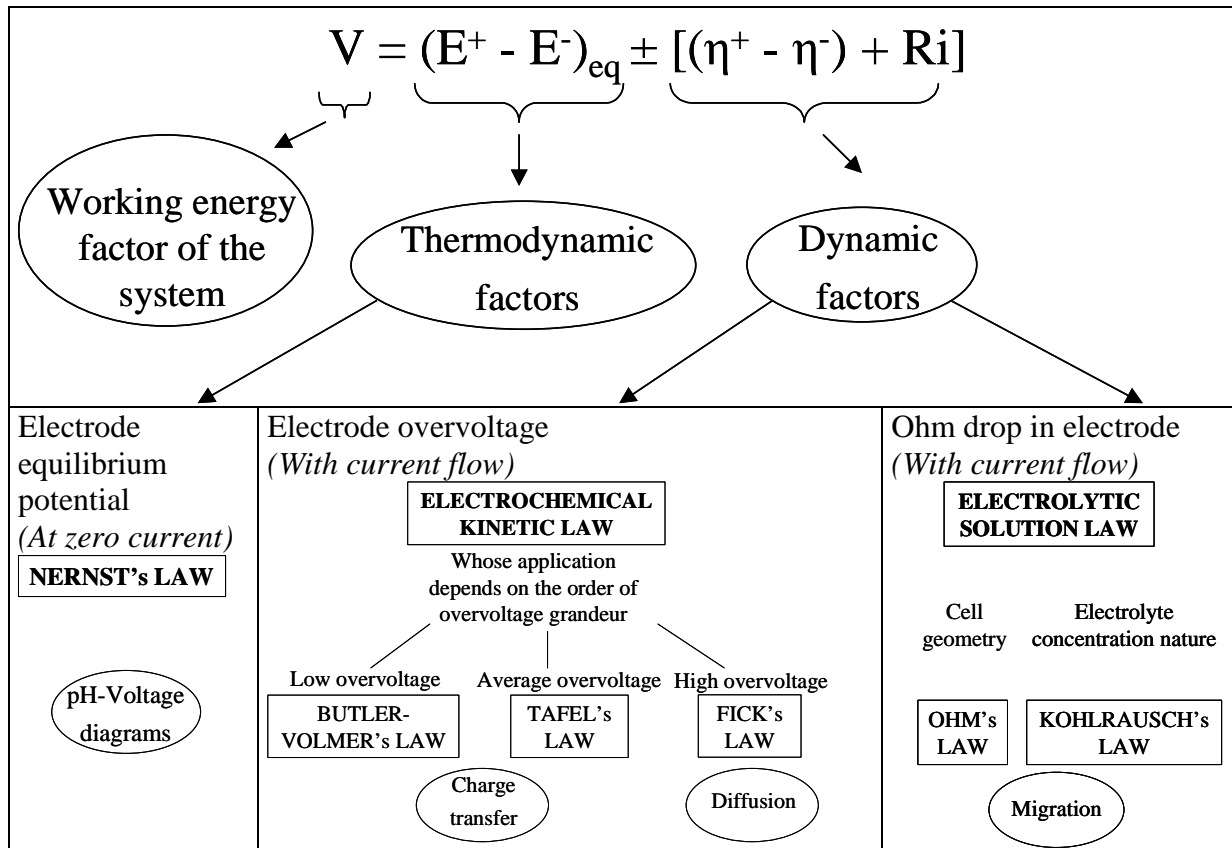
		Specific resistivity ( $\Omega\text{cm}$ )	Density (g/ml)
$\text{PbO}_2$	Massive	$2 \times 10^{-4}$	9.4
	Porous active material	$74 \times 10^{-4}$	
Pb	Dense metal	$0.2 \times 10^{-4}$	11.3
$\text{H}_2\text{SO}_4$ solution	SG 1.250 or 4.3molar	1.230	1.250
	1.070 or 1.1 molar	2.000	1.070
$\text{PbSO}_4$	-	$0.3 \times 10^{10}$	6.3

### 1.5.5 Voltage at the terminals of an electrochemical cell

The table below resumes all factors that relate to the voltage at two terminals of an electrochemical cell with current flows (during charging or discharging).



Table 4: Expression of voltage at two terminals of an electrochemical cell when a current flows [27]



### 1.5.6 Current-related heat effects (the Joule effect) [1]

Current flow through any conducting object generates a heat that is proportional to the voltage drop caused by the current itself according to:

$$dQ_{\text{Joule}}/dt = \Delta E \cdot i \quad (39)$$

In which:

$Q_{\text{Joule}}$  : generated heat (Joule effect) [J]

$t$  : time [s]

$\Delta E$  : voltage drop caused by the current [V]

$i$  : current as a function of time [A]

This heat is called the Joule effect; it always means loss of energy. The negative absolute value should be used in Eq. (39) for consistency with the arithmetical sign of the thermodynamic parameters (lost energy always has the negative sign).

In an electrochemical cell, the voltage drop caused by the current consists in the difference between the cell voltage under current flows  $V$  and the open-circuit cell voltage  $E$ . Eq. (39) becomes:

$$dQ_{\text{Joule}}/dt = (V - E).i \quad (40)$$

Eq. (40) describes a composite parameter of

- the “genuine” Joule effect  $dQ/dt = i^2R$ , which describes the heat generation by the current flow  $i$  through the ohm resistance  $R$  of the conducting elements and the electrolyte, and
- the irreversible heat effect  $T \cdot \Delta S_{\text{irreversible}}$ , which causes voltage drops between the electrode surface and the electrolyte on account of reaction hindrance. This additional heat is caused by additional entropy of reaction  $\Delta S_{\text{irreversible}}$ , which cannot be compensated when the reaction is reversed.

Both effects, however, cannot be separated in the electrochemical cells in normal conditions. For this reason, the sum of both is usually called the Joule effect.

The difference  $V - E$ , when measured as cell-voltage deviation, includes the overvoltage and ohm drops shown in Table 4. In general:

**Polarization = overvoltage + ohm voltage drops**

The Joule effect can be described as the energy generated per unit of time:

$$dQ_{\text{Joule}}/dt = (V - E).i \quad [\text{W}] \quad (40)$$

Or in its integrated form for a period ( $t$  in hours)

$$Q_{\text{Joule}} = \int_0^t \{(V - E).i\} dt \quad [\text{Wh}] \quad (41)$$

## 1.6 CAPACITY OF LEAD ACID BATTERY [1, 25]

### 1.6.1 Capacity

The energy that the battery delivers during a discharge is described as the *capacity* generally in Ampere – hour (Ah). The energy output of a battery is defined as follow:

$$C = \int_0^t I(t) dt \quad (42)$$

When the discharge current is constant (E.g. in laboratory experiment), Eq. (42) can be rewritten:

$$C = I \cdot \Delta t \quad (43)$$

According to the conditions of discharge or to the discharge parameters (discharge current – discharge rate, voltage limit, temperature) by which the capacity is determined, the obtained capacity is not the same [1].

*Nominal capacity* is the battery capacity given by the manufacturer. It is determined in specific conditions of discharge rate, voltage limit and temperature, which are fixed and generalized for each kind of battery application. For instance, the nominal capacity of SLI

batteries is generally determined at the discharge rate of C/20. It means that a SLI battery with a 100 Ah nominal capacity will supply a 5 A (100/20) current during 20 hours (C/20 rate) of discharge until a given voltage limit at 20°C or room temperature. Similarly, the nominal capacities of stationary and traction batteries are usually evaluated at discharge rate of C/10 and C/5.

*Voltage limit* is the condition of end-of-discharge to evaluate the capacity. Theoretically, the voltage limit is applied to avoid deep discharge, or in other words to prevent the active materials from degradation and to prevent polarity inversions (cf. 3.1.2). The voltage limit value depends on the discharge rate; the higher is the discharge rate the lower is the voltage limit. Practically, voltage limits are also chosen according to battery configuration (single cell, series or parallel configurations), battery technologies (flooded or VRLA batteries) as well as battery applications (SLI, traction, stationary) [1].

*Battery capacity evaluation* is the process used to determinate the *battery capacity*: cycles of charge-discharges or a discharge test after a full charge. This makes the difference between the battery capacity and its *measured capacity*, which is determined also by a test of discharge but without doing a full charge before. In contrast with the nominal capacity of the battery, the measured capacity varies with the time and depends on its “electric history”, other words on its previous utilization. The measured capacity is also sensitive to degradations after a certain number of charge-discharge cycles, overcharge periods or a standby period at a weak state of charge [25].

### 1.6.2 State of charge

The State Of Charge (SOC) of a battery can be defined as the capacity left, which is the charge quantity liberated during a discharge achieved in a given condition of current, temperature and voltage limit. In the standards, SOC often corresponds to the ratio between the capacity left and the nominal capacity:

$$\text{SOC} = \frac{C_{\text{left}}}{C_{\text{no min al}}} = \frac{C_{\text{no min al}} - C_{\text{used}}}{C_{\text{no min al}}} = 1 - \text{DOD} \quad (44)$$

$C_{\text{used}}$  : the capacity used.

DOD : Depth Of Discharge, which is the ratio between the capacity used and the nominal capacity.

$$\text{DOD} = \frac{C_{\text{used}}}{C_{\text{no min al}}} \quad (45)$$

The SOC varies from 1 (or 100%) at the *state of full charge* to 0 (or 0%) at the *discharged state*. The state of full charge and discharged state will be defined in detail in the next chapters (cf. 2.1.4.1 and 3.1.2). Sometimes, the nominal capacity is not the initial maximal capacity of the battery. So, the SOC can be superior to 1.

### 1.6.3 State of health

The State Of Health (SOH) of a battery can be defined as the charge quantity liberated during a discharge executed in a given condition of current, temperature and voltage limit after a full

charge. In the standards, SOH often corresponds to the ratio between the measured capacity and the initial capacity (nominal capacity):

$$\text{SOH} = \frac{C}{C_{\text{no min al}}} \quad (46)$$

The SOH varies also from 1 (or 100%) to 0 (or 0%). However, in practice, the SOH is between 1 and 0.8 (or 100% and 80%), as it is considered in general that a battery reaches its end-of-life when it liberates less than 80% of its initial capacity (or nominal capacity).

It is important to notice that Eq. (46) is only true when the measured capacity and the initial capacity are measured in the same discharge conditions (discharge current, temperature and voltage limit).

The SOH defined here allows estimating the battery aging regarding to the capacity that it is able to liberate. Nevertheless, capacity is not always a significant parameter to define battery aging, for instance in SLI and cell telephone application. In this thesis, capacity is used as the aging parameter as it concerns only stationary and motive applications.

## Conclusion of chapter 1

This chapter assembles the principal information needed to know and understand lead acid batteries: technologies, application markets, how does it work, what are its characteristics at open circuit as well as at working mode, i.e. with external current flows.

The lead acid battery technology is regrouped into two major construction types: flooded lead acid batteries and valve regulated lead acid batteries - VRLA batteries. One of the primary features that distinguish VRLA batteries from flooded lead acid batteries is the internal recombination of water dissociated by electrolysis thanks to an immobilized electrolyte.

The application market of lead acid batteries is divided into three main segments: starting, lighting and ignition lead acid batteries - SLI batteries, motive lead acid batteries, essentially heavy-duty applications, and stationary lead acid batteries for back-up supply.

When a lead acid cell is in service, at discharge i.e. to supply electricity to a DC load or in charge i.e. to re-establish its chemical energy reserve thanks to a generator, its voltage  $V$  is different or shifted from the equilibrium value, or its open circuit value  $E$ . The equilibrium voltage of a cell relates to the maximum energy that can be converted by its reactions, electrical energy into chemical energy and vice versa, called Gibb free energy change  $\Delta G$ , by the relation:  $\Delta G = -nEF$ . During charge and discharge, the difference of the cell voltage from its equilibrium value  $\Delta V = V - E$  is attributed to ohmic loss and non-ohmic polarizations, which result, *in fine*, in heat evolution.

Regarding reactions of a lead acid cell, one important remark is that main reactions (charge and discharge of active materials) and side reactions (water electrolysis, oxygen recombination, corrosion, etc.) occur simultaneously in the cell at open circuit as well as at charge and discharge. This situation has a significant influence on lead acid battery behaviors, in particular at open circuit and during charge. It has to be taken into account in lead acid battery managements. This characteristic of lead acid batteries will be analyzed through this thesis: at charge with the electrolyte destratification by gassing (chapter 2), and at maintaining the charge of stationary lead acid batteries, where the secondary reactions are responsible at the same time of the self-discharge phenomenon and of the principals failure modes - dry-out, corrosion of the positive grid, thermal runaway – leading to end of life of these batteries (chapter 4).

## **CHAPTER 2 - CHARGE OF LEAD ACID BATTERIES: FROM TRADITIONAL CHARGE TO ACCELERATED CHARGE WITH EARLY DESTRATIFICATION**

### **Introduction**

As mentioned in chapter 1, main reactions and side reactions simultaneously occur in lead acid cell. During charging, this co-existence of the side reactions with charge reactions of active materials, in one side, can influence, i.e. reduce, the charge efficiency; producing a negative effect. But in another side, gassing (i.e.  $O_2$  and  $H_2$  evolution) can be used to reduce the stratification phenomenon of the electrolyte, thus having a positive effect.

In practice, a charge process has to answer three principal conditions: reasonable or desired charge duration, sufficient state of charge and acceptable electrolyte homogeneity.

In general, charge durations are imposed or demanded according to applications. For instance, a 12 to 14-hour charges for charging batteries during night, when batteries are discharged during day; a 8-hour charge for 3 shifts/day in industrial batteries (traction batteries). Currently, new applications appear needing reduced charge duration: 4-hour charge in the case of grid storage due to reduced durations of the slack period during the night (e.g. 1 to 5 am), in the case of a fast charge of batteries in electric buses, the total charge duration is of the order of an hour during noon break-times or waiting times at terminal stops.

Two conditions of the sufficient SOC and the acceptance electrolyte homogeneity are mainly governed by following important factors: charge acceptance and current of gas evolution for destratification, called gas current.

In a typical charge process, which lasts from 8 to 14 hours, in order to make the management easier, the destratification is done at the end of the charge when the charge acceptance is considered to be negligible and the gas current is assimilated to the applied current.

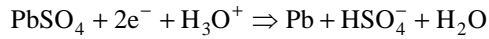
Nowadays, the reduction of charge time required by new applications (4 hours, 1 hour or less) drives to design and develop new charge processes.

In this chapter, first of all, the charge acceptance notion, the electrolyte stratification phenomenon and the destratification by gassing are presented. Then, variations of charge acceptance and gas current during a typical charging process are analyzed. This analysis shows difficulties in the control of the destratification phase in the case of accelerated charges, i.e. durations less than 8 hours, and thus the demand of a new charge process for reduced charge times. This is the reason why, in the next part, we search to control the destratification phase by charge acceptance measurement solutions. Finally, a new charge method using charge acceptance measurement is implanted. It is tested with a commercial charger of IES-Synergy Society.

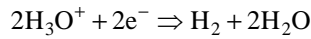
### **2.1 CHARGE OF LEAD ACID BATTERY**

#### **2.1.1 Reminder of reactions during charging**

Negative electrode:

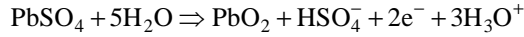


Reaction 5

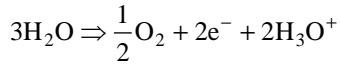


Reaction 10

Positive electrode:

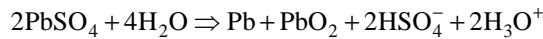


Reaction 6



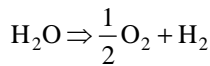
Reaction 11

Overall reactions of charge:



Reaction 7

Overall reaction of water electrolysis:



Reaction 12

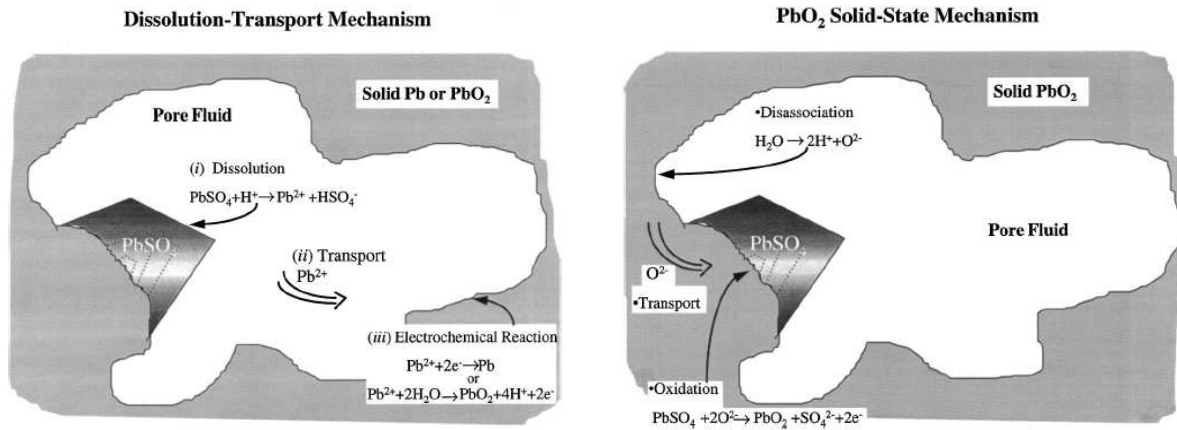


Figure 25: Schematic description of the dissolution-transport mechanism within a solution-filled cavity of porous Pb (or PbO<sub>2</sub>) electrode; schematic description of a proposed solid-state charge mechanism within the PbO<sub>2</sub> electrode [28].

Petkova et al. [29] described the mechanism of PbSO<sub>4</sub> reduction to Pb comprises following elementary processes:

- Dissolution (chemical reaction) of PbSO<sub>4</sub> crystals to Pb<sup>2+</sup> and HSO<sub>4</sub><sup>-</sup> ions.
- Diffusion (transport) of Pb<sup>2+</sup> ions to the active centers where the electrochemical reaction of Pb<sup>2+</sup> reduction to Pb proceeds (charge-transfer).
- Surface diffusion of Pb atoms to the sites of Pb nucleation and crystal growth (crystallization).
- Diffusion and migration of HSO<sub>4</sub><sup>-</sup> ions out of the pores of negative active material. This step is very slow as the HSO<sub>4</sub><sup>-</sup> ions have a very low mobility. Electro-neutralization of the HSO<sub>4</sub><sup>-</sup> ions proceeds through diffusion of H<sub>3</sub>O<sup>+</sup> ions from the bulk solution into the pores of the negative active material. As the transference number of H<sub>3</sub>O<sup>+</sup> and HSO<sub>4</sub><sup>-</sup> ions is 0.9 and 0.1 respectively, the H<sub>3</sub>O<sup>+</sup> ions have 9 times higher mobility than HSO<sub>4</sub><sup>-</sup> ions. The electrochemical reaction continues only at

the sites of active material where the  $\text{HSO}_4^-$  ions are electrically neutralized. If the negative charges of  $\text{HSO}_4^-$  ions generated by electrochemical reaction are not neutralized, the pore volume will be charged negatively and the electrochemical reaction will stop at this particular site.

- The  $\text{H}_2\text{SO}_4$  concentration in the pores increases and a concentration gradient is formed between  $\text{H}_2\text{SO}_4$  in the pores and the bulk of the electrolyte (stratification phenomenon, cf. 2.1.3). Under its action,  $\text{H}_2\text{SO}_4$  diffuses towards the bulk solution. This is a low process.

Similar processes take place at the positive electrode where  $\text{PbSO}_4$  is oxidized to  $\text{PbO}_2$ .

## 2.1.2 Charge acceptance

### 2.1.2.1 Definitions

Several definitions of the charge acceptance, in term of a current, of a flooded lead acid battery can be found in the literature [1, 2, 5, 15, 30, 31].

Berndt defines the “acceptance” as *the share of the current that actually is “accepted” by the battery and could be retrieved by subsequent discharge* [1]. Indeed, the charge current is partly involved in side reactions, mainly gassing. According also to Berndt [1], charge acceptance is determined by the balance between the kinetic parameters of the main charge current and the gassing current. In other words, it depends on the rate of the main and side charge reactions. This definition is difficult to use in practice because this “acceptance” cannot be directly measured, but only evaluated, by taking into account the losses through side reactions. This definition of the charge acceptance is associated to faradic efficiency ( $\eta_{\text{Faraday}}$ ) as the following:

$$\eta_{\text{Faraday}} = \frac{I_{\text{ACCEPTANCE}}}{I_{\text{CHARGE}}} \quad (47)$$

In which:

$I_{\text{ACCEPTANCE}}$  : charge acceptance

$I_{\text{CHARGE}}$  : charge current

Charge acceptance may also be defined as the maximum current a battery can absorb for its main charge reaction. This corresponds to the maximum value that can be reached in the case of the first definition. Although this concept is easily understandable, measurement of such a charge acceptance is very difficult.

A very different definition is the total charge current (main and side reactions) under a constant charge voltage. The result can widely vary with the chosen voltage value. This includes for instance charge currents under float charges (charge with very low rates, cf. 4.1.2.).

Gassing becomes noticeable when voltage is above a threshold value, called here *gassing voltage*. The gassing voltage depends on temperature, charge rate, alloy quality, battery age and history. Moreover, as “noticeable” is subjective, it depends also on the observer



appreciation. The gassing voltage is statistically situated between 2.3 and 2.6 V/cell. In this thesis, the charge acceptance of the flooded lead acid battery is assumed to be the charge current passing through its electrodes at a gassing voltage. Thele [5] has used a similar definition for modeling the charge acceptance of flooded lead acid batteries.

### 2.1.2.2 Charge acceptance profile

As mentioned in 1.5.3, the overall charge reaction consists of four partial steps: charge transfer, mass transfer, chemical reaction and crystallization. Corresponding to each step, a respective overvoltage appears when this step is the determining-rate of the reaction (cf. 1.5.4). The charge acceptance profile is in fact an image that describes the charge reaction rate, which is limited by one or many partial steps of the charge reaction. In other words, the acceptance profile is drawn based on electrochemical kinetic parameters. At their turn, these electrochemical kinetic parameters depend on many conditions such as the initial state of the battery (depth of discharge), the history, and the rate of charge.

At the beginning of the charge process, as there are a lot of  $\text{PbSO}_4$  crystals and initially no concentration gradient, the charge-transfer reaction is generally the determining-rate. According to Takehara et al. [32], the charge-transfer process and the mass transfer process are the rate-determining steps for the oxidation of  $\text{PbSO}_4$  to  $\text{PbO}_2$  and for the reduction of  $\text{PbSO}_4$  to  $\text{Pb}$  respectively. Many authors [2, 5, 29, 32, 33] reveal also that the depletion of  $\text{Pb}^{2+}$  ions is the limiting process of the overall reaction.

### Charge-transfer as determining-rate

When the charge-transfer rate is the determining-rate, the hindrance of this reaction causes the formation of active overvoltage  $\eta_a$ . (cf. 1.5.4.3). The charge-transfer rate is:

$$\frac{i}{nF} = i_0 \left[ \exp\left(\frac{\alpha}{RT} \eta_a\right) - \exp\left(-\frac{(1-\alpha)}{RT} \eta_a\right) \right] \quad (31)$$

Thus, the exchange current density  $i_0$  of the electrode reaction, the transfer coefficient and the active overvoltage have important roles in the charge process.

### Diffusion as determining-rate

The rate of diffusion reaction is given by the first law of Fick (for one dimension):

$$\frac{i_{j,D}}{nF} = D_j \frac{c_j - c_{j,o}}{d} \quad (23)$$

Applying it to the lead acid cell gives:

$$\frac{i_{\text{Pb}^{2+},D}}{nF} = D \frac{c_{\text{Pb}^{2+}} - c_{\text{Pb}^{2+}}^0}{d} \quad (48)$$

In which:

$c_{\text{Pb}^{2+}}^0$  : concentration of  $\text{Pb}^{2+}$  ions at equilibrium

$c_{\text{Pb}^{2+}}$  : concentration of  $\text{Pb}^{2+}$  ions at the reactive surfaces, i.e. at Pb and  $\text{PbO}_2$  surfaces.

$d$  : gap distance between Pb or  $\text{PbO}_2$  and  $\text{PbSO}_4$  surfaces, which can be assumed as the thickness of diffusion layer [cm]

Therefore, the rate of the diffusion reaction depends on the diffusion constant  $D$ , which is a function of the material, the temperature and the concentration of the sulfuric acid. It is also inversely proportional to the thickness of the diffusion layer.

The diffusion rate is also proportional to the difference in concentration of the  $\text{Pb}^{2+}$  ions  $c_{\text{Pb}^{2+}}$  at the reactive surface and their equilibrium concentration  $c_{\text{Pb}^{2+}}^0$ .

During charging, the concentration of the  $\text{Pb}^{2+}$  ions in the electrolyte (at the  $\text{PbSO}_4$  surface as well as at the reaction electrode surfaces) is always smaller than the one at equilibrium. The  $\text{Pb}^{2+}$  ion concentration change, which is given by Sauer, Thele et al. [2, 5], is defined by the balance of the absorption rate of  $\text{Pb}^{2+}$  ions,  $q$ , due to the generation of Pb and  $\text{PbO}_2$  and the dissolution rate of the  $\text{Pb}^{2+}$  ions,  $s$ , from  $\text{PbSO}_4$  crystals:

$$\frac{\partial c_{\text{Pb}^{2+}}}{\partial t} = s - q \quad (49)$$

In which:

$q = I/nF$  : consumption rate of  $\text{Pb}^{2+}$  ions due to the electrochemical process (charge transfer) and therefore directly proportional to the charge current  $I$ . The current  $I$  is positive during the charge.

$s$  : dissolution rate of the  $\text{PbSO}_4$  crystals [mole.s<sup>-1</sup>]

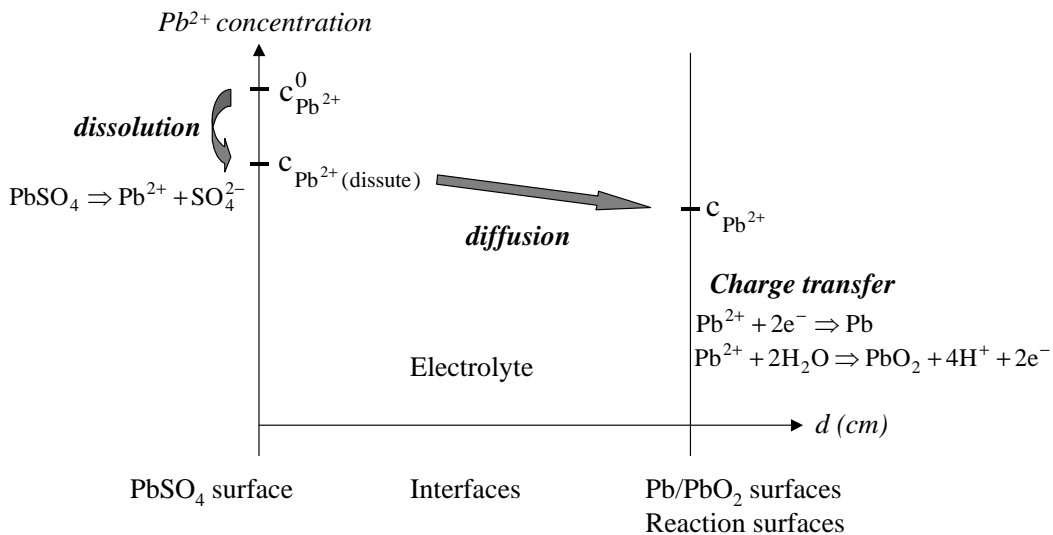


Figure 26: Evolution of  $\text{Pb}^{2+}$  ion concentration at the interface area consisting of active material surface and  $\text{PbSO}_4$  crystal surface during charging:  $c_{\text{Pb}^{2+}}^0$  concentration at equilibrium,  $c_{\text{Pb}^{2+}}(\text{dissute})$  concentration at  $\text{PbSO}_4$  surface,  $c_{\text{Pb}^{2+}}$  concentration at reactive surfaces, i.e. Pb and  $\text{PbO}_2$  surfaces.

According to Sauer, Thele et al., the limitation of the  $\text{PbSO}_4$  dissolution process is assumed to be the main cause for depletion of  $\text{Pb}^{2+}$  ions. When the depletion of  $\text{Pb}^{2+}$  ions is the limiting process of the overall reaction, the charge reaction rate is obtained from the  $\text{PbSO}_4$  dissolution rate, which is defined by Sauer in [2] as follows:

$$s = \frac{DV_{\text{PbSO}_4}}{r^2} (c_{\text{Pb}^{2+}} - c_{\text{Pb}^{2+}}^0) \quad (50)$$

In which:

$V_{\text{PbSO}_4}$  : overall crystal volume of  $\text{PbSO}_4$  [cm<sup>3</sup>]

$r$  : average radius of all  $\text{PbSO}_4$  crystals [cm]

$c_{\text{Pb}^{2+}}$  : concentration of  $\text{Pb}^{2+}$  ions at the  $\text{PbSO}_4$  surface (i.e.  $c_{\text{Pb}^{2+}}$  (dissute) in Figure 26).

Therefore, the dissolution rate is proportional to the diffusion constant and to the overall crystal volume of  $\text{PbSO}_4$  but is inversely proportional to the square of the crystal radius.

### **Dissolution-precipitation mechanism at positive electrode**

Or according to Takehara [32], the oxidation of the  $\text{PbSO}_4$  through the dissolution-precipitation mechanism can be written as follows:



And then the following equation for the rate of this reaction may be written:

$$\frac{i}{nF} = A(t)k c_{\text{Pb}^{2+}}^x c_{\text{H}^+}^{-y} \quad (51)$$

In which:

$A(t)$  : interface area, which changes with the proceeding oxidation;

$c_{\text{Pb}^{2+}}, c_{\text{H}^+}$  : concentration of  $\text{Pb}^{2+}$  ion and  $\text{H}_3\text{O}^+$  ion in the sulfuric acid solution, they depend on the concentration of sulfuric acid solution;

$x$  and  $-y$  : reaction order of  $\text{Pb}^{2+}$  ion and  $\text{H}_3\text{O}^+$  ion respectively for the anodic reaction;

$k$  : potential dependence constant.

As shown in Eq. (51), the charge-transfer reaction rate depends on the concentration of sulfuric acid solution and the interface area  $A(t)$ .

### **Diffusion rate at negative electrode**

Always according to Takehara the rate of charge reaction of the negative electrode depends on the rate of diffusion reaction, which can be obtained by:

$$\frac{i_D}{nF} = \frac{DA(t)}{d} (c_{Pb^{2+}}^0 - c_{Pb^{2+}}) \quad (52)$$

In which:

$A(t)$  : interface area;

$d$  : gap distance between Pb and PbSO<sub>4</sub>, which can be assumed as the thickness of diffusion layer [cm];

$c_{Pb^{2+}}^0$  : concentration of Pb<sup>2+</sup> ions at equilibrium (solubility of PbSO<sub>4</sub>);

$c_{Pb^{2+}}$  : concentration of Pb<sup>2+</sup> at the Pb surface.

In both cases of negative and positive electrode charge, the reaction interface area  $A(t)$  plays an important role in the charge reaction rate. The charge reaction rate is proportional to  $A(t)$ .

### Charge acceptance profile

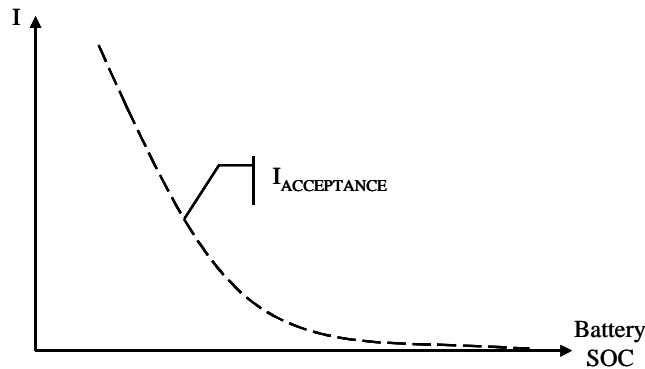


Figure 27:

*Charge acceptance as a function of battery state of charge (SOC), following an asymptotic profile*

In brief, apart from the temperature, the battery age, history and the rate of charge, the charge reaction rate or the charge acceptance at a fixed charge rate changes depending:

- the interface area between active materials and PbSO<sub>4</sub> crystals, which is related to the volume and the crystal radius of PbSO<sub>4</sub>. During the charge, for both negative and positive electrode, the total volume as well as the crystal radius of PbSO<sub>4</sub> crystals decrease with the state of charge. This results in an increase of the diffusion layer and so a decrease of the diffusion rate, cf. Eq. (48). Moreover, according to Eq. (51) and (52), the decrease of interface area leads directly to the decrease of reaction rates. So, the decrease of interface area with processing charge is one of the reasons explaining the falling down of the acceptance with the SOC;
- the concentration of H<sub>2</sub>SO<sub>4</sub> in the pores of active material, which increases with progressing charge and involves the decrease of the diffusion coefficient, as well as of the solubility of PbSO<sub>4</sub> crystals. For these influences, the increase of the H<sub>2</sub>SO<sub>4</sub>

concentration is also attributed to the decrease of the charge acceptance with the augmentation of the SOC.

In brief, the charge acceptance decreases with the increase of the battery SOC, following an asymptotic profile (cf. Figure 27).

### 2.1.3 Electrolyte stratification

#### 2.1.3.1 Phenomenon

At room temperature the density of sulfuric acid is 1.834, which is more than 1.8 times the density of water. This difference in density can cause problems during recharge, as sulfuric acid takes long time to diffuse towards the bulk solution, relatively higher density causes it to settle downward relative to the water. This problem can be seen in more detail by examining the chemical reactions that occur during charging.

When the lead acid battery is being charged, the sulfuric acid is produced in the porous volume of both electrodes. This porous volume is inferior to 20% of the total volume of the electrolyte. During charging, the sulfuric acid concentration in the pores increases progressively and becomes higher than the one in the bulk solution. When coming out of these pores, the electrolyte has a higher concentration of sulfuric acid near the positive and negative electrodes, which corresponds to a higher density. This causes it to pour down along the electrodes under effect of gravity and increases the acid concentration at the bottom of the cell. This is the process of *stratification*, in which the electrolyte at the bottom has a higher acid concentration than the one on the top of the cell.

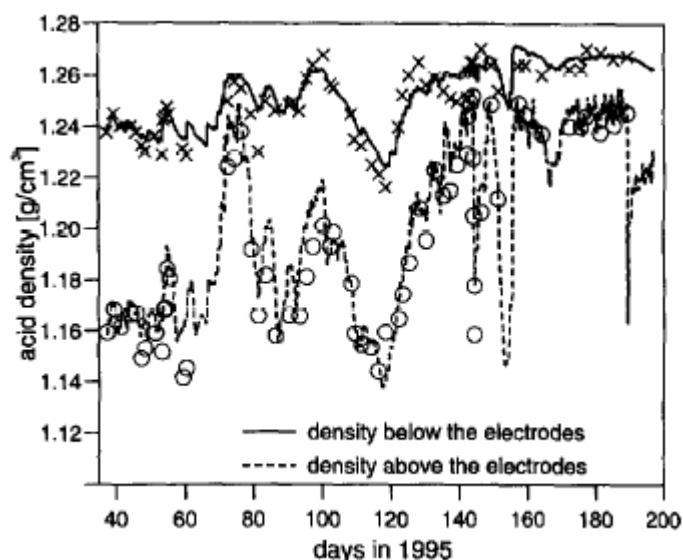


Figure 28: Sulfuric acid density at the top and the bottom of electrodes during a 160 days period under typical conditions of an autonomous photovoltaic system. The measurement was manually carried out on a 200 Ah/2 V flooded lead acid battery [42].

The bibliography work of Y. Guo et al. gives a quite full summary of lead acid applications, which suffer from the stratification phenomenon [34]. The electrolyte stratification is an ubiquitous phenomenon in lead-acid batteries and the severe stratification often occurs in large-scale batteries, PV applications, and batteries at a high rate of discharge or charge [35-

39]. It is known that the degradation of the automotive battery performance often appears in the bench-life testing because of the acid stratification. In the application of photovoltaic systems [38-43], the discharge current of the batteries is very small and they are seldom completely charged due to low limited charge voltage and also to limited amount of sunshine per day. The frequent undercharge makes the electrolyte stratification to become increasingly serious. These problems also appear in valve-regulated lead-acid batteries with poor convection because of their design of starved electrolyte and less overcharge [44-46].

### 2.1.3.2 Consequences

Battery voltage depends on acid concentration. In a stratified cell, the equilibrium voltage is higher at the bottom (cf. 1.4.2.1).

At charge with voltage restriction, higher polarization is distributed at the top of a stratified cell. Consequently, the cell is heterogeneously charged and it can happen that the top portion is overcharged while the bottom portion is undercharged.

At discharge, this same bottom part of the stratified cell, where polarization is higher, is preferentially discharged and reaches more rapidly the criterion of end of discharge (cf. section 3.1) while it is not met yet at the top part. In this case, the discharge of the cell continues, the bottom part thus suffers over-discharge.

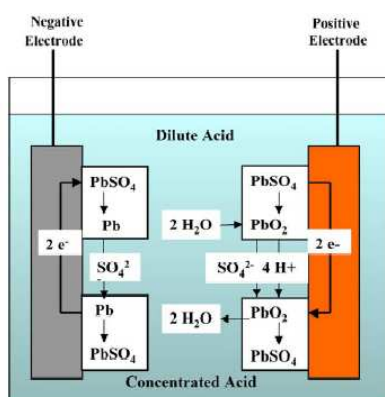


Figure 29: Stratification effect on positive and negative electrodes: concentration pile that discharges the bottom part and charges the top part of electrodes [47]

In the case of a stratified cell at open circuit, concentration pile effect can take place as illustrated by Ruetschi [47] in the Figure 29. Within the electrolyte stratification, the *emf* of the electrode top part (dilute electrolyte) is lower than the one of the electrode bottom part. This results to an equivalence of a *concentration pile* in short circuit on the electrode itself. A current appears inside each electrode where the top part is charged and the bottom part is discharged.

These situations during charging, discharging and open-circuit of the stratified cell bring to an excessive sulfating the electrode bottom parts, and thus, to an accelerated aging process of the cell (cf. Figure 30). It is known that the lead sulfate takes considerably more volume than the active materials at charged state ( $\text{PbO}_2$ ). Moreover, it has a completely different morphology and crystallographic structure compared to  $\text{PbO}_2$ . If there is an excessive sulfation during cycling in the stratified electrolyte condition, the morphological shape-change of the positive active mass is accelerated.  $\text{PbO}_2$  material gradually loses its structure (i.e. loss of coherence between particles) and cannot participate any longer in the discharge process. This phenomenon is called *softening* of the mass. The soft mass layer becomes more and more

thicker and finally the active material falls down from the plate to the container bottom. This is called *shedding* [47-49].



Figure 30: Stratification effect on a positive plate: softening and shedding of the active material at the bottom of the plate [48].

### 2.1.3.3 Destratification by gassing

In flooded lead acid batteries, the stratification of electrolyte can be readily recovered by agitation such as by gassing. As mentioned in 2.1.2.1, when the applied current exceeds the charge acceptance, or in other words when the voltage is prolonged beyond a gassing value, the current share that produces gases (called gassing current), becomes noticeable. In a traditional charge, an overcharge phase at constant current is added at the end of charge (cf. 2.1.5) in which gassing is produced to destratify the electrolyte.

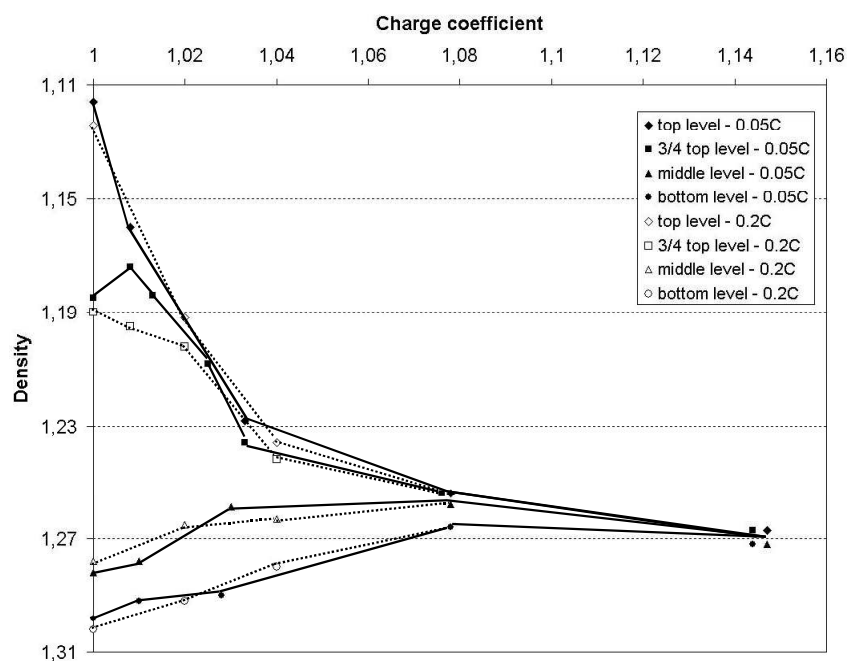


Figure 31: Electrolyte density measured at four levels of the cell as the function of the charge coefficient evolution during overcharge phases at 0.05C or at 0.2C. Beyond 8% of overcharge, the electrolyte is almost homogeneous without depending on the overcharge rate [50].

The work of J. Alzieu and J. Robert [50] shows in Figure 31 that for a flooded battery, beyond about 8% of overcharge (8% more of the electrical quantity, which equals to the one obtained during the previous discharge), the electrolyte is almost homogeneous and independent on the overcharge rate. It is clear that, the destratification is more efficient at the beginning of the overcharge phase, below 5% of overcharge.

In practice, as the electrical quantity (Ah) used during the previous discharge is usually unknown, a 10 to 20% of the total electrical quantity accepted during the two previous charge phases (cf. Figure 32) is applied at the end of the charge process to destratify the electrolyte.

## 2.1.4 Charge definitions [51]

### 2.1.4.1 Full charge

As explained in 2.1.2, the charge acceptance decreases following a descending profile during the charge. A complete state of charge is an asymptotic state that is never reached. This is the reason why what is called a *full charge* is not a real full charge. It is just a trade-off between a desired charge duration and a high enough state of charge.

According to charge standards, the full charge is considered to be reached when there is no charge current or voltage evolution during at least 2 hours. This criterion of full charge is evidently vague as the observation of a non-evolution depends on the sensibility of the measurement apparatus used. Moreover, at the end of charge, the temperature rise due to inevitable losses (cf. 1.5.6), involves a slight decrease of the electrolyte resistance and as consequence of the battery voltage. This decrease can mask the increase of the voltage related to the effective charge, which becomes lower and lower but never zero. The association of these two processes results in the voltage evolution profile as the appearance of a maximum level that is almost flat but usually can be detected by a reasonable effort of measurement. A similar phenomenon takes place in the electrolyte density evolution: this maximum area is then classified, in practice, like a non-evolution period of the observed parameters allowing the validation of the full charge criterion.

Taking also into account the stratification phenomenon during charging, a full charge that can be obtained at the end of a lead acid battery charge is in reality the result of a trade-off between a reasonable charge duration, a sufficient state of charge and an acceptable electrolyte homogeneity.

### 2.1.4.2 Normal charges

The normal charge of lead acid batteries consists in reaching the maximum level of full charge while respecting the standards and constraints of the operating fields.

The initial charge current is limited by the standards at  $C_{\text{nominal}}(\text{Ah})/5(\text{hours})$ , or written in a simple way  $C/5$  or  $0.2C$  (e.g. 20 A for a battery whose the nominal capacity is 100 Ah). Most of commercial chargers have an initial current slightly inferior to this limitation, generally between  $0.15C$  and  $0.18C$ . After a complete discharge (100 % DOD), this current can be maintained during 3 to 5 hours before the charge acceptance becomes inferior to this initial value. The current profile at the last phase of charge as well as the criterion of end of charge vary according to the charger brands and recommendations of battery manufacturers. They can take into account also maximum charge durations dictated by utilization constraints.



Therefore, the normal charge is more or less complete in different cases. But, this is not the essential criterion. The primary condition that has to be respected during a charge concerns the electrical quantity for electrolyte destratification and not the perfect charge of active materials. The gassing current is limited by the standard at  $C/20$ . A normal charge usually lasts from 12 to 14 hours and the last 3 hours are used considered for gassing.

#### 2.1.4.3 Accelerated and fast charges

*Accelerated charges* apply high currents together with reduced charge durations (less than 8 hours). A charge lasting less than 1 hour (i.e. the charge rate is  $C/1$ ) is generally called *fast charge*.

Two fundamental points associated to the accelerated charge of lead acid batteries are:

**The accelerated charge is just a partial charge.** Within a reduced charge time, for instance 1 hour, the battery just approaches in a very relative manner the asymptotic state of full charge. The final state of charge depends on the charge rate, the initial depth of discharge, the rate of this discharge, the duration of possible standby period between the discharge and the charge, the temperature. In practice, after a full discharge, the final maximum state of charge that can be reached during 1 hour is between 60 to 85%.

**The destratification step is mandatory.** The necessary gas volume for electrolyte homogenization is the same as for a normal charge (cf. Figure 31). But, the gas evolution rate has to be intense to preserve the characteristic of a fast charge.

#### 2.1.5 Charge acceptance and gassing current variations during a IUi typical charge process of lead acid batteries

A typical traditional charge of lead acid batteries is composed of three phases, usually called I(W)Ui charge (cf. Figure 32).

The first phase is a constant current phase (or a constant power phase) (A), in which the current value ( $I_1$ ) is usually limited by the maximum power of the charger, as initial charge acceptance of a discharged battery is high. During this phase, the voltage increases with the increase of the SOC up to the gassing value as the internal resistance increases progressively. Within this phase, the major part of charge, 60 to 90%, is accomplished. As the voltage increases, the gassing current also increases, but it remains insignificant compared to the charge current up to a threshold value.

The second phase (B) is performed at a constant gassing voltage. During this phase, the charge current decreases asymptotically to a low value following the charge acceptance profile (cf. Figure 27), while gassing current is almost invariable as the voltage is fixed at the gassing value.

The third and last phase is a constant current phase (C), which is called overcharge or destratification phase. This provides constant current ( $I_2$ ), called *overcharge current*, whose value is higher than the charge acceptance, thus producing significant gas evolution that destratifies the battery electrolyte.

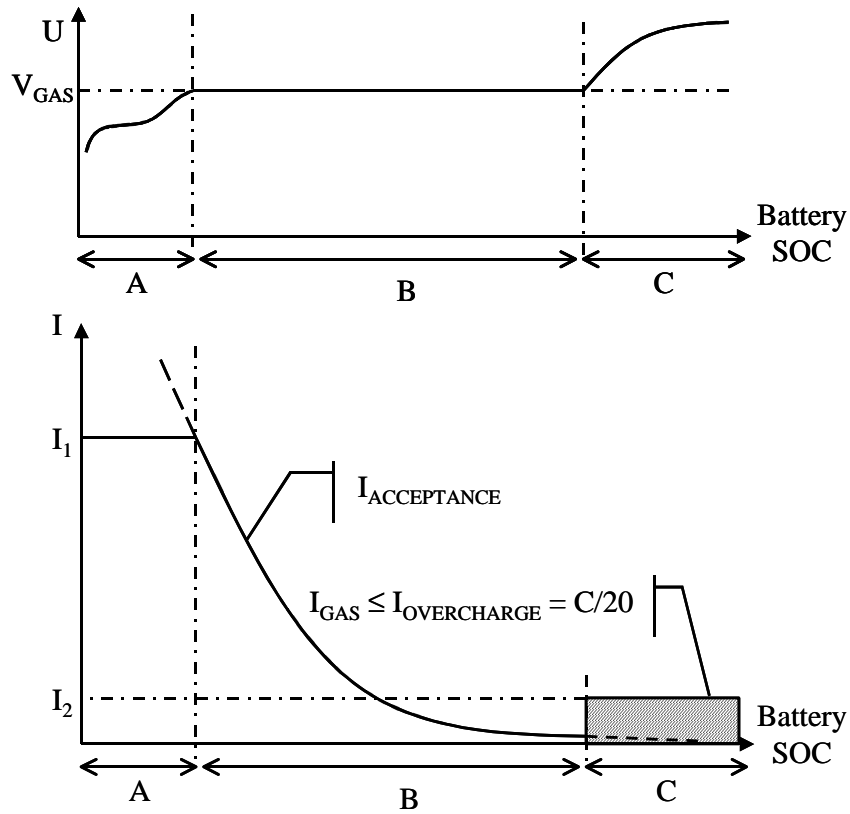


Figure 32: IUi charge of lead acid batteries: (A) constant current phase at  $I_1$ , (B) constant voltage phase at gassing value  $V_{GAS}$  and (C) overcharge or destratification phase at constant overcharge current  $I_2 = C/20$ .

Figure 33 illustrates the relationship between the current and the potential of the positive electrode during three phases of the charge; the ratio of the active material current  $i_{AM+} = i_{PbSO_4/PbO_2}$  and of the oxygen current  $i_{O_2} = i_{H_2O/O_2}$  is just an image to illustrate the principle, the contribution of gassing current in the first and second phases being pretty amplified in order to be easily observed.

The characteristic of  $i_{AM+}$  is sensibly straight at the beginning of the charge. With progressing charge, it moves towards the abscissa of the potential as the state of charge increases. The characteristic of  $i_{O_2}$  evaluates following an exponential function with the increase of the voltage.

On the phase A at current constant  $I_1$ , the voltage increases slightly as the characteristic of  $i_{AM+}$  evaluates slightly and the slope of the characteristic of  $i_{O_2}$  is sufficiently low that its influence is almost negligible

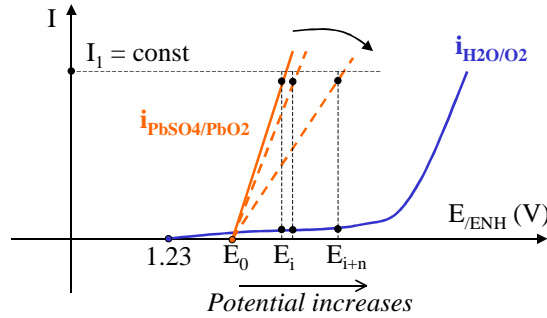
It is shown that, if the constant current  $I_1$  were continued to be applied to the battery without the voltage limitation, the potential would increase up to values where the gas evolution would be very important and this current would not match any more the battery acceptance profile. Therefore, the fixed gassing voltage phase (phase B) plays the role to limit the gassing current and enables the battery to be charged at its charge acceptance rate.

At the end of charge (at the end of phase B), the characteristic of  $i_{AM+}$  is almost en parallel with the potential abscissa, the charge acceptance is almost mixed up with the gassing current,

the battery is no more charged. The battery is imposed at the current constant  $I_2$  for destratification (phase C). During this phase, the voltage is fixed at high values by overcharge current  $I_2$ .

The first and the third phases (phases A and C) are both at constant current, but their effect is different: in the first phase, the supplied current contributes most all to the proper charge while in the third phase it is essentially dedicated to gassing.

Phase (A)



Phase (B)

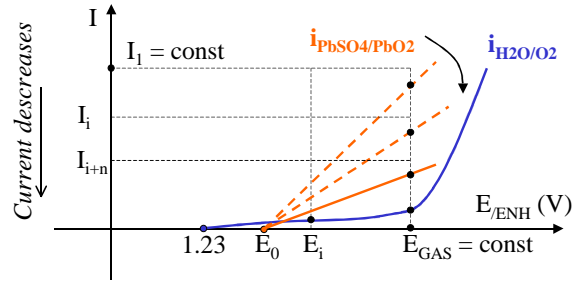
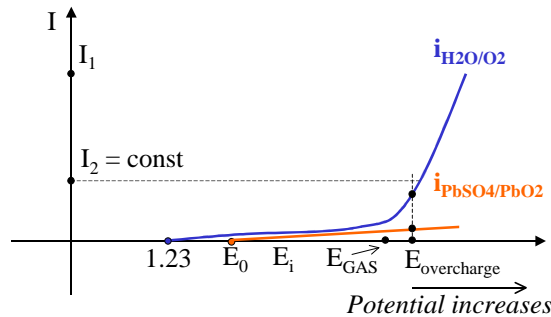


Figure 33: Relationship between current and potential of the positive electrode during each phase of IUi charge.

Phase (C)



Phase (A): the battery is charged with constant current  $I_1$ , the potential  $E$  increases up to the gassing value.

Phase (B): the battery is charged at the constant potential gassing  $E_{GAS}$  (i.e. at its charge acceptance). The charge acceptance decreases progressively.

Phase (C): the battery electrolyte is destratified by gassing at constant current  $I_2$ , the potential increases. The battery is almost no longer charged.

### 2.1.5.1 Gassing Voltage

As defined in 2.1.2.1, beyond the gassing voltage value the gassing current becomes noticeable compared to the current of proper charge reactions or in other words with the charge acceptance.

The gassing voltage value can be obviously observed on the voltage profile during charging with a constant current. As shown in Figure 33, in the first charge phase of constant current (phase A), the voltage variation is almost decided by the profile of the active material charge current  $i_{AM+}$  and in the third charge phase of overcharge constant current, it is essentially determined by the profile of the gassing current  $i_{O2}$ . The moment where the voltage profile transfers from the charge to overcharge profile is marked by a transient phase of an abrupt jump from one level (low level where the gassing current is sufficiently low and does not influence on the battery voltage) to a higher one (high level where the gassing current is

important and fixes the voltage at high values). The gassing voltage value is the inflection point between these two levels (cf. Figure 34).

An industrial charger is usually not programmed to detect the inflection point of the voltage profile. Thus, an experimental gassing value has to be predicted to limit the charge current according to the charge rate and the kinds of positive grid alloys.

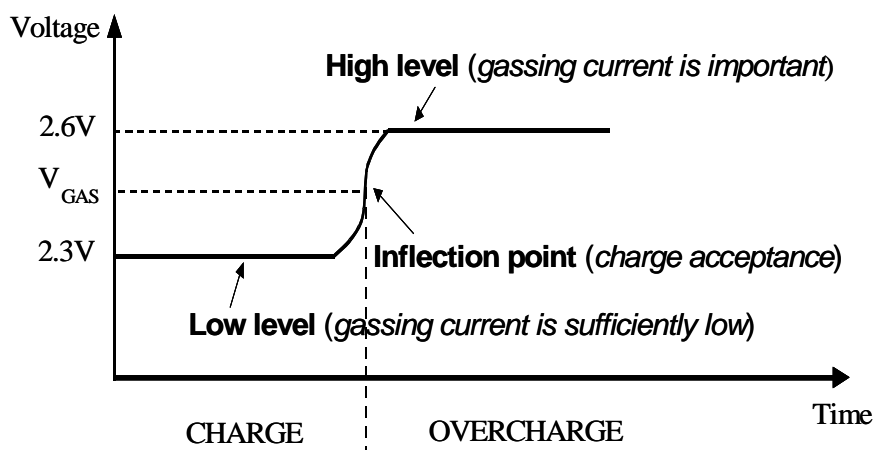


Figure 34: Voltage variation of the battery as a function of time during a charge followed by an overcharge at a constant current: it jumps from a low level to a high level, for instance 2.3 V to 2.6 V. The gassing voltage corresponds to the inflection point between two levels.

Increasing the gassing voltage can be one way to charge more rapidly the battery, but it is limited by the increased water electrolysis with the voltage [1]. Berndt shown in his experiment that when increasing the gassing voltage the charge current increases as well because of the raising of the gassing and the charge acceptance. In this example, it is shown that when the voltage reached the gassing value of 2.23 V/cell 79% SOC is reached, and this value is 97% in the case of 2.4 V/cell gassing voltage. However, the water decomposition is seven times faster in the second case. This is the reason why an increase of gassing voltage is only used when a certain level of charge has to be reached within a limited time.

The transient voltage values depend at the same time on rates of charge reactions and gassing reactions, or in other words, on the balance between these two reaction rates. Therefore, transient voltage values, like the charge acceptance and the gassing current, vary with many parameters such as temperature, rate of charge, alloy quality, battery age and history.

It is found in experiments that the slope of transient phase decreases with battery age. Indeed, an aged battery has a lower gassing voltage than a new one. This change can create problems as the gassing voltage of the charger is fixed. A bad situation can happen when the voltage of an aged battery is not able to reach the fixed gassing voltage value of the charger, so the battery continues to be charged with a constant current and produces undue gas evolutions.

### 2.1.6 Control of Destratification phase

The destratification phase is mandatory for flooded lead acid batteries longevity, but the electrical quantity supplied for gassing has to be controlled to prevent shedding of active materials from the electrodes, to reduce water loss by electrolysis and corrosion, to reduce depletion of the electrolyte, to comply with the recommended venting rate associated to

hydrogen high flammability and sometimes to have a quite high faraday efficiency (e.g. in the case of photovoltaic applications, to use the most efficiently the available sun power). The overcharge electrical quantity control means the control of the gassing current that is injected into the battery.  $C/20$  is often considered as a convenient gassing rate.

The destratification phase is usually performed at the end of charge when the charge acceptance is small enough to be negligible. Supplied current is then considered mainly for gassing. The destratification phase is thus evaluated and controlled by the control of the supplied current. This is the case of charge processes lasting enough long time, typically from 10 to 14 hours.

Establishment of the 8-hour shifts (three shifts/day) required the constructors to develop 8-hour charge programs, sometimes qualified as *accelerated charge*. This reduced charge time can be performed without changing fundamentally the charge methods: at the end of charge (e.g. last 3 hours), a constant current of  $C/20$  is applied for destratification. It is important to keep in mind that although the charge acceptance is not yet negligible, it is already inferior to  $C/20$ . As the gassing current is part of this applied current, its value never exceeds the  $C/20$  rate (cf. Figure 35).

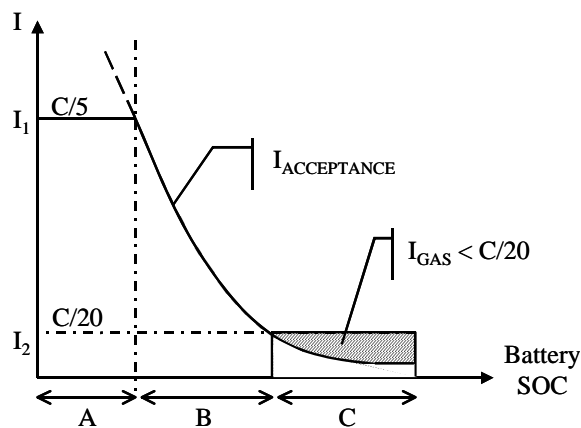


Figure 35: Control of destratification phase at an accelerated  $I_{Ui}$  charge. Charge acceptance may not be negligible during overcharge phase, overcharge rate is set at  $C/20$ , gas rate never exceeds  $C/20$ .

However, reducing the charge time even more, below the 8 hours, presents difficulties, especially when the charge acceptance is still superior to  $C/20$ . Two bad situations can happen in this case (cf. Figure 36):

- On one hand, if the charge acceptance is higher than  $C/20$  and the constant current for destratification phase is fixed at  $C/20$ , it is supplied only for the proper charge and not for gassing. There is no destratification. (a)
- On other hand, if the constant current of destratification phase is increased to be superior to the charge acceptance (superior to  $C/20$ ), the destratification control can become delicate. In fact, the charge acceptance is not known, neither the current value share for destratification (the gassing current). The gassing current, as well as the electrical quantity for the destratification, cannot be controlled and can become too high and damage the battery. (b)

The first situation has to be avoided because it retards the charge process and there is no destratification. The second situation could be a way to homogenize the electrolyte in accelerated and fast charges with the condition that the current share for gassing has to be controlled.

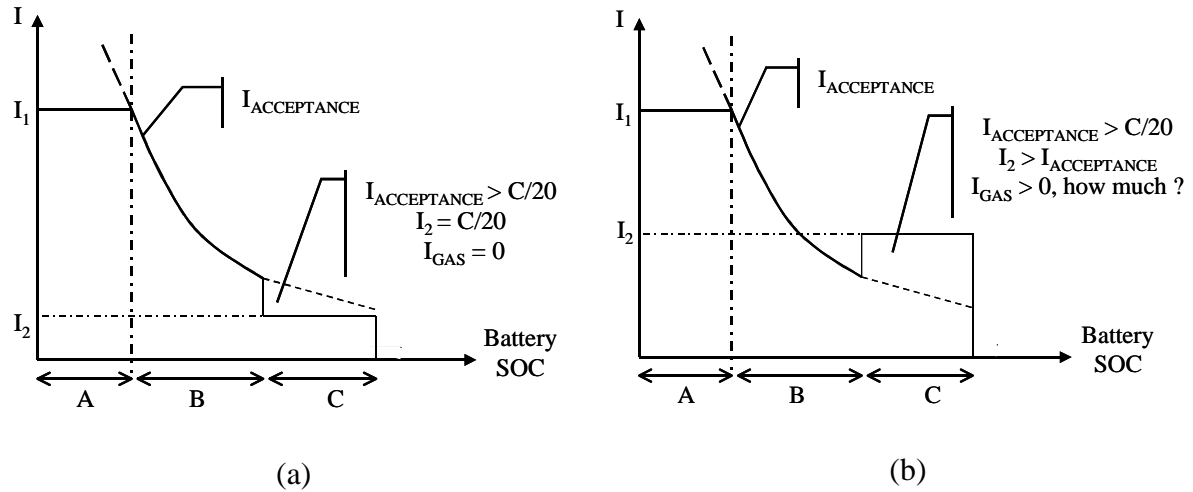


Figure 36: when at phase (C) charge acceptance is still greater than  $C/20$ , 2 situations can happen: (a)  $I_2$  is set at  $C/20$  that involve no  $I_{GAS}$ , (b)  $I_2$  is set greater than  $I_{ACCEPTANCE}$  there is current share for gassing but it cannot be properly controlled.

In order to control the gassing current, assuming that during an overcharge phase, the supplied current ( $I_{OVERCHARGE}$ ) is the sum of charge acceptance ( $I_{ACCEPTANCE}$ ) and gassing current ( $I_{GAS}$ ), we have to find a way to measure the charge acceptance during the overcharge phase (phase C) so that the gassing current can be calculated as follows:

$$I_{GAS} = I_{OVERCHARGE} - I_{ACCEPTANCE} \quad (53)$$

## 2.2 CHARGE ACCEPTANCE MEASUREMENTS

As defined in 2.1.2.1, the charge acceptance that has to be determined is the charge current under a gassing voltage. Thus, in principle, acceptance value can be obtained in provoking a transition from overcharge to charge, so the current (the voltage) decreases from overcharge value to acceptance value (gassing value) respectively. This action can be operated by controlling either the current or the voltage.

The first method of charge acceptance measurement during the overcharge phase proposed by P. Izzo in his thesis work using the current ramps in the charge algorithm for batteries of photovoltaic application [48]. The second method tested in this thesis is using voltage squares.

### 2.2.1 Current ramps

#### 2.2.1.1 Principle

The method proposed by Izzo can be applied during the overcharge phase in the following way (cf. Figure 37):

- Linearly decreasing current ramps are periodically imposed on the battery (e.g. the period to execute the current ramps is 20 minutes) and the voltage decreases as well.
- While the current share for gassing is high, the voltage value stays high (high level).
- While the current share for gassing is almost negligible, the voltage transients toward the gassing value ( $V_{GAS}$ ). The current at this gassing value is the charge acceptance.

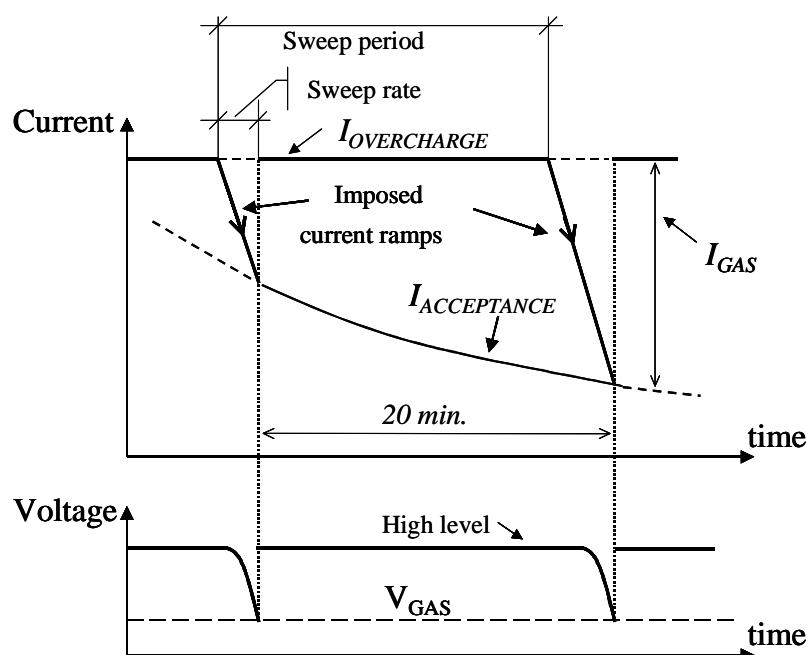


Figure 37: Principle of current ramp method: at overcharge, periodically, e.g. every 20 minutes, the current follows a decreasing ramp. When the gas evolution is almost zero the battery voltage reaches a gassing value. At this moment, charge current response is obtained and the current is reestablished to the overcharge value [48].

### 2.2.1.2 Experimental

Laboratory experiments were carried out to answer the two following questions for a given battery at charge:

- What is the gassing voltage value?
- What is the charge acceptance response of the battery at this gassing value?

It is known that the presence of a maximum in  $dV/dI$  versus current ramps, or in other words the appearance of the voltage inflection point, indicates the gassing point (cf. 2.1.5.1). With such way, the question of the gassing voltage must to be no longer posed: whatever the alloy type, the temperature or the battery age, the crossing of the charge acceptance has to be observed by a transient phase between a high voltage, associated to the gas evolution, and a low voltage, related to the proper charge. The expected behavior has to consist of an inflection point between two voltage levels. The current associated to this inflection point is considered to be the charge acceptance of the battery as it marks a limit between the important current of gas evolution, which fixes the battery voltage at a high value, and a sufficient low gassing current, which does not significantly influence the battery voltage. Determination of this inflection point can be achieved by imposing a decreasing or increasing current ramp onto the battery. We chose operating both variation directions in order to take into account a potential difference.

Regarding the choice of the applied current ramps, the following remarks should be kept in mind:

- The amplitude of the current ramp is also the desirable one to homogenize the electrolyte. This value is usually limited by the standards at  $C/20$ . In order to observe

the gassing point, the current is swept from  $C/20$  to 0 (A) and vice versa. This is the different point compared to Izzo's principle, where the current ramps decrease linearly and stop at the value at which the voltage reaches a determined gassing value.

- It is desirable that the period at which the current sweep is carried out is long. In contrast, the sweep rate is better to be fast. In fact, the final objective of the overcharge phase is to destratify the electrolyte by applying to the battery a constant current value. The current ramp is just a step to measure and up date the charge acceptance value. Therefore, the period to execute this measurement step should be long and the sweep rate should be quick to preserve the characteristic of the overcharge phase and the characteristic of an accelerated charge.
- The saw-toothed waveform was chosen instead of half saw-toothed waveform illustrated in the principle to verify the gassing point, as the transient phase would occur two time, in the ramp-down as well as in the ramp-up direction.

The charge process is done at the current regulation mode without voltage restriction.

The tests were operated on the flooded lead acid battery 12V-70Ah, Monobloc Equipa-Fulmen 070430 A-A, used in photovoltaic applications.

The battery was subjected to several charge/discharge cycles as follows:

- Discharge of 3 Ah; current ramp charges in which ramp amplitudes were 2, 4, 10 or 30 minutes.
- Discharge of 15, 30 Ah and complete discharge with the voltage limit at 10 V; current ramp charges with 10 minute ramp amplitude.
- Discharge of 15 Ah; normal charge at 3 A constant current with 14.5 V limit voltage.

The depths of discharge were chosen in such a manner that a discharge-charge cycle could be done during a working day shift (less then 8 hours).

The current ramps were supplied by a bipolar alimentation and amplifier (KEPCO BOP 20-20M), which is controlled by a function generator (HP 33120A).

The battery voltage and current and temperatures of the battery and of the ambient are recorded using JUMO Logoscreen 500.

### 2.2.1.3 Results and discussion

Figure 38 shows voltage and current profiles during a current ramp charge process as a function of time. Looking at the voltage profile, it is clear to distinguish charge and overcharge profiles separated with the transient phase. At charge, the current sweep does not produce a considerable variation on the voltage profile compared to the one at overcharge. This can be easily explained in observing again the Figure 33.

During the charge phase, the voltage profile is determined by the active material charge reaction. The gassing current is almost negligible (cf. Figure 33, b). Therefore, while the current is swept from high to low value or vice versa, the voltage is always determined by the active material charge current. As the charge acceptance decreases steadily, its value happens to reach the maximum current value. This is done in the transient phase.



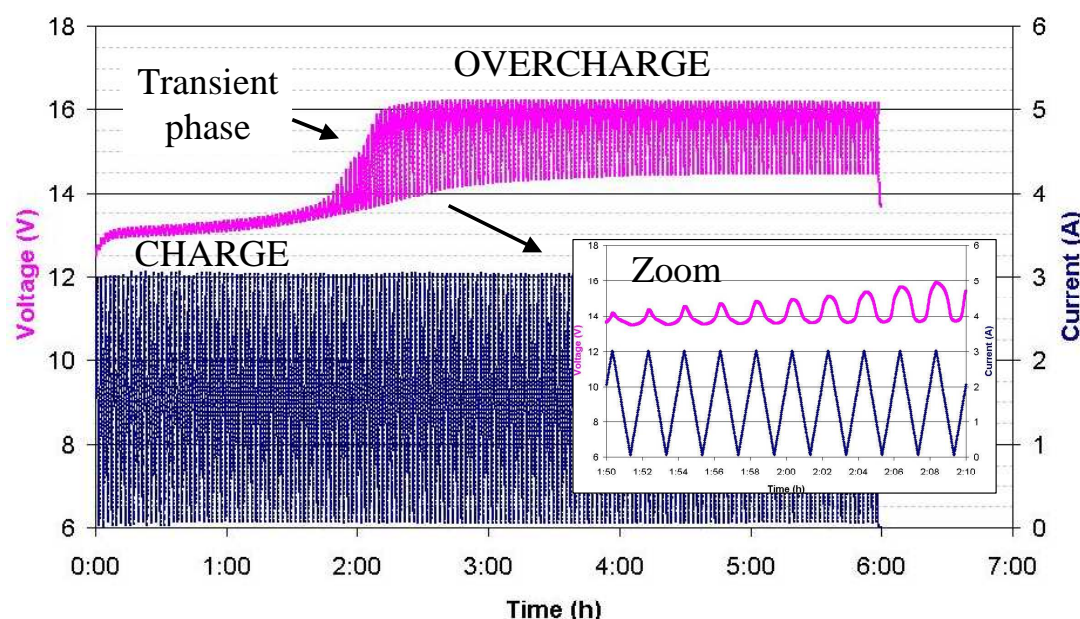


Figure 38: Voltage and current profiles vs. time in a charge with current ramps of 2 minutes (1 minute ramp-up + 1 minute ramp-down). The charge phase, the transient phase and the overcharge phase are obviously observed at the voltage profile.

At overcharge (phase C) the maximum value of the current always exceeds the charge acceptance of the battery. The voltage profile is determined by the gassing current profile as the acceptance current is very low and its profile stays below the gassing profile (cf. Figure 33, c). While the applied current decreases (ramp-down), the overcharge point would transfer to the charge point where the voltage is defined again by the proper charge current. During the ramp-up, in contrast, the increase of the applied current involves the transfer of the charge point to the overcharge point where the voltage depends on the gassing current. As shown in Figure 38, beyond to the transient phase, the voltage increases slightly at the beginning, then stays almost stable when the current is at the maximum injected value, 3 A. This confirms the fact that the voltage is determined by the gassing current and the charge acceptance is almost negligible or the battery is no longer charged.

So the first conclusion that can be made is that sweeping the current from a low value to values beyond to the charge acceptance value can provoke the charge/overcharge transition and vice versa.

The primary objective of the test is to find the gassing voltage point that induces the charge acceptance response of the battery. Figure 41 shows an extract of voltage and currents profile during the overcharge. In this case, the inflection value is 14.7 V for both ramp-up and ramp-down directions. However, the two correspondent charge acceptance values are not the same, for instance they are 0.3 A and 1 A for ramp-down and ramp-up respectively at 2 hours 33 minutes of charge.

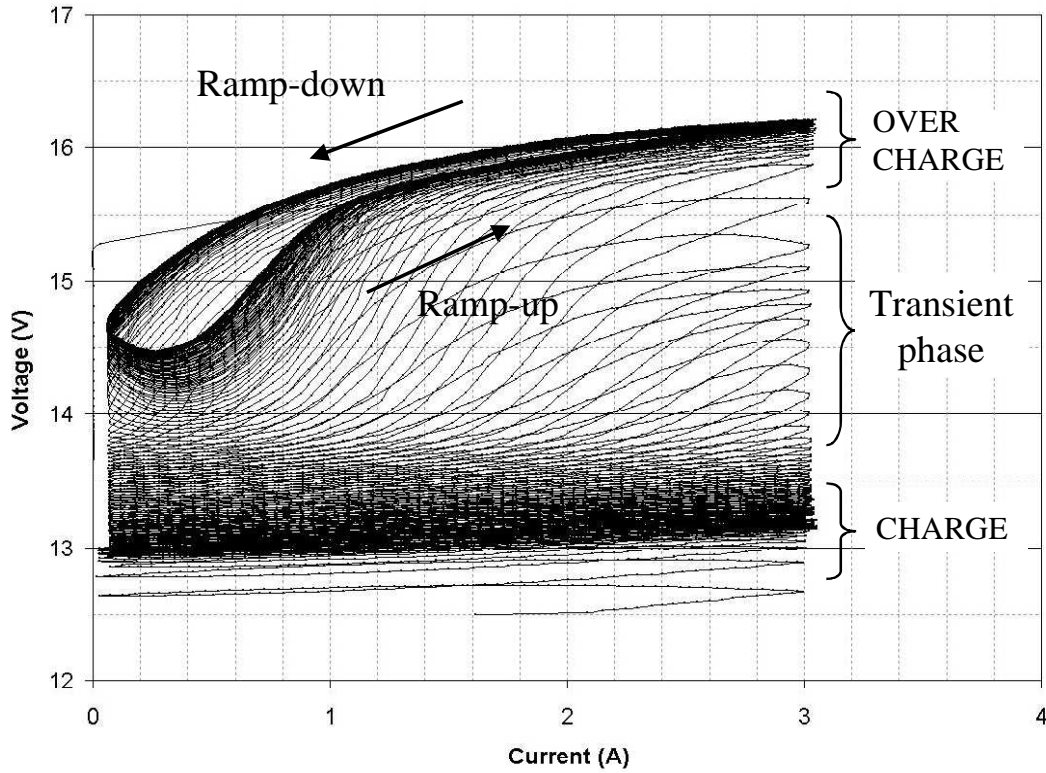


Figure 39: Voltage profile vs. current in a charge with current ramps of 2 minutes (1 minute ramp-up + 1 minute ramp-down): charge phase, transient phase and overcharge phase are obviously observed.

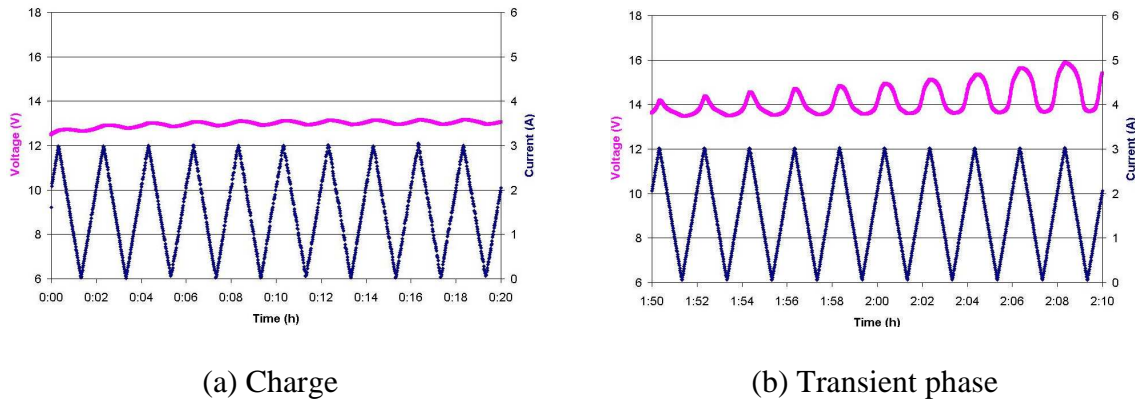


Figure 40: Zooms on voltage and current profiles at charge (a): current sweep does not produce a considerable variation in the voltage profile, at transient phase (b): voltage begins to increase considerably with current sweep.

Figure 42 represents the charge acceptance response of the battery at the gassing voltage of 14.7 V during overcharge. At this same value, there were two profiles of charge acceptance correspond to the ramps-down and ramp-up. An average difference of 0.6 A is found between them, with the charge acceptance profile of ramp-up being higher position. This difference, current-voltage hysteresis, can be associated to the process of charge and discharge of the double layer capacitance when the current increases and decreases [52, 53]. Another remark is that these both current profiles have a normal form of the battery charge acceptance, they follow the asymptotic profile to a low value.

The same discharge/charge cycles were carried out with lower sweep rates, at 4, 10 and 30 minutes. Using the same definition of gassing point, the gassing values are equal to 14.5, 14.0-14.3 and 13.9-14.3 V at 4, 10 and 30-minute ramp charges respectively. Figure 43 illustrates the correspondent charge acceptance profiles at these gassing points.

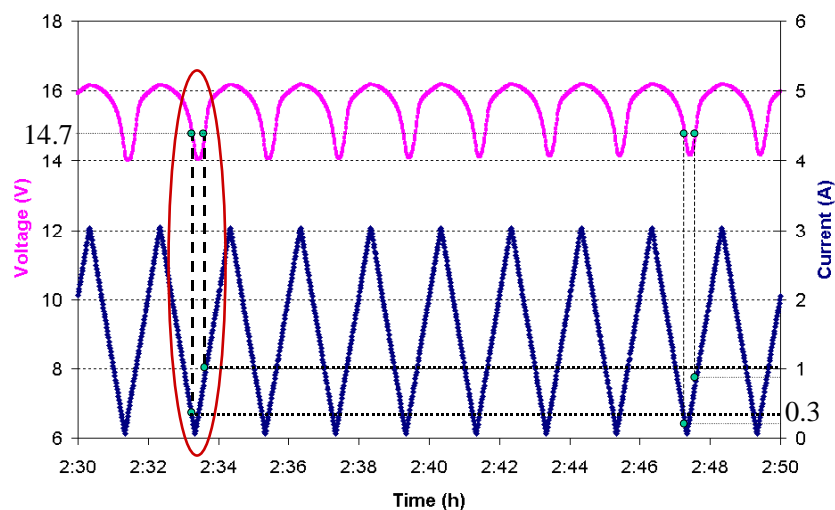


Figure 41: Zooms on voltage and current profiles at overcharge: at inflection points of voltage profile, it equals to 14.7 V in this case, charge acceptance response of the battery is obtained. Corresponding to ramp-down and ramp-up, there are two different values of charge acceptance.

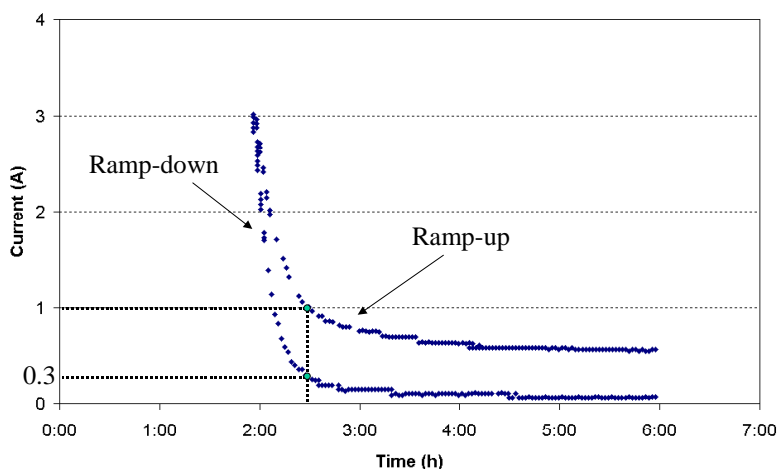


Figure 42: Charge acceptance response of the battery at 14.7 V gassing value. Two different charge acceptance profiles were obtained. Charge acceptance profile of the ramp-down is about 0.6 A lower than the one of the ramp-up.

These remarks are obvious:

- Hysteresis almost does not change in decreasing the sweep rate from 2 to 4 minutes. The noticeable decrease of hysteresis is observed at 10 minutes (0.4 A instead of 0.6 A) at 4 minute ramps. Even at 30 minute ramp, a 0.2 A hysteresis is still present. So it can be seen that hysteresis decreases with a decrease of sweep rate. It should be kept in mind also that if the sweep rate is decreased several times, the charge acceptance response corresponding to the ramp-up and ramps-down could not be the same because the charge acceptance varies with charge time.

- When decreasing from 2 to 10 and finally to 30 minute, it seems that the charge acceptance profiles corresponding to the ramp-down do not change, just the profiles of the ramp-up fall more and more toward the ramp-down ones.

Different cycles with deeper depths of discharge have been carried out with similar results.

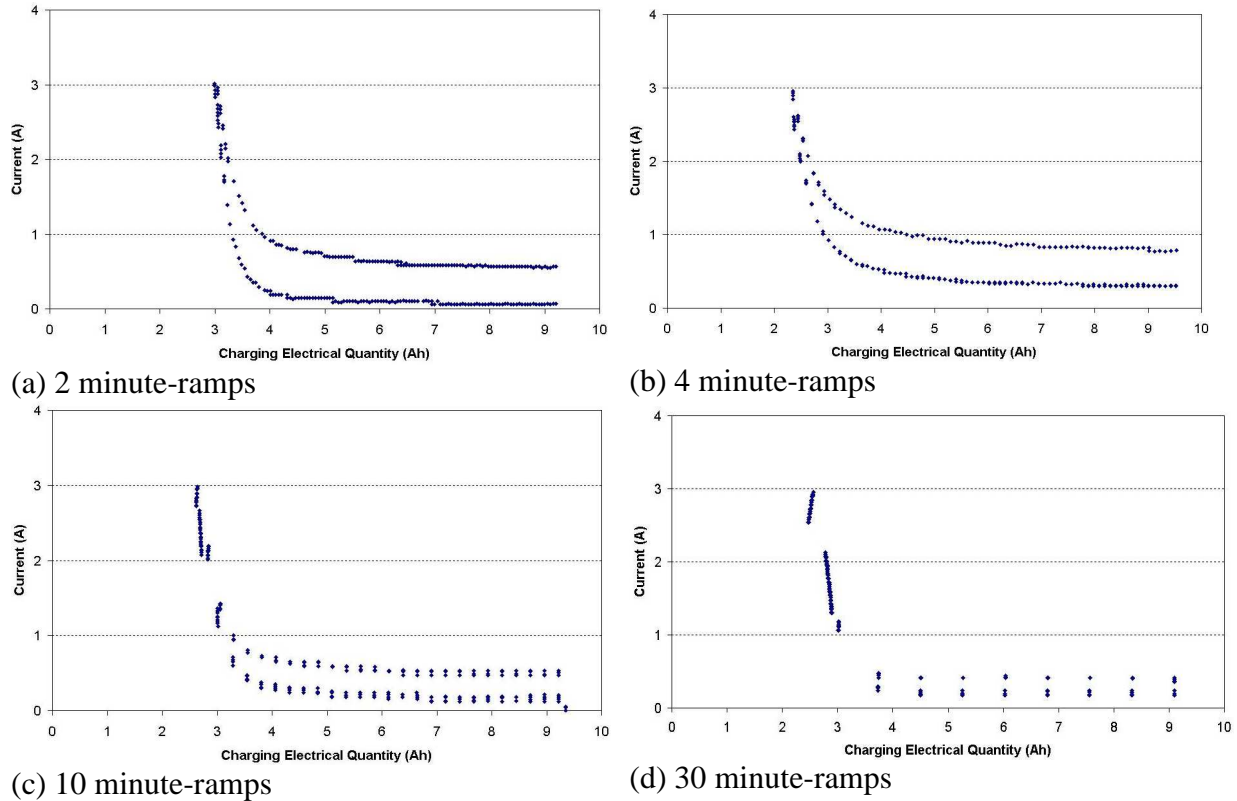


Figure 43: Charge acceptance profile responses of the battery at gassing voltage at different ramp tests, 2 – 4 - 10 and 30 minutes, following a 3 Ah discharge. Voltage-current hysteresis always appears.

#### 2.2.1.4 Conclusions of current ramp method

Using current sweep of ramps can provoke transitions from charge to overcharge and from overcharge to charge. Corresponding gassing points and charge acceptance values can be obtained. Nevertheless, this requires a considerable long sweep rate to limit hysteresis and to have accurate current-voltage information. This is the result why, this method is not suitable to use in those applications requiring accelerated charges.

### 2.2.2 Voltage squares

#### 2.2.2.1 Principle

Two results of the ramp current tests that should be taken into consideration for voltage square tests are:

- Gassing points situate between 13.9 and 14.7 V for a 12 V battery. During charging, it could be sufficient to decrease the battery voltage to these values to determine charge acceptance.

- The ramp form can retard the battery voltage to reach the gassing values. Square form can be used instead to avoid this inconvenient.

Basing upon the charge acceptance definition, the principle of the voltage square method to measure the charge acceptance is resumed as follows: during overcharge phase at constant current, the voltage is periodically brought back to a chosen gassing value for a very short time, called measurement step; at this gassing value, charge acceptance response of the battery is measured. This method, differing from the method of current ramp, requires knowing the gassing voltage value. This value is predicted according to the charge rate and the type of positive grid alloys.

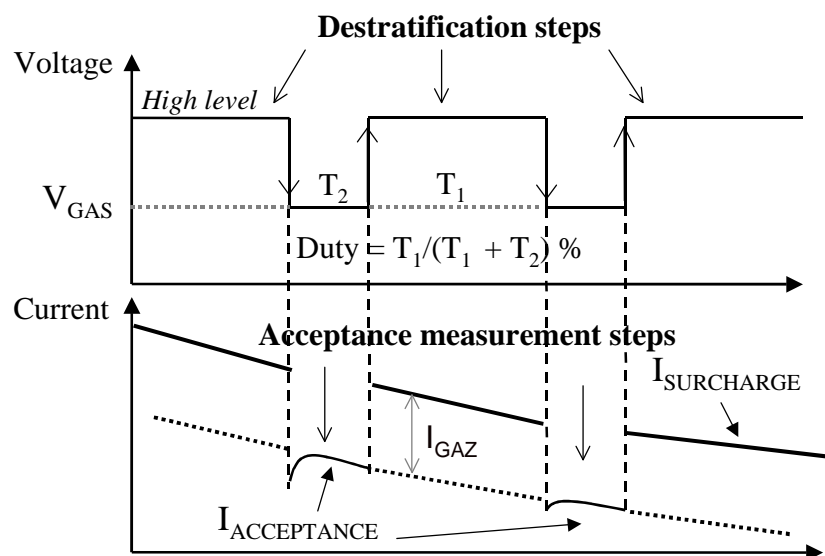


Figure 44: Principle of voltage square method: at overcharge, successive steps of destratification at overcharge current and of acceptance measurement at gassing voltage are periodically applied.

Regarding the duty ratio at which the voltage square is carried out, the efficiency of destratification phase as well as the characteristic of an accelerated charge should be kept in mind as mentioned in the choice of the period and the sweep rate in ramp current method (cf. 2.2.1.2). It is better that voltage squares are executed with a high duty ratio, or in other words with measurement steps as short as possible.

### 2.2.2.2 Experimental

The same equipments of the ramp current tests were used for square voltage tests.

The duty cycle of square voltage was set at 80% (about 3 minute-measurement for every 15 minutes).

Gassing voltage values were chosen taking into account the ramp current test results and even more: 13.8 – 15.0 V.

Different charge rates, 3 – 5 – 10 A, were applied; the results were compared to one another.

The depth of discharge was fixed at 15-20 Ah.



The charge test to measure charge acceptance by voltage squares, called here Charge&Destratification charge test (C&D charge test), is carried out as follows: charge the battery at constant current ( $I$ ) until the battery voltage reaches a determined gassing value ( $V_{GAS}$ ); then overcharge steps at constant overcharge current ( $i$ ) ( $i$  can be manually changed according to charge acceptance value obtained) and charge measurement steps at constant  $V_{GAS}$  are successively imposed. At the overcharge step of  $i$  current, the limited voltage is set at a very high value that the battery will never reach (e.g. 18 V) so that it is alike in the case of no voltage restriction. Every overcharge step and measurement step last 15 and 3 minutes respectively.

Our first cycle of tests consists to evaluate the battery charge acceptance response at different gassing voltage values (from 13.8 to 15.3 V). To simplify the C&D test program, the overcharge current value ( $i$ ) is set to be equal to the constant current of the first charge phase ( $I$ ). They are both fixed at 3 A.

Our second cycle of tests consists to compare C&D charge acceptance measurement with the one obtained at a charge IU (a classical charge without the overcharge phase, cf. 2.1.5). The depth of discharge, the charge rate and the gassing voltage value are the same in both cases (15Ah, 10 A and 14.8 V respectively).

### 2.2.2.3 Results and discussion

#### Evaluate charge acceptance responses of the battery at different gassing voltage values

The first gassing voltage that we tested was 14.5 V and the results are presented in Figure 45.

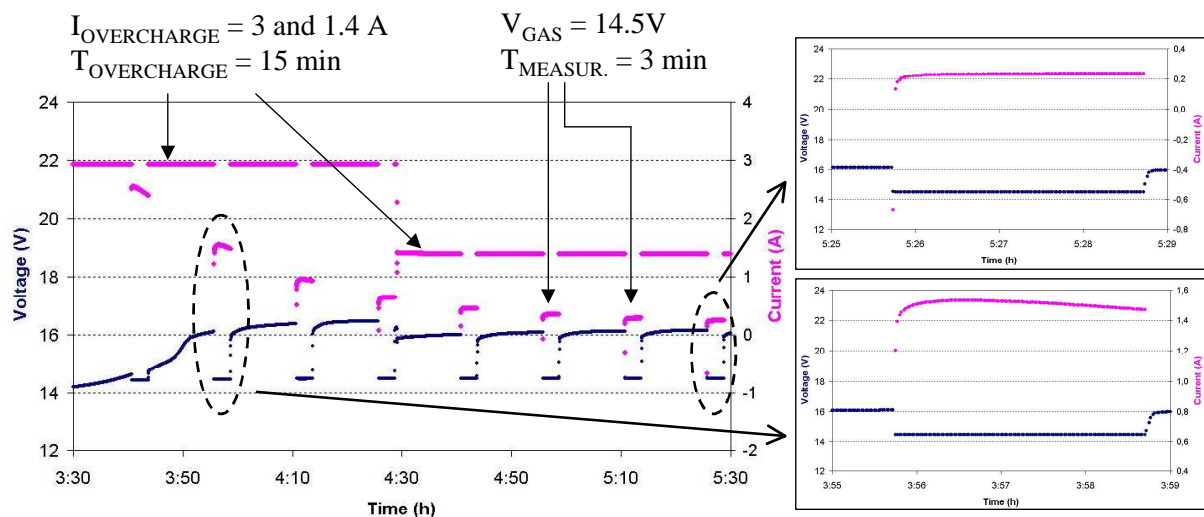


Figure 45: Voltage and current of the battery are presented as functions of time during a charge test with acceptance measurement by voltage square method (C&D test): successive steps of overcharge for 15 min at 3 A and 1.4A and of acceptance measurement for 3 min at 14.5V gassing voltage were periodically done. Two zooms on the current profile at 14.5 V gassing voltage show transient values, sometimes negative, at the beginning of the acceptance current measurement steps.

It can be observed that while the voltage is brought back to the fixed gassing value at 14.5 V, the current at first drops abruptly to a very low value (that can be negative) for a short time (around 5 seconds) then it increases to reach stabilized values. As mentioned above, this transient phase of current response can be related to the fact that the double-layer capacitance

is discharged when the battery voltage falls from a given potential to a lower one [52, 53]. According to this hypothesis, the higher the voltage gap between the overcharge value and the gassing value, the more deeply the double layer capacitance is discharged and therefore the lower the current falls down before stabilizing. This is confirmed by results of C&D tests with gassing values of 13.8 V and 14.8 V.

From the Figure 46, it is clear that at 13.8 V the current falls down to very negative values (-12 A), and takes about 1 minute 30 seconds to stabilize, while at 14.8 V the current becomes stable after some seconds (5 seconds) as shown on Figure 47.

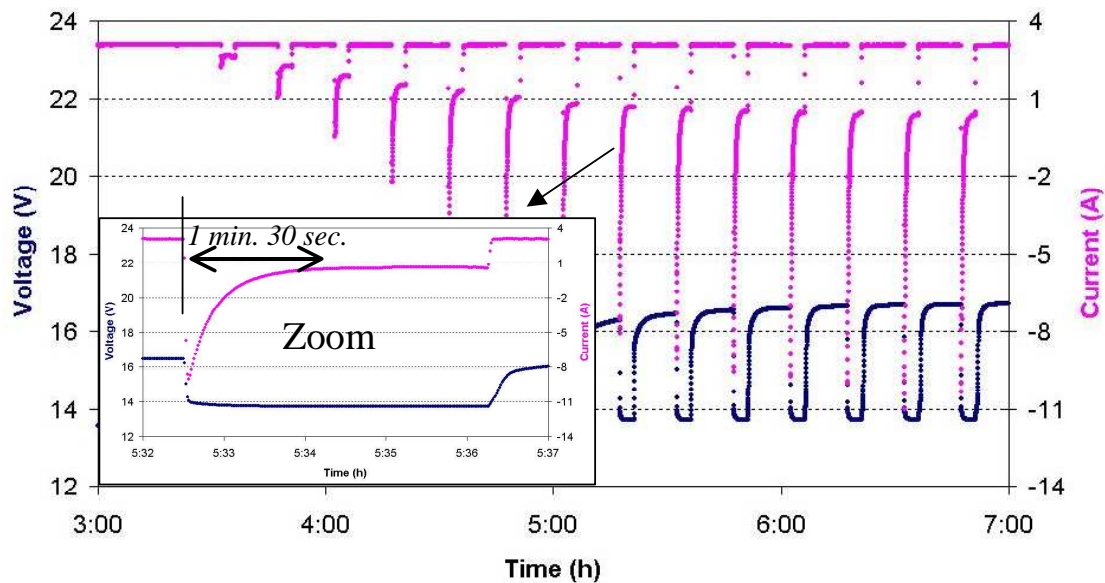


Figure 46: C&D test with 13.8V gassing value: successive steps of overcharge lasting 15 min at 3 A, and of acceptance measurement lasting 3 min at 13.8 V were periodically done. Zoom on the current profile under 13.8 V shows very negative transient value at the beginning of acceptance current measurement step.

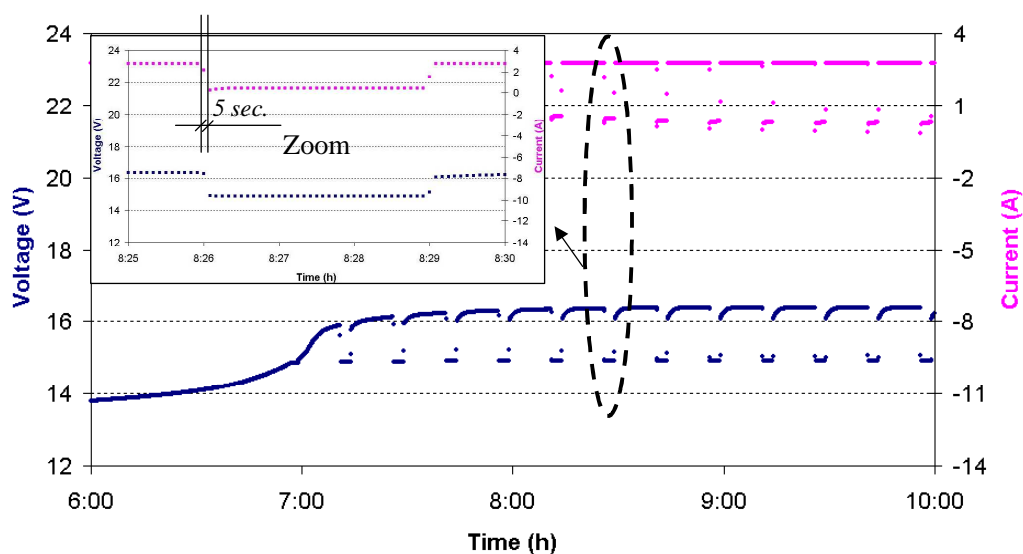


Figure 47: C&D test with 14.8V gassing value: successive steps of overcharge for 15 min at 3 A, and of acceptance measurement for 3 min at 14.8 V were periodically provided. Zoom of current profile under 14.8 V shows that charge acceptance is almost stabilized after 5 seconds.

The voltage gap between the overcharge and the gassing value should not be too high to avoid negative transient current values. This voltage gap depends directly on two factors: the applied overcharge current, which decides overcharge voltage and the set gassing voltage. As mentioned above, overcharge current is controlled in such a manner that share current for gassing is limited at  $C/20$ . So one way to reduce this voltage gap is to increase the imposed gassing value. But, it should be noted that, increasing gassing voltage means increasing gas evolution (cf. 2.1.5.1). Anyway, this share current for gassing during charging the acceptance measurement step can be estimate and accounted also for electrolyte destratification. Moreover, what is accounted is the imposed share current for gassing which is far stronger than the gas evolution current under the gassing voltage.

### Comparison of charge acceptance measured in C&D test with the one in IU test.

It is shown in Figure 48 that the current values measured at 14.8 V in C&D test forms a current profile that matches well with the one obtained from IU charge.

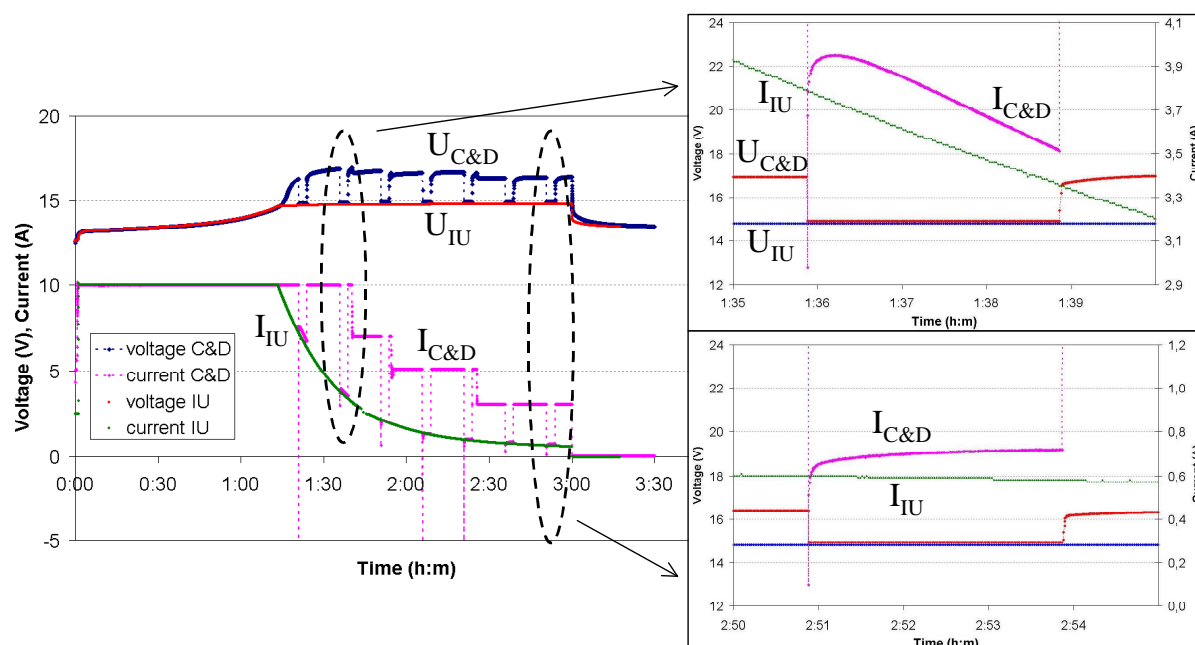


Figure 48: Comparison of the charge acceptance measured by C&D test and the charge acceptance obtained from IU charge. Gassing voltage was set at 14.8 V for both tests. Regardless of the transient values, charge acceptance measures of C&D test matches well with charge acceptance at a fixed gassing voltage of IU charge.

Now let's take a closer look in zooming two measurement steps at the beginning and at the end of the overcharge phase of the C&D test. As already observed, there is always a transient phase at the beginning of measurement steps. Transient values are far lower than the charge acceptance values of IU charge. Then the current increases and follows a profile that is almost parallel with the charge acceptance profile of the IU charge, but slightly greater. In this case of 14.8 V, it takes about 5 seconds to get rid of the influence of this transient phase shown in both zooms of Figure 48. So two situations can happen regarding the data obtained:

- If current data is measured at a transient point (e.g. earlier than 5 seconds) its value can be negative and it is a wrong charge acceptance value.



- If current data is measured beyond 5 seconds, this value can be a little smaller or higher than the one of charge acceptance, but stays close to it.

The first situation, especially when data measured is negative, should be avoided. The second situation can be used despite of a little gap between the two charge acceptance values because this difference is just some hundreds mA, it is small compared to  $C/20$  (3.3A for a 70 Ah battery) that is the recommended gassing current for destratification. Moreover, it is possible to take into account this difference when setting the percent of electrical quantity.

#### 2.2.2.4 *Conclusions of voltage square method*

C&D with voltage square test gives promising results for the charge acceptance measurement, which match well with the ones obtained from an IU charge at the same gassing voltage value. Nevertheless, set gassing voltage values at which charge acceptance measurement steps are carried out and the duration of these steps as well as the moment to get the current data have to be set in such a manner to avoid inaccurate voltage-current information. Many experimental tests show that gassing values should be between 14.3-14.8 V for a 12 V battery and duration of about 5 seconds is convenient to measure and collect the data.

This method can be used in accelerated charges as well as in fast charges.

### 2.3 NEW CHARGE ALGORITHM WITH EARLY DESTRATIFICATION FOR ACCELERATED CHARGES

Nowadays, many applications of lead acid batteries require reduction of the charge duration, for instance, a 4 hour-charge for lead acid batteries in grid energy storage or 1 hour-charge for lead acid batteries in electric buses. Such reductions of charge time imply the use of a new charge process.

One way to reduce the charge duration is to perform an early destratification step without waiting for the end of charge. Early electrolyte destratification by gassing is possible. It can start as soon as the power of the charger is available, i.e. as soon as the charge acceptance becomes lower than the nominal current of the charger. However, limitation of this gassing is not possible using traditional charge methods when charge acceptance is higher than  $C/20$ . Indeed, not only the current value share for destratification (gassing current) can become too high and damage the battery, but also it becomes very difficult to estimate and thus to control the electrical quantity supplied for the destratification.

The new charge method proposed here (Charge&Destratification charge method – C&D) focuses on the reduction of the charge time for vented lead acid batteries using early destratification, which is performed and controlled using charge acceptance measurements during the charge.

#### 2.3.1 Objectives

This new charge method aims to reduce the charge time for flooded lead acid batteries in controlling the destratification phase as follows:

- Starting early the destratification phase, when the charge acceptance is not yet negligible. Practically, destratification can start as soon as the charge acceptance becomes lower than the charger nominal current.
- Controlling the total electrical quantity for gassing (or for destratification); for instance 7% of the total charged electrical quantity.
- Maintaining the gassing current at a value not too high.

### 2.3.2 Principle

Figure 49 represents the principle of the C&D charge method with early destratification in order to reduce charge time, consisting in the following steps:

- *I* step at constant current or constant power during which the voltage increases continuously up to the gassing voltage  $V_{GAS}$ . This step is similar to the *A* phase of the IUi charge (Figure 32).
- *IIa* steps, dedicated to charge acceptance measurement. These steps consist in fixing the voltage at  $V_{GAS}$ . To get rid of transient effects, a certain latency time is included between the voltage fixation and the current measurement. This latency time is a few seconds, for instance 3 to 10 seconds.
- *IIb* steps of overcharge during which an overcharge current  $I_{OVERCHARGE}$  is supplied to the battery.  $I_{OVERCHARGE}$  is determined from the measured charge acceptance  $I_{ACCEPTANCE}$  and a convenient gassing current  $I_{GAS}$ :

$$I_{OVERCHARGE} = I_{ACCEPTANCE} + I_{GAS} \quad (54)$$

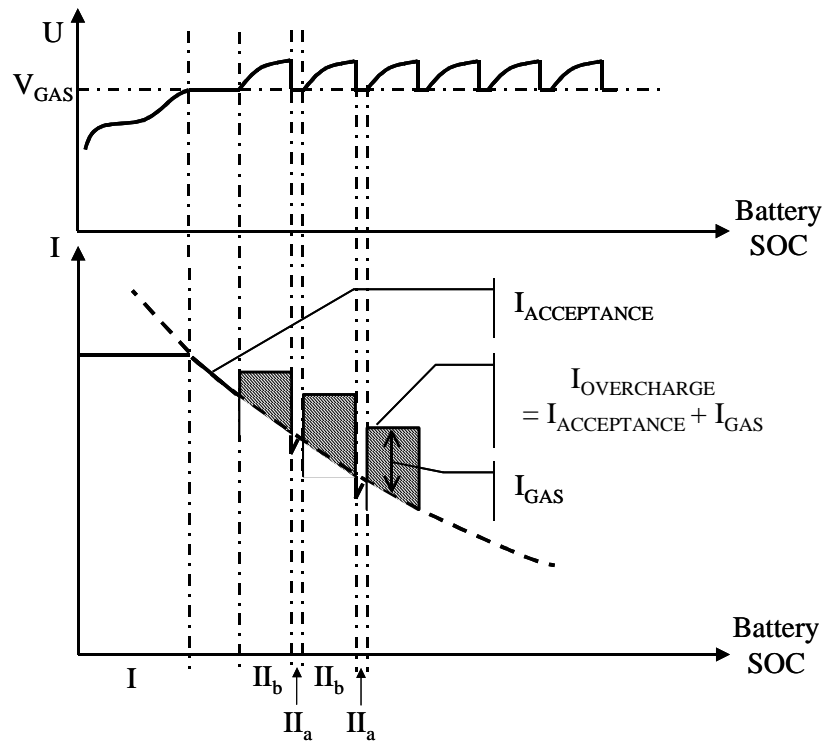


Figure 49: C&D principle to reduce charge time for flooded lead acid batteries: (*I*) constant current step, (*IIa*) charge acceptance measurement steps at gassing voltage, (*IIb*) overcharge steps at overcharge current ( $I_{OVERCHARGE}$ ) which equals to the total sum of charge acceptance ( $I_{ACCEPTANCE}$ ) and gassing current ( $I_{GAS}$ ):  $I_{OVERCHARGE} = I_{ACCEPTANCE} + I_{GAS}$ .

Two ways to determine a convenient gassing current value are considered:

- For the shortest duration of charge, gassing current  $I_{GAS}$  is set at the maximum value the battery can afford (e.g. C/20).
- For applications where the charge duration is set in advance (e.g. 4 hours), gassing current  $I_{GAS}$  is calculated taking into account the electrical quantity for destratification ( $Q_{DES}$ ) and the remaining charge time ( $T_{remain}$ ).

$$I_{GAS} = Q_{DES} / T_{remain} \quad (55)$$

The  $Q_{DES}$  is calculated as a function of the depth of the preceding discharge. As mentioned above, during the first charge step at constant current, i.e. from the beginning of the charge to the moment when the battery voltage reaches the gassing value, 60 to 90% charge is accomplished. In practice,  $Q_{DES}$  can be set as a percentage, e.g. 15%, of this electrical quantity that has been provided to the battery during the first step of the charge (*I* step).

In order to update regularly the charge acceptance value, the *Ila* and *Ilb* steps are repeated  $n$  times until  $Q_{DES}$  is reached.

### 2.3.3 Experimental

In the context of MICROSCOPE project - Grid connected inverter combined with energy storage for production optimization – a 4-hour charge algorithm of C&D type has been developed at EDF R&D in cooperation with Montpellier II University. This algorithm is integrated to 12 and 48 V commercial chargers of IES-Synergy Society without any modification of the charger maximum power.

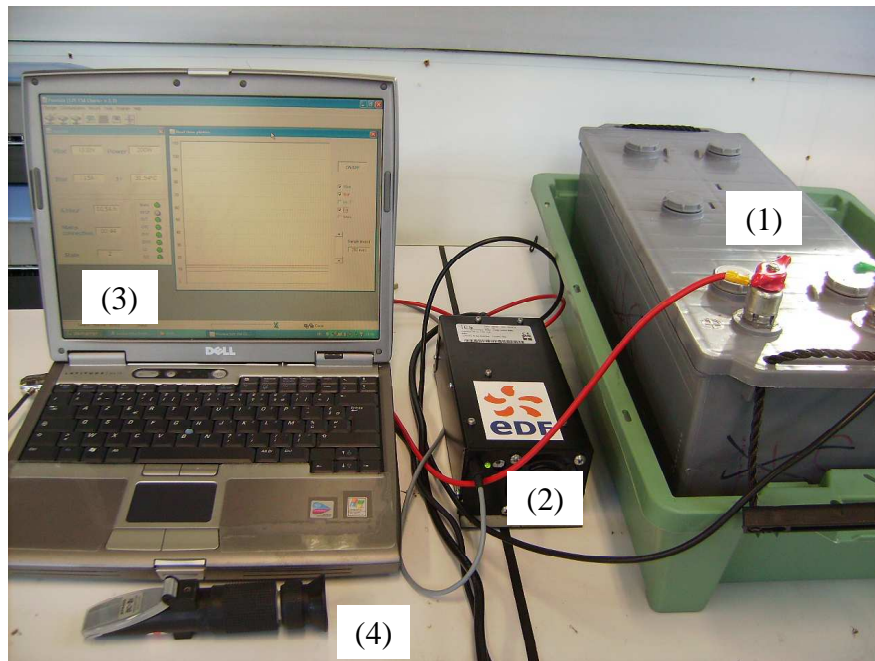
Table 5: IES-Synergy charger: electrical characteristics, integrated C&D and IU*i* charge profiles

Electrical characteristic of the IES-Synergy charger	Max output power: 222 W $\pm$ 3% Max output current: 15 A $\pm$ 2% Nominal battery voltage: 12 V
C&D charge profile (Figure 49)	$V_{GAS}$ : 14.6 V $Q_{DS}$ : 11% of total charged Ah during I step $I_{GASmax}$ : C/20 $I_{GAS}$ : $Q_{DES}/T_{remain}$ Total charge duration: 4 hours Duration of $II_a$ step: 5 seconds Duration of $II_b$ step: 60 seconds
Traditional charge IU <i>i</i> profile (Figure 35)	$V_{GAS}$ : 14.6 V $I_1$ : 15 A $I_2$ : 3 A Duration of the overcharge phase: until 17% of charged Ah accepted during phase A and phase B is obtained

In this application, batteries are charged by the grid during the night at lack period, i.e. from 1 to 5 am, and by the photovoltaic panels during the day except during the time when they supply energy to the grid. They are usually discharged in average of about 50% DOD.

The C&D charge and the traditional IU*i* charge are achieved by IES-Synergy charger using a prototype of compressed lead acid battery 140Ah/12V developed at EDF R&D. The battery was charged with a IU*i* profile followed with a 8-hour charge at 14.6 V then discharged at

50% DOD before being tested with the IES-Synergy charger. These cycles were operated with BITRODE Battery Charge and Test System, Module Type LCN 200A – 12V.



*Figure 50: Montage of the charge of the compressed battery (1) with either IUi or C&D profiles using the 12 V commercial charger IES-Synergy (2); voltage and current are at the output of the charger recorded by Provista logical via computer (3; electrolyte density is measured by the Battery Coolant Checker (4).*

During charging with IES-Synergy charger, the charged electrical quantity, the voltage and the current at the output of the charger were recorded by Provista logical via a computer. Battery voltage and current were measured by HOBO logical (via a shunt to measure the current). The electrolyte density is manually measured at the top of the battery using Atago Refractometer BC-2E – Battery Coolant Checker.

### 2.3.4 Results and discussion

Figure 51 shows the battery voltage, battery current and measured density profiles during the C&D charge. In the  $I$  step of constant current, the measured charge acceptance and the gassing current are clearly observed. This means that the duration of the charge acceptance measurement at 5 seconds can ensure accurate information of the battery current response. On the voltage profile, a slight increase of  $V_{GAS}$  is observed which can be explained by the contribution of drop voltages on the cables. These drop voltages, depending on the resistance of the cable and the current flow, decrease with the decrease of the charge current.

The  $I$  step at 15 A lasts about 3 hours, meaning that 45 Ah is charged. According to the C&D algorithm, the  $I_{GAS}$  has to be 11% of this value, so 4.95 A. As soon as the battery voltage reaches 14.6V, the overcharge step is done to homogenize the electrolyte. At the beginning of this step, the  $I_{OVERCHARGE}$  is limited at 15 A by the maximum output current of the charger then it is equal to about 3 A. It means that during 1 hour of early destratification, the overcharged Ah is less than 3 Ah, so 6.7%, which is less than 11% expected. In this case, the setting of  $I_{GAS}$  at 3 A instead of 4.95 A programmed was due to a calculation error of the program integrated in the charger.

Nevertheless, an obvious improvement of the electrolyte density stratification can be observed when using the early destratification. This result fits with the electrolyte density evolution illustrates on Figure 31 showing that most of the stratification is removed with a 5% overcharge. During the  $I$  step at constant current, the density increases slightly with the battery voltage. As soon as the  $I_{OVERCHARGE}$ , which is the sum of the measured charge acceptance and the calculated gassing current, is applied the density increases with an obvious higher rate. This reveals that the early destratification process has effectively started. After 4 hours of charge, the electrolyte density at the top is around 1.26. It should be noted here that, at the end of this C&D charge, the acceptance is still high, 6.5 A. This shows that C&D charge is, of course, not a complete charge, but is just a partial charge. This is the second reason why the electrolyte density is not higher.

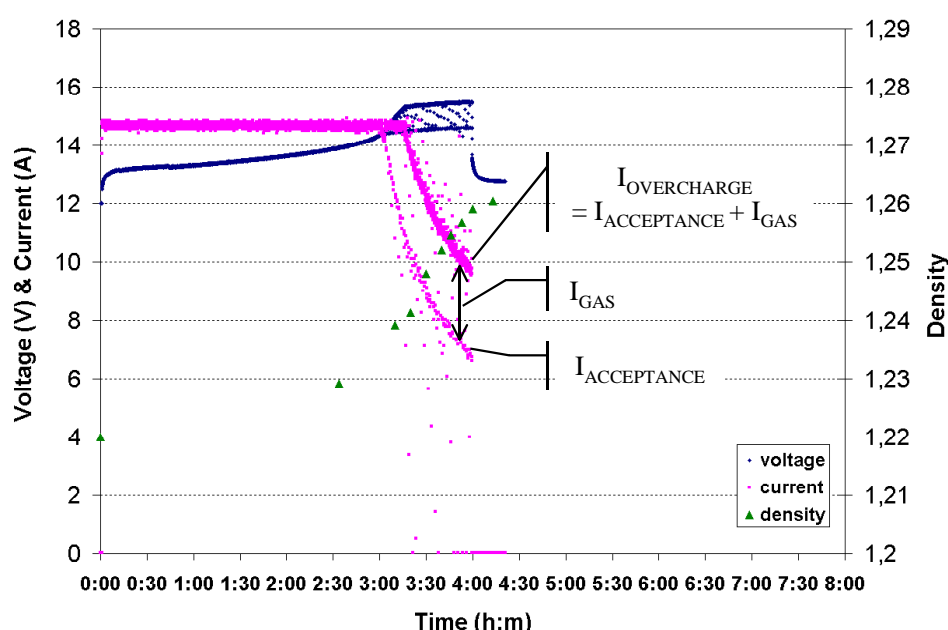


Figure 51: Voltage, current and electrolyte density profiles measured during C&D charge. The battery had been discharged with 50% DOD. The total charge time was 4 hours.

A traditional IUi charge was also operated on the same battery (cf. Table 5). Results of this charge, battery voltage, current and electrolyte evolutions, are illustrated in the Figure 52. Similar to the C&D charge, during the  $I$  step at constant current, the density increases slightly. When the battery voltage reaches the gassing value, 14.6 V, the density increases faster phase after phase. Electric quantity during the 3<sup>rd</sup> phase is 17% of charged Ah during the first and second phases ( $I_1 + U$ ). The electrolyte density reaches 1.275 at the end of charge lasting 7 hours 15 minutes.

Compared to C&D charge, at IUi charge without early destratification, after 4 charge hours, the electrolyte density is about 1.235, which is lower than in the case with early destratification, i.e. 1.26. This confirms again efficiency of the early destratification. It is clear that, within 4 hours of C&D charge, the battery is not charged as well as in the case of 8 hours of traditional IUi charge regarding the state of charge. But, within half reduced charge duration compared to a traditional IUi charge, it can be acceptable in condition that refresh charge is periodically achieved to establish a good state of charge, e.g. once a week.

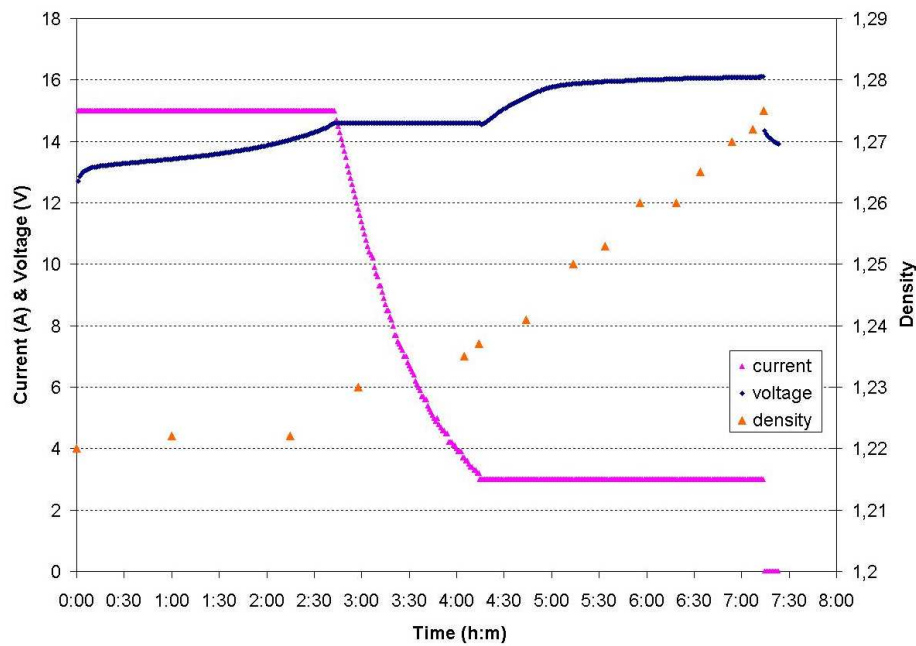


Figure 52: Voltage, current and electrolyte density profiles measured during IU charge. The battery had been discharged with 50% DOD. The total charge time was 7 hours 10 minutes.

### 2.3.5 Conclusions

A new charge method is proposed for fast charges and accelerated charges using early destratification with charge acceptance measurements. The following conclusions can be drawn:

- The overcharge phase, which begins as soon as the charge acceptance becomes lower than the maximum output current of the charger – the early destratification phase, can efficiently homogenize the electrolyte.
- Thanks to the charge acceptance measurement, the overcharge current as well as the electrical quantity for destratification can be calculated and controlled.
- The charge time can be reduced with a factor of two compared to a traditional IU charge with the same charge regime. This factor can be higher if increasing the initial charge rate. Accelerated charges should be used only if fresh charges are periodically achieved to re-establish a good state of charge of the battery after several accelerated charges.

## Conclusion of chapter 2

Electrolyte stratification is a common problem of vented lead acid batteries, in which the electrolyte on the bottom tends to be more concentrated than at the top. The stratified battery, exposed to accelerated aging process, loses its capacity prematurely. One way to homogenize the electrolyte is to provoke a sufficient strong gas circulation to mix the electrolyte by a forced convection.

It is known that gas evolutions due to water electrolysis always occur at the same time with charge reactions in lead acid batteries. They increase with the increase of the charge voltage and become noticeable beyond a gassing point, called gassing voltage. At this gassing voltage, charge current contributes mostly to proper charge reactions, or in other words the battery is charged with its charge acceptance. The definition of the charge acceptance in this thesis is the current response of the battery at a gassing voltage. Therefore, a noticeable gas flow can be produced by applying a current superior to the charge acceptance, or by applying a voltage that exceeds the gassing value; this is called the destratification phase.

The destratification by gassing is necessary for battery longevity, but the gas current has to be controlled to prevent the shedding of active materials, the depletion of the electrolyte and the excessive hydrogen evolution, which increases the flammability risk. In a classical charge process, which lasts in general from 8 to 14 hours, the destratification phase is achieved at the end where the charge acceptance is sufficiently small to be negligible, so that the current of gas evolution (gas current) is roughly assimilated to the applied current. This makes the evaluation of gas current easier, as well as the global management of the charge. In practice, 10 to 15% of overcharge is supplied to the battery for electrolyte destratification. Nowadays, many applications of flooded lead acid batteries require reduction of the charge duration, for instance, a 4 hour-charge for lead acid batteries used for grid energy storage or 1 hour-charge for lead acid batteries in electric buses. These are called accelerated charge and fast charges. Such reductions of charge time imply the use of a new charge process. In accelerated charges and fast charges, indeed, there is not enough time available for the charge acceptance to become negligible to operate electrolyte destratification by gassing.

In this thesis, we propose to achieve the destratification phase as long as the power of the charger is available even though the charge acceptance is still strong. We then talk about an *early destratification*. In this case, in order to control the gas current, it is necessary to know the charge acceptance. Two methods of charge acceptance measurement were studied and tested. The first method, following the suggestions of P. Izzo, consists to impose from a current value superior to the charge acceptance decreasing current ramps to detect on the response of the battery voltage an inflexion point, which characterizes the gassing voltage. This method, supposed to affranchise the influences of the temperatures, compositions of the positive grid alloy, etc on the obtained results, turns out to be inapplicable for accelerated charges. It appears indeed that the response time of the battery imposes to practice current ramps whose slopes are so slow that the resulting measurement duration becomes incompatible with the concept of “fast” charge. We then replaced the “Izzo’ ramp” with a new method of charge acceptance estimation. This method consists to impose periodically to the battery a voltage that equals to the gassing voltage. This gassing value is predicted according to the charge rate and the battery characteristics. The current response is characterized with a sudden drop of the intensity, which can reach transitorily a negative value, then with a rapid increase. The intensity tends then asymptotically towards the acceptance value. Our experimental results

show that some seconds are enough to obtain an utilizable image of the charge acceptance for the management algorithm of the early destratification phase.

During the charge algorithm with early destratification, as long as the charger power is available, a succession of steps of acceptance measurement at constant voltage and of steps of destratification at a constant current superior than the charge acceptance is imposed to the battery. This sequence - measurement at imposed voltage then destratification at imposed current – is periodically repeated, e.g. every minute.

The modification of a “12 hours” charger with an algorithm of the early destratification, enables the battery to be available for a discharge in duration of the order of 4 to 6 hours. This division of the charge duration of a factor two is obtained without increasing the charger power. Evolution towards a rapider charge requires increasing the initial charge rate, so using more powerful chargers. For a fast charge whose duration is less than one hour, the estimation of charge acceptance is no longer sufficient; one has to take into account its derivative. A patent of EDF and University Montpellier II has been submitted in November 2008 about this subject.



## CHAPTER 3 - DISCHARGE OF LEAD ACID BATTERY – POLARITY INVERSION

### Introduction

Polarity inversion is a frequent phenomenon during deep discharges of lead acid batteries. In general, it is better to avoid this phenomenon because of its harmful effects on the battery. In this thesis, our initial objective is to measure both negative and positive capacities of a cell. As two electrodes have rarely the same capacity, within this operation, the polarity inversion of the electrode, whose capacity is lower, is unavoidable, but one does not know if it concerns a negative or a positive electrode. Utilization of a reference electrode helps answering this question.

The first part of this chapter presents the theoretical principles and hypothesis of lead acid battery polarity inversion. The second part treats this phenomenon in details through results of laboratory experiments on different kinds of conventional lead acid batteries. Two kinds of reference electrodes manufactured ourselves at the laboratory have been used.

### 3.1 THEORY ABOUT THE DISCHARGE OF LEAD ACID BATTERY AND POLARITY INVERSIONS

#### 3.1.1 Reminder of discharge reactions

At the negative electrode:



Correspondent equilibrium potential:

$$E(\text{Pb}/\text{PbSO}_4) = E_0(\text{Pb}/\text{PbSO}_4) + \frac{RT}{nF} \ln \left( \frac{a_{\text{H}^+}}{a_{\text{HSO}_4^-}} \right) = -0.996 - 0.0296 (\log a_{\text{HSO}_4^-} - \log a_{\text{H}^+}) \quad (56)$$

At the positive electrode:



Correspondent equilibrium potential:

$$E(\text{PbSO}_4/\text{PbO}_2) = E_0(\text{PbSO}_4/\text{PbO}_2) + \frac{RT}{nF} \ln a_{\text{H}^+}^3 a_{\text{HSO}_4^-} = 1.631 + 0.0296 (\log a_{\text{HSO}_4^-} + \log a_{\text{H}^+}^3) \quad (57)$$

Overall discharge reaction:



Correspondent equilibrium voltage:

$$E = E(\text{PbSO}_4/\text{PbO}_2) - E(\text{Pb}/\text{PbSO}_4) = 1.931 + 0.0592 \log a_{\text{H}^+} a_{\text{HSO}_4^-} \quad (58)$$

### 3.1.2 Discharge cell voltage and end-of-discharge criterion

As described in chapter 2 (cf. 2.1.2.2), during a charge at a constant voltage, the charge acceptance of the battery decreases following asymptotic profile. This decreasing of charge acceptance can be related to the decrease of the reaction interface area and the increase of the acid sulfuric concentration in the pores of the active material. During discharging at a constant current, a similar phenomenon takes place, and the battery voltage diminishes steadily.

The cell voltage at a discharge can be described by this formulary:

$$V = E - (\eta_a + \eta_d + \eta_r + \eta_{cr}) - RI \quad (59) \text{ (cf. Table 4)}$$

With progressing discharge, the equilibrium voltage gradually decreases because of acid dilution. Furthermore, the gradual increase of the internal resistance with progressing discharge leads to an increase of the polarization and the ohm voltage drop (cf. 1.5.4). These two situations result to the decrease of the cell voltage during discharging.

In general, the discharge is stopped when the cell voltage reaches a voltage limit, called the end-of-discharge voltage, which is specified by the battery manufacturer. This end-of-discharge is fixed by the battery manufacturer in order to avoid deep discharges and the risk of battery polarity inversion, which are critical for both electrodes [1]. During discharging, lead Pb and lead dioxide PbO<sub>2</sub> are reacted with H<sub>2</sub>SO<sub>4</sub> of the electrolyte and precipitated to a new chemical compound, lead sulfate PbSO<sub>4</sub>, whose structure is very different from these original substances. The initial structure of the active material is largely lost when this conversion goes carried too far.

- This is especially critical for the positive electrode, because the conducting bridges between the lead dioxide particles are degraded and the particles may partially lose contact between themselves and with the grid, which means that they can no longer participate in the electrochemical reactions. The mechanical strength of the active material is also weakened when the bonds between the particles re-destroyed and the tendency to material loss (shedding) is increased.
- For the negative electrode, deep discharges are critical because of the danger of reversal. Expanding additives of the active material may then be lost by oxidation.
- The danger that lead dendrites grow during the subsequent recharge is increased in lead acid batteries by the fact that most of the acid is consumed during deep discharge, and the residual electrolyte may become diluted. In such a solution, the solubility of lead is increased markedly and therefore so is the tendency to form thin fibers (dendrites) that surround the separator and form short-circuit when the battery is recharged. As a remedy, often sodium sulfate Na<sub>2</sub>SO<sub>4</sub> is added to the electrolyte to reduce the solubility of lead when the battery is discharged.

In practice, the capacities of negative and positive electrodes are not quite the same. The battery capacity is limited by the lowest electrode capacity. This can be caused by several factors. In general, for batteries at long open-circuit periods, the self-discharge rate of the negative electrode is higher than the one of the positive electrode, especially in the batteries with antimony grid alloys (cf. 4.1.1.3). For heavy-duty batteries, the age mechanisms are not the same at the negative and the positive electrodes. The positive electrode, which suffering for the corrosion phenomenon including the grid growth, formation of electric passivation layers and the degradation of the positive material (cf. 4.1.3.1), usually losses more rapidly its

capacity. The capacity difference of the negative and positive electrodes can be attributed also to designs and manufactures. Some manufactures attempt to over-proportion the negative electrode to prevent it from the polarity inversion during discharging, which can cause the oxidation of expanding additives meaning the definitive lost of these latter. So, when the discharge test is stopped, the capacity obtained is in fact the capacity of either negative or positive electrode and not both of them.

### 3.1.3 Diffusion of sulfate ions

At discharge, the sulfate ions  $\text{HSO}_4^-$  consumed at both electrodes, i.e. at reactive interfaces, are renewed at the positive electrode by diffusion and at the negative electrode by diffusion and migration from the bulk electrolyte (cf. Eq. (21)). The transport of  $\text{HSO}_4^-$  ions is executed in majority by diffusion, as the transference number of  $\text{HSO}_4^-$  is very small, 0.1. The ion current flow in the electrolyte is ensured essentially by  $\text{H}_3\text{O}^+$  ions.

The local concentrations diminish with progressing discharge and the lowest concentration is normally met at the proximity of the reactive interfaces. The cell voltage drop, which marks the end of discharge, can be attributed to the fact that the concentration of sulfate ions tends to zero at the proximity of one of interfaces. It means the diffusion cannot bring any more necessary sulfate ions to the reactive interface to supply the reaction with the demanded discharge rate. This unavailability or too low diffusion of sulfate ions at a demanded discharge rate can be explained taking into account the hindrance caused by the sulfate crystals, i.e. the discharge product, which fills the pores and prevents the sulfate ions to pass through.

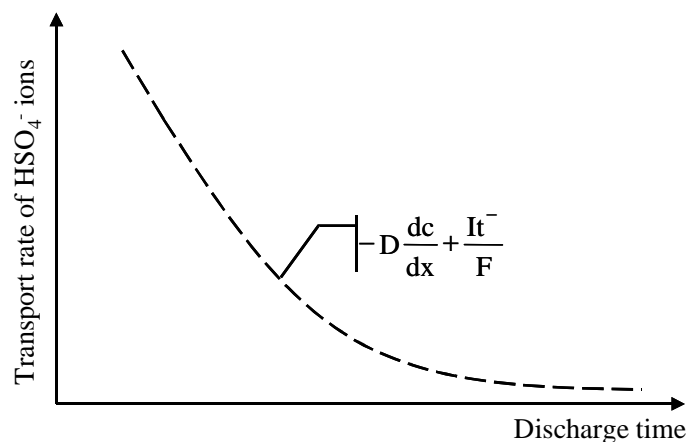


Figure 53: Evolution of the transport rate of  $\text{HSO}_4^-$  ions by diffusion and migration from the bulk electrolyte to the reactive interface as a function of the discharge time.  $\text{HSO}_4^-$  ions are transported essentially by diffusion.

### 3.1.4 Proposed mechanisms of polarity inversion

A definition of polarity inversion of a cell is theoretically given by Gory in [54] is that a cell is inversed when its positive electrodes become negative and vice versa.

As described in 1.1, regarding chemical and structural points of view, the two electrodes are different. So this definition of polarity inversion as well as the possibility for this phenomenon to take place may seem a bit confusing. But it is known that at the end of discharge the two electrodes are covered with the same material, i.e. lead sulfate  $\text{PbSO}_4$ .

Moreover, in the case of lead acid cell, it is known that both two electrodes are, before formation, made of lead oxide ( $\text{PbO}$ ). From these features, inversion is supposed to be possible.

At discharge with polarity inversion, oxidation degrees of lead change as illustrated in Figure 54.

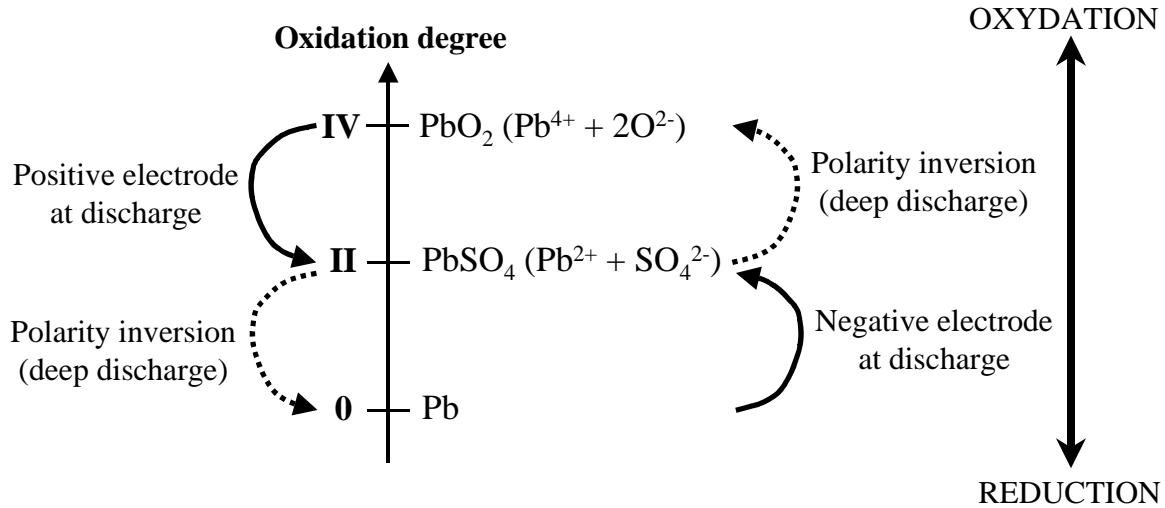


Figure 54: Oxidation degrees of lead; state variations of active materials at discharge with polarity inversion [6]

#### Proposed mechanism by Izzo [48]

Regardless of the total polarization ( $\Sigma\eta$ ) and the ohm voltage drop ( $RI$ ) during discharging, polarity inversion can be attributed to the sign inversion of the electromotive forces  $E$  of a cell. This inversion of a cell consists of two successive inversions of each electrode polarity.

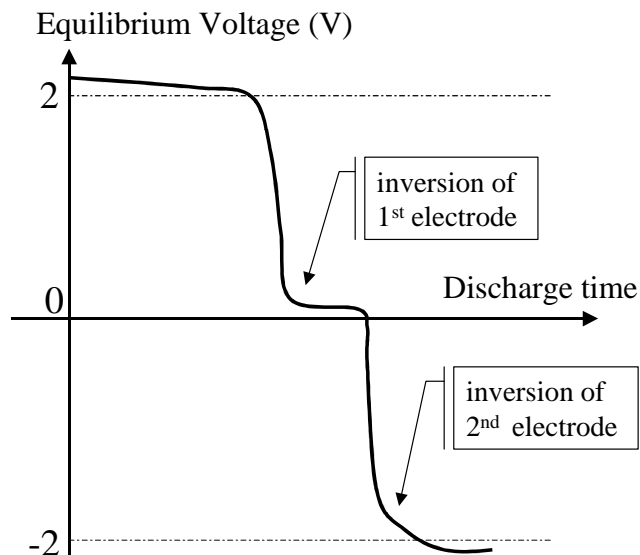


Figure 55: Evaluation of the equilibrium voltage of the cell during discharging with polarity inversions of two electrodes, one after the other [48].

For instance, the polarity of positive electrode is inversed first. While the concentration of sulfate ions tends to zero at the reactive interface of the positive electrode, this leads  $0.0296\log[\text{HSO}_4^-]$  tends toward  $-\infty$  and  $E(\text{PbSO}_4/\text{PbO}_2)$  tends to fall toward  $-\infty$ . As soon as  $E(\text{PbSO}_4/\text{PbO}_2)$  reaches a value which equals or is inferior to  $E(\text{Pb}/\text{PbSO}_4)$ , i.e.  $\leq -0.2996$  V,

$\text{PbSO}_4$  is converted to  $\text{Pb}$ . The discharge of the positive electrode becomes the charge of the negative electrode. The equilibrium voltage of the cell becomes:

$$E_{\text{Mi-INVER}} = E(\text{PbO}_2 / \text{PbSO}_4) - E(\text{Pb} / \text{PbSO}_4) = E(\text{Pb} / \text{PbSO}_4) - E(\text{Pb} / \text{PbSO}_4) = 0 \quad (60)$$

Then at its turn, the negative electrode polarity is inverted.  $0.0296 \log[\text{HSO}_4^-]$  tends toward  $+\infty$  and  $E(\text{Pb} / \text{PbSO}_4)$  increases toward  $+\infty$ . It meets the value of  $E(\text{PbSO}_4 / \text{PbO}_2)$  and  $\text{PbSO}_4$  is consumed to produce  $\text{PbO}_2$ . The discharge of the negative electrode becomes the charge of the positive electrode. The equilibrium voltage of the cell becomes:

$$\begin{aligned} E_{\text{INVER}} &= E(\text{PbO}_2 / \text{PbSO}_4) - E(\text{Pb} / \text{PbSO}_4) = E(\text{Pb} / \text{PbSO}_4) - E(\text{PbO}_2 / \text{PbSO}_4) = -E \\ &= -1.931 - 0.0592 \log a_{\text{H}^+} a_{\text{HSO}_4^-} \end{aligned} \quad (61)$$

Taking into account the Joule losses ( $IR$ , simplified from the total overvoltage and the ohm drop, cf. 1.5.6) during discharging, Gory proposed second principle of the polarity inversion regarding the total cell voltage during discharging  $V$ , which equals to  $E - RI$  without distinguishing the inversion processes of negative and positive electrodes.

Proposed mechanism by Gory [54]:

Figure 57 illustrates the variation of the equilibrium voltage  $E$  and the voltage  $V$  during an inversion as functions of time for a cell in a series configuration with two other cells.

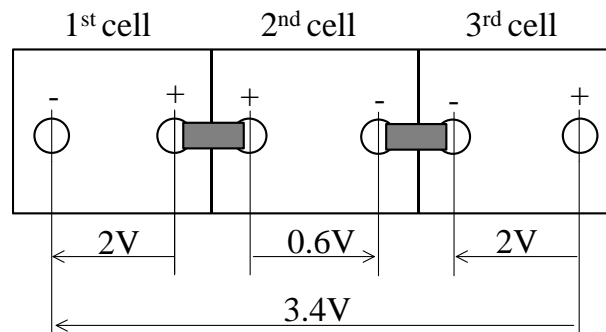


Figure 56: Battery with three cells in series configuration. One cell is inverted, its voltage equals to minus 0.6 V [54]

The equilibrium voltage, which can be measured by cutting off the current rapidly, decreases rapidly to zero after the beginning of the voltage decrease corresponding to the normal end-of-discharge, passing by zero at point A, then it slowly increases in the inversed direction. Point A corresponds to the zero equilibrium voltage before the inversion: the pores are filled with lead sulfate crystals and the electrolyte cannot any more enter and reach the remaining active materials. The current continues to pass through the battery thanks to the equilibrium voltages of the other cells (1<sup>st</sup> and 3<sup>rd</sup> cells). It is going to decompose the sulfate with the inversed reactions. The inversion therefore takes place and an equilibrium voltage, whose sign is opposed from the initial one, appears. If  $E_{\text{INVER}}$  is its absolute value, we have  $V_{\text{INVER}} = -E_{\text{INVER}} - IR_{\text{INVER}}$  in keeping always the positive direction of the discharge current. The equilibrium voltage and the Joule's losses have the same sign like in a cell at charge.

The cell voltage decreases quickly beyond the limit of the normal end-of-discharge, passes by zero at the point B, at the moment where the equilibrium does not yet become zero but just

compensated with the ohm lost. It increases next, in a manner quantitatively very incomplete because of the deep sulfation, towards minus 2 V. When the equilibrium voltage equals to zero, the cell voltage equals to the Joule losses.

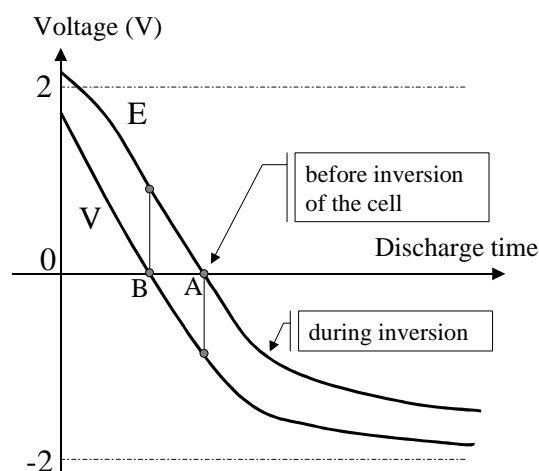


Figure 57: Variation of the equilibrium voltage  $E$  and the cell voltage  $V$  during the polarity inversion of the cell without distinguishing the two electrodes of the cell [54].

In brief, two proposed mechanisms associate the polarity inversion of electrodes to the limited diffusion of sulfate ions at the end-of-discharge. This is an initial foundation we take into account to explain and discuss the results obtained during ours experiments.

## 3.2 EXPERIMENTAL

### 3.2.1 Initial objective

The objective of our experimental work is to determine the capacities of the negative electrode and the positive electrode of a cell, so the limited-capacity electrode.

### 3.2.2 Tools

Batteries: flooded batteries

- 70 Ah/12 V Monobloc Fulmen 070430 A-A: flat-plate, cycled in a photovoltaic post.
- 140 Ah/12 V Solar Monobloc Fulmen ASSSOLARBLOC140/12: tubular-plate, maintained in float charge.
- 140 Ah/12 V: flat-plate, compress, cycled tests.
- 110 Ah/12 V heavy-truck SLI Exide D02075W01-A: flat-plate, stored at open circuit.

Generator: The discharge with limited voltage at minus 2 V/cell was executed by the bipolar alimentation and amplifier KEPCO (BOP 20-20M)  $\pm 20$  V/20 A.

Temperature measurement: two thermocouples JUMO, type K are used to measure temperatures of ambient and of the battery.

Density measurement: electrolyte densities are manually measured before and during discharging by the portable density meter Densito 30PX.

Recorder: battery voltage, current, temperature and ambient temperature were recorded with Personal Daq 56<sup>TM</sup> USB Acquisition Systems.

### 3.2.3 Electrode potential measurement using reference electrodes

The principle of electrode potential measurement by using reference electrode is presented in the chapter 1 (cf. 1.2.1 electrochemical cell). The working electrode and the reference electrode can be in two different solutions, which are related by ionic bridge, or in the same solution and they are isolated from each other by a separator. In this thesis, both methods were used (cf. Figure 58 and Figure 59).

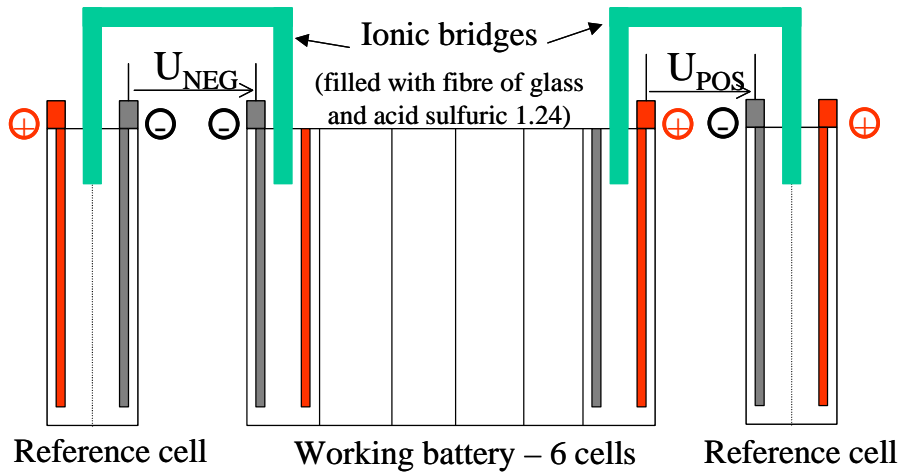


Figure 58: Schema of electrode potential measurement by using reference cell with ionic bridges. Two difference reference cells are used to determine the negative electrode potential of the first cell ( $U_{NEG}$ ) and the positive electrode potential of the sixth cell ( $U_{POS}$ ). According to the way to connect the measurement channels, the values obtained are  $U_{POS} = V_+$  and  $U_{NEG} = (-V_-)$ .

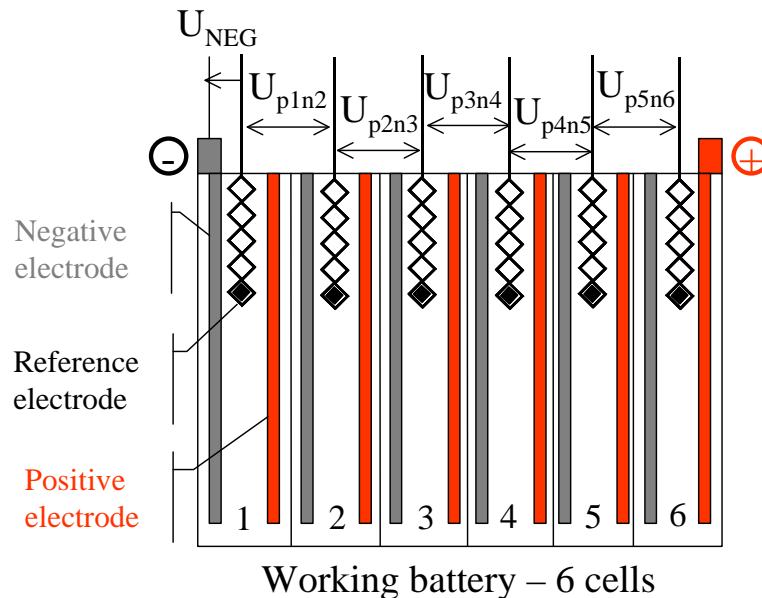


Figure 59: Schema of principle for the measurement of the electrode potential and the pseudo cell voltage by using reference electrodes. The battery consists of 6 cells in series configuration. The negative terminal is negative electrode of the first cell; the positive terminal is the positive electrode of the sixth cell.


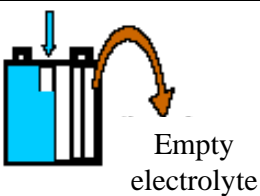
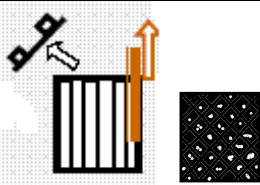

In the second case where reference electrode is an extra electrode that is added to the battery to measure the potential of the working electrode, these criterions have to be kept in mind:

- The potential of the reference electrode has to be constant, i.e. it must not participate to reactions of the working electrodes.
- The material of the reference electrode has to be chemically stable at the contact with the battery electrolyte.
- Input impedance of the recorder has to be sufficient strong to get rid of all current circulation via the reference electrode.

It is clear from Figure 59 that the voltage measured, e.g.  $U_{p1n2}$ , is not the one between two electrodes of the same cell but between a negative electrode and a positive electrode of two successive cells. It is called the voltage of a *pseudo cell*.

### **Reference electrode manufacture and maintaining the charge**

The material chosen to manufacture reference electrode is Pb, which is taken from a lead acid negative electrode. The steps of manufacturing reference electrodes are presented below.

			
1. Wagging + open circuit for 24 hours	2. Rinsing with tap water	3. Scissoring and taking out cells. Taking negative plates	4. Cutting the negative plate into several slices. Eliminating most of active material

5. Charge reference electrodes with a current of 10 mA/g for 72 hours with limited voltage at 2.65V/cell.

6. Reference electrodes are at open circuit for minimum 24 hours before using.

7. As Pb is not completely stable in the electrolyte of lead acid battery because of the self-discharge caused by the secondary reactions (cf. 1.3.2 and 4.1.1), the potential of the reference electrodes has to be periodically controlled. When it clearly deviates from the initial value, reference electrodes have to be recharged. In our experiments, the reference electrodes are systematically recharged after each test of discharge.

### **Reference cell manufacture and maintaining the charge**

Reference cells of 2 V were manufactured following the laboratory prototype of EDF R&D. States of charge of reference cells are periodically controlled by density measurements. Charges at 10 mA/g for 72 hours with limited voltage at 2.65V/cell are performed to establish a good state of charge.



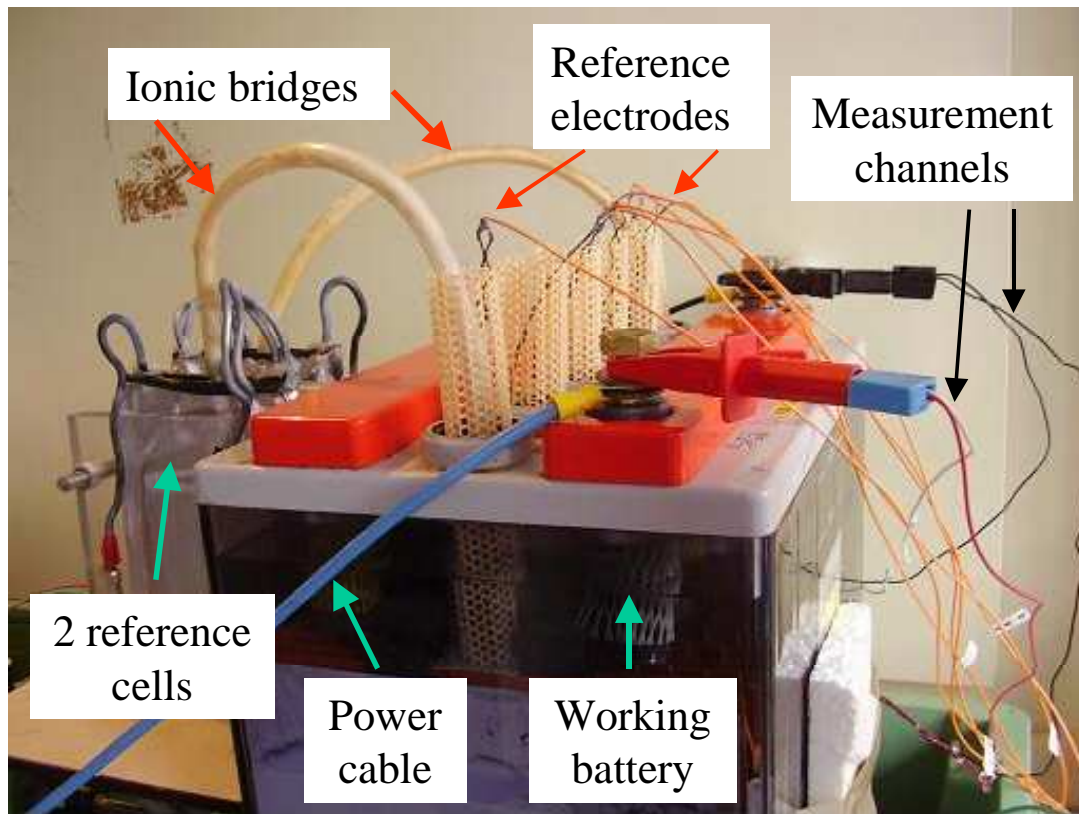


Figure 60: Experimental measurement schema of electrode potentials and pseudo-cell voltages using reference cells with ionic bridges and reference electrodes on a tubular plate battery.

### 3.3 POLARITY INVERSION OF FLAT-PLATE BATTERY

#### 3.3.1 Experimental

Table 6: Experimental procedures of the 70 Ah/12 V flat-plate battery. Densities before and after discharge test:  $d_{BDCH}$ ,  $d_{ADCH}$

Time	Services	Remarks
02/04/2007	Picked up from a photovoltaic station	$U = 12.69 \text{ V}$ $d = 1.275$
7 days	Charge at 4 A, 14.3 V	
2 months	Open circuit	$d_{BDCH1} = 1.28$
	Discharge at 4 A, limited voltage at $-12 \text{ V}$ (1 <sup>st</sup> )	$d_{ADCH1} = 1.17$
7 days	Charge at 4 A, 14.6 V	$d_{BDCH2} = 1.22$
	Discharge at 4 A, limited voltage at $-12 \text{ V}$ (2 <sup>nd</sup> )	$d_{ADCH2} = 1.16$
7 days	Charge at 4 A, 14.6 V (1 days) then at 13.8 V (6 days)	$d_{BDCH3} = 1.22$
	Discharge at 4 A, limited voltage at $-12 \text{ V}$ (3 <sup>rd</sup> )	$d_{ADCH3} = 1.16$
14 days	Charge at 4 A, 14.6 V	$d_{BDCH4} = 1.27$
	Discharge at 4 A, limited voltage at $-12 \text{ V}$ (4 <sup>th</sup> )	$d_{ADCH4} = 1.17$

The tests of discharge are manually stopped. Discharge rate at  $C/17.5 = 4 \text{ A}$  is chosen so that the discharge lasts during the night in order to facilitate the supervising and the test stop. After discharge tests with polarity inversion, prolonged charges within voltage restriction are achieved.

### 3.3.2 Results and discussion

The following graphics present the results of the 4<sup>th</sup> discharge.

Figure 61 shows the potential profiles of the 1<sup>st</sup> negative electrode and the 6<sup>th</sup> positive electrode related to the reference cells. These results match well with the results measured using reference electrodes.

According to the material of the reference electrode (a Pb electrode) and the way to connect the measurement channels (cf. Figure 58), in this graphic we can note that, at the beginning of the discharge test, the potential of the positive electrode ( $V_+$ ) is a little higher than 2 V while the one of the negative electrode ( $-V_-$ ) is around 0 V giving a cell voltage ( $U$ ) of:

$$U = V_+ - (-V_-) \sim 2 \text{ V}$$

#### **Polarity inversion profiles**

It is clear that polarity inversion of a cell consists of two steps corresponding to two potential profiles of the positive and negative electrodes. In this case, the positive electrode first reaches the limit of a normal discharge after 6 hours of discharge. Its potential rapidly falls down from about 2 V to zero and beyond this moment, it maintains at this zero value. The potential of the positive electrode changes from 2 V to 0 V, which is similar to the potential of the negative electrode (the reference electrode is a negative electrode). It is said that positive electrode is inverted. The absolute potential value of the negative electrode continues to slightly decrease toward minus 2 V, but still stays close to 0 V. The cell voltage value is also close to 0 V. Then, after 18 hours of discharge, the potential of the negative electrode abruptly drops to minus 2 V from the value of the order of 0 V. At its turn, the negative electrode is said also inverted. At this moment, polarity inversion of cell appears, the opposite situation compared to the one before inversion takes place: potential of the positive electrode ( $V_+$ ) is around 0 V and the one of the negative electrode ( $-V_-$ ) is a little inferior of minus 2 V leading the cell voltage to  $U = V_+ - (-V_-) \sim -2 \text{ V}$ . The polarity of the cell is inverted. These observations validate the proposed principles of Izzo and Gory regarding the profile of cell voltage.

Two differences between the potential profiles of positive and negative electrodes during inversion are observed. Firstly, the positive electrode takes more time to inverse than the negative electrode does. It takes about 2 hours to fall down close to 0 V from 2 V while for the negative electrode, it takes just some minutes to drop down from around 0 V to minus 2V. Secondly, the inversion of the negative electrode is marked with a variation of the potential similar to “coup de fouet” phenomenon, which is not present at the potential profile of the positive electrode.

#### **“Coup de fouet” phenomenon:**

- “Coup de fouet” is a voltage dip followed by a recovery at the start-of-discharge of a full-charged battery or is a voltage maximum followed by a recovery at the start-of-charge of a deep-discharged battery. Main parameters are the trough voltage, in the order of 10 to 80 mV/cell, the “plateau” voltage, the trough duration and the plateau duration.
- Delaille [55] revealed that “coup de fouet” always reflects the positive electrode behavior.

- The commonly accepted interpretations about causes of the “discharge coup de fouet” and “charge coup de fouet” are the nucleation of the lead sulfate crystals and the nucleation of the lead dioxide respectively [55-59]. In his thesis work, Delaille revealed that mass-transport limitations in the pore, probably due to the electrode texture, are likely to take a significant part in the origin of the “coupe de fouet” at charge as well as at discharge [55].

Indeed, after inversion, the negative electrode at discharge can behave like a positive electrode at charge, i.e. the supplied discharge current decomposes lead sulfate crystals  $\text{PbSO}_4$  to lead dioxide  $\text{PbO}_2$ . Moreover, as the discharge is far deeper than a normal discharge, the criterion of a deep-discharged state for the “charge coup de fouet” to take place is largely fulfilled.

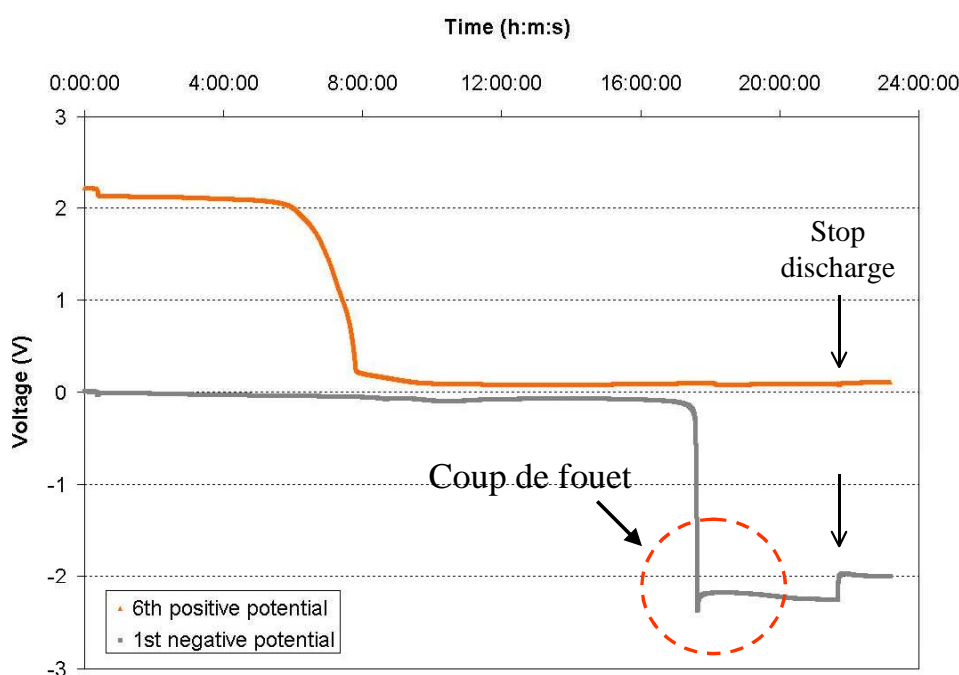


Figure 61: 70 Ah/12V battery, 4<sup>th</sup> discharge with -12V end of discharge. Potential profiles of the first cell negative electrode (battery negative terminal,  $-V_-$ ), and of the sixth cell positive electrode (battery positive terminal),  $V_+$ . Coup de fouet phenomenon at the inversion negative profile. We chose to present  $-V_-$  at the place of  $V_+$  to avoid crossing the profile of the positive electrode  $V_+$ .

### **Voltage scattering phenomenon on cells in a series configuration**

Figure 62 shows voltage profiles of six pseudo cells in a series configuration. They are similar one another regarding the shape of the voltage profile which consists of a positive electrode inversion followed by a negative electrode inversion which is remarked with a “coup de fouet”. However, these inversions do not take place at the same time. This confirms the voltage scattering phenomenon on cells in a series configuration. In this case the dispersion of voltage is more remarkable at positive electrodes than at negative electrodes. The first positive inversion was after 6 hours and 30 minutes of discharge while the last positive inversion was after 10 hours. It is well known that, in a normal discharge, the weakest cell voltage imposes the stop-discharge, thus limiting the discharged battery capacity.

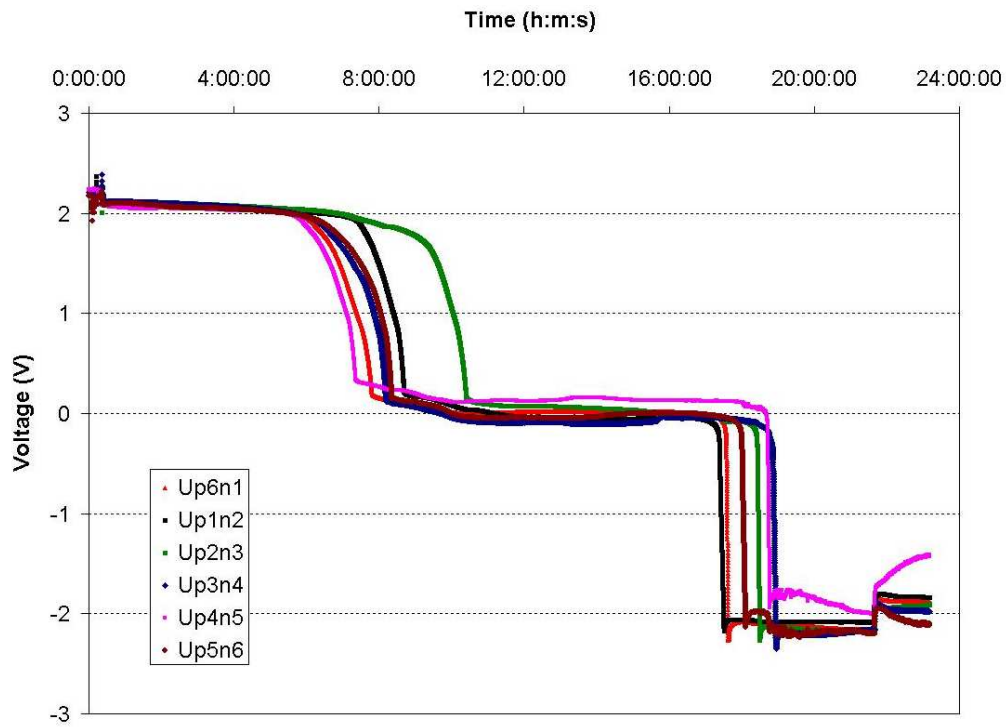


Figure 62: 70 Ah/12V battery, 4<sup>th</sup> discharge with -12V end of discharge. Potential profiles of pseudo cells. Scattering voltage phenomenon on cells in series configuration.

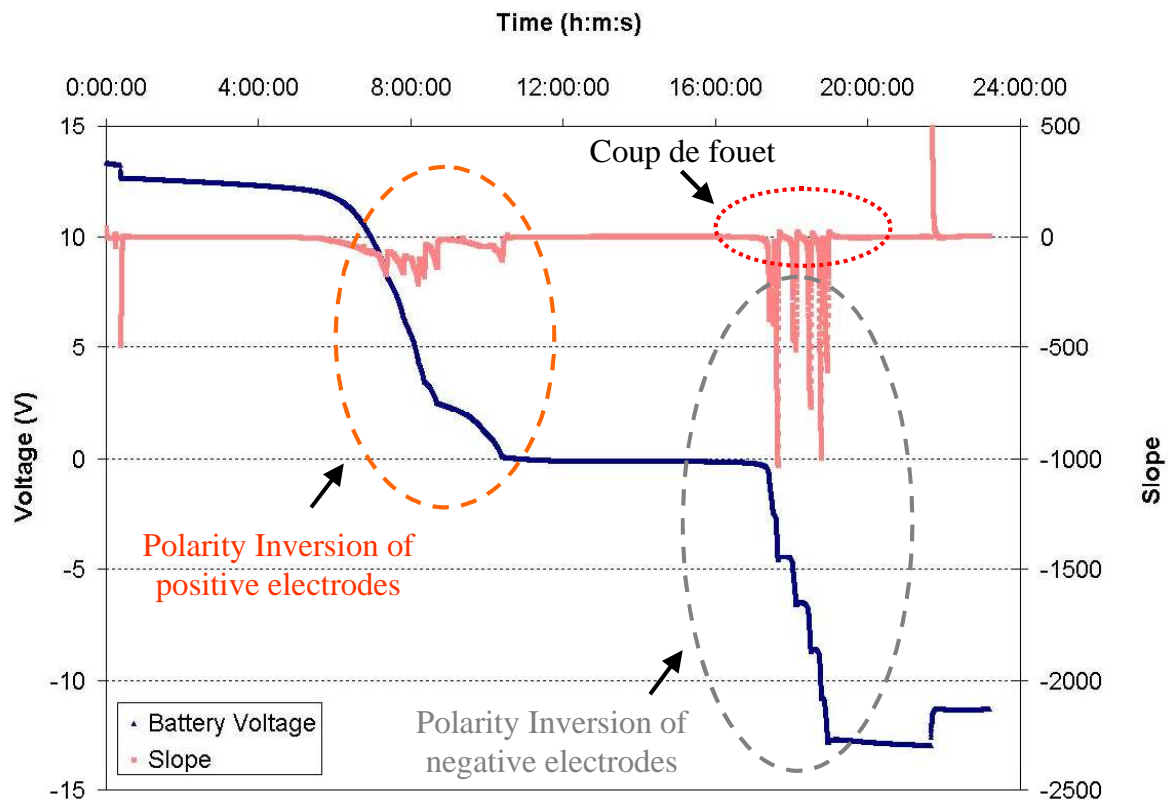


Figure 63: 70 Ah/12V battery, 4<sup>th</sup> discharge with -12V end of discharge at  $C/17.5 = 4$  A. Battery voltage profile and calculated slope voltage profile. Six negative inversions and six positive inversions can be seen with the slope profile.

### Distinguishing the positive and negative inversions

The total voltage between two terminals of the battery during discharging is illustrated in Figure 63.

It is possible to distinguish the positive and negative inversion groups with a 0 V plateau voltage between them, but not each inversion. In observing the slope profile of the battery voltage, each inversion can be easily detected by an abrupt decrease of the slope value. It is clear that, slopes of the positive inversions are smaller than slopes of the negative inversion. The appearance of the “coup de fouet” at the negative inversion profile is remarked with a small positive value of the slope.

### Heat delivered during polarity inversions

The temperature of the battery was recorded and presented in Figure 64. Ambient temperature was 19 to 22.5°C. It is obvious that, during inversions, the temperature of the battery increases. This due to 2 phenomena: reversible heat of the inversed reactions, i.e. charge reactions and irreversible heat caused by polarization, including Joule effect, which is very strong at polarity inversion condition.

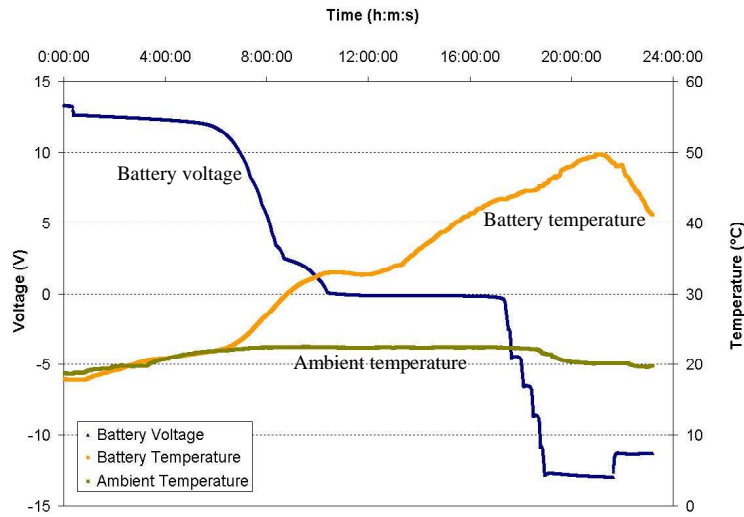


Figure 64: 70Ah/12 flat-plate battery. Battery voltage and temperature, ambient temperature profiles as a function of the charge time. Battery temperature increases strongly when the battery polarity is inversed.

As mentioned in chapter 1 (cf. 1.5.6) regarding the current-related heat effects, heat generation is proportional to polarization. When the cell polarity is inversed, overvoltages of both electrodes strongly increase.

$$dQ_{\text{Joule}}/dt = (V - E) \cdot i \quad [\text{W}] \quad (40)$$

$$Q_{\text{Joule}} = \int_0^t \{(V - E) \cdot i\} dt \quad [\text{Wh}] \quad (41)$$

It is well known that, when a 2 V cell is short circuited, all of its chemical energy is converted into heat. This phenomenon can be explained using the Eq. (40) as showed in Figure 65.

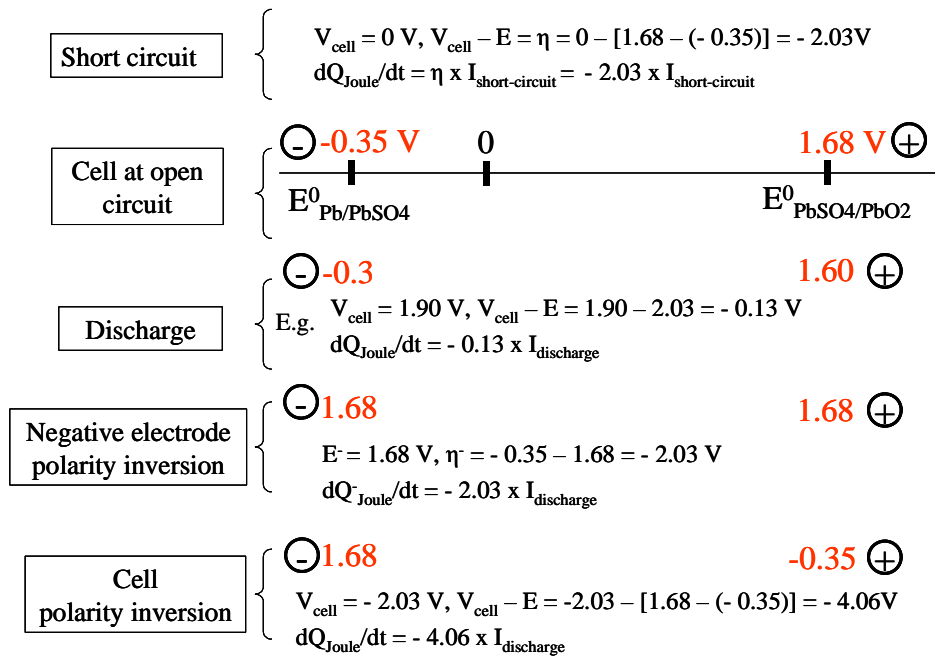


Figure 65: Negative and positive electrode potentials and calculation of polarizations during discharging, short circuit, negative electrode inversion and cell inversion.

At short circuit, the cell voltage equals to 0 V and the polarization equals to the cell voltage at open circuit, e.g. 2 V. According to the internal resistance of the cell, the battery is strongly heated, even burned out. When the cell polarity is inverted, a similar situation is obtained regarding the polarization evolution. As revealed in Figure 65, the polarization corresponding to the negative inversed electrode reaches already 2 V like in the case of a short circuit. If accounting both electrodes, the cell polarization is 4 V, the double compared to the one at short circuit. As the discharge current is fixed, the battery should not be burned out like in the case of a short circuit, though its temperature increases strongly compared to a normal discharge.

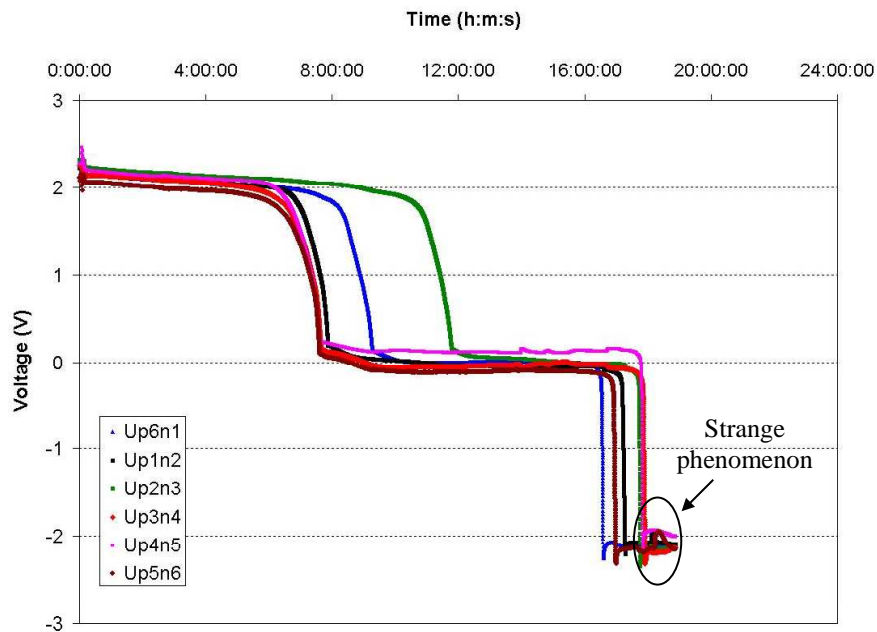


Figure 66: 70 Ah/12V battery, 3<sup>rd</sup> discharge with -12V end of discharge. Potential profiles of pseudo cells. Appearance of a voltage hump after inverting the negative potential.

### Voltage hump

In the 3<sup>rd</sup> discharge, a strange phenomenon of a voltage hump (cf. Figure 66), which is not presented in other tests, appears at the end of the procedure. We will return to this phenomenon when discussing results obtained with tubular batteries.

## 3.4 POLARITY INVERSION OF TUBULAR PLATE BATTERY

### 3.4.1 Experimental

Table 7: Experimental procedures of the 140Ah/12V tubular-plate battery. Several discharge rates are tested C/20, C/14 and C/10.

Time	Services	Remarks
15/05/2007	Picked up	U = 12.40 V d = 1.2
14 days	Charge at 4 A, 13.8 V	
7 days	Open circuit	
	Discharge at 7 A (C/20), limited voltage is – 12 V (1 <sup>st</sup> )	
2 days	Charge at 7 A, 14.6 V	
	Discharge at 14 A (C/10), limited voltage is – 12 V (2 <sup>nd</sup> )	
3 days	Charge at 14 A, 14.6 V	
7 hours	Open circuit	
	Discharge at 10 A (C/14), limited voltage is – 12 V (3 <sup>rd</sup> )	

### 3.4.2 Results and discussion

The following graphics present the results of the 1<sup>st</sup> discharge at C/20.

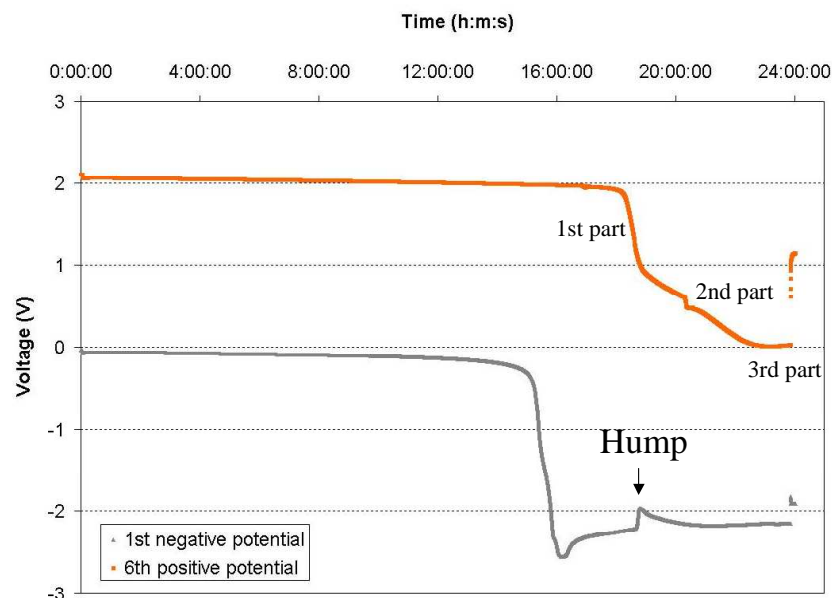


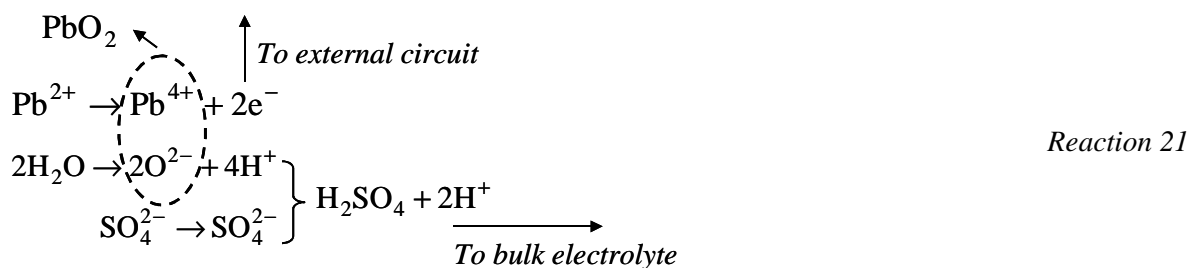
Figure 67: 140 Ah/12V tubular-plate battery, 1<sup>st</sup> discharge with –12V end of discharge (C/20). Potential profiles of the first cell negative electrode and of the sixth cell positive electrode. Coup de fouet phenomenon and voltage hump at the negative profile. Three slopes of the inversed positive potential profile.



Figure 67 shows that in this battery, it was the negative electrode whose polarity was inversed first. The shapes of potential profiles are slightly different than the ones of the 70Ah/12V flat-plate battery analyzed above for both negative and positive electrodes.

### Negative electrode

For the negative electrode, a similar “coup de fouet” phenomenon was also observed but the trough duration was almost an hour in this case vs. some minutes in the case of the 70Ah/12V flat-plate battery. Basing on the proposed interpretation of the causes of the “coup de fouet”, this phenomenon can be explained as follows. At the moment where the negative electrode polarity is inversed, the electrode had been very deep discharged and was covered with a lot of lead sulfate crystals,  $\text{PbSO}_4$  (cf. Figure 68). At some places on the electrode surface, sulfuric acid could not be any more in contact with the remaining active material, Pb. As the discharge current was continued to be applied to the battery and the transport of  $\text{HSO}_4^-$  is totally hindered, remaining Pb cannot be oxidized into  $\text{Pb}^{2+}$  as no more  $\text{HSO}_4^-$  is able to cross the  $\text{PbSO}_4$  barrier. In this case, at the active interface, which is located behind the  $\text{PbSO}_4$  barrier, electrons ( $e^-$ ) are no more taken from Pb to form  $\text{Pb}^{2+}$  but are taken from  $\text{Pb}^{2+}$  to form  $\text{Pb}^{4+}$ , following the reaction:



Two remarks can be made:

- As the  $\text{H}_2\text{SO}_4$  concentration is low, the sulfate ion in solution is  $\text{SO}_4^{2-}$
- $\text{H}_3\text{O}^+$  can still cross the barrier while  $\text{SO}_4^{2-}$  cannot.

So,  $\text{PbO}_2$  forms in negative active material behind the  $\text{PbSO}_4$  barrier, and  $\text{H}_2\text{SO}_4$  is released into that closed space, near the active interface. Here the normal discharge reaction can then take place in parallel with the  $\text{PbO}_2$  formation:



These reactions, Reaction 21 and Reaction 22, result a displacement of  $\text{PbSO}_4$  on the backside of the barrier to inner sites, closer to the active interface.

$\text{PbO}_2$  crystals formed at the negative electrode are thermodynamically stable at the inversed potential of the negative electrode. They should not react with Pb to reform  $\text{PbSO}_4$  because of the lack of  $\text{SO}_4^{2-}$  ions.

An extra polarization, i.e. crystallization polarization, was demanded to create first lattices of  $\text{PbO}_2$ . This polarization made appear the dip voltage at the beginning of the negative inversion which is considered to the similar “coup de fouet” phenomenon.



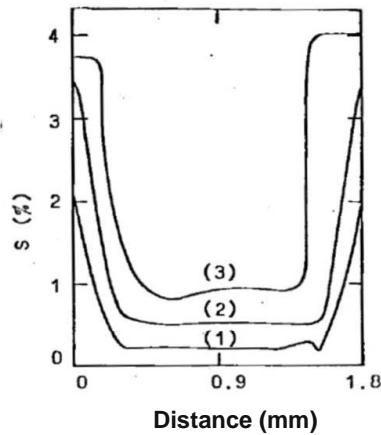


Figure 68: Characteristic of lead acid battery on discharge: the “U curves”. [60]

Profiles of  $S$  (10% in mass of  $PbSO_4$ ) in the middle of a positive electrode according to a cross section at the electrode interface: 25% (1), 50% (2) and 100% (3) states of discharge.

During discharging,  $PbSO_4$  appears in favor at the area close to electrode interfaces. At 100% state of discharge,  $PbSO_4$  forms a layer that prevents the discharge continuing at a fixed rate.

Always at the negative electrode, after about 2 hours and a half of inversion, a hump voltage, which was in the opposite direction of the “coup de fouet” appeared. This phenomenon was already observed at the 3<sup>rd</sup> discharge of the 70 Ah/12 V flat-plate battery. We suggest that as the charge reaction consumes  $PbSO_4$  crystals on the backside of the barrier layer, it can hole the barrier and thus liberate reactive surfaces. Sulfuric acid  $H_2SO_4$  could enter into the pores and meet the remaining active material and the discharge reaction could take place with a higher rate. Moreover, as  $SO_4^{2-}$  ions are available,  $PbO_2$  produced inside the negative electrode could short-circuit with Pb remaining active material to form  $PbSO_4$ . In addition, the concentration of the solution at proximity of the reactive surface increases and the equilibrium voltage increases as well. These three acts would lead to the increase of the negative potential.

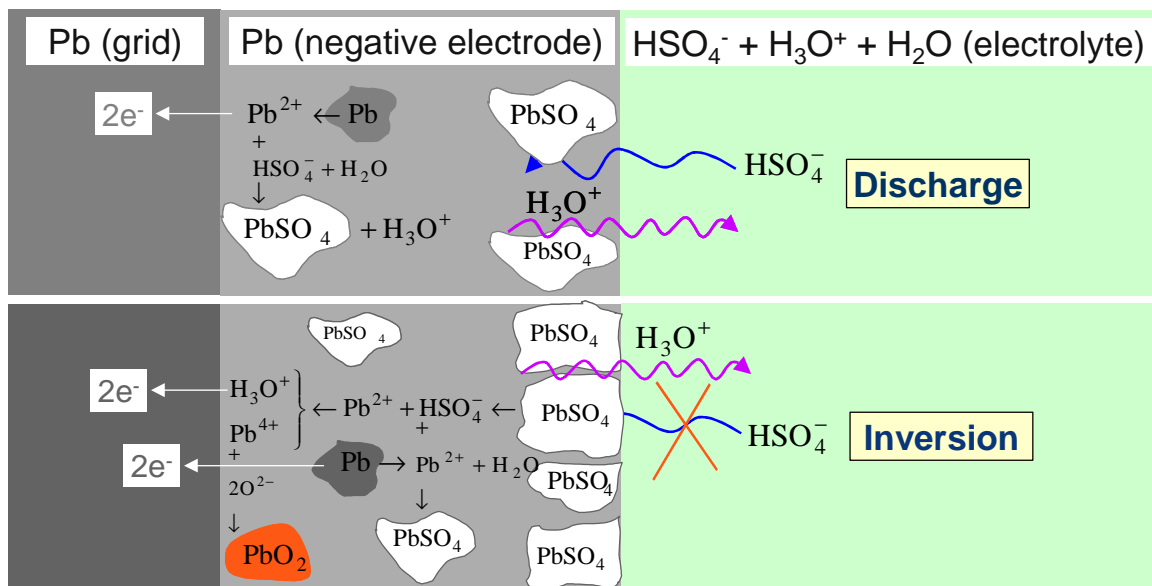


Figure 69: Processes of discharge and of polarity inversion at the negative electrode. Polarity inversion appears when a layer of  $PbSO_4$ , preventing sufficient acid sulfuric diffusion from the bulk electrolyte into the reactive surface, forms at the interfaces of the electrode. The reaction of inversion, which is identical to the reaction of the positive electrode on charge, consumes  $PbSO_4$  and produces  $PbO_2$  inside the negative electrode.

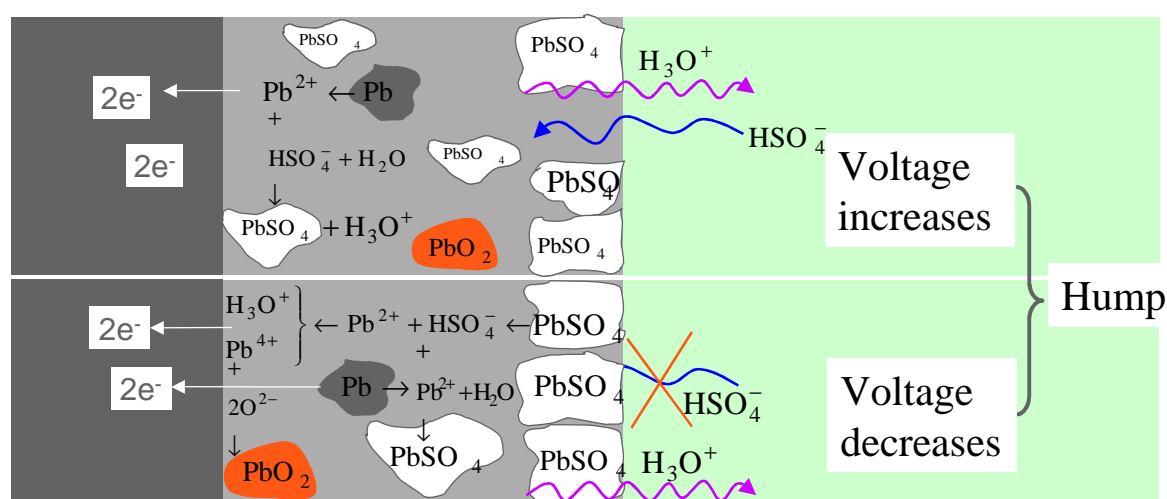


Figure 70: Formation process of hump voltage: the consumption of  $\text{PbSO}_4$  of the reaction of inversion leads to a breakdown of the  $\text{PbSO}_4$  layer, the diffusion of acid sulfuric is again sufficient for the discharge reaction taking place in advance than the reaction of inversion. Moreover,  $\text{PbO}_2$  produced inside the negative electrode can be short circuit with the Pb, remaining active material, to form  $\text{PbSO}_4$ . The voltage increases.  $\text{PbSO}_4$  invades rapidly the short circuit area. The refilling of  $\text{PbSO}_4$  layer corresponds to the return of the voltage to the inversion value.

The discharge reaction as well as the short circuit reaction reform  $\text{PbSO}_4$ . These  $\text{PbSO}_4$  crystals refill rapidly the  $\text{PbSO}_4$  layer and this layer separates again some reactive surfaces from  $\text{H}_2\text{SO}_4$ . The voltage returns to the inversion value. These decrease and increase of the electrode voltage form humps on negative potential profile. According to this interpretation of hump phenomenon, it is clear that hump appears only when the reaction of inversion has already taken place for a certain time, i.e. polarity electrode is already inverted.

### Positive electrode

The positive potential profile has also some differences compared to the one of the 70Ah/12V flat-plate battery. The shape of the potential profile from the beginning to the end of the inversion did not steadily blow down but broke into three different parts with three distinguished slopes whose values decrease with time to zero at the end. They reflect the decrease of the discharge reaction rate and the increase of the charge reaction rate until both rates are equals, when the positive potential reaches 0 V and remains stable. A little trough voltage was also observed.

One remark for both electrodes is that the positive electrode always took more time, about five times more, than the negative electrode to completely reach the inversed potential value, i.e. counting from the beginning, where the potential begins to abruptly drop, to the end of the inversion, where the potential reaches 0 V or minus 2 V for the positive and the negative electrodes respectively.

## Pseudo cells

Figure 71 presents the voltage profiles of six pseudo cells. They well reflect the shape of the negative electrode with the presence of the similar “coup de fouet” phenomenon at the beginning and of the hump, sometimes two successive humps, at the middle of the inversion. Potential humps occur almost at the same time on every negative electrode, i.e. after about 2 hours and a half counted from the beginning of the inversion. The voltage profiles of pseudo

cells are also clearly associated to the profile of the positive potential with three different slopes during the whole inversion. The little trough voltage observed on the positive potential profiles above, opposite to the direction of humps, was reproducible. We remarked once that, the trough voltage on the 6<sup>th</sup> positive electrode potential appears just after the appearance of the hump on the 5<sup>th</sup> negative electrode potential. We suppose that, this trough would be a mirror of the hump, as the movement of sulfuric acid to the negative electrode when the  $\text{PbSO}_4$  wall is holed, would cause a drop of acid density at the positive electrode. Nevertheless, the inversion takes place inside the electrode and not at the surface faced to the bulk electrolyte.

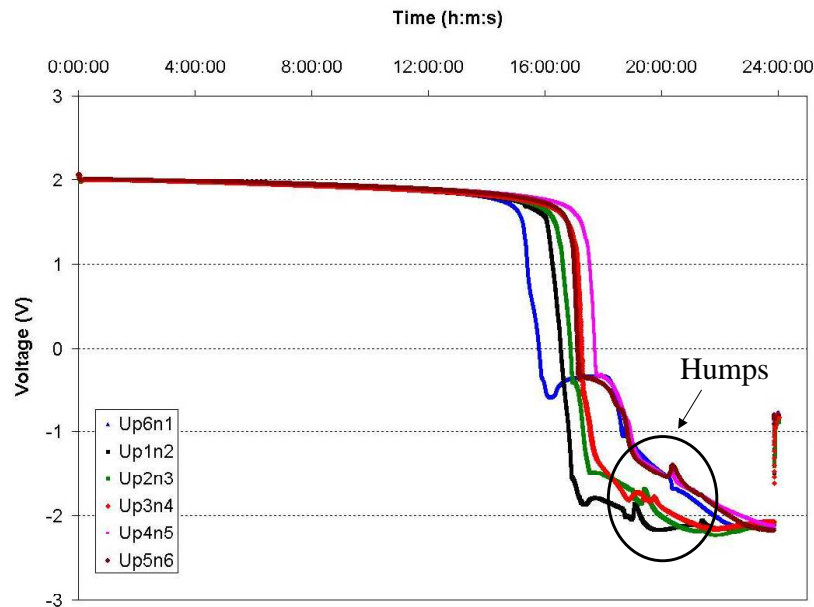


Figure 71: 140 Ah/12V tubular-plate battery, 1<sup>st</sup> discharge with  $-12\text{V}$  end of discharge (C/20). Potential profiles of pseudo cells. Appearance of voltage humps after inverting negative potential.

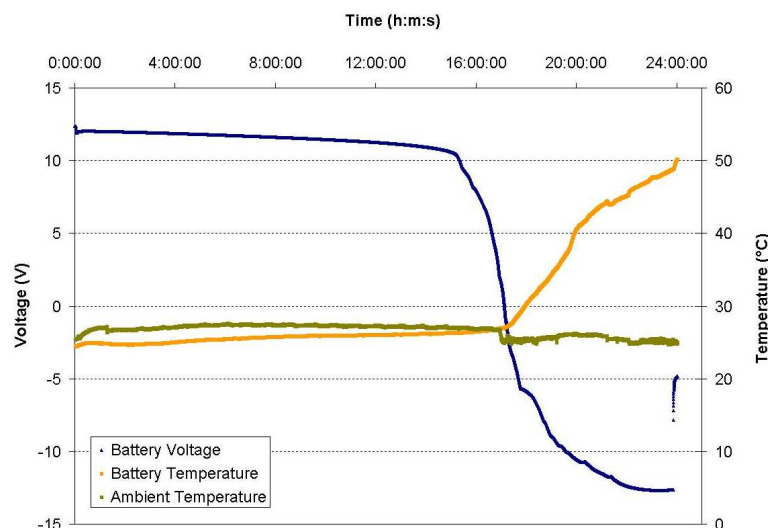


Figure 72: 140Ah/12V tubular-plate battery. Battery voltage and temperature, ambient temperature profiles as a function of charge time. Battery temperature increases strongly when the battery polarity is inverted.

### **Rate of discharge current before and after polarity inversion**

During discharging with current  $I$ ,  $\text{HSO}_4^-$  ions are consumed with the rate  $I/F$  and are renewed from the bulk electrolyte by diffusion to the positive electrode with the rate  $Ddx/dc$  and by diffusion and migration to the negative electrode with the rate  $Ddx/dc + It/F$ .

$$\frac{I}{F} = -D \frac{dc}{dx} + \frac{It}{F} \quad (62)$$

At the beginning of the discharge, the ability of the transport rate is greater than the consumption rate of discharge current; the battery is discharged with the later rate.

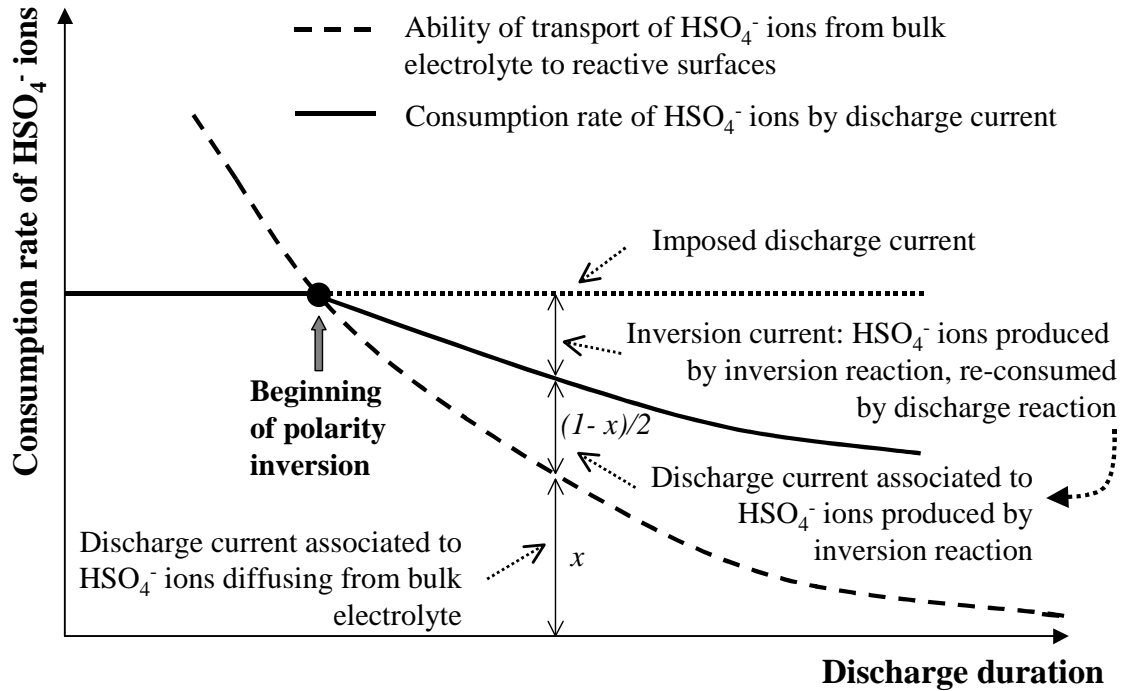


Figure 73: Consumption rate of  $\text{HSO}_4^-$  ions or rate of discharge reactions before and after polarity inversions. After polarity inversion, the discharge reaction rate is higher or at least equals to the inversion reaction rate.

At the moment when the transport rate is lower than the consumption rate of the discharge current, the concentration of sulfate ions tends to zero at some active interfaces and the cell voltage drops abruptly, which marks the end of a normal discharge. Beyond this moment, if the discharge continues with the same discharge current value, the number of sulfate ions reaching the active interface becomes too low for the discharge reaction and the polarity inversion happens. At the beginning of polarity inversion, most of the applied current is used for discharge reactions with the transport rate of  $\text{HSO}_4^-$  ions. This rate decreases with discharge time (cf. Figure 53). The exceed part of the imposed discharge current supplies inversed reactions. This current share for the inversion reaction increases with discharge time. The inversion reactions produce  $\text{HSO}_4^-$  ions, which are re-consumed by discharge reaction. So  $\text{HSO}_4^-$  ions supplied for discharge reactions come from two sources:  $\text{HSO}_4^-$  ions transported from bulk electrolyte and  $\text{HSO}_4^-$  ions produced by inversion reactions. If the discharge process is prolonged even though polarity inversions have already take place for a long time, the transport rate from bulk electrolyte tends to zero,  $\text{HSO}_4^-$  ions are renewed only by inversion reactions.

If  $x$  is the current proportion associated to the discharge reaction, which consumes  $\text{HSO}_4^-$  ions diffusing from the bulk electrolyte, the current proportion related to the inversion reaction or to the discharge current, which uses  $\text{HSO}_4^-$  ions produced by the inversion reaction is  $(1-x)/2$ . As the current proportion associated to the discharge reaction, which consumes  $\text{HSO}_4^-$  ions diffusing from the bulk electrolyte has to be included between 0 and 100%,  $x$  is positive and inferior to 1.

Total current proportion related to the discharge current is:

$$x + \frac{1-x}{2} = \frac{1}{2} + \frac{x}{2} > 0.5 \quad (63)$$

It is clear that the discharge reaction rate is higher or at least equals to the inversion reaction rate if there is no more diffusion of  $\text{HSO}_4^-$  ions from the bulk electrolyte to reactive interfaces ( $x = 0$ ).

### **Reestablishment of electrode potentials when discharge stop**

Are inversed potentials stable when cutting off the discharge current? From Figure 61 and Figure 67, it is clear that, the less prolonged the inversion is, the less difficult to reestablishment of electrode potentials. For instance, when the current is cut off, the potential of the positive electrode of the 140Ah/12V, having suffered for about 6 hours at the inversed potential, increases immediately from its inversed value, 0V, to 1.2V (cf. Figure 67). While, the potential of the positive electrode of the 70Ah/12V battery, subjected to the inversed potential for about 13 hours, cannot return to its initial value, it stays at the inversed value, 0V, when the current is turned off (cf. Figure 61).

It is well known that, the active material utilization ratio is just about 50%. When the inversion is not too prolonged, it produces only a certain quantity of the second kind of active material, i.e. active material of the opposite polarity. These two kinds of active material, carried by metal grid and more or less bathed with electrolyte, form several cells in short circuit, which can be rapidly discharged. As the active material of primitive formation is more abundant compared to the material formed by inversed reactions, this latter is consumed first. In addition, the cell gets back very slowly its initial potential as it is deeply sulfated. In the case the electrode is too deeply sulfated and inversed, the inversed potential is stable for so long time that a simple stop-current cannot help it to return to the initial state of polarity. A prolonged charge with low rate is required.

## **3.5 ANALYZING A DEFECTIVE BATTERY BY USING POLARITY INVERSION DISCHARGE**

### **3.5.1 Experimental**

The battery TC5, whose voltage is 11.3 V, was subjected to the test of discharge at C/20, i.e. 7A, with polarity inversion in order to find out which electrode(s) is (are) defective.

### **3.5.2 Results and discussion**

By observing the entire discharge voltage profile of the battery as a function of time, it is clear that there were 2 under-charged electrodes, which limit the battery capacity. The initial voltage before discharge was 11.3 V. At start-discharge, it dropped rapidly to 10.5 V, about

2V less compared to a normal voltage of a 6-cell battery. After 3 hours and 30 minutes of discharge, this voltage fell abruptly to 7.9 V, about 4 V less compared to a normal voltage of a 6-cell battery. Two possibilities lead to this same result:

- Two electrodes of the same nature, two negative or two positive could be inverted; these other discharge normally.
- Two electrodes of different natures, one negative and one positive could be inverted; these other discharge normally.

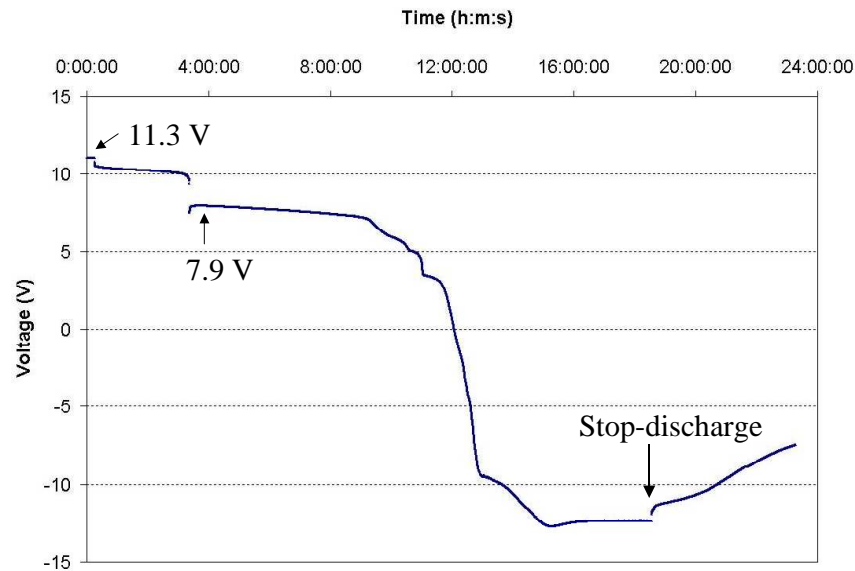


Figure 74: Battery TC5 total voltage during discharging with polarity inversion. Battery voltage drops to 7.9 V after about 3 hours and 30 minutes of discharge at C/20, 4 V less than nominal voltage. Two cells should be defective.

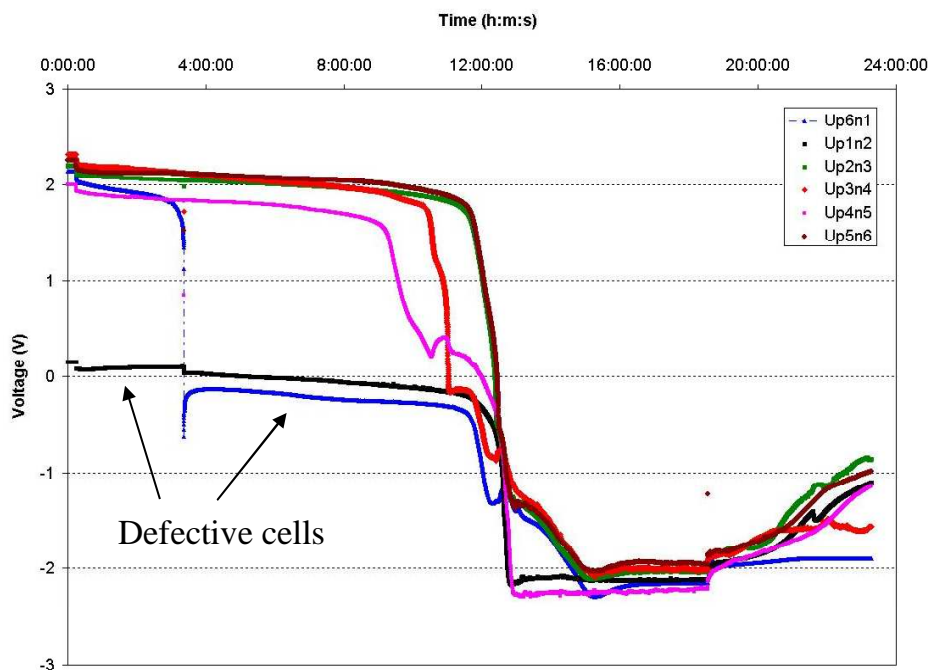


Figure 75: TC5 compressed 140 Ah/12V flat-plate battery, discharge with -12V end of discharge at C/20, potential profiles of pseudo cells. Two cells,  $U_{p6n1}$  and  $U_{p1n2}$ , are defective.

Figure 75 illustrates the pseudo cell voltages of the battery. It shows that the pseudo cell consisting of 1<sup>st</sup> positive electrode and of 2<sup>nd</sup> negative electrode,  $U_{p1n2}$ , and the pseudo cell consisting of 6<sup>th</sup> positive electrode and of 1<sup>st</sup> negative electrode,  $U_{p6n1}$ , are affected. These two voltages are now presented in the same graphic of the 1<sup>st</sup> negative electrode potential and the 6<sup>th</sup> positive electrode potential (cf. Figure 76).

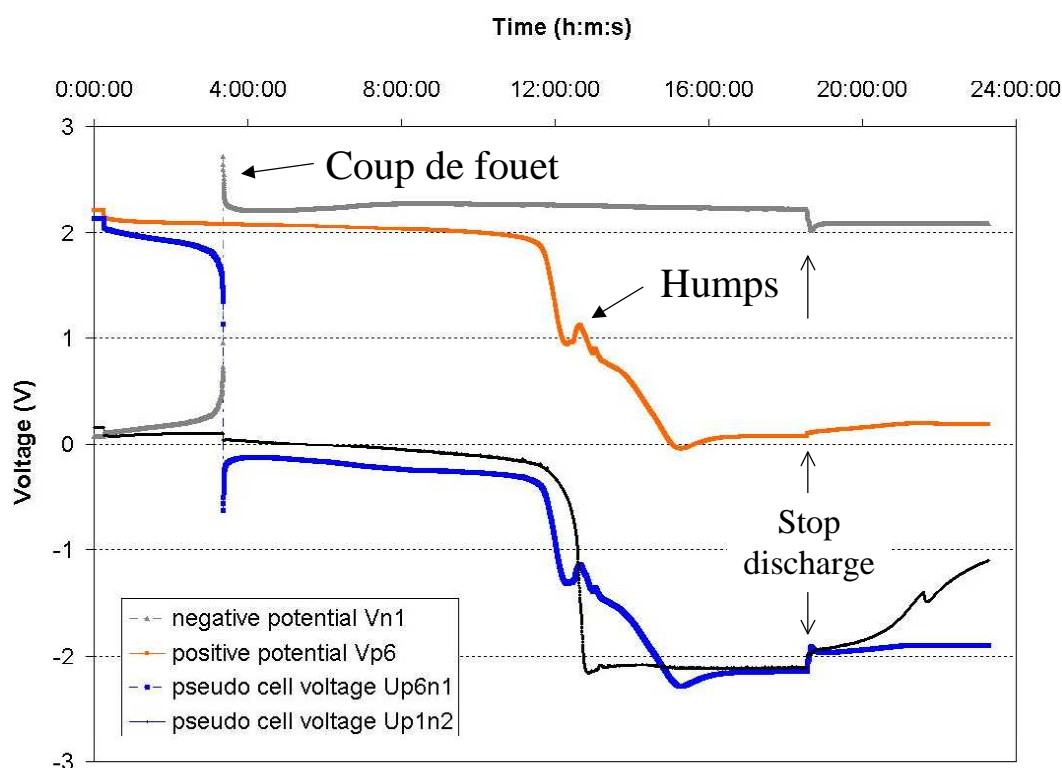


Figure 76: Potentials of negative and positive electrodes at two terminal cells; voltage profiles of two defective cells,  $U_{p6n1}$  and  $U_{p1n2}$ .

For  $U_{p6n1}$ , it shows that the negative electrode is affected and inverted after only 3 hours and 30 minutes of discharge. A “coup de fouet” is also obvious.

For  $U_{p1n2}$ , its voltage is close to 0V at the start-test, meaning that one electrode had already been completely discharged and inverted. The remaining electrode is inverted after about 12 hours 30 minutes of discharge. The shape of this inversion resembles the shape of a negative inversion, which is characterized by a very abrupt fall of the potential. Moreover, the phenomenon of hump, which appeared on the potential profile of the positive electrode, is not present on this profile. We can conclude that the completed discharged electrode of the cell  $U_{p1n2}$  from the beginning is a positive electrode. Therefore, two defective electrodes are the negative and the positive electrodes of the 1<sup>st</sup> cell. This can be caused by a short circuit between them. The result of another test confirmed that in the electrolyte of this cell, there were ions of Fe, which should develop the oxido-reduction “shuttle” phenomenon and should discharge the electrodes.

Regarding hump phenomenon, in this battery, humps appear at the positive potential profile and not at the negative one. This confirms that, hump phenomenon can occur at either negative or positive potential profile. A surprising inverted hump appeared at the  $U_{p1n2}$  pseudo cell voltage profile after the discharge current was cut off.



### 3.6 ANALYZING EVOLUTION OF SEPARATED STATES OF CHARGE OF NEGATIVE AND POSITIVE ELECTRODES USING POLARITY INVERSION DISCHARGE

#### 3.6.1 Experimental

Some details on 110 Ah/ 12 V heavy truck SLI batteries used for test are follows:

- Nine positive electrodes: grids 64g Pb/Sb + 0.111kg of material, out put of active material: 118Ah/kg for C/20. Thus, under test of discharge of C/20, the capacity of positive electrode must be  $9 \times 0.111 \times 118 = 117.9\text{Ah}$ .
- Eight negative electrodes: grids Pb/Ca 64g + 0.103kg of material, out put of active material: 145Ah/kg for C/20. Under test of discharge of C/20, the capacity of positive electrode must be  $8 \times 0.103 \times 145 = 119.5\text{Ah}$ .
- Composition of grids: Pb/Sb = Sb 1,6%  $\pm$  0,1 + impurities (As 0,1%  $\pm$  0,02 / Se 0,03%  $\pm$  0,0025 / Sn 0,12%  $\pm$  0,04); Pb/Ca = Ca 0,12%  $\pm$  0,01 / Sn 0,20%  $\pm$  0,02 / Al 0,0175%  $\pm$  0,0025.
- Date of fabrication: 06/09/2006.

Three batteries 110 Ah/12 V heavy truck SLI Exide of the same manufacture lot on the 6<sup>th</sup> September 2006, B101-103-105, were subjected to different tests of discharge (DCH) and charge (CH) as shown in Table 8. The first test on B101 was operated on the 19<sup>th</sup> September 2007; the battery was self-discharged for bout 12 months. They were the 17<sup>th</sup> and 18<sup>th</sup> October 2007 for the B103 and B105 respectively, so more than 13 months of self-discharge.

Table 8: Experimental procedures of 110Ah/12V flat-plate batteries, B101, B103 and B105.

Battery	Test	Description
B101	DCH -12.0V (1)	Discharge at 18 A, limit-stop-voltage at -12.0V (18 - 12)
	CH IU <sub>i</sub>	Charge at C/10 (I) and limited voltage at 14.0 V (U) for 11 hours than at C/20 (i) without voltage restriction for 3 hours
	DCH -12.0V (2)	18 - 12
B103	DCH -12.0V (1)	18 - 12
	CH 13.6 V	Charge at C/10 and limited voltage at 13.6 V for 168 hours
	DCH -12.0V (2)	18 - 12
	CH 13.6 V + C/200	After the charge 13.6 V, continue to charge at C/200 without voltage restriction for 168 hours
	DCH -12.0V (3)	18 - 12
B105	DCH 10.5 V (1)	Discharge at 18 A, limit-stop-voltage at 9 V
	CH 13.6 V	18 - 12
	DCH -12.0V (2)	18 - 12

Comparison of the following couples of discharge are operated:

- B101 – DCH(1) with B105 – DCH(1) to show differences between a normal discharge and a discharge with polarity inversion
- B101 – DCH(2) with B103 – DCH(2) to compare the efficiency of CH IU<sub>i</sub> and 13.6 V
- B103 – DCH(2) with B103 – DCH(3) to figure out the efficiency of CH C/200



### 3.6.2 Results and discussion

Before discussing on the results, it should be reminded that the initial capacities of two electrodes are almost the same; they are 118 and 119 Ah for the positive and negative electrodes respectively.

Figure 77 shows the discharge potential profiles of a negative and a positive electrode of B103, which was at open circuit for thirteen months. It is obvious that, the negative electrode finishes its discharge far earlier than the positive electrode. The remaining capacity of the negative electrode is just about 50% of the positive one. We remind here that the battery tested contains antimony in positive grid alloys. This explains why the negative electrode self-discharges much faster than the positive electrode.

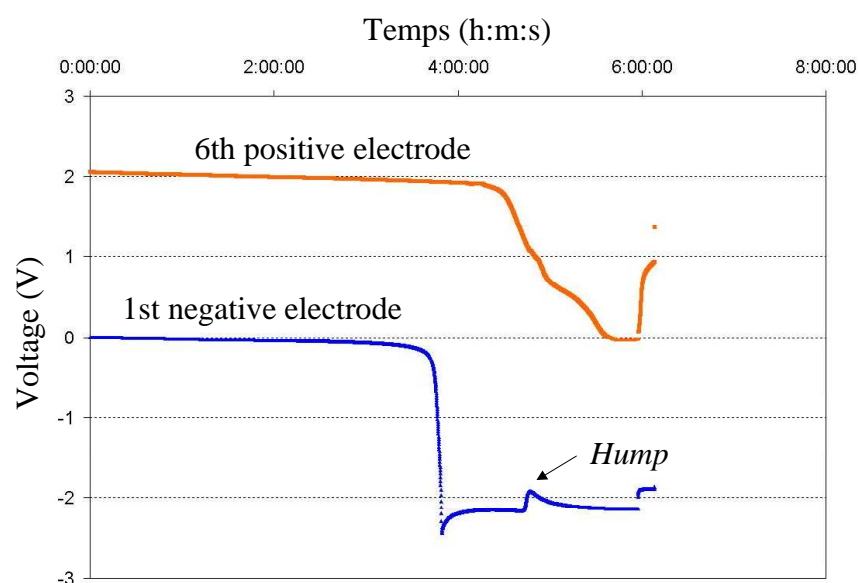


Figure 77: B103, first discharge with  $-12V$  end of discharge. Potential profiles of the first cell negative electrode (battery negative terminal), and of the sixth cell positive electrode (battery positive terminal).

Familiar shapes of negative and positive potential profiles are observed. The negative electrode marks its polarity inversion with an abrupt potential drop to  $-2V$  and a “coup de fouet”. Then, after 1 hour from this beginning, the potential hump appears. When the discharge current is switched off, the negative potential reestablishes far more slowly than the positive potential, as the negative electrode is inversed far earlier. The positive electrode takes more time, about 1 hour, to reach its value of the inversed potential level,  $0V$ .

#### 3.6.2.1 B105 – DCH(1) with B101 – DCH(1)

Figure 78 (a) shows that after 2 hour and 15 minutes of discharge, at  $9V$ , a first inversion takes place; it is also the criterion to stop discharge in practice. The remaining capacity of the B105 battery after 13 months of self-discharge is  $40.5Ah$ ,  $36.8\%$  of its nominal capacity.

Figure 78 (b) shows a complete discharge test where all cells of the B101 battery are inversed. Without regarding the potential profiles of negative and positive electrodes, according to the shape of the battery voltage, we can conclude that the negative electrode is inversed before the positive electrode and limits the battery capacity. We can also obtain complete

information about average capacity of six negative and six positive electrodes: 44 % and 86 % respectively compared to nominal capacity (110 Ah), with 6 V is the limit-stop-discharge for negative electrodes and minus 6 V for positive electrodes.

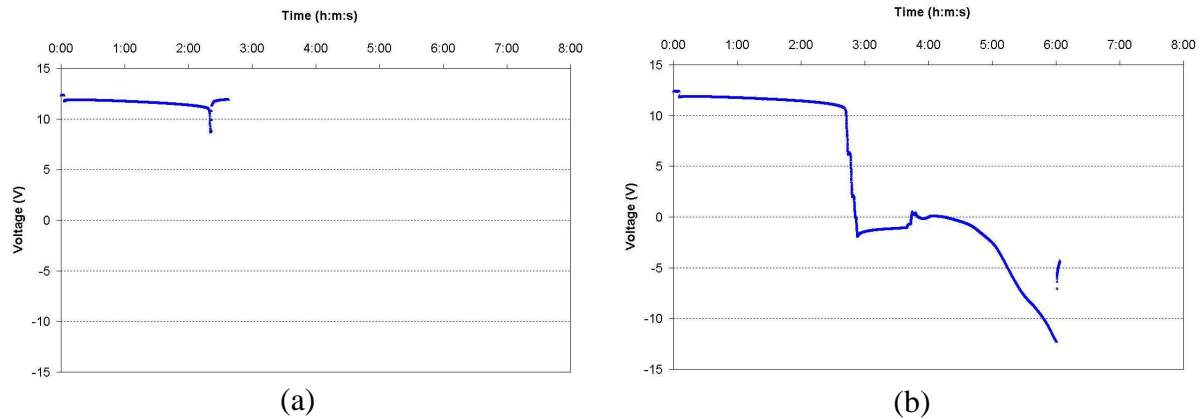


Figure 78: Discharge voltage profiles of B105 with limit-stop-discharge at 9 V (a) and of B101 at minus 12.0 V (b). B101 and B105 had been at open-circuit for 12 and 13 months respectively before the tests.

### 3.6.2.2 B101 – DCH(2) with B103 – DCH(2)

Two charge methods, IUi and prolonged IU, were tested on B101 and B103, whose history and SOC are almost similar each other. These two charge methods show the same efficiency in recovering battery SOC after very deep discharges with polarity inversion. The negative electrode reaches 65% of its nominal capacity and it is 90% for the positive electrode. It reveals also that, both charge methods are not sufficient to well charge deeply sulfated batteries, especially to well charge the negative electrode.

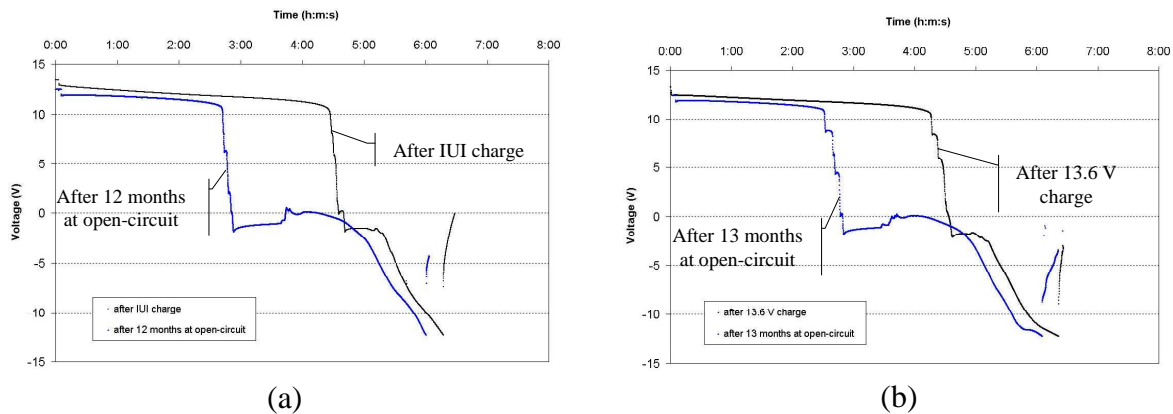


Figure 79: Discharge voltage profiles of B101 after 12 months at open-circuit and after an IUi charge (a). Discharge voltage profiles of B103 after 13 months at open-circuit and after a 13.6 V charge (b).

## 3.6.2.3 B103 – DCH(2) with B103 – DCH(3)

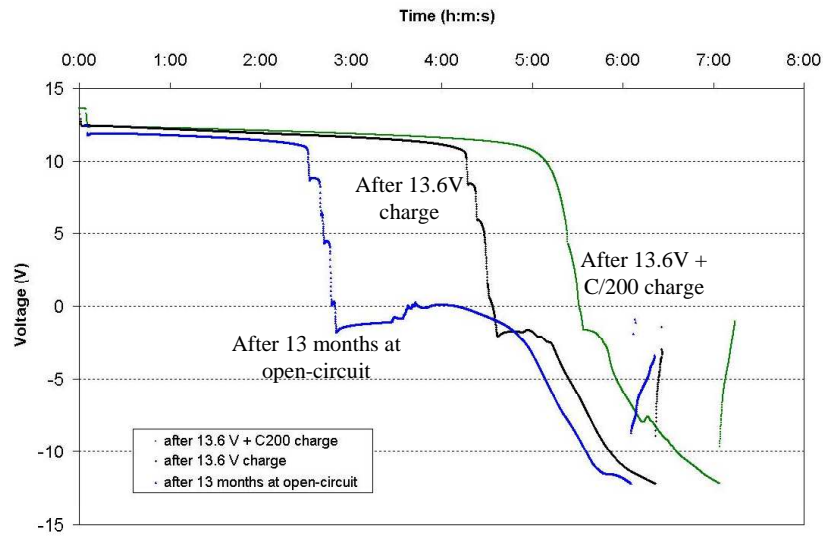


Figure 80: Discharge voltage profiles of B103 after 13 months of self-discharge (blue), after a one week at 13.6 V charge (black) and after 2 weeks at a 13.6 V + C/200 charge (green). Discharge rate is 1.8C/10

It is clear from Figure 80 that a prolonged charge with constant low current is necessary to recover battery SOC after a prolonged self-discharge period and polarity inversions. After this charge, SOC of the negative and positive electrodes are 90 % and 98 % respectively.

Table 9: Results of experimental tests subjected to B103. Calculated % of remaining capacity compared to nominal capacity  $C_{nominal} = 110 \text{ Ah}$

B103	Charged Ah	Discharged Ah at +6V	Discharged Ah at -6V	% negative capacity compared to $C_{nominal}$	% positive capacity compared to $C_{nominal}$
DCH -12V (1)	-	47.5	93	43	84.5
CH 13.6V	160	-	-	-	-
DCH -12V (2)	-	78.9	98.6	71.7	89.6
CH 13.6V	126.8	-	-	-	-
C/200	80.6	-	-	-	-
DCH -12V (3)	-	94.9	106	86.3	96.3

## 3.7 CONCLUSIONS OF POLARITY INVERSION

The following conclusions can be drawn from the study presented in this thesis on the polarity inversion:

**Mechanism of polarity inversion:**

The principle of polarity inversion relates to the limit diffusion of  $\text{HSO}_4^-$  ions from bulk electrolyte to supply discharge reactions. When the transport rate of  $\text{HSO}_4^-$  ions from bulk electrolyte is inferior to the imposed rate of discharge reaction, the exceed current will feed inversion reactions, i.e. charge reactions of the opposed electrode. Inversion occurs, potential value of the negative electrode becomes potential value of the positive electrode and vice versa. The  $\text{HSO}_4^-$  ions supplied for the discharge reaction come from two sources: by diffusion from the bulk electrolyte and as the produce of charge reactions. The discharge reaction rate is always superior or at least equals to the inversion reaction rate.

Once the inversion already occurs, the hump voltage, i.e. a quick increase followed by a return of the potential to the inversion level potential, can take place on either negative or positive electrodes. This phenomenon clarifies more the inversion process, which happens in the milieu of the electrode, in the back of the sulfate layer that prevents a sufficient diffusion of  $\text{HSO}_4^-$  ions to the remaining active materials. The inversion process consists of consuming the sulfate crystals of the latter layer and producing sulfate crystals in the deep of the electrode. The sulfate layer tends to move toward the heart of the electrode.

### **Distinction of negative and positive electrode inversions – application suggestion:**

The negative electrode inversion marks the difference to the positive electrode inversion with a very abrupt drop of potential and a presence of “coup de fouet”. It reaches far more rapidly its inversed potential value than the positive electrode does. These features allow recognizing an inversion if it is a negative inversion or a positive inversion without using reference electrodes.

This result can influence the surveillance of batteries subjected to charge/discharge cycles. In fact, on batteries consisting cells in a series configuration, the inversion of one electrode polarity (a voltage drop of 2 V) goes usually unnoticed within the only observation of the total voltage of the battery on discharge. From the nominal voltage of 48 V, which constitutes a standard current of photovoltaic station or a backup installation, EDF has carried out a surveillance system, which detects during discharging the first inversion of electrode polarity. The principle is: the intermediate voltages at the medial level (half battery voltage) are measured. The comparison of the voltage difference of the half batteries during discharging allows detecting the first inversion. Before the inversion, the voltage difference between two half batteries does not exceed generally 200 to 300 mV. The first inversion makes this difference overrun 1500 mV. For more details, in order to avoid being entrapped with two weak cells, which would be distributed to each half battery, in practice, the battery is divided into four parts and it is the maximum difference that constitutes the surveillance parameter.

The result obtained in this thesis would allow distinguishing between a first positive inversion and a first negative inversion and using this information to:

- authorize or not the pursuit of the discharge (if it is a first positive inversion, the discharge can continue but not the case of a first negative inversion as the oxidation of expanding additives can not be recovered).
- react on the subsequent management.

### Conclusion of chapter 3

In this chapter, the polarity inversion phenomenon during very deep discharge has been discussed.

In the case of a full traditional discharge, the current is interrupted when the voltage at the terminals of the cell begin to drop. The two electrodes, not having the same capacity, it is the weaker that determines the end of discharge and one does not know its concerns the negative or the positive electrode. Using a reference electrode help knowing this information but one does not have any information about the capacity of the other electrode unless extending the discharge until the voltage drop of the second electrode. The first electrode, forced to continue the discharge beyond its capacity, is subjected to a polarity inversion process. In other words, inside the negative electrode for example appears positive active material, i.e. lead dioxide: the potential of the negative electrode becomes then the potential of the positive electrode; *vice versa* for the positive electrode. Such an operation makes electrode tired and so, in a general manner, has to be avoided. The inversion of a negative electrode is even particularly detrimental in term of destroying by oxidation the lignosulfonates, which is an essential additive for its longevity. We consider, however, that in our case, the risk is negligible in the even that each tested battery has been subjected to only two or three cycles.

The tests have been carried out on 12 V batteries, i.e. six cells in a series configuration. In this case, only the terminals of the battery are accessible. They correspond to the negative electrode of the first cell (negative terminal) and the positive electrode of the sixth cell (positive terminal). The potential of these two separated electrodes of the terminals as well as the voltages of pseudo cells in a series configuration were analyzed. Two kinds of reference electrodes were used, giving the same results.

First results obtained from discharges of the flat-plate battery gave us not only the capacities of each electrode but also the potential profiles of electrodes and of pseudo cells during inversion. We obtained different potential profiles for the negative and positive electrodes with the presence of “coup de fouet” phenomenon at negative electrodes and not at the positive electrodes. These results allow recognizing if an inversion is on the negative or on the positive electrode without using reference electrodes. These results encouraged us to continue our exploration into this research, as the literature about this phenomenon is scarce.

Next, we operated deep discharges with polarity inversions on a tubular-plate battery. The results obtained clarify several aspect of this process: the mechanism of inversion in which the concentration of the sulfuric at the reactive surfaces tends to zero and inversion reactions (charge reactions of the opposed electrode) take place to produce  $\text{PbO}_2$  at the negative electrode and Pb at the positive electrode; the rate ratio between these inversion reactions and the discharge reactions with progressing inversion; different behaviors of potential profiles during inversion and when the discharge is switched off; high polarizations cause important heat losses.

We then applied discharges with polarity inversion to analyze a defective compress lead acid battery. The obtained results show that the first cell was short-circuited and lost most of its capacity. Another test confirmed these results by revealing that there was Fe in the electrolyte of this cell that developed the oxido-reduction “shuttle” phenomenon thus discharged the cell.

Discharges with inversion have been used to study state of charge evolutions of negative and positive electrodes of SLI heavy struck batteries exposed to different conditions: prolonged open circuit, IU<sub>i</sub> charge, float charge at 13.6 V, equalization charge with imposed low current at C/200. The obtained results give the self-discharge rates of both negative and positive electrodes as well as effects of different charge processes on deeply sulfated batteries. The equalization charge with an imposed low current and long duration is necessary to recover the capacity loss of the battery under prolonged open circuit, especially the capacity of the negative electrode. These results are used in the fourth chapter.

This work is a significant discovery for us about polarity inversion in particular and about lead acid battery in general.

## CHAPTER 4 - NEW METHOD OF MAINTAINING THE CHARGE OF STATIONARY LEAD ACID BATTERIES

### Introduction

Backup power supply is one of the main applications of lead acid batteries. Nowadays, VRLA batteries subjected to traditional float charges encounter the problem of short service life. This drives us to continue the work done at EDF R&D since 2000 on methods of maintaining the charge of stationary lead acid batteries. First of all, an overview is taken on stationary lead acid batteries concerning the self-discharge phenomenon, traditional float charges and standby battery failure modes. Then, a new method of maintaining the charge of standby batteries using low currents and periodical charges is studied and tested on different kinds of lead acid batteries including lead acid batteries with Sb grid alloys (SLI heavy truck batteries) and Sb free lead acid batteries (SLI car batteries and AGM VRLA batteries). Finally, a new management system with low current charges is proposed especially for VRLA batteries with expected targets of improved reliability and increased battery life span.

### 4.1 LEAD ACID BATTERIES IN STATIONARY APPLICATIONS

Secondary reactions such as corrosion, water decomposition and oxygen recombination are the main cause of self-discharge of stationary lead-acid batteries. Maintaining the charge of standby batteries is necessary to compensate self-discharge. However, if the maintaining-charge current is too high, it can accelerate these side reactions, which can thus become the cause of several failures of standby batteries. An appreciated method of maintaining the charge for stationary lead acid batteries is a trade-off between their state of charge and state of health.

#### 4.1.1 Secondary reactions as causes of self-discharge

Apart from electronic short-circuits caused by contact between current-conducting elements and by oxido-reduction “shuttle” of impurity ions present in the electrolyte, e.g.  $\text{Fe}^{2+}$  and  $\text{Fe}^{3+}$  (cf. 1.3.3.4), the self-discharge phenomenon in stationary lead-acid batteries is due to the simultaneous presence of main reactions, i.e. charge and discharge of active materials and unavoidable side reactions such as corrosion, water decomposition and oxygen recombination. At open circuit, the battery voltage does not only correspond to the equilibrium voltage of principal reactions but depends on the mixed voltage of both main and side reactions [1]. Its value is between the equilibrium voltage value of the principal reactions and the one of the secondary reactions. Water electrolysis is one of the principal secondary reactions and its potential difference is 0.7 to 0.75 V lower than the potential difference of the charge-discharge reactions (depending on electrolyte density and temperature). In these conditions, at open circuit, secondary reactions are produced at the expense of principal reactions; the battery is thus discharged or “self-discharged”. However, the influence of these secondary reactions is quite weak as the kinetics of oxygen and hydrogen evolutions are very slow. The battery potential difference at open circuit is smaller but very close to the potential difference of principal reactions.

The self-discharge caused by secondary reactions concerns only the positive or the negative electrode. The self-discharge of the negative electrode is mainly related to the evolution of hydrogen and to the reduction of oxygen, while the self-discharge of the positive electrode is

principally associated to the evolution of oxygen and to the corrosion of positive grids.

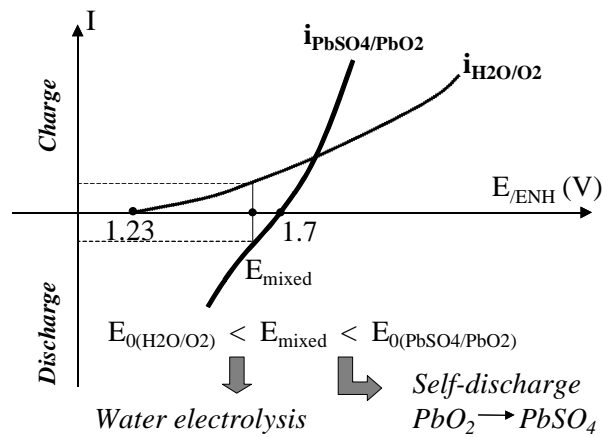
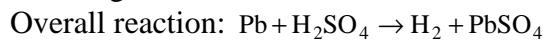
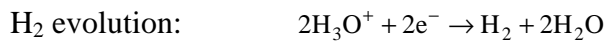


Figure 81: Establishment of a mixed potential  $E_{mixed}$  at the positive electrode at open circuit. Its value is between the equilibrium voltage value of the principal reactions  $E_{0(PbSO_4/PbO_2)}$  and the one of the secondary reaction  $E_{0(H_2O/O_2)}$  which leads to water electrolysis and self-discharge of the positive active material.

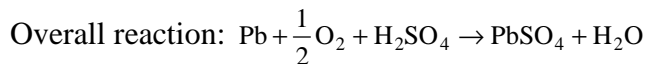
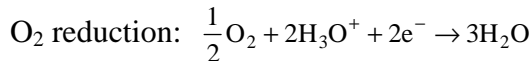
#### 4.1.1.1 Self-discharge reactions at the negative electrode

##### 1. Self-discharge due to hydrogen evolution



Reaction 23

##### 2. Self-discharge due to oxygen reduction

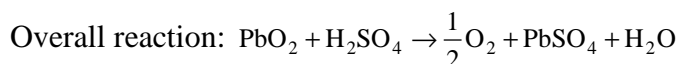
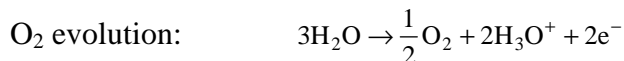


Reaction 24

Thus, in the presence of sulfuric acid, Reaction 23 and Reaction 24 cause self-discharge of the negative electrode with lead sulfate  $\text{PbSO}_4$  as the final product.

#### 4.1.1.2 Self-discharge reactions at the positive electrode

##### 1. Self-discharge due to oxygen evolution



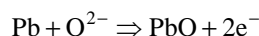
Reaction 25

##### 2. Self-discharge due to corrosion

When lead oxides supply the  $\text{O}^{2-}$  ions to neutralize the  $\text{Pb}^{2+}$  ions:



Grid corrosion:  $\text{Pb} \Rightarrow \text{Pb}^{2+} + 2\text{e}^-$



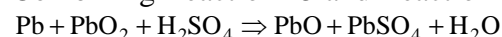
*Reaction 15*

Discharge of  $\text{PbO}_2$ :  $\text{PbO}_2 + \text{H}_2\text{SO}_4 + 2\text{e}^- \Rightarrow \text{PbSO}_4 + \text{O}^{2-} + \text{H}_2\text{O}$

*Reaction 26*

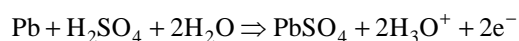
Combining Reaction 15 and Reaction 26, we have:

*Reaction 27*



When the grid is on contact with the electrolyte:

Grid corrosion:  $\text{Pb} \Rightarrow \text{Pb}^{2+} + 2\text{e}^-$



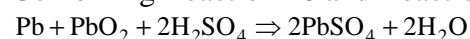
*Reaction 16*

Discharge of  $\text{PbO}_2$ :  $\text{PbO}_2 + \text{H}_2\text{SO}_4 + 2\text{H}_3\text{O}^+ + 2\text{e}^- \Rightarrow \text{PbSO}_4 + 4\text{H}_2\text{O}$

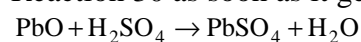
*Reaction 28*

Combining Reaction 16 and Reaction 28, we have:

*Reaction 29*



The formed lead oxide ( $\text{PbO}$ ) in Reaction 27 is converted into lead sulfate according to Reaction 30 as soon as it gets in contact with sulfuric acid:



*Reaction 30*

And the result is Reaction 29.

#### 4.1.1.3 Self-discharge rate [1]

It is clear that side reactions taking place at negative and positive electrodes are independent of one another and self-discharge rates are not equal between the positive and the negative electrode.

Self-discharge rates depend on a lot of factors such as temperature, grid alloys and the battery state of charge.

The rates of side reactions depend on temperature as well as the rates of self-discharge. This dependence is often described by the Arrhenius equation below:

$$k = k_0 e^{\left(-\frac{E_a}{RT}\right)} \quad (64)$$

In which:

$k$  : rate constant of the reaction

$k_0$  : pre-exponential factor or simply the *prefactor*, is an empirical relationship between the temperature and the rate coefficient  $k$ . It is determined experimentally.

$E_a$  : activation energy

$R$  : molar gas constant ( $8.3143 \text{ J} \cdot \text{mol}^{-1} \cdot \text{K}^{-1}$ )

Generally, the approximation holds true that a temperature increase of 10 K (degrees Centigrade) the reaction rate doubles. In electrochemical reactions, this means that equivalent currents are doubled, e.g. a temperature increase of 20 K means a current increase by a factor

of 4; a rise in temperature of 30 K corresponds to a factor of 8 [1].

In lead-acid batteries with antimony grid alloys, the self-discharge rate of the negative electrode is several times stronger than the self-discharge rate of the positive electrode, depending mainly on the battery age and the antimony content in the alloy of the positive grid. Indeed, at charge, the Sb metal, whose equilibrium potential is above that of the negative electrode, dissolves (corrodes) progressively from the positive grid, diffuses through the electrolyte and is precipitated (reduced) at the negative electrode. As this contaminated electrode has a lower hydrogen overvoltage, this results in a greater hydrogen gassing rate [1]. The more aged battery is, the more serious this “antimony affect” is. Sometime, this greater self-discharge rate of the negative electrode is masked by an extra negative active material quantity. In antimony-free lead-acid batteries, e.g. VRLA batteries with Pb/Ca grid alloys, the self-discharge of the negative electrode is largely reduced. It should be kept in mind that the electrode with stronger self-discharge rate limits the capacity of the cell.

The self-discharge rate depends also on the battery state of charge as it affects gassing reactions. It is clear that the self-discharge is easier when more active materials are available, or in other words hydrogen  $H_2$  and oxygen  $O_2$  evolution cannot occur at a surface covered by lead sulfate  $PbSO_4$ .

#### 4.1.2 Traditional method of maintaining the charge: float charge - a trade-off between state of charge and state of health

In order to compensate for the self-discharge of lead-acid batteries, a current whose value exceeds the self-discharge of the limit-capacity electrode has to be supplied. Traditionally, a voltage whose value is slightly higher than the battery open circuit voltage is applied to compensate the difference between mixed potentials and equilibrium potentials of the principal reactions. This is called “float charge”.

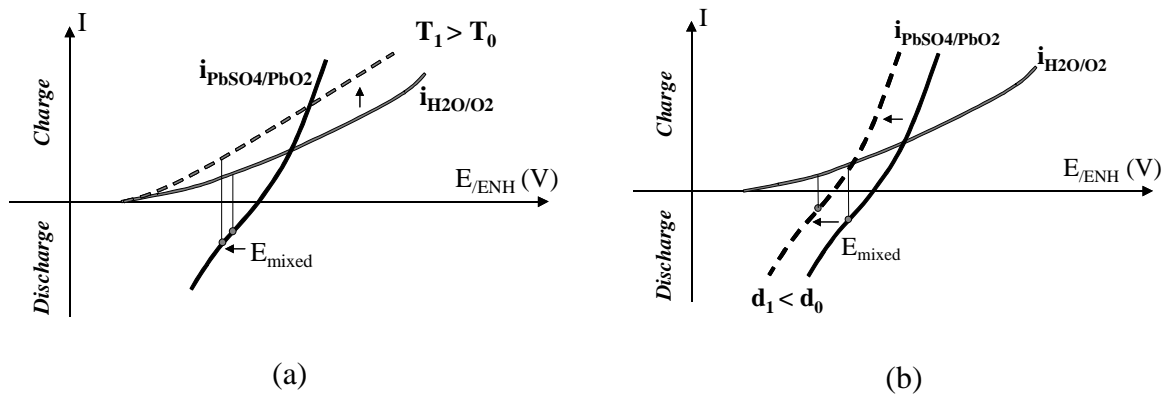


Figure 82: Principle schema to illustrate the dependence of mixed voltage ( $E_{mixed}$ ) on temperature ( $T$ ) and electrode density ( $d$ ). The movement of  $E_{mixed}$  due to temperature or electrolyte change is determined here by the movement of either oxygen curve or positive active material curve with time.

In reality, equilibrium potentials depend on a lot of factors such as temperature, electrolyte density, grid alloys [1, 15]. Moreover, as a constant voltage is applied between two terminals of a cell, the potential distribution is not properly shared between the negative and the positive electrode [61-65]. In batteries with cells in a series configuration, the phenomenon of voltage scattering on cells is also present [1, 65-67]. In addition, it should be kept in mind that the float polarization increases gas evolution rates at both electrodes. It is very difficult or even

impossible to choose a value of float voltage, which can take into account all of these phenomena without paying the piper. Convenient practical values for float voltage have been empirically determined. To get rid of the risk of under-charge, batteries in float charge are permanently overcharged.

#### 4.1.2.1 Bimodal float voltage distribution between the negative and positive electrodes – difference between vented and VRLA batteries.

The electrode reactions on float charge are described in detail by Berndt and Teutsch [61]. During float charge, hydrogen evolution, oxygen evolution and grid corrosion proceed certainly as presented in Figure 83. The float current serves to compensate the electrode discharge caused by these side reactions in maintaining the voltage above the open-circuit value. When this float current is too low, i.e. the positive potential is slightly below its equilibrium value, or the negative electrode potential is slightly above its equilibrium value, the discharge of the electrodes would occur. Otherwise, the battery is completely charged or overcharged. In general, batteries in float charges are permanently overcharged. The float current, i.e. overcharged current, feeds electrons to secondary reactions.

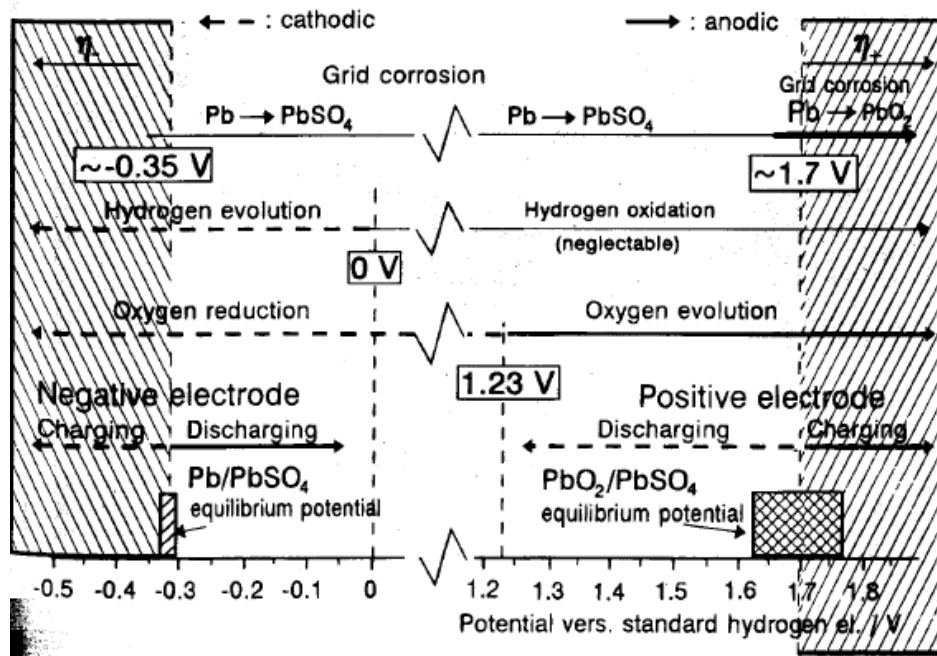


Figure 83: Reactions that occur in lead acid batteries dependent on electrode potential. Equilibrium potentials of charge-discharge reactions ( $\text{Pb}/\text{PbSO}_4$  and  $\text{PbSO}_4/\text{PbO}_2$ ) are presented in columns, because they depend on the acid concentration. Hatched areas mark polarization ranges that are shown in Figure 86 [61]

Berndt and Teutsch presented the model used for float charge describing the single cell behaviors at overcharge in [61]. Under normal float conditions as the battery is already completely charged, the charge and discharge reactions of the active materials do not occur. The equal float current flow through both electrodes can be written:

$$\text{At the positive electrode: } I_{\text{float}} = I_{\text{O}_2 \text{ ev.}} + I_{\text{corr.}}$$

$$\text{At the negative electrode: } I_{\text{float}} = I_{\text{H}_2 \text{ ev.}} + I_{\text{O}_2 \text{ re.}}$$

The balance reaction:  $I_{\text{float}} = I_{\text{O}_2 \text{ ev.}} + I_{\text{corr}} = I_{\text{H}_2 \text{ ev.}} + I_{\text{O}_2 \text{ re.}}$

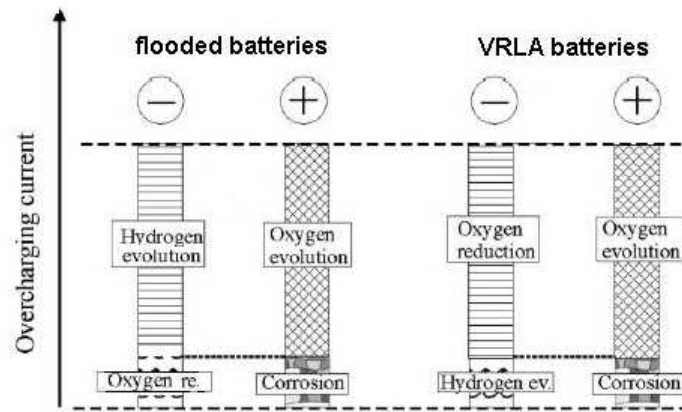


Figure 84: description of equal float current flows through both electrodes in the normal conditions at flooded batteries and VRLA batteries. Supposing that the recombination efficiency at the VRLA battery is 100%.

As shown in 1.5.4.3, in general for electrochemical reaction the current is an exponential function of the electrode potential (cf. Eq. (32)). At high overvoltage, current/voltage curve forms a straight line, called “Tafel line”.

$$\eta_a = \frac{RT}{\alpha n F} \ln(|i|) - \frac{RT}{\alpha n F} \ln(|i_0|) = a + b \log(|i|) \quad (32)$$

This is applied also for the  $\text{H}_2$  and  $\text{O}_2$  gas-evolving reaction in lead acid batteries, since they are polarized by more than 0.3 V already at the battery open-circuit voltage. Tafel lines for hydrogen and oxygen evolution have been confirmed in literatures. A slope  $b$  of about 0.12 V per current decade is nearly always found for hydrogen evolution, while the corresponding slope for oxygen evolution is between 0.07 and 0.14 V per current decade [1, 15]. Feder and Carosella revealed that at float charge of a vented lead acid battery, the negative electrode is polarized more than the positive electrode [68].

In the case of VRLA batteries, the principal reactions at the negative electrode during floating are hydrogen evolution and oxygen reduction. As the rate of  $\text{H}_2$  evolution rate is low thanks to the utility of antimony free grid alloys, essential float current is for the oxygen recombination. As mentioned in chapter 1 (cf. 1.3.3.2), the rate of the oxygen reduction reaction is determined by the rate of oxygen diffusion from the positive electrode to the negative electrode, which does not depend on the electrode potential. If the diffusion of oxygen is sufficiently fast, which is the case in VRLA batteries, the recombination oxygen will occur, as the potential condition - inferior to 1.23V - is already satisfied at the negative electrode. The negative electrode is thus only polarized by the hydrogen evolution reaction. Therefore, in VRLA batteries the positive electrode takes essential polarization and the negative electrode can be depolarized during float charges.

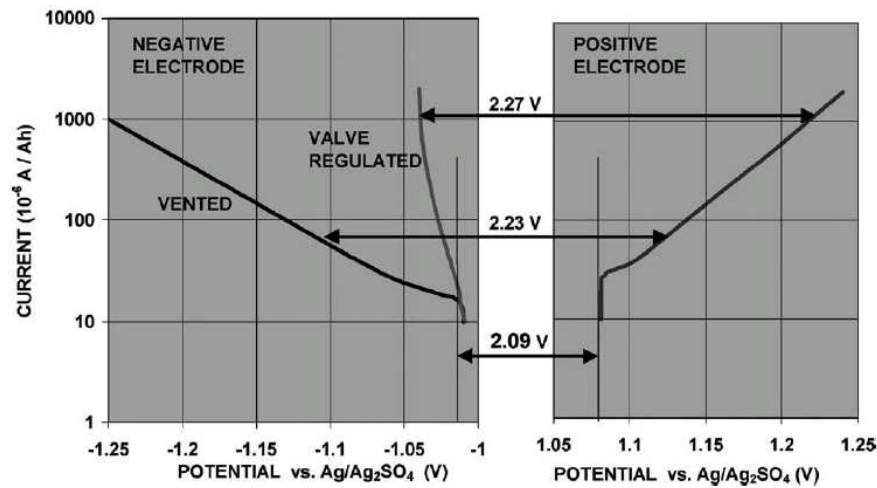


Figure 85: Expected polarization curves of positive and negative electrodes, when measured against silver–silver sulfate reference electrodes. This figure demonstrates that the positive electrodes of valve-regulated batteries are subjected to much higher potentials than the positive electrodes in vented batteries [62]

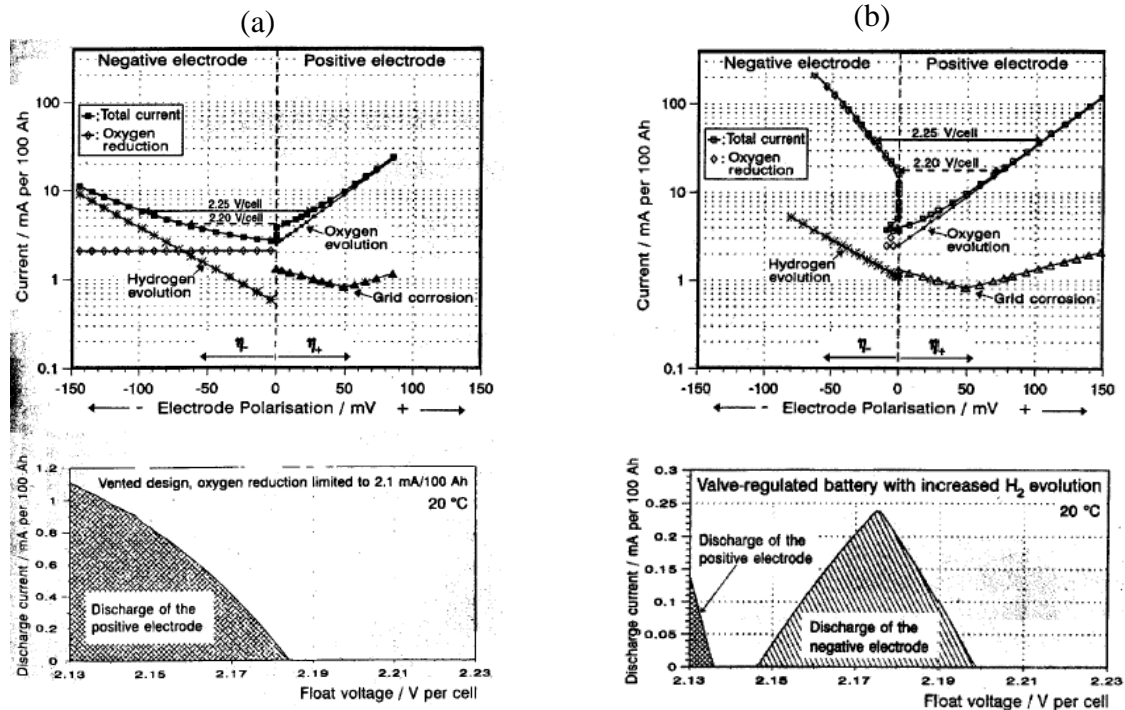


Figure 86: Mathematical models: currents vs. electrode polarization; at 2.20V/cell float voltage: (a) discharge current of the positive electrode of flooded battery and (b) discharge current of the negative electrode of VRLA battery [61]

#### 4.1.2.2 Cells in series configuration – scattering problem

In general, in order to obtain a desirable voltage value, one battery is composed of several cells connected in series configuration. A usual phenomenon observed in these assemblies is the voltage scattering between the individual cells [1, 65-67]. One example given by Berndt [1] shows that for a mean float voltage of 2.38V per cell, a normal distribution curve with a standard deviation of  $\pm 33\text{mV}$  and a difference between the maximum and the minimum

values of 170mV are noticed. There are many reasons producing the voltage scattering. Two of them are found in industrial installations, despite the rigorous manufacturing process control and special industrial conditions [67]. The first reason is due to the difference in the characteristics of the cells, even in the same production batch. The second one relates to the reality that in industrial installations, it is impossible to control self-discharge condition and state of charge characteristics of each cell before using.

It is revealed above that the polarization is not properly symmetrical for negative and positive electrodes. The voltage scattering thus reflects the voltage dispersion of negative electrode in flooded batteries [68] and of the positive electrode in VRLA batteries [61, 66].

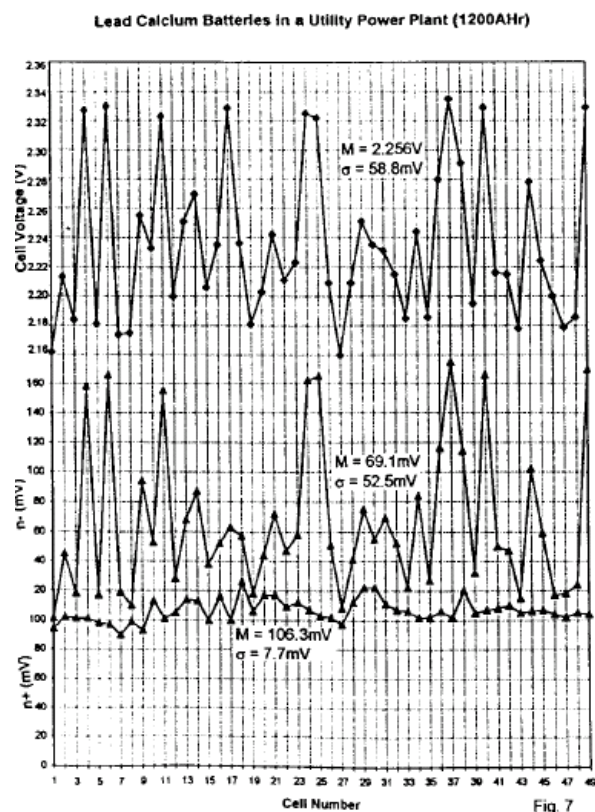


Figure 87: Distribution of 113 V on 50 vented cells Pb-Ca in series configuration for 9 years of float charge.  $\eta^-$  and  $\eta^+$  are potentials of the negative and positive electrodes.

Voltage dispersion appears obviously at the negative electrodes and its presence is far smaller at the positive electrodes [68].

### 4.1.3 Secondary reactions as causes of failure modes

At float charges, if both electrodes are well polarized, i.e. float potentials exceed the equilibrium ones; float currents will serve only to produce side reactions. The higher the float current is, the stronger the rates of side reactions are, especially the rates of gas evolution reactions.

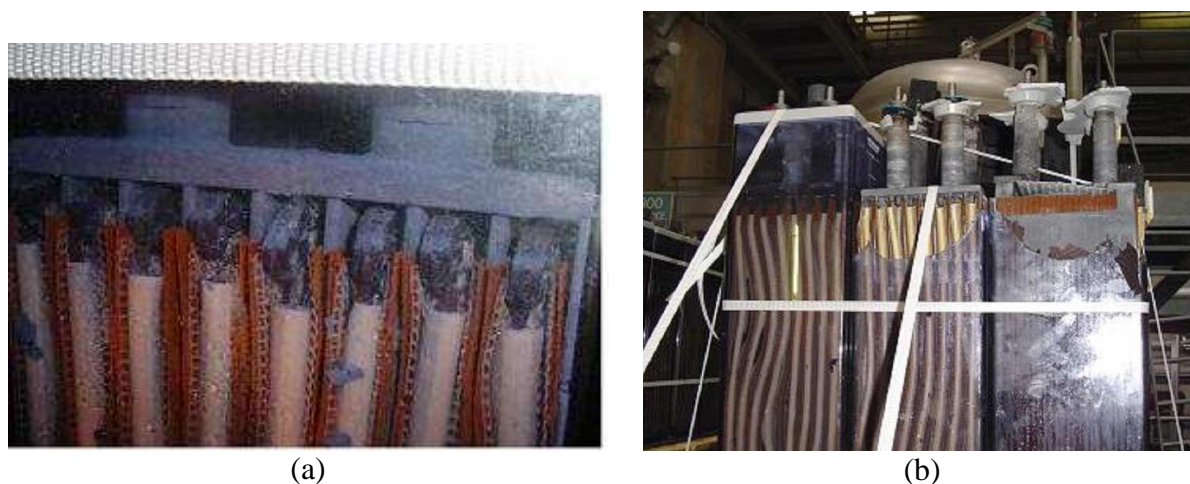
Secondary reactions are not only the cause of self-discharge, but also the cause of many failure modes of stationary lead acid batteries under constant float voltages. Flooded and VRLA technologies can be affected by corrosion, including creeping, and degradation of positive electrodes [1, 47, 49, 69-73]. VRLA batteries are moreover subjected to electrolyte drying out and thermal runaway [1, 49, 71, 73, 74].

#### 4.1.3.1 Corrosion

Corrosion leads to the increase of the oxide multi-layers  $PbO_x$  (cf. 1.3.3.3) and is the cause of different failure modes [47, 49, 75-81]:



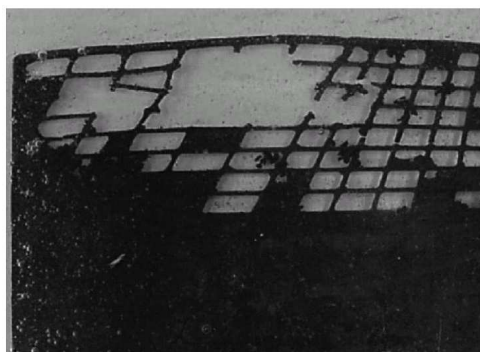
- The oxides, corrosion products, take more volume than the metallic grid. The result is an expansion of the positive grid into three dimensions, in particular into the dimension of each bar of the grid. Under such mechanical stresses, the grid bars get longer and the grid dimension increases, this is called “grid growth” or “grid creeping”. This distortion can provoke internal short-circuits when the grown grid comes into contact with the negative top-bar (cf. Figure 88).
- The formation of an electric passivation layer (barrier layer) at the interface between a positive grid and its active material prevents all electrical contact between them. The passivation layer is sometimes said to be a closely structured  $\text{PbSO}_4$  layer (high-resistance layer) formed at the grid active-material interface, or lower oxides of lead, such as  $\text{PbO}$ , that are generated in a high-pH environment.
- When the grid growth becomes excessive, apart from the passivation layer other causes of gradual loss of contact between the active material and the grid are noticed. The first one is the displacement of the active material away from the grid as it is not able to follow the grown grid. The second one is the gradual disappearance of the metallic grid, i.e. the grid is consumed by corrosion and can no longer take the role of electric conductor (cf. Figure 89).



*Figure 88: Due to corrosion, short-circuit took place and caused explosion accident in a standby tubular battery: (a) positive plate lengths were increased and touched the negative collective bar, (b) positive plates were distorted; the positive terminal obviously became more higher than the negative terminal; battery was destroyed after explosion (source: EDF).*

VRLA batteries under float charges, along with their grid design and their characteristic of the oxygen recombination, seriously suffer the corrosion consequences. Usually, 4% grid growth over the battery lifetime is the design limit. In most VRLA batteries, the grid sections are smaller; grid growth rates thus should be higher. There is some evidence that designs with absorbed and limited amounts of electrolyte are less tolerant to growth and, therefore, suffer greater capacity losses [78]. Moreover, in VRLA batteries, in order to lower the self-discharge rate, Pb/Sb alloys are replaced by Pb/Ca alloys, where the electric passivation of the positive grid alloy, called the “antimony-free effect” occurs [77, 82]. In addition, the operation potential of the positive electrode under float charge is higher in VRLA designs (cf. 4.1.2.1). For instance, the potential of the positive electrode is likely to be 50 to 100 mV higher than in a flooded battery [78]. Different publications have demonstrated that there is a zone of positive polarization where the corrosion is minimum (cf. 4.2.1.2). According to Brecht et al. [83], the corrosion rate is minimum when the positive polarization is between 30 and 70 mV

and increases to almost double at 150 mV. Therefore, the increase of the grid growth due to corrosion is further encouraged in VRLA batteries under float charges.



*Figure 89: Corroded positive plate of a starter battery, at the end of 5 years of service life in a passenger car [47].*

#### 4.1.3.2 Water loss

Water electrolysis, i.e. evolutions of hydrogen at the negative electrode and oxygen at the positive electrode, as well as positive grid corrosion cause water loss of the electrolyte (cf. 1.3.3). In VRLA batteries, despite of the recombination of oxygen at the negative electrode, water loss always occurs. This is due to the evolution of hydrogen, which cannot be re-oxidized to water at the positive electrode, at least not at significant rates. Other causes of water loss such as container leakages, water evaporation, which are not mentioned in this thesis, aggravate the situation.

#### Dry-out

Water loss is not a problem as long as the electrolyte level can be refilled like in the case of flooded batteries. However, in the cases where maintenance intervals are not being properly respected or float charge rates are too high, water loss can reduce the capacity of the battery and finally limit the battery lifetime. Water loss induces a higher acid concentration, which results in an increase of the electrode equilibrium potentials. This means that oxygen and hydrogen overvoltages at open-circuit increase which lead to the growth of gas evolutions or of self-discharge rates. This would require an increase of float currents and of charge currents. If this demand is ignored, an insufficient state of charge and sulfation of plates can occur. If the electrolyte level is below the plate edges, the part of the plates above the acid level cannot be charged properly and this part of the plates will then undergo sulfation as well [47]. A dangerous case can happen when there is short-circuit in a non-electrolyte area; ignition of hydrogen can take place and provoke explosion (cf. Figure 88).

In the case of VRLA batteries, as water cannot be refilled, water loss can become a serious problem, especially at high temperatures or excessive float voltages. Electrolyte “dry-out” is often observed. Apart of the increase of gas evolutions as mentioned above, the electrolyte decrease leads also to a decrease in the contraction of separator, when the electrolyte content is under 90 % [71]. As separators in actual batteries initially retain about 95% of the electrolyte, separators shrinkage is not appreciable. This shrinkage can bring later to poor contacts between the plates and the separators, increasing the internal resistance. The increase of acid concentration due to water loss can induce also an increase of oxygen recombination efficiency [49]. This chemical reaction of oxygen reduction is a strong heat source. Oxygen evolution is higher with the increase of acid concentration. Excessive recombination efficiency can increase dramatically the temperature of the battery and can lead to a so-called thermal runaway.



### Thermal runaway

Thermal runaway is a current phenomenon observed at VRLA batteries [1, 84-87]. It is defined as an unstable state of operation where heat generation increases faster than heat can dissipate [1]. It is also described as the increase at charge or float current that occurs as a result of increase in cell temperature from initial applied constant potential. In other words, thermal runaway is usually considered to be the result of positive feedback of current and temperature when a cell is placed on float charge at constant potential [86]. The initial float current flowing through the cell causes an increase in cell temperature that causes an increase in current that further increases the temperature until both current and temperature reach high values.

Two main source of heat during charging are the reversible heat effect of the cell reactions and the Joule heating caused by the charge current. The internal oxygen cycle represents a special form of Joule heating, it is a strong heat source (cf. 1.5.6).

The important parameters that mainly influence the internal oxygen cycle are the applied float voltage, the ambient temperature and the separator dry-out or the electrolyte saturation level in the separator pore volume. High floating voltages and high temperatures induce more water loss, which in turn reduces the electrolyte saturation in the separator pore volume. The lower the saturation is, the more favorable condition for the internal oxygen cycle to take place.

According to J. Hu et al. [87], when the saturation is low, there is more gas space in the AGM separator for oxygen generated from the positive plates to transport to the negative plates, where the oxygen recombination occurs. Oxygen reduction shifts the potential of the negative electrode to a less negative value. Since the applied voltage was unchanged, the potential of the positive electrode shifts more positively, which in turn leads to the generation of more oxygen on the positive plates. So the floating current response becomes increasingly high. The thermal runaway occurs. In fact, the increased current at a constant float voltage is mainly used for oxygen evolution on the positive plates and the oxidation of Pb by O<sub>2</sub> on the negative plates to produce PbSO<sub>4</sub> (cf. reaction of self-discharge by O<sub>2</sub> reduction).

According to B. Culpin [86], at high saturations, oxygen transport by the pressure-assisted route gives good recombination efficiencies of the order of 95 ÷ 97%, but only at low float currents. At low saturations oxygen transport is mainly by pure diffusion and the recombination efficiency is high even at high current. This high recombination current generates much more heat than when gassing overvoltage occurs and thermal runaway takes place.

These same authors shown that the battery is out of control and thermal runaway occurs at a specific saturation of the separator around 80 ÷ 85 % even at low applied float voltages.

B. Culpin resumed the thermal runaway procedure in three stages:

- Stage 1: recombination efficiency is low, water loss is high, temperature and current rise slowly due to the small and slowly increasing internal resistance and low recombination efficiency.
- Stage 2: the recombination efficiency, even at high currents is high because of the change in oxygen transport mechanism through the separator. Heat generation increases rapidly because of a combination of increased recombination rate and increased internal resistance of the separator.

- Stage 3: the current rapidly decreases to zero as a result of the rapid increase in separator resistance. In fact, the internal resistance increases rapidly when the saturation is below 80 %, e.g. at 40% saturation the separator has a resistance 30 times of that in a fully saturated state.

J. Hu et al. presented some consequences when thermal runaway occurs:

- The very high temperature and violent oxygen evolution accelerated the corrosion of the positive grid.
- The negative active material after thermal runaway has lost its dendrite lead structure and is composed of sand-like poorly crystallized  $\text{PbSO}_4$  particles. After thermal runaway, the contact between the positive active material particles are very poor and many big  $\text{PbSO}_4$  crystals remain even though the battery temperature has risen to a very high value and the charge current has exceeded 15 A. Apparently the violent oxygen evolution caused many  $\text{PbSO}_4$  crystals to loose conductivity so that they become inactive. The resistance of both positive and negative plates increases about 20 times.

## 4.2 NEW METHOD OF MAINTAINING THE CHARGE - LOW CURRENT METHOD

### 4.2.1 New method of maintaining the charge

The new method of maintaining the charge using low currents and periodical charges was invented by J. Alzieu and G. Dillenseger in 2006 [88]. It was tested on Pb-Ca SLI motor car batteries and presented in detail on the PhD thesis of G. Dillenseger [6]. The following work continues to study this new method and its effect on different kinds of lead acid batteries including SLI heavy truck batteries with antimony grid alloys, SLI car batteries antimony free and AGM VRLA batteries.

#### 4.2.1.1 Heritage of intermittent charges

In order to limit the overcharge problem, instead of continuous charge, periodic charges (ON phases) are applied and the rest of the time the battery is kept on open circuit or open-circuit voltage (OFF phases) [89]. This is called intermittent floating or charge. This method is executed based on the principle that a battery on open-circuit for a given time (from some seconds to some weeks) loses a part of its capacity, which can be restored by a charge.

Table 10: Bibliography summary of characteristics of intermittent charges for VRLA batteries [6].

Characteristic	Gun et al. [93]	Reid, Glasa [89]	Yuasa [94]	Giess [92]	Rossinot et al. [90]
Phase OFF	Open-circuit	2.17V/cell	Open-circuit	2.15V/cell	Open-circuit
Duration	$\approx 15$ s	-	$\approx 2$ months	108 h	$\approx 1100$ s
Fin condition	End-voltage	-	End-voltage 2.125 V/cell	-	End-voltage 2.16V/cell
Phase ON	Constant current	Constant voltage	12 Ah	Constant voltage	Constant current
Fin condition	-	2.375 V/cell	charged	2.25V/cell	23.8 mA/Ah
		-		-	End-voltage 2.34V/cell
$\alpha$ = duration ON/(ON +OFF)	0.0625	0.5	$\approx 0.1$ to 0.03	0.357	0.0054

Different researches have shown positive results of intermittent charge vs. floating charge concerning reduced average overcharge [90, 91], increased efficiency of charge phases [90] and reduced thermal runaway in VRLA batteries [92]. However, if the intermittent charge parameters (threshold voltages, charge voltage or current, duration of ON phases and OFF phases...) are not optimized, the risk of under charge, especially under charge of the negative electrode of VRLA batteries is frequent [91]. Improving intermittent charge parameters is still an open subject of research.

#### 4.2.1.2 Benefit of corrosion minimum

Different publications about positive electrode corrosion have demonstrated that there is a potential zone where corrosion is at a minimum (cf. Table 11). This minimum would be at positive polarizations ( $\eta^+$ ) between zero (at open-circuit) and polarizations at float charges ( $\eta^+ \approx 100$  mV). According to Brecht et al. [95] this minimum zone is situated in the range of [30;70] mV. This also shows that neither open-circuit on intermittent charges nor overcharge by traditional float charges can place the positive electrode potential in the minimum corrosion zone.

Table 11: Bibliography summary of positive polarization ( $\eta^+$ ) associated to a corrosion minimum [6].

Reference	Analysis type	Minimum span (mV)	$\eta^+$ min (mV)
Lander 1956 [96]	Grid without active material, few hours	$30 < \eta^+ < 200$	“flat”
Ruetschi 1964 [97]	Grid without active material, few hours	$100 < \eta^+ < 250$	180
Willihnganz 1968 [81]	Service life (accelerated), some years	$50 < \eta^+ < 100$	No defined
Brecht et al. 1989 [83, 95]	Grid growth (accelerated), some years	$30 < \eta^+ < 70$	40
Berndt 1996 [61]	Review of literature	$40 < \eta^+ < 80$	60
Ruetschi 2004 [47]	Review of literature	$20 < \eta^+ < 80$	60

#### 4.2.1.3 Principle of the new maintaining charge method

Taking into account this minimum corrosion zone, a new method for maintaining the charge of standby lead acid batteries, called *Low-current* method, has been developed at EDF [6, 88, 98]. This method is derived from the intermittent charge: open-circuit periods are replaced by constant low current periods. These constant currents, whose values are smaller than traditional float currents, are intended to compensate, at least partially, self-discharge currents, and preferably place the battery in the minimum corrosion zone.

The choice of piloting the current instead of the voltage to supply low positive polarizations relates to the fact that maintaining a voltage with a value very close to the battery open voltage is difficult and can accidentally discharge the battery [92]. Moreover, the scattering phenomenon when a voltage is applied to the battery consisting of cells in series configuration is unavoidable. Monitoring the voltage share for each cell is difficult and expensive while applying a current ensures that every cell receives a given current value.

Although these low currents alone are not supposed to maintain the full state of charge, they can compensate most of the self-discharge. They thus enable the intervals between recharge phases to be considerably extended so that water losses and corrosion associated to these charges would be reduced.

Expected results are: (i) a slow down of the corrosion rate of positive grids, (ii) a reduction of the need of periodical charges.

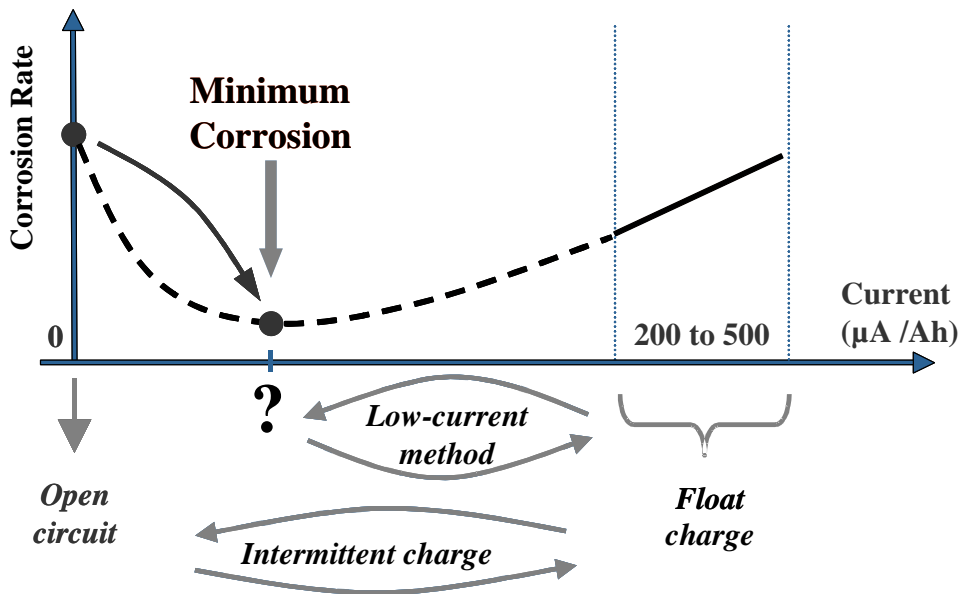


Figure 90: Low-current method is derived from intermittent charge: open circuit periods are replaced by low currents, whose values are smaller than float current (200 to 500  $\mu\text{A}$ ). Battery should be in the minimum corrosion zone.

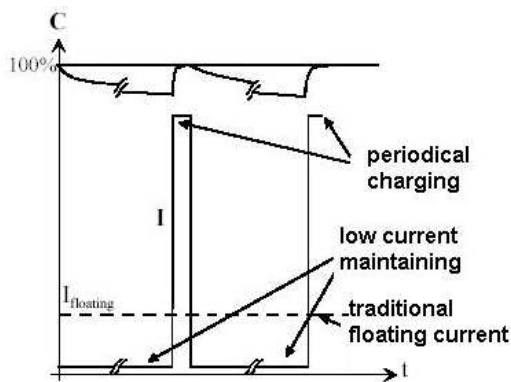


Figure 91: Principe of new charge strategy using low-current and periodical charges

#### 4.2.2 Experimental

In backup applications, maintaining the charge of stationary batteries is an opposite situation from the accelerated charges studied in chapter 2 in terms of very weak charge regimes. This leads to a comparable problematic of main and side reactions monitoring, which differs from a traditional situation. In fact, in very weak charge regimes, faraday efficiency deteriorates, meaning that the proper charge and secondary reactions take place jointly. It should be noted also that charge voltages lead to increased rates of side reactions.

This drives us to the following questions:

- At a given ambient temperature and given battery, what is the rate of self-discharge?
- At the same ambient condition and the same battery, beyond which current value, the self-discharge is compensated? This is clear that this current is not only equal but has to exceed self-discharge current.
- At this current, how does positive grid corrosion behave?

The answers obtained will serve to determine the parameters of the new low current method: regimes and durations of low current phases and periodical charge phases.

Laboratory experiments aim to evaluate the state of charge of batteries subjected (1) to open circuit, (2) to float charges and (3) to polarizations whose values are intermediate between zero and float polarizations, i.e. low current charges. Several current values below float currents have been tested.

Two methods to evaluate the battery state of charge were used to clarify this question:

- Measurement of lead sulfate content in the battery active materials by a chemical titration. This procedure requires the destruction of the battery
- Battery capacity measurement by discharge test.

In order to compare these two methods, evolutions of the lead sulfate content as well as of the capacity will be converted to current. At open circuit, increases of sulfate content and losses of capacity correspond to self-discharge currents.

We started different experiments with antimony-free vented SLI batteries, Exide L01033C24A, 40 Ah-12V. During the experiments, capacity measurement results of these batteries shown a high degree of dispersion, which we attributed to the fact that they are not suitable for repetitive charge-discharge cycles. We then continued these experiments with two other types of more robust batteries: heavy truck SLI flooded lead-acid batteries, Exide 110 Ah/12 V D02075W01-A, low antimony grid alloys and EnerSys 400 Ah/2 V VRLA AGM batteries.

Low currents were applied using METRIX power supplies AX 502 2.5A – 30 V. As their accuracy does not allow a fine control of currents as low as a few mA, these power supplies were used as voltage regulators and the low currents were set using resistors in series.

Positive polarizations were evaluated using a lead acid battery reference electrode, which was first charged and then stabilized at open circuit. A current path between the tested cell and the reference electrode was provided by a tube filled with immobilized electrolyte (cf. 3.2.3, Figure 58).

The discharge-charge cycles were performed with BITRODE Battery Charge and Test System, Module Type LCN 100A – 5V.

Voltages, currents, positive polarizations and temperatures were recorded with Personal Daq 56<sup>TM</sup> USB Acquisition Systems.

#### *4.2.2.1 Lead sulfate content measurement [6]*

Batteries used for lead sulfate measurements were antimony-free vented SLI batteries, Exide L01033C24A, 40 Ah-12V. The plates were pulled out of the batteries and rinsed with distilled water for one week before picking up active material samples. Lead sulfate contents on the later samples were measured chemically: the successive formation of complexes is achieved using nitric acid, acetic acid, xylenol orange and titriplex III (EDTA). The last complex is reached using a titrated solution of EDTA. The final stage of this reaction induces a color change: violet to yellow. Sulfate content was calculated from the sample mass and the quantity of EDTA used.

### 1. Open circuit

In order to estimate the rate of self-discharge, we measured the lead sulfate content of the batteries 40Ah/12V, which were in open circuit for different durations: 5, 9.5, 20.5, 21.5 months at ambient temperatures; 177 days at 60°C that we considered to be equivalent to 2838 days at 20°C according to the Arrhenius law (acceleration factor  $2^4 = 16$ ).

### 2. Low-current compared to open circuit

Four batteries were subjected first to open circuit during 231 days, then to low currents of 25, 50, 100 and 200  $\mu\text{A/Ah}$  during 356 days at room temperatures ( $23 \pm 4^\circ\text{C}$ ) and were finally opened to analyze their lead sulfate content.

#### *4.2.2.2 Capacity measurement by discharge test*

Before beginning the experiments, we had a preliminary remark that the measurements of self-discharge, even after several months at open circuit, represent only a weak portion of the capacity, e.g. about 10%. The expected results concern differences between reduced rates of self-discharge. These results were supposed to be a few percent of the nominal capacity, which is less than the natural dispersion we generally observe in capacity measurements (e.g. between several batteries taken at random from the same lot of fabrication).

Two methods are *a priori* possible:

- Testing with a big enough number of batteries to obtain precise and meaningful statistical averages. We haven't chosen this method because the number of batteries required is too big for our test facilities.
- Comparing the capacity results of every single battery subjected to n months of self-discharge or floating or low-currents to its own capacity measured after a full charge. This is the chosen method.

Tests of discharge with the limit-stop-discharge voltage at minus 2 V/cell, which provoke the polarity inversion of the cell, were used for flooded batteries 110 Ah/12 V to determine the capacity of both negative and positive electrodes using reference electrodes (cf. 3.6). Although such a deep discharge is detrimental for lead acid batteries, it was decided to proceed because only some tests were necessary for the whole experiment. The battery capacity was taken as an average of six positive electrodes, whose discharge was measured individually. The test of discharge with polarity inversion was operated one time on a VRLA battery to determine the limit-capacity electrode. The other tests were executed at the limit-stop-discharge voltage at 1.8 V/cell.

### 1.Exide 110Ah/12V, SLI heavy truck batteries, 1.6%Sb

As presented in 3.6.1, these batteries were stocked at open-circuit for one year or more before subjecting to our tests. In order to estimate the initial state of charge, batteries were discharged at 18 A. A “full” IUi charge of one week at 11A (C/10) and 13.6V followed by one week at 0.55A (C/200) without voltage restriction were executed to reestablish a good state of charge. The same discharge-charge was performed before these batteries were subjected to low currents, float charge and open circuit. We called “first reference capacities” the capacities we measured during this cycle. After 6 months under this service, the batteries were discharged at the same rate (18A), and then they were recharged and discharged (second

reference capacities) again one more time. All of these experiments were done at ambient temperatures.

## 2. EnerSys 400 Ah/2 V, AGM VRLA batteries, new

These batteries were self-discharged at open-circuit during two months before testing. Fifteen discharge-charge cycles were executed in order to stabilize the battery capacity. A refresh charge at 2.27 V during one week followed by a discharge test at C/10 (reference capacity), then a charge IU<sub>i</sub> (C/10 – 2.4 V during 5 hours – C/80 during 2 hours) and another charge at 2.27 V during one week were operated before the batteries were subjected to service at 46°C: open circuit, low-current and float charges. After one month, the batteries were discharged to determine their final capacities. These experiments were repeated one more time at 50°C.

## 3. EnerSys 400 Ah/2 V, AGM VRLA batteries, old

These batteries were taken from the field and replaced by new ones after six-year service, which corresponds to their mid-life (they are designed to last twelve years or more). These batteries were first subjected to fifteen discharge-charge cycles in order to stabilize their capacities. The last capacity obtained is the reference capacity. They were then subjected to tests at room temperatures ( $18 \pm 3^\circ\text{C}$ ): open circuit, low-currents of 29 and 105  $\mu\text{A}/\text{Ah}$  and float charge at 2.27V (current response is 414  $\mu\text{A}/\text{Ah}$ ). After six months, these batteries were discharged with the same rate (C/10) to determine their final capacities.

### 4.2.3 Sulfate content measurement – results & discussion

#### 4.2.3.1 Lead sulfate content at open-circuit

The level of lead sulfate of batteries at open circuit at ambient temperature and at 40°C and 60°C in equivalent days at 20°C is presented in the Figure 92. Equivalence is based on the Arrhenius law, i.e. kinetic reaction doubled every 10-Celsius degree.

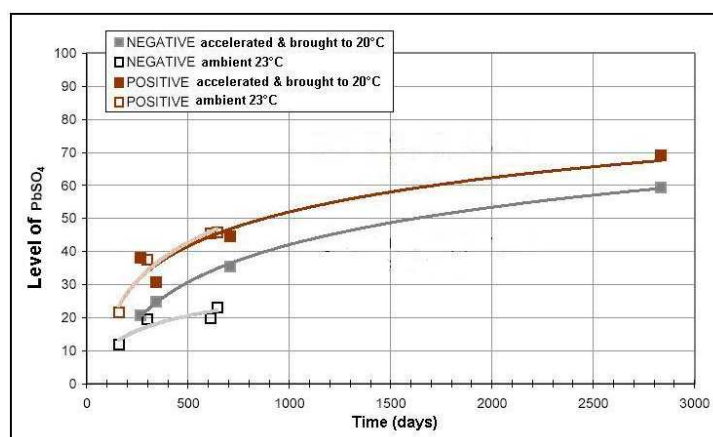


Figure 92: Lead sulfate levels (% mass) of four batteries at open circuit at ambient temperature ( $23 \pm 3^\circ\text{C}$ ). Level of lead sulfate in equivalent days at 20°C of four batteries at open circuit in a thermal enclosure (40°C and 60°C) [6].

We have some remarks on the sulfate level results under open circuit in Figure 92:

- A significant difference is observed between positive and negative electrode self-discharge kinetics.

- Sulfation at the positive plate maintained at 40°C and 60°C matches up well, when using the Arrhenius law, with the sulfation at ambient temperature, but it is not the case of the negative plate. In this case, the sulfation is less rapid at high temperature than what is predicted from ambient by the Arrhenius law.

The results illustrated in the Figure 92 show that after 231 days at open circuit the level of PbSO<sub>4</sub> are about 16% and 30% at the negative and positive electrodes respectively. After 600 days, they are 21% at the negative electrode and 45% at the positive electrode.

#### 4.2.3.2 Lead sulfate content at low currents

Table 12: After 231 days at open circuit, four batteries were subjected to low-currents during 356 days at room temperatures  $23 \pm 4^\circ\text{C}$ . Contents of lead sulfate were measured at the negative active material (NAM) and the positive active material (PAM). Active material samples were taken from the middle of the negative and positive plates.

Executed service during 356 days	Applied Current ( $\mu\text{A}/\text{Ah}$ )	Obtained PbSO <sub>4</sub> content (% mass)		Calculated PbSO <sub>4</sub> content (% mol)		PbSO <sub>4</sub> content variation during service (% mol)	
		NAM	PAM	NAM	PAM	NAM	PAM
Initial state (231 days at open circuit)	-	16	30	11.5	24.4	-	-
Self-discharge (Open-circuit)	0	21	45	15.4	37.3	3.9	12.9
Low current	25	16.8	24.0	12.1	19.4	0.6	-5
Low current	50	11.5	19.1	8.1	15.4	-3.4	-9
Low current	100	1.9	8.6	1.3	6.8	-10.2	-17.6
Low current	200	1.4	4.8	1	3.8	-10.5	-20.6

Table 12 gives the results of PbSO<sub>4</sub> contents at initial state (after 231 days on open-circuit), and PbSO<sub>4</sub> final contents (after 356 more days at open-circuit and at constant low currents varying from 25 to 200  $\mu\text{A}/\text{Ah}$ ). Sulfate content variations during 356 days are the difference between final and initial sulfate contents.

From the % of mass obtained of PbSO<sub>4</sub> contents, the % of mol of PbSO<sub>4</sub> contents can be calculated as follows.

At the negative electrode we have:

$$\text{PbSO}_4(\% \text{ mass}) = \frac{\text{PbSO}_4(\% \text{ mol}) \times \text{PbSO}_4(\text{g})}{\text{PbSO}_4(\% \text{ mol}) \times \text{PbSO}_4(\text{g}) + [1 - \text{PbSO}_4(\% \text{ mol})] \times \text{Pb}(\text{g})} \quad (65)$$

so:

$$\text{PbSO}_4(\% \text{ mol}) = \frac{\text{PbSO}_4(\% \text{ mass}) \times \text{Pb}(\text{g})}{\text{PbSO}_4(\text{g}) - \text{PbSO}_4(\% \text{ mass}) \times [\text{PbSO}_4(\text{g}) + \text{Pb}(\text{g})]} \quad (66)$$

Calculating the same way at the positive electrode:

$$\text{PbSO}_4(\% \text{ mol}) = \frac{\text{PbSO}_4(\% \text{ mass}) \times \text{PbO}_2(\text{g})}{\text{PbSO}_4(\text{g}) - \text{PbSO}_4(\% \text{ mass}) \times [\text{PbSO}_4(\text{g}) + \text{PbO}_2(\text{g})]} \quad (67)$$

From the variations of sulfate content and the duration of the experiments, currents equivalents can be calculated using the first Faraday's law (cf. 1.5.2.3), they are called *Effective current*.



$$\text{Effective current: } I_{\text{Effect}} = \text{PbSO}_4 \text{ content (\% mol)} \times \frac{m}{M} \times \frac{nF}{t} \quad (68)$$

According to the manufacturer Exide, the masses of active materials of L01033C24A, 40 Ah-12V battery are 365g of PbO<sub>2</sub> and 300g of Pb.

The Effective current at open circuit ( $I_{\text{Effect}}^0$ ) is the self-discharge current ( $I_{\text{selfdischarge}}$ ). It will be presented with a negative value in Table 13, as the battery is discharging.

$$I_{\text{Effect}}^0 = I_{\text{selfdischarge}} \quad (69)$$

Applying Eq. (68) to the battery at open circuit, we have the self-discharge current of the negative electrode ( $I_{\text{Effect}}^{0-}$ ) and of the positive electrode ( $I_{\text{Effect}}^{0+}$ ):

$$I_{\text{Effect}}^{0-} = I_{\text{selfdischarge}}^- = 0.039 \times \frac{300}{207} \times \frac{2 \times 96500}{356 \times 24 \times 3600} = 0.00035 \text{ A} = 9 \text{ } \mu\text{A} / \text{Ah}$$

$$I_{\text{Effect}}^{0+} = I_{\text{selfdischarge}}^+ = 0.129 \times \frac{365}{239} \times \frac{2 \times 96500}{356 \times 24 \times 3600} = 0.0012 \text{ A} = 30 \text{ } \mu\text{A} / \text{Ah}$$

Current Balance is the result theoretically expected when applying a current to the battery. So it is the subtraction of the applied low current and the self-discharge current at open-circuit.

$$\text{Current Balance: } I_{\text{Balance}} = I_{\text{Applied}} - I_{\text{selfdischarge}} \quad (70)$$

Table 13: Equivalent currents obtained from the variations of sulfate level and the duration of the experiments. Calculated current balances and side reaction rates.

Executed service during 356 days	Applied Current $I_{\text{Applied}}$ ( $\mu\text{A}/\text{Ah}$ )	Effective current $I_{\text{Effect}}$ ( $\mu\text{A}/\text{Ah}$ )		Calculated Current Balance $I_{\text{Balance}}$ ( $\mu\text{A}/\text{Ah}$ )		Calculated rate of side reactions $I_{\text{Side-reac}}$ ( $\mu\text{A}/\text{Ah}$ )	
		NAM	PAM	NAM	PAM	NAM	PAM
Initial state (231 days at open circuit)	-	-	-	-	-	-	-
Self-discharge (Open-circuit)	0	-9	-30	-9	-30	-9	-30
Low current	25	-1.4	12	16	-5	-26.4	-13
idem	50	8	22	41	20	-42	-28
idem	100	23	42.6	91	70	-77	-57.4
idem	200	24	50	191	170	-176	-150

Side reactions are always present inside the lead acid cell at open circuit as well as under low currents. At open circuit, the side reaction rate is the self-discharge current. Under low currents, side reaction rates can be calculated by subtracting the effective currents to the applied current.

$$\text{Side reaction rate under low currents: } I_{\text{Side-reac}} = I_{\text{Effective}} - I_{\text{Applied}} \quad (71)$$

In Figure 93, Effective Currents (EC) are compared to Current Balances (CB) and Side Reaction Rates (SRR) for negative and positive plates.

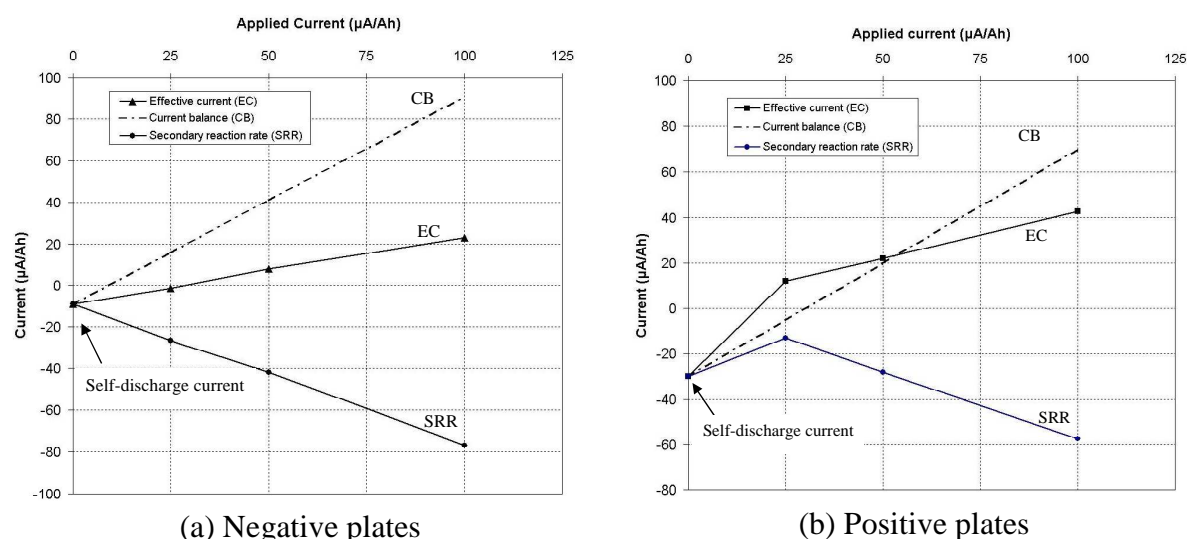


Figure 93: Equivalent currents calculated from the variations of sulfate levels vs. applied currents: (a) negative plates, (b) positive plates. Current balance (CB) is the sum of the self-discharge currents and the applied low currents. Effective current (EC) is the equivalent currents corresponding to sulfate content variations. Side reaction rate is the subtraction of the effective current and the applied currents.

At open-circuit in Figure 93, variations of sulfate content in mole percent are +3.9% for the NAM and +12.9% for the PAM [98]. One can calculate from these sulfate content variations the self-discharge currents during 356 days of the experiment:  $-9 \mu\text{A/Ah}$  and  $-30 \mu\text{A/Ah}$  for the negative and positive electrodes respectively. The self-discharge rate of the positive electrode is more than three times faster than the self-discharge rate of the negative electrode.

The lowest tested current,  $25 \mu\text{A/Ah}$ , induces a drastic change in the sulfate content evolution inside the active materials. The sulfate content in the NAM remains almost constant (0.6 % increase) while the sulfate content in the PAM decreases by 5%. So, the positive plate behaves worse than the negative plate at open-circuit but it has a better behavior as soon as the battery receives the lowest applied current.

#### a. Negative plates

Figure 93 (a) shows the calculated current balances and the effective resulting currents for the negative plates.

According to the lead sulfate content variation at  $25 \mu\text{A/Ah}$ , the effective current for NAM is  $-1.4 \mu\text{A/Ah}$ . This negative value means that the low current compensates only partially the self-discharge. The current balance at  $25 \mu\text{A/Ah}$  is:  $25 - 9 = 16 \mu\text{A/Ah}$ .

The difference between the current balance and the effective current can be associated to losses of the applied current. Another explanation could be an increase of the secondary reactions involved in the self-discharge process under the polarization resulting from the applied current. These two hypotheses are in fact the same as secondary reactions involved in the self-discharge process and loss reactions during charging are identical: mainly hydrogen evolution and some oxygen recombination.

#### b. Positive plates

Figure 93 (b) shows the calculated current balances and the effective resulting currents for the positive plates.

A surprising result is observed for the 25  $\mu\text{A}/\text{Ah}$  applied current. The effective current (12 $\mu\text{A}/\text{Ah}$ ), is higher than the calculated current balance (-5  $\mu\text{A}/\text{Ah}$ ). Of course, one cannot have an efficiency that is higher than 100%. The low current effect is then not only a compensation of the self-discharge process, but a modification and/or a rate reduction of the secondary reactions involved in this process. Indeed, one observes a minimum of the side reaction rate at 25  $\mu\text{A}/\text{Ah}$  (cf. Figure 93).

Secondary reactions at the positive electrode are the oxygen evolution and the positive grid corrosion.

Oxygen evolution takes place at open-circuit, charge and discharge potentials. This reaction is known to increase its rate with positive polarization, so it cannot be the reason of the reduction of the self-discharge process observed in this case.

On the contrary, corrosion can slow down under positive polarization. This phenomenon is well known in the field of corrosion of metals as anodic protection, or more generally as corrosion passivation.

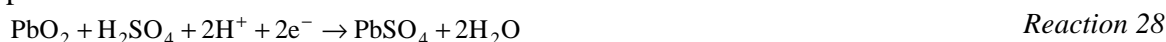
In the case of lead acid batteries, it is also well known that corrosion reactions are different at open-circuit and during charging. More exactly, corrosion reactions of the positive grid consist of two steps:



In which,  $\text{O}^{2-}$  ions are brought by migration from the active material.

Only the first step (Reaction 15) operates at open-circuit while these both steps occur during charging.

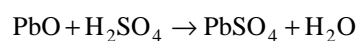
Indeed, at open-circuit, divalent lead ( $\text{Pb}^{2+}$ ) is the stable state for lead. Only the first step of the corrosion reaction occurs but not the second step (Reaction 17) in which  $\text{Pb}^{2+}$  would oxidize into  $\text{Pb}^{4+}$ , because  $\text{Pb}^{4+}$  is not the thermodynamically stable state for lead. On the contrary, as at open-circuit the two electrons of Reaction 15 cannot be evacuated by the external circuit, they are used by reduction of  $\text{Pb}^{4+}$  into  $\text{Pb}^{2+}$  in the discharge reaction of the positive active material:



The combination of Reaction 15 and Reaction 28 is then:

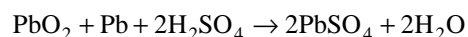


When  $\text{PbO}$  is not protected with a dense  $\text{PbO}_2$  layer, it reacts chemically with sulfuric acid to form  $\text{PbSO}_4$  as follows:



Reaction 30

The overall corrosion reaction at open-circuit is then:



Reaction 29

When this reaction occurs, usually in prolonged open-circuit conditions, positive grids are no more protected. Indeed, the formation of lead sulfate in the corrosion layers leads to mechanical stress, causing the formation of cracks and the destruction of the protective layer.

During charging (under low currents), Reaction 17 takes place. Under positive polarization,  $\text{Pb}^{4+}$  (in  $\text{PbO}_2$ ) is indeed the stable species of lead.  $\text{PbO}_2$  produced in Reaction 17 is formed in the outer part of the corrosion layer. As it is dense, issued from the dense inner layer, and stable in sulfuric acid solution, it takes the role of protecting the  $\text{PbO}$  inner layer and the positive grid from the electrolyte [1, 47, 79].

Under positive polarization, grid corrosion, which is part of the self-discharge process of the positive electrode, is then slowed down by the formation of a protective layer of dense  $\text{PbO}_2$ . Therefore, for the positive electrode, this can be the reason why the effective current is sensibly higher than the calculated current balance, as long as corrosion is important part of the positive self-discharge process. Benefit of 25  $\mu\text{A}/\text{Ah}$  low current is then triple:

(i) Compensation of the self-discharge:

For intermittent charge, in the prospect of replacing open-circuit periods by low current periods, it is obvious that periodical charges would no longer be necessary or at least would be required less frequently.

(ii) Slowing down of the corrosion rate:

As evoked previously, several authors indicate a minimum corrosion zone. This minimum is generally situated at positive polarizations in the [30, 80] mV range. Indeed, at 25  $\mu\text{A}/\text{Ah}$ , the strong effect observed can be attributed to an important reduction of the corrosion rate. But in this case the positive polarization is in the order of 2 mV (cf. Figure 94), much lower than the preceding published values. It must be noticed that our results, obtained from long duration tests (over 19 months) at room temperatures, differ from these published results, generally obtained at accelerated conditions.

(iii) Reduction of water consumption:

It concerns water involved in corrosion reactions. In these reactions, the oxygen is taken from the positive active material. In turn, the active material takes oxygen from water of the electrolyte. The oxygen, finally locked in the corrosion product layers, cannot be recombined to reform water. So, the decrease of water consumption due to corrosion is important for the battery life span.

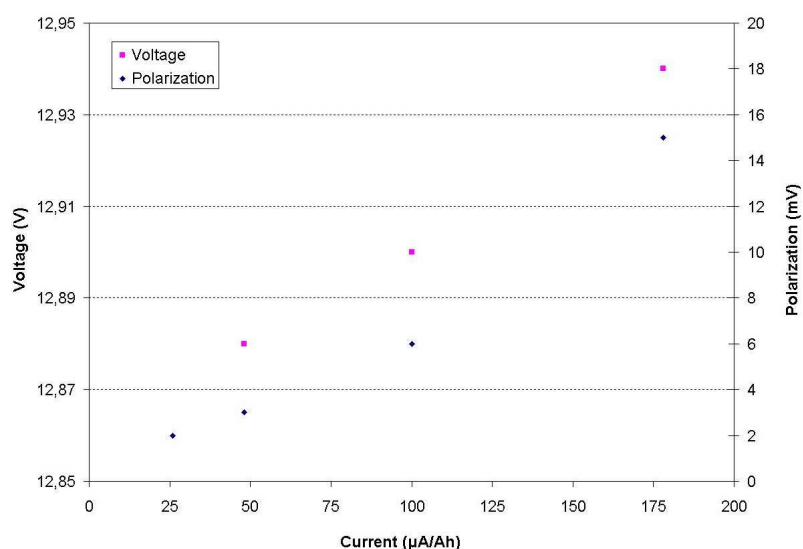


Figure 94: Positive polarizations and battery voltages vs. currents. Imposed low currents: 26, 48, 100 and 178  $\mu\text{A/Ah}$ . Tested battery: flooded flat-plate 140 Ah/12 V

## 4.2.4 Capacity measurement – results & discussion

### 4.2.4.1 Exide 110 Ah/12 V, SLI heavy truck batteries, 1.6%Sb grid alloys

Figure 95 shows the potential of the negative and positive electrodes versus the reference electrode and the voltage of the pseudo cell consisting of these two electrodes. It is clear that the negative electrode finishes the discharge far before the positive electrode. This confirms that the negative electrode has a smaller state of charge, which could be the result of a higher rate of self-discharge, and it was the limit-capacity electrode of the cell (cf. 3.6).

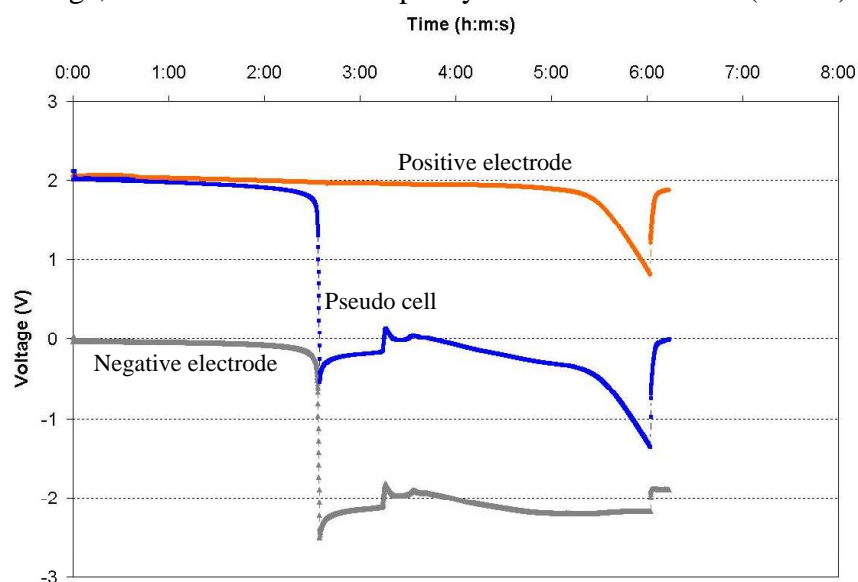


Figure 95: Profiles of voltages between the negative electrode of the 1<sup>st</sup> cell (negative terminal)/ the positive electrode of the 6<sup>th</sup> cell (positive terminal) and the reference electrodes; and of the voltage of the pseudo cell consisting of these two electrodes during a test of discharge with polarity inversion of the battery B104 after six months at open circuit.

The principle results of negative and positive electrode capacities are presented in the table below.

Table14: Capacity of the SLI flooded batteries 110 Ah/12 V, which were at open circuit or subjected to low-current during six months as well as their capacities before (1<sup>st</sup> reference) and after (2<sup>nd</sup> reference) this service.

Batteries	Reference capacity (Ah)				Applied current during 6 months (μA/Ah)	Final Capacity (Ah)	
	1 <sup>st</sup>		2 <sup>nd</sup>			Negative	Positive
	Negative	Positive	Negative	Positive			
101	87.2	108.6	84.2	102.3	(at 13.6V) ~ 364	92.7	111.8
102	97.9	106.5	86.0	111.8	100	53.0	118.1
103	94.9	106.0	81.6	107.5	25	58.6	118.4
104	98.8	112.3	85.3	103.8	0	46.1	100.4

Figure 96 shows the relative difference between the final capacity of negative and positive electrodes after 6 months under service and the first and second reference capacities. For instance, the battery B104 loses  $(100.4 - 112.3)/100.4 = -10.6\%$  of its positive capacity after 6 months of self-discharge relating to its first reference capacity; and the battery B103 positive capacity increases by  $(118.4 - 107.5)/107.5 = +10.1\%$  after 6 months at 25 μA/Ah relating to its second reference capacity.

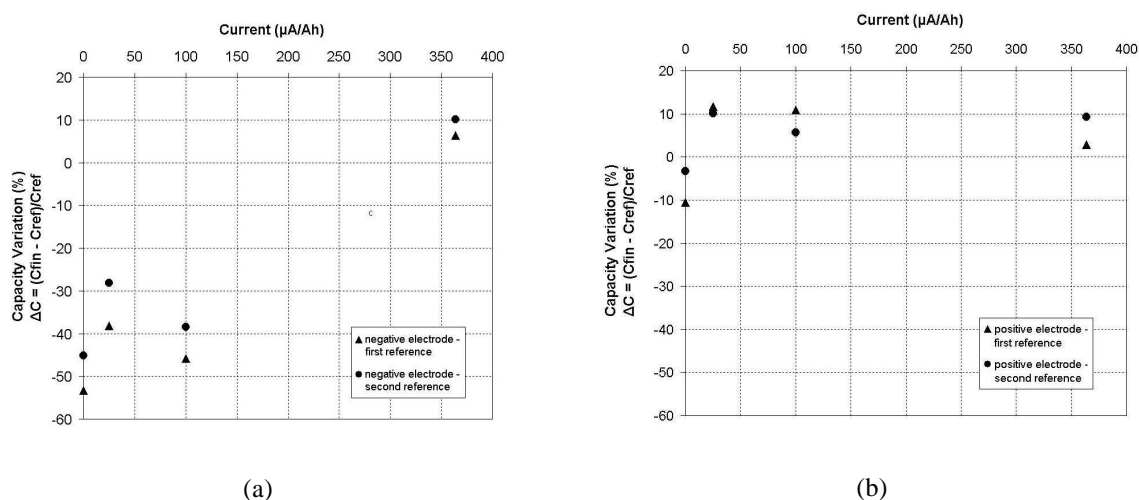


Figure 96: Relative differences ( $\Delta C$ ) between the final capacity of (a) the negative electrode and (b) the positive electrode of the SLI flooded batteries ( $C_{fin}$ ), measured after 6 months during which they were at open circuit or subjected to low-current at ambient temperature, and their reference capacities ( $C_{ref}$ ), measured after a “full charge” before service (1<sup>st</sup> reference) and after service (2<sup>nd</sup> reference).

It is clear to observe the capacity evolutions of the batteries with antimony grid alloys from the Figure 96 that:

- The self-discharge rate of the negative electrode is far higher than the self-discharge rate of the positive electrodes. For B104 at open circuit for 6 months the positive lost about 5% its capacity while it is in the order of 50% for the negative electrode, 10 times greater.
- For the batteries subjected to low-currents, B102 and B103 at 100 and 25 μA/Ah respectively, the state of charge of the positive electrodes is well maintained, even improved as soon as the lowest current is applied while it is not the case of the negative electrodes. They loose about 30 to 45% their capacities. Low-currents thus are not sufficient to compensate the self-discharge of negative electrodes of batteries

with antimony grid alloys.

- For the battery subjected to float charge at 2.27 V/cell with the equivalent float current of 364  $\mu\text{A}/\text{Ah}$ , the state of charge of both negative and positive electrodes is well maintained.
- At the positive electrode, a surprising maximum appears at the low current of 25  $\mu\text{A}/\text{Ah}$ .
- The reference line (0%) is not where it is expected, i.e. above the experimental results.

The reference line (0%) situated under the experimental results can be explained by the fact that the batteries were not in a full state of charge before the discharge test to determine reference capacity. The reference capacity is supposed to be the maximum capacity the battery would be able to discharge after a full charge. But what is a full charge? We all know that absolute full charge of a lead acid battery does not exist (cf. 2.1.4.1). It is an asymptotic state. What we generally call a full charge is in fact the result of a compromise between the search of a high state of charge and the time we can spend on this operation. In practice it is considered that the end of charge is reached, when there is no charge current or voltage evolution during at least two hours. Our charges lasted far more than these two hours. Our full charge procedure for SLI heavy truck batteries lasted two weeks: one week at C/10 limited by 13.6 V followed by one week at C/200 without voltage restriction. Density and voltage measurements shown stable values for the last days of charge. Despite all these cares, we must consider that our full charge procedures were not sufficient to reach states of charge as high as after a few months of float charges or even low current charges (cf Figure 97).

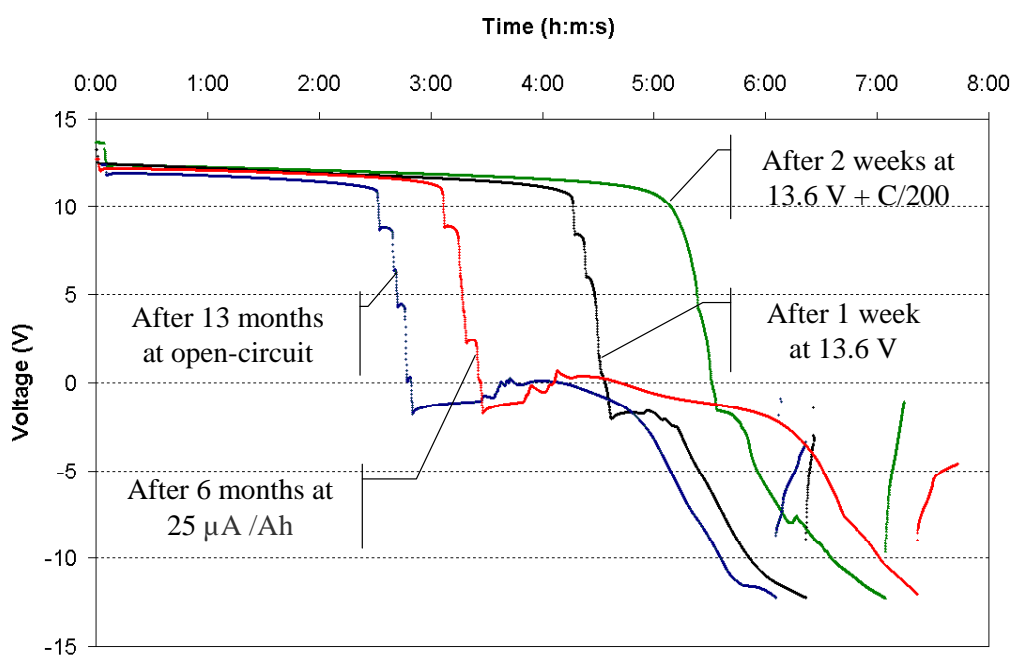


Figure 97: Discharge voltage profiles of B103 after thirteen months of self-discharge (blue), after a one week at 13.6 V charge (black), after two weeks at a 13.6 V + C/200 charge (green) and after six months at 25  $\mu\text{A}/\text{Ah}$  (red) (cf. 3.6). After six months at 25  $\mu\text{A}/\text{Ah}$ , the negative electrode loses 45% of its capacity while the positive electrode capacity gains 11.7% (cf. Table 14).

From the capacity variation and the test duration, we can calculate the effective current. The currents balances and the side reaction rates are calculated as the same way in the section 4.2.3.2. These equivalent currents of the positive electrode are present in Figure 98. One can find here the same phenomenon observed already in the measurement of sulfate levels: the

side reaction rate; i.e. the corrosion rate, has reduced and reached a minimum, when the low current of 25  $\mu\text{A}/\text{Ah}$  is applied on the battery.

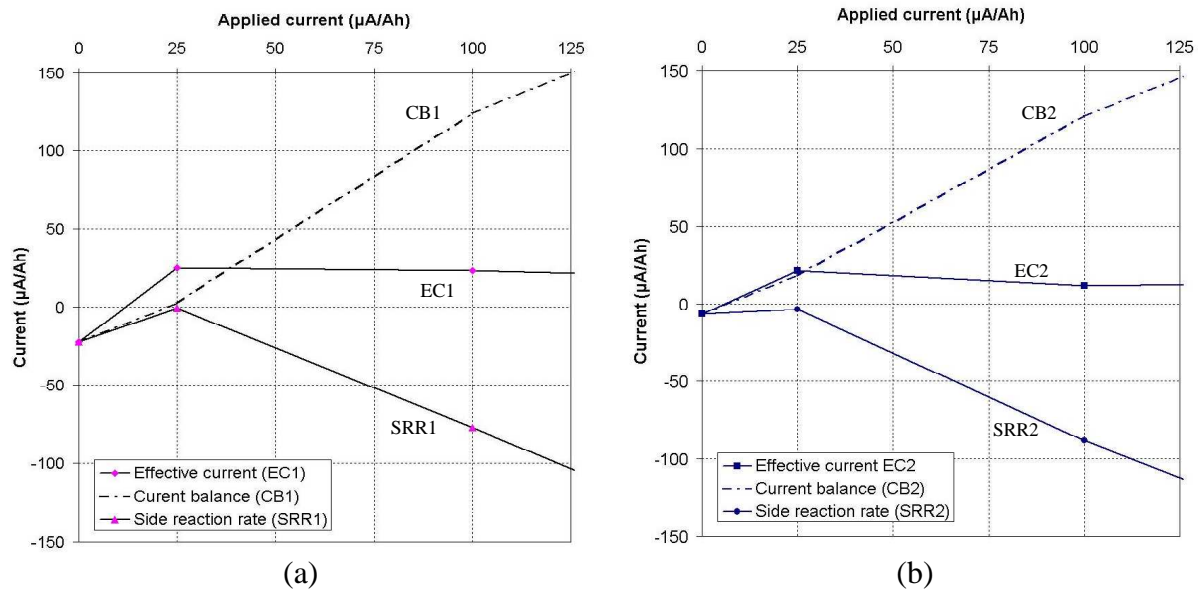


Figure 98: Equivalent currents calculated from the capacity variations and the test duration (6 months) vs. applied currents for the positive electrode: (a) capacity evaluation calculated from the 1<sup>st</sup> reference capacity, (b) capacity evaluation calculated from the 2<sup>nd</sup> reference capacity.

#### 4.2.4.2 EnerSys 400 Ah/2V VRLA AGM batteries, new

The test of discharge with polarity inversion shown that in this lot of VRLA batteries the capacity of the positive electrode was smaller than the capacity of the negative electrode. Thus it was the positive electrode that limited the capacity of the cell. Results shown here are positive electrode capacities.

Table15: Capacity of the VRLA batteries before (reference capacity) and after being at open circuit or subjected to low-current during 1 month at 46°C and 50°C (final capacity). Current values at 46°C and 50°C, equivalent current values at 20°C.

Batteries	Reference capacity (Ah)	Applied current during 1 month at 46°C ( $\mu\text{A}/\text{Ah}$ )	Equivalent current values at 20°C according to Arrhenius law ( $\mu\text{A}/\text{Ah}$ )	Final Capacity (Ah)
B111	436	~ 500 (at 2.2V)	74	437.8
B112	434	200	29.6	439.5
B113	432	50	7.4	412.7
B114	435	0	0	401.0
Batteries	Reference capacity (Ah)	Applied current during 1 months at 50°C (mA)	Equivalent current values at 20°C (Arrhenius law)	Final Capacity (Ah)
B111	455.9	~ 800 (at 2.22V)	100	461.0
B112	442.1	200	25	434.5
B113	460.7	100	12.5	449.8
B114	465.1	0	0	421

The low-current effect obtained with lead sulfate contents of antimony free batteries is confirmed by the capacity evolution. A remarkable reduction of the self-discharge rate is observed as soon as a few mA current is provided. In the case of VRLA batteries, self-discharge rate decreases in a quite homogeneous manner while increasing applied current



values, and over 25  $\mu\text{A}/\text{Ah}$  no more self-discharge is observed. This is already observed in the case of the positive electrode of the SLI batteries, at the smallest current tested (25  $\mu\text{A}/\text{Ah}$ ). No self-discharge is observed as it gives the best capacity result. We have to bear that supplying continuously an anodic current can help to maintain or reestablish the protecting lead oxide layer at the grid surface.

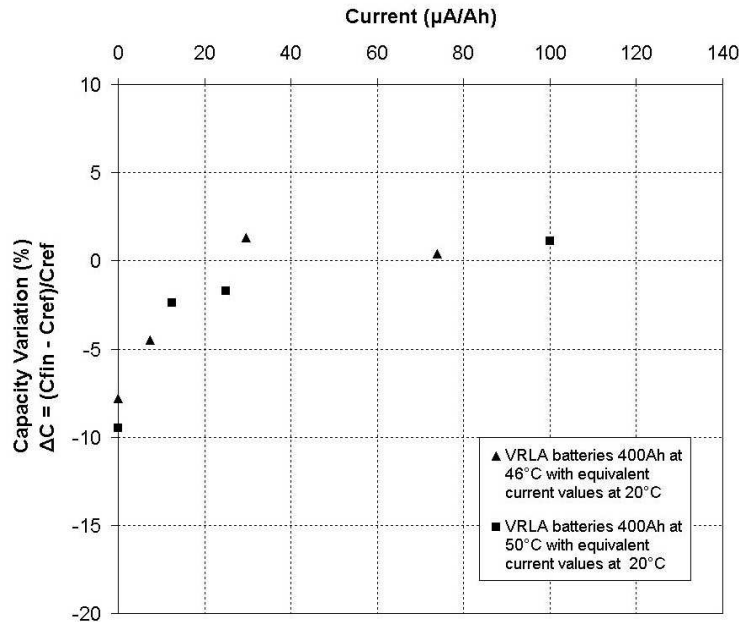


Figure 99: Relative difference ( $\Delta C$ ) between the final capacities of the VRLA batteries ( $C_{fin}$ ), measured after one month during which they were at open circuit or subjected to low-current at 46 and 50°C, and their reference capacities ( $C_{ref}$ ) measured after a “full charge” before this service. The current values are the equivalent values at 20°C according to the Arrhenius law.

In this case of VRLA batteries, “full charges” were classical IUi charges, followed by one week at a constant voltage: 2.27 V/cell. As density measurement cannot be performed, we could not verify if the density was stable. Current measurements show stable values for the last days of this charge procedure. But as mentioned above, our “full charge” procedures do not really give full states of charge; the reference line (0%) was again observed slightly under the experimental results.

#### 4.2.4.3 EnerSys 400 Ah/ 2V AGM VRLA batteries, old

Table 16 gives the capacities of VRLA batteries before ( $C_{ref}$ ) and after ( $C_{fin}$ ) six months at open-circuit, at low currents of 29 and 105  $\mu\text{A}/\text{Ah}$ , and at 2.27V float charge. These experiments were done at room temperatures ( $18 \pm 3^\circ\text{C}$ ). The battery at open-circuit for six months lost  $(264 - 327)/327 = -19.3\%$  of its capacity compared to its reference capacity; the capacity of the battery subjected to 105  $\mu\text{A}/\text{Ah}$  increased by  $(329 - 313)/329 = +5.1\%$ .

Figure 100 (a) shows the capacity variations given for each battery in percent of their reference capacities. These percentages are also the state of charge variations induced by the applied currents during the 6 months of experiments. The capacity variations are converted to the equivalent currents or as named above the effective currents. These effective currents are presented as a function of the applied current in Figure 100 (b). The currents balances and the side reaction rates are calculated as the same way in the section 4.2.3.2. At open-circuit, the capacity reduction of 63Ah after six months allows calculating the average self-discharge current, which is 36  $\mu\text{A}/\text{Ah}$ .

Table 16: Capacities of the VRLA batteries, which were subjected to open circuit, to 29 and 105  $\mu\text{A/Ah}$  low-currents and to 2.27 V float charge during six months at room temperature ( $18 \pm 3^\circ\text{C}$ ) as well as their reference capacities before this service.

Battery	Reference Capacity $C_{\text{ref}}$ (Ah)	Applied Current during 6 months at room temperatures $18 \pm 3^\circ\text{C}$ ( $\mu\text{A/Ah}$ )	Final Capacity $C_{\text{fin}}$ (Ah)	Capacity Variation $(C_{\text{fin}} - C_{\text{ref}})/C_{\text{ref}}$ (%)
B115	340.0	$\sim 414$ (float charge at 2.27V)	379.0	11.8
B116	313.0	105	329.0	5.1
B117	318.0	29	308.0	-3.1
B118	327.0	0	264.0	-19.3

The capacity variation has a strong increase for the lowest applied current (29  $\mu\text{A/Ah}$ ). It appears that this low current, whose value is 80 % of the average self-discharge current (36  $\mu\text{A/Ah}$ ), compensates 84 % of the self-discharge. Such a high efficiency (superior to 100%) suggests that these VRLA batteries could be positive limited at this mid-life state. Further experiments confirmed that these batteries were indeed positive limited. Increases of the state of charge at 105  $\mu\text{A/Ah}$  and at float charge (414  $\mu\text{A/Ah}$ ) indicate that the charge procedure we used does not lead to a real full charge. Charge is then completed slowly at currents beyond 50  $\mu\text{A/Ah}$ .

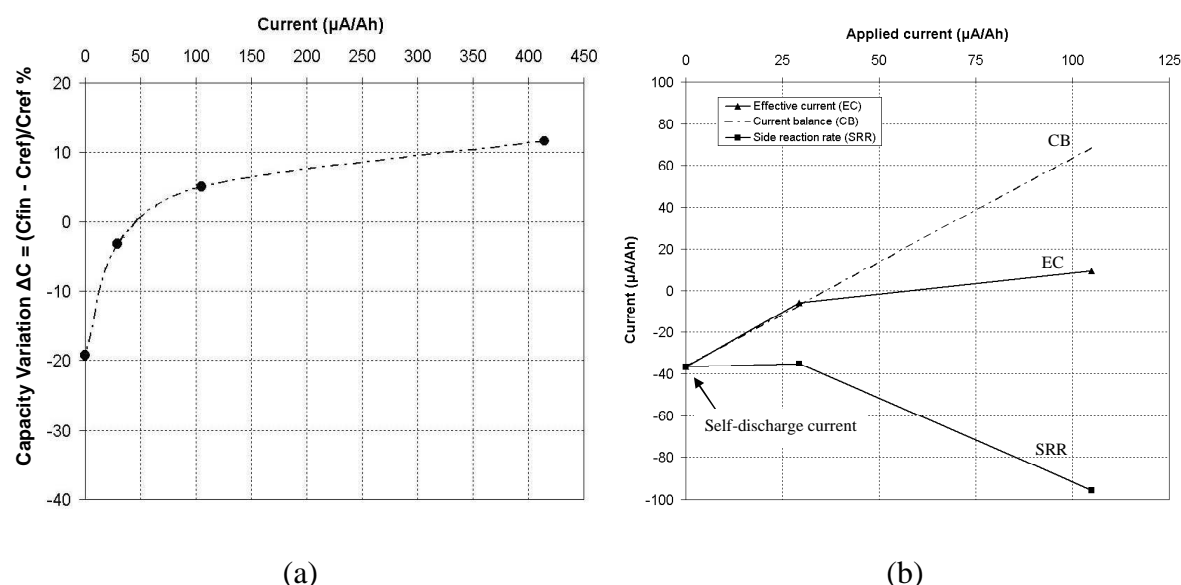


Figure 100: VRLA Batteries were tested during six months at room temperatures ( $18 \pm 3^\circ\text{C}$ ). (a) Relative capacity variations (state of charge variations) vs. applied currents. (b) Equivalent currents calculated from the variations of sulfate levels vs. applied currents.

#### 4.2.5 Conclusion

A new method of maintaining the charge for standby batteries using low-currents and periodic charges is proposed. The following conclusions can be drawn from the study presented on the influence of low currents on reducing self-discharge:

- When accelerated by temperature, self-discharge kinetic of positive electrode tends to follow the Arrhenius law. Self-discharge kinetic of negative electrode appears to be less accelerated by temperature than what is predicted by the Arrhenius law.
- In antimony-free lead acid batteries, the self-discharge rate of the positive electrode is higher than that of the negative electrode. In lead-acid batteries with antimony alloys,

the self-discharge rate of the negative electrode is several times stronger than the positive one.

- Low-currents beyond 25  $\mu\text{A}/\text{Ah}$ , about 10 times smaller than traditional float currents, appear to be able to maintain good states of charge for both positive and negative plates of an antimony-free lead acid batteries, while the float charge (about 400  $\mu\text{A}/\text{Ah}$ ) is seen to be necessary for maintaining the charge of lead-acid batteries with antimony grid alloys, especially for negative plates.
- The effect of 25  $\mu\text{A}/\text{Ah}$  low current on the positive active material is much higher than a simple compensation of the self-discharge but a reduction of the corrosion rate which is, with the oxygen evolution, responsible of the self-discharge at open circuit. This can be explained by a passivation phenomenon of the positive grid corrosion. In other words, it constitutes an anodic protection of the positive grid.
- The use of low-current periods in place of open-circuit periods in the intermittent charge method should increase the life span of VRLA batteries, as it both lowers the water consumption and the corrosion rate of positive grids.

According to experiment results, we supposed that when combined with low currents in the order of 25 to 50  $\mu\text{A}/\text{Ah}$ , a refresh charge every six months or every single year is sufficient to maintain antimony-free batteries in a good state of charge. Higher currents, as traditional float currents (10 times higher), are not necessary and not suited, as they would increase corrosion and water loss. We consider using a refresh charge only when the battery has been subjected to a discharge service.

### 4.3 NEW MANAGEMENT SYSTEM FOR ANTIMONY-FREE STANDBY BATTERY

Valve regulated lead acid batteries - VRLA batteries - have been developed and used for about thirty years in standby applications. They have shown several advantages compared to flooded lead acid batteries: spill-proof, reduced weight, free from excessive gas evolution or acid spillage, reduced maintenance and reduced cost. However, limitations have been also observed concerning system reliability and battery service life.

Several reliability prediction methods have been used such as complete discharge test [99], open-circuit voltage measurement [46], conductance testing [100], internal resistance and impedance measurements [99, 101-105]. Among these, the complete discharge test is well known as the most reliable one but it requires service interruption. This has driven EDF R&D to develop the *Stationary Multibat* system, which consists of a new design of the electrochemical storage and an adapted electronic battery management system [106]. This system, combining redundancy and automated periodical capacity measurements, increases reliability and allows a real time monitoring of the battery state of health. Redundancy not only ensures the continuity of service in the case of a cell failure, but also enables complete discharges to be periodically performed without service interruption.

Standby VRLA batteries maintained under a constant float voltage to compensate self-discharge encounter the problem of short service life, e.g. about 3-4 years compared to the so-called 20-year design and to the 20-year lifetime of conventional lead acid batteries in similar conditions [107]. Indeed, VRLA batteries under float charges are permanently overcharged and different failure modes have been observed, such as corrosion of positive grid alloys, electrolyte dry-out and thermal runaway [1, 47, 49, 70, 108].

A new management system for standby VRLA batteries has been developed at EDF using the *Stationary Multibat* system [106] to ensure system reliability and the Low-current method

[98] to improve the battery life span.

Figure 101 (a) describes a simplified schematic diagram of the Stationary Multibat system. Three battery-pack strings in parallel instead of one pack are used in order to improve the system reliability. In case of a cell failure such as an open circuit, the system loses only one battery-pack string, i.e. one-third of the total capacity. This configuration also allows each string to be discharged completely across the test resistance to evaluate its real state of health. Each battery string is periodically (e.g. every six months) discharged and charged.

Figure 101 (b) describes how to integrate and to operate Low-current method of maintaining the charge on the Stationary Multibat system:

- A resistance branch is added to reduce the traditional float current with a factor of 5 to 10. In standby state, Programmable Logic Controllers (PLC)  $K_1$  and  $K_2$  are open; the battery is maintained at charge with a low current via the resistance  $R$ .
- On backup demand, a voltage drop appears on the DC bus, the battery immediately provides electricity to the DC load via the diode  $D$ . Then PLC  $K_1$  closes; DC load is directly supplied by the battery.
- During the periodical discharge test (e.g. every six months) to evaluate the battery state of health, PLC  $K_2$  closes and  $K_1$  stays open. The battery-pack string is discharged across the test resistance. The low current, still provided to the battery pack string, is a parasitic but negligible effect ( $< 0.1\%$ ). Next, the charge is operated via  $K_1$ . The charge current is controlled by a Pulse Wave Modulation (PWM). When the charge finishes,  $K_1$  re-opens, the battery is re-maintained the charge with a low current via  $R$ .

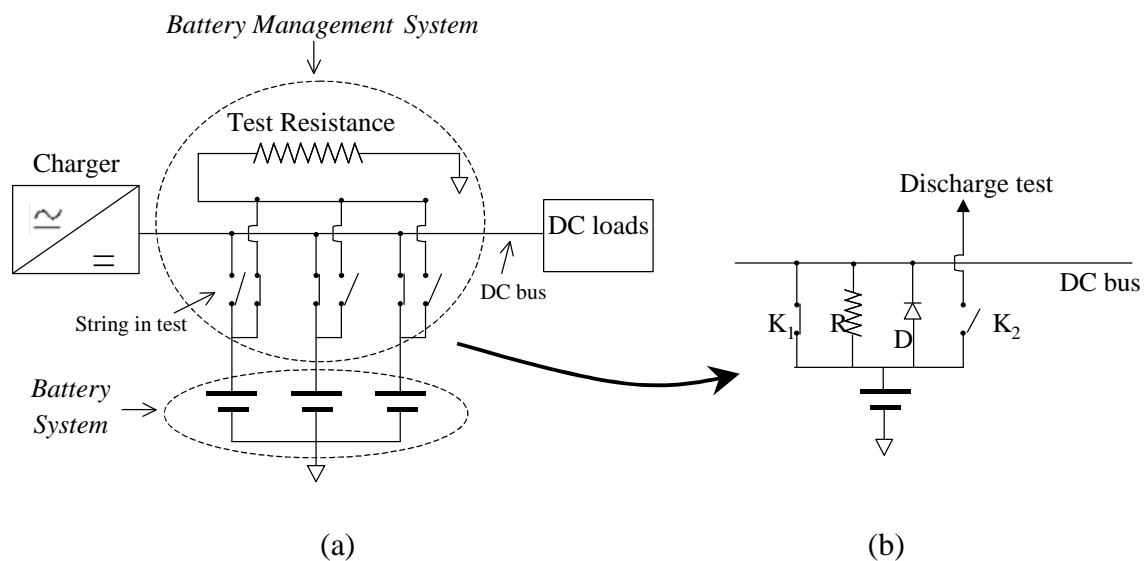


Figure 101: (a) Simplified schematic diagram of the Stationary Multibat system. (b) Zoom on the power electronic components of one of the three battery-pack strings using Low-current method.

All those operations are done sequentially and automatically so that no intervention is required from the maintenance.

This system is expected to fulfill three targets:

- Increasing the system reliability by a redundancy in the design of the battery system and by an assessment method to control battery states of health.

- Improving battery life spans by the Low-current method, leading to reduced corrosion and water loss.
- Decreasing maintenance costs.

Combining the Low-current method, battery redundancy and automated periodical capacity measurements, VRLA batteries should provide long life spans and high reliability. Several management systems of this kind are being experimentally used at EDF.

## Conclusion of chapter 4

The self-discharge phenomenon caused by side reactions such as corrosion, water decomposition and recombination is unavoidable in lead acid batteries. Self-discharge rates depend on several factors such as the state of charge, the temperature, grid alloys, etc. These rates are not equal between negative and positive electrodes and are independent of each other. In lead-acid batteries with antimony, the self-discharge rate of the negative electrode is several times stronger than the self-discharge rate of the positive electrode, depending mainly on the battery age and the antimony content in the positive grid alloy.

In order to compensate for the self-discharge of lead-acid batteries, a current whose value exceeds the self-discharge of the negative electrode has to be supplied. This is traditionally achieved by applying a constant voltage whose value is slightly higher than the battery open circuit voltage. This is called “float charge”. It has to be kept in mind that the float polarization increases gas evolution rates at both electrodes.

In antimony-free lead-acid batteries, e.g. VRLA batteries, the self-discharge rate of the negative electrode is largely reduced and is about a half of the self-discharge rate of the positive electrode. The question is: are traditional float charges really suited to antimony-free lead-acid batteries? Practical situations on field as well as experimental results say no. Standby VRLA batteries maintained under a constant float voltage to compensate self-discharge encounter the problem of short service life, when our results show that traditional float charge currents are far over what is needed to maintain the VRLA battery state of charge.

In order to reduce overcharge, intermittent charges (open-circuit and periodical charges) have been used instead of float charges and have given positive results in reducing thermal runaway and increasing the battery life span. Nevertheless, corrosion of the positive grid is also high during open-circuit periods of intermittent charges. Indeed, it is revealed in the literature that corrosion is minimum when the positive polarization is between 40 and 80 mV.

In this chapter, taking into account this minimum corrosion, a new method of maintaining the charge of antimony-free lead-acid batteries using low currents and periodic charges is studied. This is called *Low-current* method. This method is derived from the intermittent charge: open-circuit periods are replaced by constant low current periods with values are about 5 to 10 times smaller than traditional float currents.

This new method was tested on several types of lead acid batteries: SLI car batteries, VRLA batteries, SLI heavy truck batteries with antimony grid alloys. It was compared to no charge (open circuit) and traditional float charges. The obtained results shown that low currents, 5 to 10 times smaller then float currents, could maintain good states of charge of antimony free lead acid batteries including SLI car batteries and VRLA batteries. Whereas, float charges seemed necessary to ensure a good state of charge of batteries with antimony grid alloys, in particular, of its negative electrodes. At 25  $\mu\text{A}/\text{Ah}$  (more than 10 times smaller than traditional float currents), corrosion reduced drastically. The effect of this 25  $\mu\text{A}/\text{Ah}$  on the positive active material was much higher than a simple compensation of the self-discharge, but also a reduction of corrosion by keeping the battery in a corrosion passivation zone. However, the positive polarization response of this current was just of the order of 2 mV, much lower than the preceding published values. It must be noticed that our results, obtained from long duration tests (over 19 months) at room temperatures, differed from these published

results, generally obtained at accelerated conditions. Besides reducing corrosion, the Low-current method would have also the advantages of reducing water loss due to corrosion and the need of periodical charges.

The battery management system of three parallel strings individually controlled (Stationary Multibat system), associated to the implementation of the low current method, has been used at six electrical substations of EDF. Recently, the Direction of Hydraulic Production has decided to adopt this new technology for backup batteries ensuring the security of hydraulic power plants. Twenty systems of this kind will be installed by the second semester of 2009.

## GENERAL CONCLUSION

Lead acid batteries have been used for more than 150 years. Compared with newer energy technologies, such as nickel-metal hydride and lithium-ion batteries with ability to pack a lot of energy into a small space and deliver a steady current over a long period, it has to be admitted that they look old-fashioned. It is, nevertheless, a mistake to dismiss something just because it is old. Another way of looking at it is that lead acid batteries are tried and trusted. They may just need to be used in the right ways. And that is what has been happening: three PhD theses have been done in the past at EDF and the University Montpellier II. They have given promising conclusions for lead acid batteries and their applications. In this thesis, these conclusions are confirmed, improved and new possibilities are opened.

A traditional charge process of lead acid batteries lasts generally from 10 to 14 hours. The common use of 3 shifts of 8 hours has driven manufacturers to develop 8-hour charge algorithms. These charge algorithms involve an adaptation of classical algorithms without radical changes. In both cases, the electrolyte destratification phase, called overcharge phase, is achieved at the end of the operation, where the battery charge acceptance is sufficiently low. In this way, the current of gas evolutions, called gas current, is almost equal to the total current, making the evaluation of the gas current easier and thus facilitating the global management of the charge.

New applications of lead acid batteries require, in general, a reduction of the charge duration; we are talking here about accelerated charges. The accelerated charges do not include a final phase just for destratification where it is partially controlled. It has to be thus carried out in parallel with the proper charge, called here an early destratification. The global charge rate during this operation is much higher than the one of classical charges. For instance, a factor of 4 to 5 is used in the case of grid storage due to reduced durations of the slack period during the night or a factor of 10 to 20 is applied in the case of a fast charge of batteries in electric buses, where the total charge duration is of the order of an hour.

In this thesis, a new charge algorithm for accelerated charges and for fast charges is developed applying early destratification. Charge acceptance measurements are achieved in order to evaluate and control gas currents. This algorithm has been implemented in a commercial charger. A flooded lead acid battery charged with this new algorithm has shown a good evolution of its electrolyte density within a half reduced charge duration compared to a classical charge of the same initial rate.

Backup supplies are one of the main applications of lead acid batteries. Stationary VRLA batteries, maintained under a constant float voltage to compensate for self-discharge, encounter the problem of short service life. In this application, almost opposed to the case of fast charges because of very low charge rates, at least a part of the problem is similar: within these low charge rates, the charge and the side reactions take place jointly.

The float currents have to exceed side reaction rates to prevent batteries from under-charge. Nevertheless, too high float currents cause failures of lead acid batteries because of side reactions. In fact, gas evolution increases with the increase of charge polarizations and the corrosion rate is demonstrated to increase when the positive polarization is over  $[40 \div 80]$  mV. At a typical float polarization voltage of the order of 120 mV/cell, the float current response of the battery is about 10 times stronger than the self-discharge current; batteries are overcharged.

In order to reduce overcharge, intermittent charges (open-circuit and periodical charges) have been used instead of float charges and have given positive results in reducing thermal



runaway and increasing the battery life span. Nevertheless, corrosion of the positive grid is also high during open-circuit periods of intermittent charges.

In this thesis, a new method of maintaining the charge of antimony-free lead-acid batteries using low currents and periodic charges is studied. This is called *Low-current* method. This method is derived from the intermittent charge: open-circuit periods are replaced by constant low current periods with values about 5 to 10 times smaller than traditional float currents. The low current of 25  $\mu\text{A}/\text{Ah}$  (more than 10 times smaller than traditional float currents) can maintain good states of charge of antimony free lead acid batteries. The effect of this 25  $\mu\text{A}/\text{Ah}$  on the positive active material is much higher than a simple compensation of the self-discharge; it is also a radical reduction of corrosion by keeping the battery in a corrosion passivation zone. However, the positive polarization response of this current is just of the order of 2 mV, much lower than the preceding published values. Besides reducing corrosion, the Low-current method has also the advantages of reducing water loss due to corrosion and the need of periodical charges.

This Low-current method combined with battery redundancy and automated periodical capacity measurement has been now used in several MV/LV substations and in some hydraulic power plants of EDF.

In order to evaluate the capacities of both negative and positive electrodes of the battery, we decided to operate discharges with polarity inversions. Two kinds of reference electrodes are used to measure the potentials of each electrode. Several types of flooded lead acid batteries including a flat-plate battery, a tubular-plate battery, a compress battery and SLI heavy truck batteries were subjected to this test. The obtained results enable us to determine the capacities of both electrodes and of all pseudo cells including the limited battery capacity one. They also lead us to better understand the polarity inversion phenomenon concerning the mechanism of polarity inversion and processes occurred inside electrodes. The discovery of differences between the inversed potential profiles of negative and positive electrodes allows recognizing them even when reference electrodes are not used.

This reminds me of another way of looking at research; besides pursuing the initial objective it is always a pleasure to make serendipities.

At this point I would like to talk briefly about the pleasure that I have had during my research adventure.

During my five years of electrical engineering training at Hanoi University of Technologies, I became aware of renewable energies and their applications in sustainable development. This is the reason why for my graduation dissertation, I chose to work on renewable energies, in particular, on small hydraulic plants in remote mountain villages of Thua Thien Hue district, my hometown. This was my first experience of the domain, which gave me a good mark and also a scholarship to continue my study in France. Taking a long with the desire to learn more about renewable energy applications, I did a Master of Science (M.S.) at the South Electronic Institute (IES) on electronic, systems and components with the option of photovoltaic and wind systems. During my M.S. research placement on lead acid batteries in photovoltaic installations under the supervision of Professor Glaize Christian, I encountered Alzieu Jean senior engineer at EDF R&D, and my adventure has led to this thesis. Although electronic and electrochemistry were not my initial training, I have been very pleased to study and try new things. I am carried along with my desire to study about renewable energies and their applications and what I have received pleases me very much. I think any oriented work opens up new opportunities and perspectives.

The first outlook of our work concerns the new charge algorithm with early destratification using charge acceptance measurements. This innovation has the advantage of destratifying the electrolyte whenever the charge power is available. Testing this new algorithm on accelerated

charges and fast charges (with high charge rates) should lead to further investigations. Besides, it can be used in any charge processes to assure a quite homogenized state of the electrolyte in case the charge procedure is accidentally interrupted. Aging tests should be performed to evaluate the state of health of batteries on which these new charge procedures are applied.

The discovery of low-current effects opens up the second outlook of this thesis works. As the overcharge and especially the corrosion are drastically reduced, we conclude that the battery lifespan should be improved. However, as the corrosion is a long process, a test under real conditions over a long period should be achieved. Other than back-up supply applications, the phase of maintaining the charge with an imposed low-current might be also be used in any lead acid battery applications where the battery may be at open circuit for a long time between services. This will have the advantages, besides maintaining the state of charge of the battery, of keeping it in minimum corrosion.

The innovation about acceptance measurements during charge, the discoveries on low-current effects on corrosion and on self-discharge, as well as the studies about battery behaviors during polarity inversions contribute to better understanding and use of lead acid batteries. They open the door to new ways of managements, which revolutionize the manner on dealt with lead acid batteries. This PhD thesis finally reaches its initial objective of contribution towards sustainable development.

## REFERENCES

- [1] D. Berndt, *Maintenance-Free batteries*, Second ed. Taunton, Somerset, New York, Chichester, Toronto, Brisbane, Singapore: Research studies press LTD, John Wiley & Sons INC, 1997.
- [2] D. U. Sauer, E. Karden, B. Fricke, H. Blanke, M. Thele, O. Bohlen, J. Schiffer, J. B. Gerschler, and R. Kaiser, "Charging performance of automotive batteries--An underestimated factor influencing lifetime and reliable battery operation," *Journal of Power Sources*, vol. 168, pp. 22-30, 2007.
- [3] D. U. Sauer and H. Wenzl, "Comparison of different approaches for lifetime prediction of electrochemical systems--Using lead-acid batteries as example," *Journal of Power Sources*, vol. 176, pp. 534-546, 2008.
- [4] J. Schiffer, D. U. Sauer, H. Bindner, T. Cronin, P. Lundsager, and R. Kaiser, "Model prediction for ranking lead-acid batteries according to expected lifetime in renewable energy systems and autonomous power-supply systems," *Journal of Power Sources*, vol. 168, pp. 66-78, 2007.
- [5] M. Thele, J. Schiffer, E. Karden, E. Surewaard, and D. U. Sauer, "Modeling of the charge acceptance of lead-acid batteries," *Journal of Power Sources*, vol. 168, pp. 31-39, 2007.
- [6] G. Dillenseger, "Caractérisation de nouveaux modes de maintien en charge pour batteries stationnaires de secours," in *Sciences et Techniques du Languedoc*. vol. Docteur Montpellier: Université de Montpellier II, 2004, p. 196.
- [7] "<http://www.varta.com>."
- [8] R. M. Dell, "Batteries: fifty years of materials development," *Solid State Ionics*, vol. 134, pp. 139-158, 2000.
- [9] G. Toussaint, "Amélioration du comportement électrochimique des batteries plomb acide à usage photovoltaïque." vol. Docteur en Physique et chimie de la matière et des matériaux Nancy: Université Henri Poincaré, Nancy I, 2003, p. 128.
- [10] E. Rocca, "Passivation du plomb pur et de ses alliages en milieu sulfurique et atmosphérique." vol. Docteur en sciences et génie des matériaux Nancy: Université Henri Poincaré, Nancy I, 1999, p. 157.
- [11] E. Cattaneo, H. Stumpf, H. G. Tillmann, and G. Sassmannshausen, "Continuous casting of lead-antimony alloys," *Journal of Power Sources*, vol. 67, pp. 283-289, 1997.
- [12] "[www.milbatteries.com](http://www.milbatteries.com)."
- [13] *World lead acid battery markets*. San Jose, CA, United States: Frost & Sullivan, 2002.
- [14] F. Miomandre, S. Sadki, P. Audebert, and R. Meallet-Renault, *Electrochimie, des concepts aux applications*. Paris: Dunod, 2005.
- [15] H. Bode, *Lead Acid batteries*. New York, London, Sydney, Toronto: John Wiley & Sons, 1977.
- [16] M. Pourbaix, *Atlas of Electrochemical equilibria in aqueous solutions*. Houston: National association of corrosion engineers, 1974.
- [17] "<http://en.wikipedia.org>."
- [18] "The Encyclopedia of Electrochemistry," C. A. Hampel, Ed. New York, London: Reinhold Publishing corporation, 1964.
- [19] L. Jumau, *Accumulateurs électriques*, Troisième ed. Paris: Dunod, 1928.
- [20] D. Devilliers and E. Mahé, "Cellules électrochimiques: aspects thermodynamiques et cinétiques. Applications aux générateurs et aux électrolyseurs industriels," in *L'actualité chimique*, Janvier 2003.
- [21] K. J. Vetter, *Electrochemical Kinetics, Theoretical and experimental aspects*. New York, London: Academic press, 1967.
- [22] D. R. Lide, *Handbook of chemistry and physics*, 84th edition ed.: CRC Press, 2003-2004.
- [23] C. Lefrou, *Les bases de l'électrochimie*. France: Lesson slides of electrochemical students of Grenoble Institute of Technology.
- [24] "<http://www.bath.ac.uk>."
- [25] A. Delaille, "Développement de méthodes d'évaluation de l'état de charge et de l'état de santé des batteries utilisées dans les systèmes photovoltaïques," in *Paris Centre*. vol. Docteur Paris: Université de Paris VI, 2006, p. 310.
- [26] M. Barak, *Electrochemical power sources*. London, New York: Peter Peregrinus Ltd, Institution of Electrical Engineers, 1980.
- [27] J.-C. Catonne, "Grandeurs caractéristiques d'électrochimie appliquée," *Techniques de l'Ingénieur*, vol. K 800 ou COR 900.
- [28] D. M. Bernardi, R. Y. Ying, and P. Watson, "Study of charge kinetics in Valve-Regulated Lead acid cells," *Journal of the Electrochemical Society*, vol. 151, pp. A85-A100, 2004.
- [29] G. Petkova and D. Pavlov, "Influence of charge mode on the capacity and cycle life of lead-acid battery negative plates," *Journal of Power Sources*, vol. 113, pp. 355-362, 2003.
- [30] Y. Yamaguchi, M. Shiota, M. Hosokawa, Y. Nakayama, N. Hirai, and S. Hara, "Study of charge acceptance for the lead-acid battery through in situ EC-AFM observation -- influence of the open-circuit standing time on the negative electrode," *Journal of Power Sources*, vol. 102, pp. 155-161, 2001.

- [31] Klang and K. James, "Apparatus and method for step-charging batteries to optimize charge acceptance," United States: GNB Battery Technologies, Inc. (Mendota Heights, MN), 1996.
- [32] Takehara and Zen-ichiro, "Dissolution and precipitation reactions of lead sulfate in positive and negative electrodes in lead acid battery," *Journal of Power Sources*, vol. 85, pp. 29-37, 2000.
- [33] M. Thele, E. Karden, E. Surewaard, and D. U. Sauer, "Impedance-based overcharging and gassing model for VRLA/AGM batteries," *Journal of Power Sources*, vol. 158, pp. 953-963, 2006.
- [34] Y. Guo, W. Yan, and J. Hu, "Effects of Electrolyte Stratification on Performances of Flooded Lead-Acid Batteries," *Journal of Electrochemical Society*, vol. 154, pp. A1-A6, 2007.
- [35] T. G. Chang and D. M. Jochim, "Rapid partial charging of lead/acid batteries," *Journal of Power Sources*, vol. 64, pp. 103-110, 1997.
- [36] F. Mattera, D. Desmettre, J. L. Martin, and P. Malbranche, "Characterisation of photovoltaic batteries using radio element detection: the influence and consequences of the electrolyte stratification," *Journal of Power Sources*, vol. 113, pp. 400-407, 2003.
- [37] J. F. Cole, "Installation and operation of a large scale RAPS system in Peru," *Journal of Power Sources*, vol. 116, pp. 243-247, 2003.
- [38] R. H. Newnham and W. G. A. Balasing, "Performance of flooded- and gelled-electrolyte lead/acid batteries under remote-area power-supply duty," *Journal of Power Sources*, vol. 66, pp. 27-39, 1997.
- [39] R. H. Newnham and W. G. A. Balasing, "Advanced management strategies for remote-area power-supply systems," *Journal of Power Sources*, vol. 133, pp. 141-146, 2004.
- [40] D. J. Spiers and A. D. Rasinkoski, "Predicting the service lifetime of lead/acid batteries in photovoltaic systems," *Journal of Power Sources*, vol. 53, pp. 245-253, 1995.
- [41] M. Kim and E. Hwang, "Monitoring the battery status for photovoltaic systems," *Journal of Power Sources*, vol. 64, pp. 193-196, 1997.
- [42] D. U. Sauer, "Modelling of local conditions in flooded lead/acid batteries in photovoltaic systems," *Journal of Power Sources*, vol. 64, pp. 181-187, 1997.
- [43] D. U. Sauer and J. Garche, "Optimum battery design for applications in photovoltaic systems -- theoretical considerations," *Journal of Power Sources*, vol. 95, pp. 130-134, 2001.
- [44] P. R. Stevenson, "Advanced separator construction for long life valve-regulated lead-acid batteries," *Journal of Power Sources*, vol. 116, pp. 160-168, 2003.
- [45] D. Pavlov, V. Naidenov, S. Ruevski, V. Mircheva, and M. Cherneva, "New modified AGM separator and its influence on the performance of VRLA batteries," *Journal of Power Sources*, vol. 113, pp. 209-227, 2003.
- [46] K. R. Bullock, M. C. Weeks, C. S. C. Bose, and K. A. Murugesamoorthi, "A predictive model of the reliabilities and the distributions of the acid concentrations, open-circuit voltages and capacities of valve-regulated lead/acid batteries during storage," *Journal of Power Sources*, vol. 64, pp. 139-145, 1997.
- [47] P. Ruetschi, "Aging mechanisms and service life of lead-acid batteries," *Journal of Power Sources*, vol. 127, pp. 33-44, 2004.
- [48] P. Izzo, "Etude d'un circuit électronique et algorithmique destiné à la gestion de systèmes autonomes de production d'énergie photovoltaïque," in *Sciences et technique du Languedoc*. vol. Docteur de l'Université Montpellier II Montpellier: Université Montpellier II, 2002, p. 177.
- [49] R. Wagner, "Failure modes of valve-regulated lead/acid batteries in different applications," *Journal of Power Sources*, vol. 53, pp. 153-162, 1995.
- [50] J. Alzieu and J. Robert, "Developpement d'accumulateurs au plomb a hautes performances," ANVAR1987.
- [51] H. Smimite, "Etude du comportement et gestion d'une batterie au plomb à recombinaison équipant un véhicule électrique," in *Sciences et techniques du Languedoc*. vol. Doctorat Montpellier: Université Montpellier II, 1997, p. 125.
- [52] "LEAD-ACID BATTERY TEST METHOD," United States: Ford Motor Company (Dearborn, MI), 1974.
- [53] V. Srinivasan, G. Q. Wang, and C. Y. Wang, "Mathematical Modeling of Current-Interrupt and Pulse Operation of Valve-Regulated Lead Acid Cells," *Journal of Electrochemical Society*, vol. 150, pp. A316-A325, 2003.
- [54] G. Gory, *Connaissance des Accumulateurs au Plomb et Autres generateurs electrochimiques*. Paris: Editions Semis, 1977.
- [55] A. Delaille, M. Perrin, F. Huet, and L. Hernout, "Study of the "coup de fouet" of lead-acid cells as a function of their state-of-charge and state-of-health," *Journal of Power Sources*, vol. 158, pp. 1019-1028, 2006.
- [56] P. E. Pascoe and A. H. Anbuky, "The behaviour of the coup de fouet of valve-regulated lead-acid batteries," *Journal of Power Sources*, vol. 111, pp. 304-319, 2002.
- [57] C. P. de Oliveira and M. C. Lopes, "Early stages of the lead-acid battery discharge," *Journal of Power Sources*, vol. 138, pp. 294-300, 2004.

- [58] C. Armenta-Deu and M. V. Calvo-Baza, "The initial voltage drop in lead-acid cells: the influence of the overvoltage," *Journal of Power Sources*, vol. 72, pp. 194-202, 1998.
- [59] J. H. B. Mark and W. C. Vosburgh, "The Discharge Mechanism of Certain Oxide Electrodes," *Journal of the Electrochemical Society*, vol. 108, pp. 615-621, 1961.
- [60] J. Alzieu and J. Robert, "Etude de l'hétérogénéité de fonctionnement de l'électrode positive de l'accumulateur au plomb," Ecole supérieure d'électricité. Laboratoire de génie électrique des Universités Paris VI et Paris XI, Gif sur Yvette, Compte rendu de fin d'étude d'une recherche financée par le ministère de l'industrie N° 46, Décembre 1981.
- [61] D. Berndt and U. Teutsch, "Float charging of VRLA batteries: A balancing act between secondary reactions," *Journal of Electrochemical Society*, vol. 143, 1996.
- [62] P. Ruetschi, "Silver-silver sulfate reference electrodes for use in lead-acid batteries," *Journal of Power Sources*, vol. 116, pp. 53-60, 2003.
- [63] W. B. Brecht, "Strategies for overcoming the adverse effects of imbalances in the second order reactions in valve regulated lead acid cells," in *Telecommunications Energy Conference, 1998. INTELEC. Twentieth International*, 1998, pp. 436-442.
- [64] T. G. Martinez and A. F. S. Novak, "Increased float voltage and the effects of negative self-discharge on flooded lead calcium telecommunications cells," in *Telecommunications Energy Conference, 1990. INTELEC '90., 12th International*, 1990, pp. 234-241.
- [65] S. S. Misra, T. M. Noveske, and A. J. Williamson, "Maintenance and reliability of standby battery systems: flooded vs. valve regulated lead acid battery," in *Telecommunications Energy Conference, 1994. INTELEC '94., 16th International*, 1994, pp. 250-255.
- [66] J. M. Hawkins, L. E. E. Moore, and L. O. Barling, "Aspects of the float and temperature behaviour of lead-acid batteries in telecommunications applications," in *Telecommunications Energy Conference, 1995. INTELEC '95., 17th International*, 1995, pp. 368-373.
- [67] E. Rossinot, C. Lefrou, and J. P. Gun, "A study of the scattering of valve-regulated lead acid battery characteristics," *Journal of Power Sources*, vol. 114, pp. 160-169, 2003.
- [68] D. O. Feder and G. Carosella, "The never ending pursuit of float voltage uniformity in stationary reserve battery plants," in *Telecommunications Energy Conference, 1994. INTELEC '94., 16th International*, 1994, pp. 609-617.
- [69] P. Stevenson, "Durée de vie des accumulateurs étanches," *REE, N°1*, pp. 57-60, 1996.
- [70] D. O. Feder, "1950-2001: more than one-half century of learning how to live with each new generation of telecommunication standby batteries," in *Telecommunications Energy Conference, 2001. INTELEC 2001. Twenty-Third International*, 2001, pp. 47-59.
- [71] K. Nakamura, M. Shiomi, K. Takahashi, and M. Tsubota, "Failure modes of valve-regulated lead/acid batteries," *Journal of Power Sources*, vol. 59, pp. 153-157, 1996.
- [72] C. Brissaud, G. Reumont, J. P. Smaha, and J. Foct, "Structural and morphological study of damage in lead/acid batteries during cycling and floating tests," *Journal of Power Sources*, vol. 64, pp. 117-122, 1997.
- [73] A. Cooper and P. T. Moseley, "Progress in overcoming the failure modes peculiar to VRLA batteries," *Journal of Power Sources*, vol. 113, pp. 200-208, 2003.
- [74] R. Elgh, "Tests on valve regulated lead acid batteries at different environmental temperatures and float voltages," in *Telecommunications Energy Conference, 1994. INTELEC '94., 16th International*, 1994, pp. 172-175.
- [75] D. Pavlov, "Premature capacity loss (PCL) of the positive lead/acid battery plate: a new concept to describe the phenomenon," *Journal of Power Sources*, vol. 42, pp. 345-363, 1993.
- [76] M. Shiomi, Y. Okada, Y. Tsuboi, S. Osumi, and M. Tsubota, "Study of PCL mechanism: Influence of grid/PAM state on PCL," *Journal of Power Sources*, vol. 113, pp. 271-276, 2003.
- [77] M. Kosai, S. Yasukawa, S. Osumi, and M. Tsubota, "Effect of antimony on premature capacity loss of lead/acid batteries," *Journal of Power Sources*, vol. 67, pp. 43-48, 1997.
- [78] K. Peters, "Review of factors that affect the deep cycling performance of valve-regulated lead/acid batteries," *Journal of Power Sources*, vol. 59, pp. 9-13, 1996.
- [79] J. Garche, "Corrosion of lead and lead alloys: influence of the active mass and of the polarization conditions," *Journal of Power Sources*, vol. 53, pp. 85-92, 1995.
- [80] S. S. Misra and A. J. Williamson, "Impact of grid corrosion in valve regulated lead-acid battery on standby float service," in *Telecommunications Energy Conference, 1995. INTELEC '95., 17th International*, 1995, pp. 360-363.
- [81] E. Willihnganz, "Accelerated testing of stationary batteries," *Electrochemical Technology*, vol. 115, pp. 338-341, 1968.
- [82] E. Rocca and J. Steinmetz, "Passivation phenomenon of low antimony alloys in deep discharge conditions of lead-acid batteries," *Journal of Electroanalytical Chemistry*, vol. 543, pp. 153-160, 2003.

- [83] W. B. Brecht, D. O. Feder, J. M. McAndrews, and A. J. Williamson, "The effect of positive polarization on grid growth, cell performance and life. II," in *Telecommunications Energy Conference, 1989. INTELEC '89. Conference Proceedings., Eleventh International*, 1989, pp. 12.2/1-12.2/7 vol.1.
- [84] D. Pavlov, "Energy balance of the closed oxygen cycle and processes causing thermal runaway in valve-regulated lead/acid batteries," *Journal of Power Sources*, vol. 64, pp. 131-137, 1997.
- [85] H. Giess, "Investigation of thermal phenomena in VRLA/AGM stationary lead/acid batteries with a thermal video imaging system," *Journal of Power Sources*, vol. 67, pp. 49-59, 1997.
- [86] B. Culpin, "Thermal runaway in valve-regulated lead-acid cells and the effect of separator structure," *Journal of Power Sources*, vol. 133, pp. 79-86, 2004.
- [87] J. Hu, Y. Guo, and X. Zhou, "Thermal runaway of valve-regulated lead-acid batteries," *Journal of Applied Electrochemistry*, vol. 36, pp. 1083-1089, 2006.
- [88] J. Alzieu and G. Dillenseger, "Method for maintaining the charge of a lead storage battery." vol. WO/2006/064125 France: Electricite de France, 2006.
- [89] D. P. Reid and I. Glasa, "A new concept: intermittent charging of lead acid batteries in telecommunication systems," in *Telecommunications Energy Conference, 1987. INTELEC '87*, 1987.
- [90] E. Rossinot, C. Lefrou, F. Dalard, and J. P. Cun, "Batteries in standby applications: comparison of alternate mode versus floating," *Journal of Power Sources*, vol. 101, pp. 27-34, 2001.
- [91] X. Muneret, M. Coux, and P. Lenain, "Analysis of the partial charge reactions within a standby VRLA battery leading to an understanding of intermittent charging techniques," in *Telecommunications Energy Conference, 2000. INTELEC. Twenty-second International*, 2000, pp. 293-298.
- [92] H. Giess, "The operation of VRLA monoblocs with an on/off float charge regime," in *Telecommunications Energy Conference, 2001. INTELEC 2001. Twenty-Third International*, 2001, pp. 116-120.
- [93] J. P. Gun, J. N. Fiorina, M. Fraisse, and H. Mabboux, "Increasing UPS battery life main failure modes, charging and monitoring solutions," in *Telecommunications Energy Conference, 1997. INTELEC 97., 19th International*, 1997, pp. 389-396.
- [94] A. Kita, T. Matsui, Y. Kasai, and K. Kishimoto, "Uninterruptible power system," United States: Yuasa Battery Company Limited (Takatsuki, JP), 1993.
- [95] W. B. Brecht, D. O. Feder, J. M. Mcandrews, and A. J. Williamson, "Low float technology battery," United States: C & D Charter Power Systems, Inc. (Plymouth Meeting, PA), 1990.
- [96] J. J. Lander, "Further studies on the anodic corrosion of lead in H<sub>2</sub>SO<sub>4</sub> solutions," *Journal of the Electrochemical Society*, vol. 103, pp. 1-8, 1956.
- [97] P. Ruetschi and R. T. Angstadt, "Anodic oxidation of lead at constant potential," *Journal of the Electrochemical Society*, vol. 111, pp. 1323-1330, 1964.
- [98] T. M. P. Nguyen, G. Dillenseger, C. Glaize, and J. Alzieu, "Between floating and intermittent floating: Low-current self-discharge under compensation," in *Telecommunications Energy Conference, 2008. INTELEC 2008. IEEE 30th International*, 2008, pp. 1-7.
- [99] S. Piller, M. Perrin, and A. Jossen, "Methods for state-of-charge determination and their applications," *Journal of Power Sources*, vol. 96, pp. 113-120, 2001.
- [100] M. W. Kniveton, "Reducing the cost of maintaining valve-regulated lead/acid batteries in telecommunications applications," *Journal of Power Sources*, vol. 53, pp. 149-152, 1995.
- [101] B. Hariprakash, S. K. Martha, A. Jaikumar, and A. K. Shukla, "On-line monitoring of lead-acid batteries by galvanostatic non-destructive technique," *Journal of Power Sources*, vol. 137, pp. 128-133, 2004.
- [102] F. Huet, "A review of impedance measurements for determination of the state-of-charge or state-of-health of secondary batteries," *Journal of Power Sources*, vol. 70, pp. 59-69, 1998.
- [103] E. Karden, S. Buller, and R. W. De Doncker, "A method for measurement and interpretation of impedance spectra for industrial batteries," *Journal of Power Sources*, vol. 85, pp. 72-78, 2000.
- [104] S. Rodrigues, N. Munichandraiah, and A. K. Shukla, "A review of state-of-charge indication of batteries by means of a.c. impedance measurements," *Journal of Power Sources*, vol. 87, pp. 12-20, 2000.
- [105] A. K. Shukla, V. Ganesh Kumar, N. Munichandraiah, and T. S. Srinath, "A method to monitor valve-regulated lead acid cells," *Journal of Power Sources*, vol. 74, pp. 234-239, 1998.
- [106] J. D. Desanti and G. Schweitz, "Decreasing Owning Costs of MV/LV Substations Backup Batteries," in *Telecommunications Energy Conference, 2006. INTELEC '06. 28th Annual International*, 2006, pp. 1-6.
- [107] S. S. Misra, "Advances in VRLA battery technology for telecommunications," *Journal of Power Sources*, vol. 168, pp. 40-48, 2007.
- [108] C. Dai, T. Yi, D. Wang, and X. Hu, "Effects of lead-foam grids on performance of VRLA battery," *Journal of Power Sources*, vol. 158, pp. 885-890, 2006.

# UNIVERSITÉ MONTPELLIER II

– SCIENCES ET TECHNIQUES DU LANGUEDOC –

## RESUME EN FRANÇAIS

### THÈSE

pour obtenir le grade de

#### **Docteur de l'Université Montpellier II**

*Discipline : ÉLECTRONIQUE, OPTRONIQUE et SYSTÈMES*

*Formation Doctorale : Électronique : Composants et Systèmes*

*École Doctorale : Information, Structures et Systèmes*

Présentée et soutenue publiquement  
par

**NGUYEN Thi Minh Phuong**

le 5 juin 2009

---

ETUDE DU COMPORTEMENT DE BATTERIES AU PLOMB EN  
CONDITIONS EXTREMES :

CHARGE RAPIDE, MAINTIEN EN CHARGE PAR FAIBLE  
COURANT IMPOSE, INVERSIONS DE POLARITE

INTRODUCTION DE PROCEDES DE CHARGE ATYPIQUES

---

#### JURY

M. Jean ALZIEU  
M. Didier DEVILLIERS  
M. Guy FRIEDRICH  
M. Christian GLAIZE  
M. Jack ROBERT

Examineur  
Rapporteur - Président  
Rapporteur  
Directeur de Thèse  
Examineur

## RESUME EN FRANÇAIS

Les trois principaux domaines d'application des batteries au plomb sont le démarrage des moteurs thermiques, la traction électrique et les applications stationnaires, incluant les systèmes de secours. Les évolutions des marchés, notamment celui de l'énergie, ouvrent de nouvelles applications de stockage par accumulateur au plomb : transports électriques, énergies renouvelables dont éolien et photovoltaïque, stockage réseau, qualité, secours. Dans la plupart des cas, les contraintes de l'application mènent à revoir profondément les algorithmes de charge.

Nous avons mené différentes études sur les batteries au plomb dans des conditions extrêmes : 1<sup>er</sup> cas, charge rapide pour batteries ouvertes, c'est-à-dire à des régimes de charge largement supérieurs à ceux pratiqués traditionnellement ; 2<sup>ème</sup> cas, recherche au contraire des plus faibles courants permettant de maintenir une batterie à l'état chargé ; enfin, étude du comportement de la batterie au plomb en régime de décharge extrême, c'est-à-dire jusqu'à inversion complète des polarités d'électrode.

À partir de ces travaux, un nouvel algorithme de charge rapide avec une phase de déstratification précoce a été mis au point. Deux types d'applications en résultent :

- avec augmentation de la puissance du chargeur : charge rapide ;
- sans augmentation de la puissance du chargeur : réduction de la durée de charge de l'ordre d'un facteur deux.

Concernant le deuxième volet de l'étude, une nouvelle méthode de maintien en charge par faible courant imposé a été testée sur différentes technologies de batteries au plomb. Les résultats apparaissent prometteurs, notamment dans le cas des batteries étanches en application de type secours. Une augmentation de la durée de vie est dans ce cas attendue, associée à une réduction importante de la corrosion des grilles positives et de la perte d'eau dans le temps. Enfin, l'analyse des profils de tension de la batterie en décharge profonde, avec inversion de polarité, s'est avérée un outil efficace pour mener à bien les mesures d'état de charge de chaque polarité d'électrode, nécessaires au développement de la nouvelle méthode, précitée, de maintien en charge des batteries de secours. Une industrialisation de ces deux nouvelles méthodes de gestion des batteries au plomb est en cours.



## INTRODUCTION

Inventée en 1859 par le physicien français Gaston Planté, l'accumulateur au plomb a été le premier accumulateur rechargeable. Il représente aujourd'hui le système de stockage de l'électricité le plus utilisée dans l'industrie et dans l'équipement des véhicules. Son rapport énergie/poids est modeste (35Wh/kg) mais son aptitude à fournir de fortes intensités de courant situe son rapport puissance/poids à un niveau honorable. Ces caractéristiques unies avec son faible coût, son taux de recyclage élevé (97%) et sa technologie mature, maintiennent la batterie au plomb attractive pour de nombreuses applications.

Les évolutions des marchés, notamment celui de l'énergie, et la demande de développement durable ouvrent de nouvelles applications de stockage par accumulateur au plomb : transports électriques, énergies renouvelables dont éolien et photovoltaïque, stockage réseau, qualité, secours. Dans la plupart des cas, les contraintes de l'application nouvelle mènent à revoir profondément les algorithmes de gestion, notamment de charge. Il ne faut pas non plus oublier le facteur économique qui oblige à mieux cerner et comprendre les phénomènes internes aux accumulateurs afin d'augmenter leur durée de vie.

Pour ces raisons, l'accumulateur au plomb est depuis une dizaine d'année un sujet d'étude à l'Institut Electronique du Sud (IES) en collaboration avec EDF R&D. Trois thèses se sont concrétisées sur la batterie au plomb et ses applications. En 1997, H. Smimite a travaillé sur la charge rapide, au régime 1 heure, pour la batterie étanche utilisée dans les véhicules électriques individuels. En 2002, P. Izzo a consacré son travail de thèse aux batteries pour les applications photovoltaïques, la gestion de kits photovoltaïques, c'est-à-dire de petits systèmes comportant une simple batterie de démarrage, ainsi que de grands systèmes comportant un système de stockage composé de plusieurs batteries associées en série et gérées individuellement. En 2004, G. Dillenseger a initié le développement d'une nouvelle méthode de maintien en charge pour les batteries stationnaires de secours avec des faibles courants imposés. En continuité avec les thèses précédentes, les projets en cours de EDF et de l'IES portent sur les mêmes domaines mais avec des nouvelles demandes et des nouveaux problèmes. Ils constituent le sujet de cette thèse : la charge rapide d'une durée d'une heure pour la batterie ouverte utilisée dans les bus électriques, d'une durée de quatre heures pour la batterie d'une installation photovoltaïque raccordée au réseau pour optimiser par le stockage la courbe de production électrique; la méthode de maintien en charge avec des faibles courants imposés pour différentes technologies de batteries au plomb ; la décharge profonde avec inversions de polarité.

Ce tapuscrit comporte un premier chapitre de généralités sur la batterie au plomb, rédigé à l'intention de mes collègues non électro-chimistes. Il présente le fonctionnement des batteries au plomb notamment ses comportements dans les différentes conditions expérimentales auxquelles elles seront soumises au cours des chapitres suivants. Le deuxième chapitre concerne la charge de la batterie au plomb : de la charge traditionnelle à la charge rapide des batteries ouvertes. Un nouvel algorithme de charge rapide avec une phase de déstratification précoce est développé et mis au point. Il est aujourd'hui intégré dans un chargeur commercial de la société IES-Synergy et testé sur une batterie compressée de laboratoire. La décharge de la batterie au plomb avec inversions de polarité a été étudiée dans un troisième chapitre à travers des travaux expérimentaux sur plusieurs types des batteries : batteries stationnaires plaques planes et tubulaires, batteries compressées, batteries de démarrage durcies. Le dernier chapitre concerne les méthodes de maintien en charge des batteries au plomb stationnaires. La nouvelle méthode de maintien en charge par faibles courants imposés est testée sur les batteries ouvertes avec et sans antimoine et sur les batteries étanches AGM.

## CHAPITRE 1 – BATTERIES AU PLOMB

Ce chapitre a été rédigé spécialement pour mes collègues ingénieurs électriciens, qui ne sont pas familiers avec la terminologie électrochimique. La batterie au plomb y est présentée : de sa constitution jusqu'aux principes de fonctionnement en expliquant les lois thermodynamiques et cinétiques qui la gouvernent. La première partie parle des éléments qui constituent la batterie au plomb, ainsi que des différentes technologies et domaines d'applications. La deuxième partie explique le fonctionnement de la batterie au plomb : l'énergie chimique est convertie en énergie électrique et vice-versa. La troisième partie présente les réactions dans un accumulateur au plomb : les réactions principales (charge et décharge de la matière active) et les réactions secondaires (électrolyse de l'eau, recombinaison de l'oxygène, corrosion...). Les quatrième et cinquième parties décrivent les lois thermodynamiques et cinétiques qui gouvernent l'accumulateur en circuit ouvert et sous passage de courant. La dernière partie décrit les paramètres caractéristiques de la batterie au plomb, la capacité, l'état de charge et l'état de santé.

Il y a deux types principaux de technologies de batterie au plomb : batterie ouverte et batterie étanche, aussi appelée batterie à recombinaison ou encore batterie à soupape. Cette dernière est équivalente à l'appellation anglo-saxonne : VRLA battery pour « Valve Regulated Lead Acid battery ». En fait, la principale fonction qui distingue la batterie étanche de la batterie ouverte est la recombinaison interne de l'eau dissociée par électrolyse. D'un point de vue constitutionnel, la principale caractéristique d'une batterie étanche est l'immobilisation de son électrolyte, permettant la constitution de canaux assurant un transit, en phase gazeuse, de l'oxygène produit à l'électrode positive qui sera recombiné en eau à l'électrode négative.

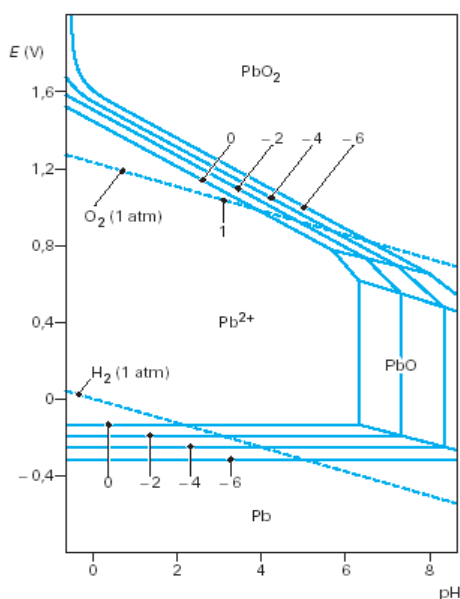


Figure 102 : Diagramme de Pourbaix : système électro-dynamique d'un accumulateur au plomb avec les couples oxydo-réducteurs :  $Pb/Pb^{2+}$  et  $Pb^{2+}/Pb^{4+}$ ,  $H_2/H_2O$  et  $H_2O/O_2$ . Les réactions secondaires de l'électrolyse de  $H_2O$ , de la recombinaison de  $O_2$  et la corrosion de la grille positive en  $Pb$  ont lieu en même temps que les réactions principales de charge ou décharge.

Les lignes notées 0 à -6 correspondent à des concentrations en  $Pb^{2+}$ , variant respectivement de 1 à  $10^{-6}$  mol/L.

La tension d'équilibre ( $E$ ) d'un accumulateur est liée à l'énergie maximale qui peut être convertie par ses réactions (énergie libre,  $\Delta G$ ) par la relation  $\Delta G = -nFE$ .

Pendant la charge ou la décharge, la différence entre la tension de l'accumulateur ( $V$ ) et sa tension d'équilibre ( $E$ ) est attribuée à des pertes ohmiques et des polarisations non ohmiques aux pertes qui se traduisent, *in fine*, par un dégagement de chaleur.

Concernant les réactions d'un accumulateur au plomb, une remarque importante est que les réactions principales et les réactions secondaires ont lieu en parallèle. Cette situation influence

le comportement de la batterie et doit être prise en compte dans sa gestion, notamment dans les cas d'utilisations extrêmes que nous avons étudiés. Cette caractéristique est analysée tout au long de la thèse : en charge avec la déstratification de l'électrolyte par dégagement gazeux (chapitre 2) ; en maintien en charge de batteries stationnaires, où les réactions secondaires sont responsables à la fois, du phénomène d'autodécharge et des principaux modes de défaillance – assèchement de l'électrolyte, corrosion de la grille positive, emballement thermique – menant à la fin de vie de ces batteries (chapitre 4).

## CHAPITRE 2 – CHARGE DE BATTERIES AU PLOMB : DE LA CHARGE TRADITIONNELLE A LA CHARGE RAPIDE

En pratique, une procédure de charge doit répondre à trois critères principaux : une durée raisonnable, un état final de charge suffisant et une homogénéité acceptable de l'électrolyte.

La stratification est un phénomène courant qui se développe pendant la charge des batteries au plomb : l'électrolyte en bas des éléments est plus concentré que l'électrolyte en haut. Une batterie stratifiée souffre d'une fatigue rapide de la partie inférieure de ces électrodes et donc vieillit plus vite. La méthode habituelle pour déstratifier l'électrolyte consiste à provoquer une circulation de gaz pour brasser l'électrolyte par la convection forcée. Ce gaz peut être de l'air injecté par une pompe ou, le plus souvent, de l'oxygène et l'hydrogène produits en fin de charge par l'électrolyse de l'eau de l'électrolyte.

Un dégagement gazeux dû à l'électrolyse de l'eau a toujours lieu dans la batterie au plomb. Il augmente avec l'augmentation de la tension de charge et devient appréciable à partir d'une valeur de tension nommée tension de dégagement gazeux. Sous tension de dégagement gazeux, le régime de charge est proche du régime maximum acceptable par la batterie pour la réaction de charge proprement-dite. Ce régime est désigné par « courant d'acceptance » dans ce tapuscrit. Un courant supérieur, correspondant à la part excédentaire, entraîne un dégagement gazeux qui brasse l'électrolyte et l'homogénéise. On parle ici d'une phase de déstratification ou d'une phase de surcharge.

La déstratification par dégagement gazeux est nécessaire pour la santé de la batterie, mais le courant de dégagement gazeux doit être contrôlé pour ne pas atteindre des valeurs excessives et protéger ainsi la batterie contre un vieillissement rapide qui en résulterait. S'ajoutent à cette raison le souci de ne pas consommer trop d'eau de l'électrolyte ainsi que d'éviter une trop forte production d'hydrogène, gaz potentiellement explosif au-delà de 4 % en volume. Au cours d'une procédure de charge classique, qui dure en général de 8 à 14 heures, la phase de déstratification est effectuée sur la fin, lorsque le courant d'acceptance est suffisamment faible pour que le courant de dégagement gazeux soit assimilable au courant total, ce qui facilite son évaluation et donc la gestion de la charge. En pratique, 10 à 15% de surcharge sont imposés à la batterie pour déstratifier l'électrolyte.

Aujourd'hui, plusieurs nouvelles applications de batteries au plomb réclament une réduction de la durée de la procédure de charge. Par exemple une charge de 4 heures dans le cas d'un stockage réseau ou encore une charge méridienne de l'ordre d'une heure pour les batteries d'un bus électrique. Dans ces cas on parle de charge rapide. Dans le cas d'une charge rapide, l'acceptance de la batterie n'a pas le temps d'attendre une valeur suffisamment basse pour être considérée comme négligeable au cours de la phase de déstratification finale.

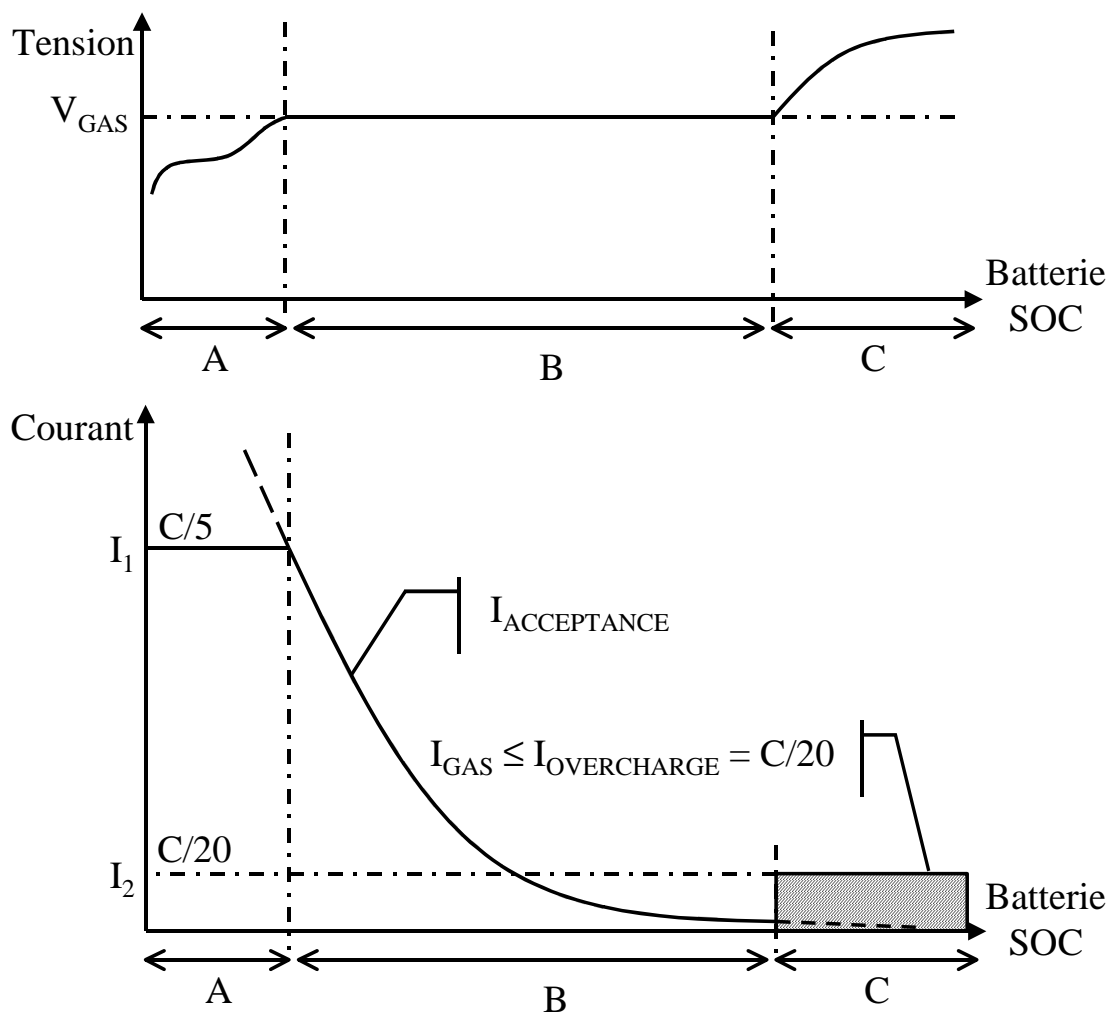


Figure 103 : La charge IUi classique : (A) phase à courant constant traditionnellement inférieur ou égale à  $C/5$ , (B) phase à tension constante  $V_{GAS}$  et phase de déstratification ou de surcharge à courant constant  $C/20$  (C).

On propose ici d'effectuer la phase de déstratification dès le début de la phase (B) (cf. Figure 103) d'un profil de charge IUi classique, c'est-à-dire alors que le courant d'acceptance est encore élevé. On parle alors d'une phase de déstratification précoce. Dans ce cas, pour contrôler le courant de dégagement gazeux il est nécessaire de connaître le courant d'acceptance. Deux méthodes de mesure de courant d'acceptance sont étudiées et testées. La première, suivant les préconisations de P. Izzo, consiste à partir d'une valeur de courant supérieure à l'acceptance de la batterie, à imposer une rampe de courant décroissante et à détecter, dans la réponse en tension de la batterie, un point d'inflexion caractéristique de la tension de dégagement gazeux. Cette méthode, censée affranchir le résultat de l'influence de paramètres tels que la température ou la composition de l'alliage de grille positive, s'est avérée inapplicable pour les charges rapides. Il apparaît en effet que le temps de réponse de la batterie impose de pratiquer des rampes de pentes tellement faibles que la durée de la mesure, qui en résulte, devient incompatible avec notion de charge « rapide ». Nous avons donc substitué à la rampe « Izzo » une nouvelle méthode d'estimation du courant d'acceptance. Cette méthode consiste à imposer périodiquement à la batterie une tension égale à la tension de dégagement gazeux pré-estimée à partir des caractéristiques de la batterie en charge. La réponse en courant se caractérise par une chute brutale de l'intensité (qui peut atteindre transitoirement une valeur négative) puis une remontée rapide. L'intensité tend alors asymptotiquement vers la valeur recherchée. L'expérience montre que quelques secondes

suffisent pour obtenir une image de l'acceptance utilisable par l'algorithme de gestion de la déstratification précoce.

À une étape de mesure d'acceptance à tension constante, succède une étape de déstratification, pendant laquelle le chargeur impose à la batterie un courant égal à l'acceptance, augmentée d'un complément, destiné à provoquer l'électrolyse de l'eau, et donc un dégagement gazeux qui brasse mécaniquement l'électrolyte.

Cette séquence – mesure à tension imposée puis déstratification à courant imposé – est répétée périodiquement, par exemple toutes les minutes (cf. ). Gérée de cette façon, la phase de surcharge peut commencer dès le début de la phase B (cf. Figure 104) d'un profil de charge IUi classique. Nous qualifions alors cette opération de « déstratification précoce » (cf. Figure 105). A son terme, l'état de charge de la batterie est de l'ordre de 90% et une utilisation en décharge est possible, l'électrolyte étant déstratifié.

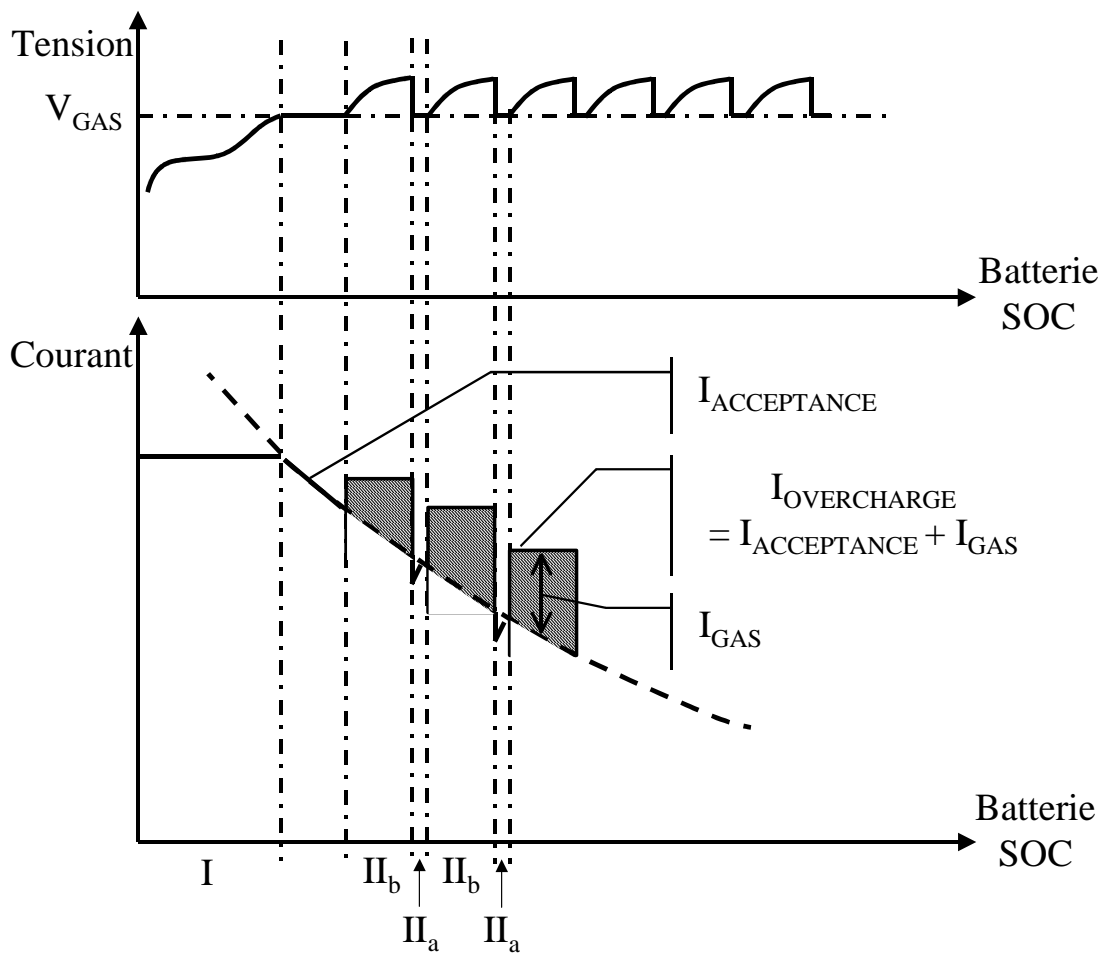


Figure 104 : Principe de la nouvelle méthode de charge rapide : (I) étape à courant constant ou puissance constante, (IIa) étape de mesure de courant d'acceptance à tension de dégagement gazeux, (IIb) étape de surcharge à courant de surcharge ( $I_{OVERCHARGE}$ ) égal à la somme du courant d'acceptance ( $I_{ACCEPTANCE}$ ) et du courant de dégagement gazeux ( $I_{GAS}$ ) choisi :

$$I_{OVERCHARGE} = I_{ACCEPTANCE} + I_{GAS}$$

La modification d'un chargeur « 12 heures » avec un algorithme de déstratification précoce, permet de rendre disponible la batterie en un temps de l'ordre de 4 à 6 heures. Cette division du temps de charge d'un facteur deux est obtenue sans modification de la puissance de

chargeur. L'évolution vers des charges plus rapides nécessite d'augmenter le régime initial (phase A) et donc d'utiliser des chargeurs plus puissants. Pour une charge d'une durée de l'ordre de l'heure, l'estimation de l'acceptance ne suffit plus ; il faut alors prendre en compte sa dérivée. Un brevet EDF/Université Montpellier II a été déposé en 2008 sur ce sujet.

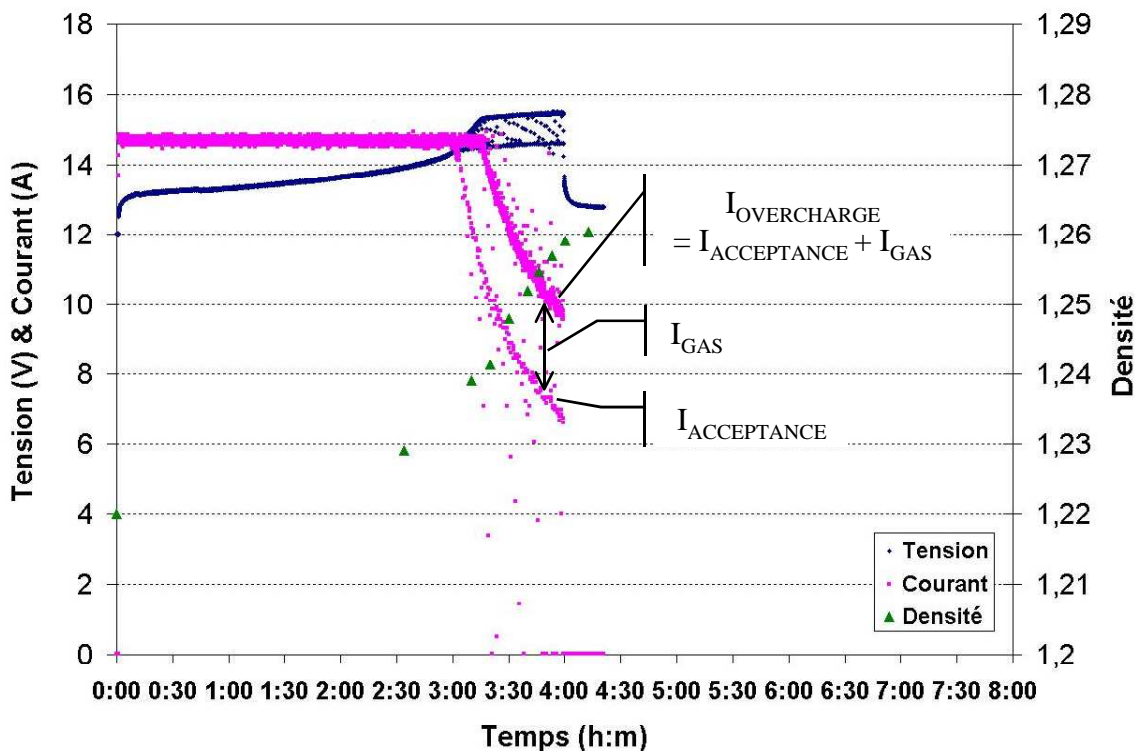


Figure 105 : Tension, courant et densité de l'électrolyte en haut de la batterie mesurés pendant une charge avec destratification précoce, pratiquée avec un chargeur industriel modifié. La durée totale de la charge est ici de 4 heures.

### CHAPITRE 3 – DECHARGE DE BATTERIES AU PLOMB : INVERSION DE POLARITE

Afin de mesurer les capacités des électrodes positives et négatives, nous avons effectué la décharge de batteries jusqu'à inversion de leur polarité. Deux types d'électrodes de référence, fabriqués par nous-même au laboratoire, sont utilisés pour déterminer les potentiels d'électrode. Le croisement des résultats a permis de valider les mesures.

Cette étude de la décharge profonde de la batterie au plomb, jusqu'à inversion complète des polarités d'électrode, a été menée pour évaluer les cinétiques d'autodécharge respectives, des électrodes positive et négative de différents types d'accumulateurs au plomb.

Dans le cas d'une décharge complète traditionnelle, le courant est interrompu lorsque la tension commence à chuter aux bornes de l'élément. Les deux électrodes n'ayant pas la même capacité, c'est la plus faible qui détermine la fin de décharge, et on ne sait généralement pas s'il s'agit de la négative ou de la positive. L'utilisation d'une électrode de référence permet de lever cette indétermination, mais on n'a alors aucune information sur la capacité de l'autre électrode, à moins de prolonger la décharge jusqu'à chute de tension de la deuxième électrode. La première électrode, forcée de continuer à se décharger au-delà de sa capacité, est alors le siège d'un processus d'inversion de polarité. Autrement dit, au sein d'une électrode négative par exemple, apparaît du matériau actif positif, c'est-à-dire du dioxyde de plomb : l'électrode négative prend alors le potentiel d'une électrode positive. Et réciproquement pour

une électrode positive. Une telle opération fatigue les matériaux d'électrode et doit donc, d'une façon générale, être évitée. L'inversion d'une électrode négative est même particulièrement préjudiciable, dans la mesure où sont alors détruits, par oxydation, les lignosulfonates qui sont un additif essentiel à leur longévité. Nous avons cependant considéré, dans notre cas, que le risque était négligeable dans la mesure où la durée de vie requise, pour chaque batterie testée, était limitée à deux, voir trois cycles.

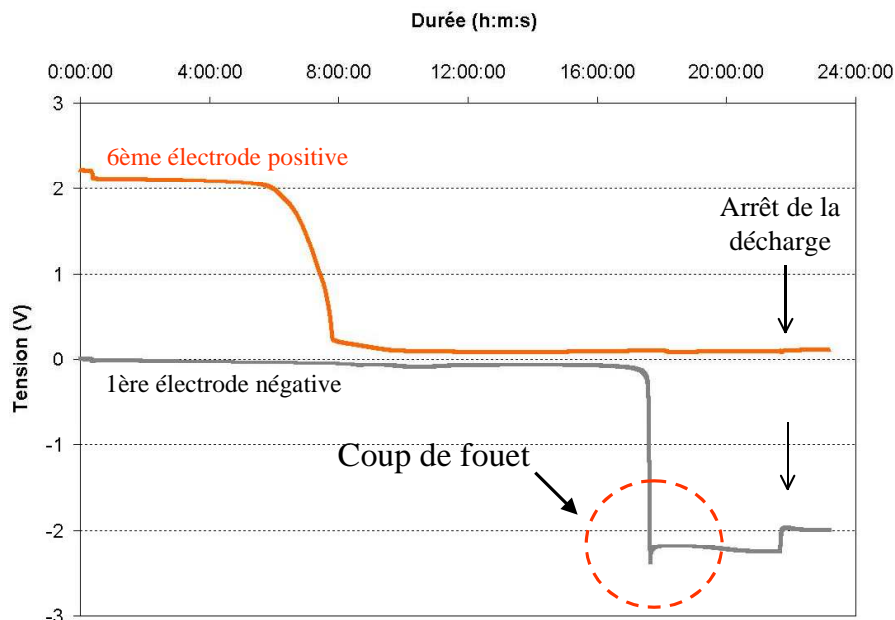


Figure 106 : Décharge (à 1,14C/20) avec inversions de polarité d'une batterie à plaques planes 70 Ah/12V. Profils de potentiel des électrodes négative et positive extrêmes associées aux deux bornes de la batterie.

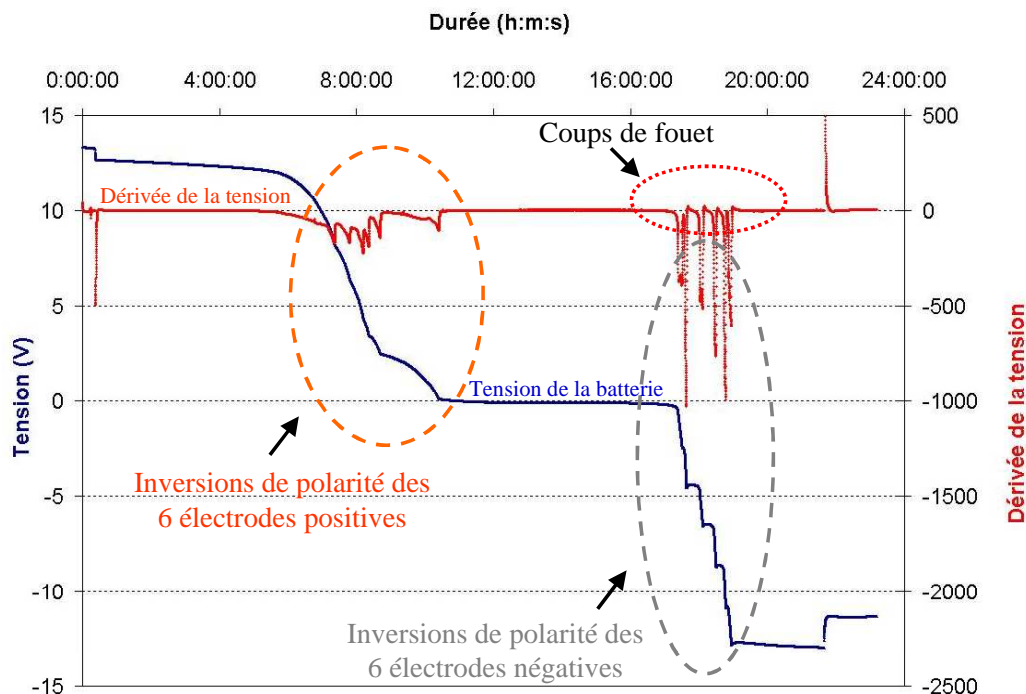


Figure 107 : Décharge (à 1,14C/20) avec inversions de polarité des douze électrodes d'une batterie à plaques planes 70 Ah/12V. Profil de tension de la batterie et représentation de la dérivée de cette tension. Les inversions des six positives et des six négatives sont nettement identifiables sur chacune de ces deux courbes.

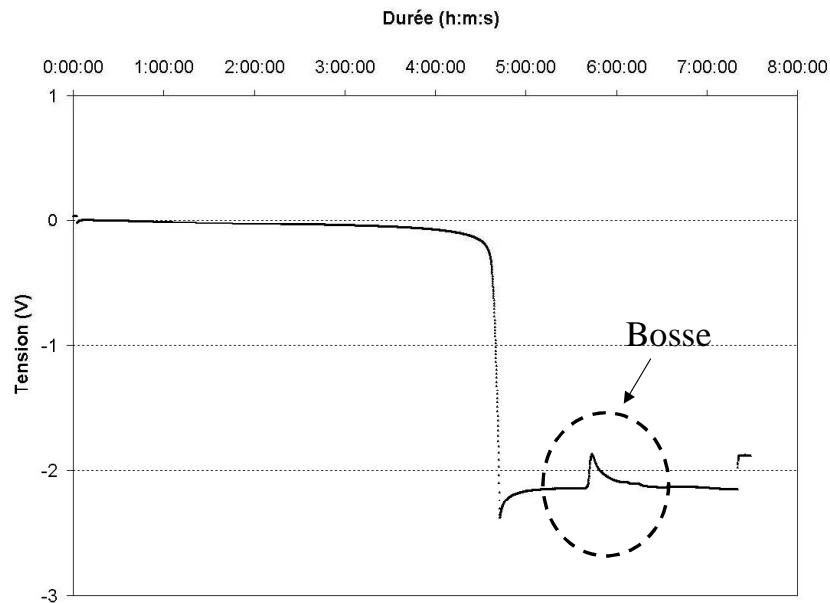


Figure 108 : Décharge (à 1,8C/10) avec inversions de polarité d'une batterie à plaques planes 110 Ah/12V. Observation d'une bosse sur le profil de potentiel de la 1<sup>ère</sup> électrode négative après la fin de son inversion.

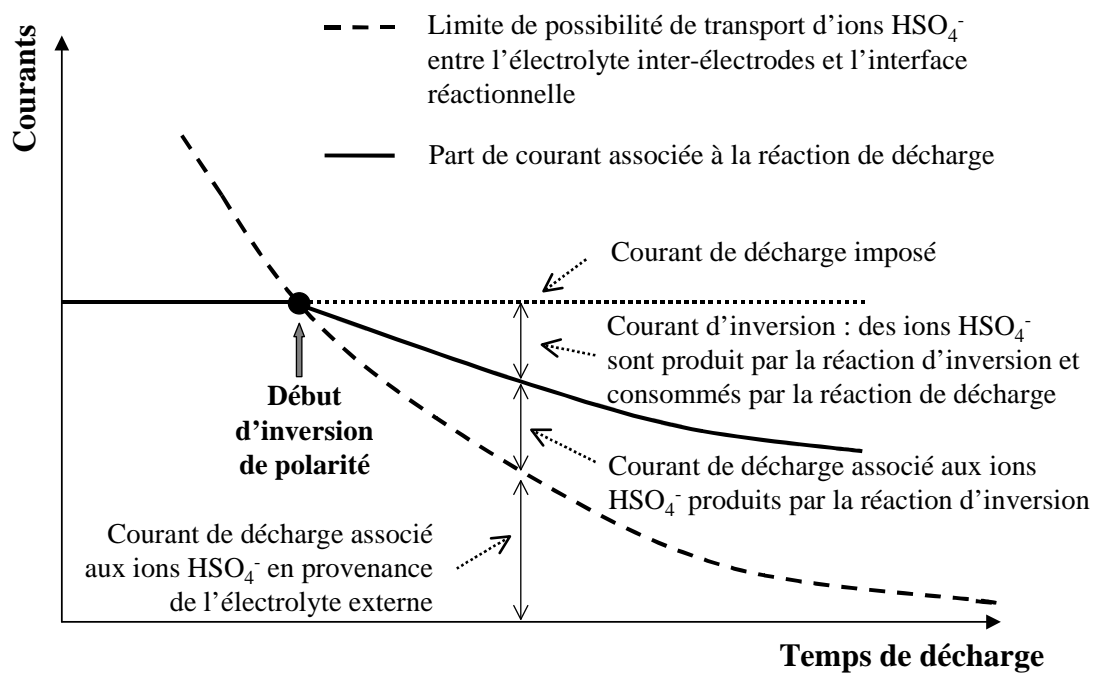


Figure 109 : Courant associé à la réaction de décharge avant et pendant une inversion de polarité. L'inversion commence lorsque la diffusion des ions  $\text{HSO}_4^-$ , depuis l'électrolyte externe, n'arrive plus à suivre le régime de décharge imposé. La réaction d'inversion libère, au sein des électrodes, des ions  $\text{HSO}_4^-$  qui sont réutilisés par la réaction de décharge qui se prolonge, parallèlement à la réaction d'inversion.

Certains essais ont été effectués sur des monoblocs 12 V, c'est-à-dire six éléments assemblés en série. Dans ce cas, seules les bornes de la batterie sont accessibles. Elles correspondent à la négative du premier élément et à la positive du sixième. Pour que nos mesures bénéficient d'un poids statistique suffisant, nous souhaitons accéder aux capacités respectives de chacune des six négatives et des six positives de la batterie 12 V. L'analyse, au cours d'une inversion



de polarité, du potentiel d'électrodes isolées a permis de distinguer des caractéristiques permettant de discriminer les deux polarités (cf. Figure 106). En fin d'inversion, par exemple, une électrode négative présente un profil de tension de type « coup de fouet », que nous avons rapproché de celui habituellement rencontré sur le profil de tension des électrodes positives en début de charge. Ou encore, la nette différence de pentes de la tension en fonction du temps entre les positives et les négatives. Ces éléments nous ont aussi permis de déterminer les capacités des douze électrodes d'une batterie 12 V à partir du seul profil de tension mesuré à ses bornes (cf. Figure 107). Au-delà de l'outil qu'a constitué l'analyse de ces profils d'inversion, l'observation surprenante de bosses sur les profils de tension d'électrode, sensiblement après la fin d'inversion (cf. Figure 108), s'est présentée tout d'abord comme une énigme – nous n'imaginions pas autre chose qu'un profil plat – puis comme une aide à la compréhension des mécanismes d'inversion (cf. Figure 109).

## CHAPITRE 4 - NOUVELLE METHODE DE MAINTIEN EN CHARGE DE BATTERIES STATIONNAIRES

L'alimentation de secours est une des principales applications des batteries au plomb. Aujourd'hui, les batteries stationnaires, en particulier les batteries VRLA, soumises aux régimes de floating traditionnels, rencontrent des problèmes de fiabilité et de durée de vie limitée. Cette situation nous a conduit à poursuivre les travaux sur les méthodes de maintien en charge préalablement engagés à EDF.

L'autodécharge due aux réactions secondaires est inévitable dans la batterie au plomb, que celle-ci soit en charge, en circuit ouvert ou en décharge. Le courant d'autodécharge dépend de plusieurs facteurs, principalement l'état de charge, la température, le type de l'alliage constitutif de la grille positive. Ces régimes d'autodécharge ne sont pas égaux pour l'électrode positive et négative. Ils sont indépendants l'un de l'autre. Dans les batteries avec antimoine, le courant d'autodécharge de l'électrode négative est plusieurs fois plus important que celui de l'électrode positive et dépend surtout de l'âge de la batterie et du taux d'antimoine de la grille positive.

Pour compenser le courant d'autodécharge, on fournit dans ce cas un courant dont la valeur est supérieure à celle de l'autodécharge de l'électrode négative. Cette situation est, en général, obtenue en appliquant aux bornes de la batterie une tension constante dont la valeur est légèrement supérieure à celle du circuit ouvert (de l'ordre de 120 mV par élément). On parle de « floating » ou, en français, de « marche flottante ». Bien entendu, la polarisation de floating fait augmenter le courant de dégagement gazeux, qui est en partie responsable de l'autodécharge.

Dans les batteries sans antimoine, comme les batteries étanches, le courant d'autodécharge de l'électrode négative est réduit. Nous l'avons évalué au tiers de celui de l'électrode positive. Un tel changement de comportement entre les accumulateurs avec antimoine et les accumulateurs sans antimoine nous a amené à nous interroger sur la pertinence d'appliquer à ces derniers les méthodes traditionnelles de charge qui ont été mises au point, depuis des décennies, avec les premiers. Une technique de maintien en charge, alternative au floating, a été ces dernières années l'objet de recherches et développements : la charge intermittente. Elle consiste à alterner des phases de repos en circuit ouvert et des phases de floating ou charge. Ces recherches ont été principalement suscitées par l'observation, notamment en ambiance chaude, de durées de vie des accumulateurs étanches réduites de façon importante, par exemple inférieures à un an. L'issue peut être dramatique, lorsque se produit le phénomène d'emballement thermique correspondant au processus suivant :

- La batterie étanche, en floating, s'échauffe sous l'effet de la réaction exothermique de recombinaison de l'oxygène.
- Cet échauffement entraîne une diminution de la résistance interne de la batterie, essentiellement due à la migration ionique dans l'électrolyte.
- La diminution de la résistance interne entraîne une augmentation du courant, donc de l'électrolyse de l'eau, donc de la recombinaison de l'oxygène, donc de l'échauffement et ainsi de suite.
- Lorsque ce phénomène diverge, la batterie fond, se déforme, peut provoquer court circuit, incendie, explosion. La charge intermittente a été conçue pour limiter les échauffements.

Des résultats positifs suivant la mise en œuvre de charges intermittentes ont été annoncés. Plusieurs équipes de recherche ont travaillé sur ce sujet, avec des choix de période (repos + charge) variées : de quelques minutes à plusieurs semaines.

Pour notre part, nous avons considéré que la phase en circuit ouvert n'était pas un passage obligatoire. Nous lui avons substitué une phase à faible courant imposé. Les raisons de cette disposition sont les suivantes :

- À très faible régime de charge d'une batterie, il est plus facile de contrôler le courant que la tension.
- Le contrôle du courant permet le contrôle de l'échauffement.
- Un courant d'intensité inférieure à celle correspondant au régime de floating est susceptible de compenser, au moins partiellement, l'autodécharge, et réduit le besoin de charge périodique.
- Plusieurs publications font état d'un minimum du régime de corrosion de la grille positive, lorsque le potentiel de l'électrode positive est compris entre celui du circuit ouvert et ceux de floating. La surtension de l'électrode positive, associée à ce minimum, est l'objet de différentes évaluations, généralement situées dans l'intervalle 30 à 80 mV.

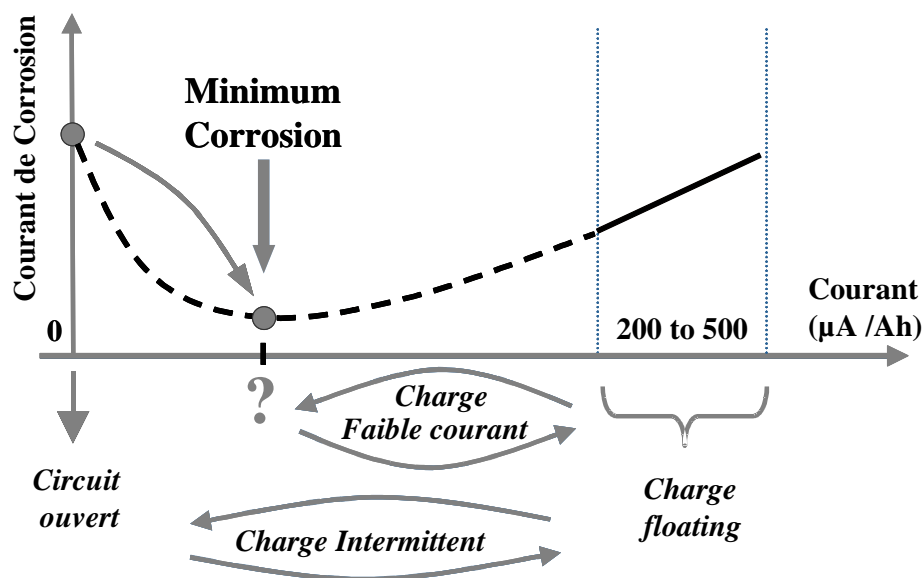


Figure 110 : La méthode des faibles courants est dérivée de la méthode de charge intermittente : les phases de circuit ouvert sont remplacées par les phases à faibles courants dont les valeurs sont de 5 à 10 fois moindres que celles des courants de floating (200 to 500 µA/Ah). L'objectif est de positionner la batterie dans la zone du minimum de corrosion.

Nous avons soumis différents types de batteries au plomb, ouverte ou étanche, avec ou sans antimoine, à des périodes de plusieurs mois sous faibles courants imposés. Alors que les régimes de floating traditionnels correspondant à des courants de charge de l'ordre de 200 à 500  $\mu\text{A}$  par Ah de batterie, les faibles courants mis en œuvre dans notre étude ont été choisis dans l'intervalle 25 à 100  $\mu\text{A}/\text{Ah}$ . Les états de charge initiaux et finaux des électrodes négatives et positives ont été mesurés suivant deux méthodes : mesure chimique des taux de produit de décharge, c'est-à-dire du sulfate de plomb, au sein des électrodes et mesure de capacités de chaque électrode par décharge jusqu'à inversion des polarités. À une variation d'état de charge en un temps donné, peut être associé, par calcul, un courant moyen effectif de charge ou décharge. Les mesures ont aussi notamment permis de calculer les courants d'autodécharge en circuit ouvert, de chaque électrode.

Les deux méthodes ont livré des résultats concordants. Ceux-ci peuvent être résumés comme suit :

- Batteries avec antimoine. L'antimoine influence le régime d'autodécharge des électrodes négatives. Dans les batteries avec antimoine, les électrodes négatives s'autodéchargent plus vite que les électrodes positives. Cette situation s'aggrave avec le taux d'antimoine et avec l'âge de la batterie. Une méthode de charge intermittente avec phase à faible courant est envisageable, mais constat est fait que le floating traditionnel est bien adaptée au maintien en charge permanent de la batterie.
- Batteries sans antimoine. La situation s'inverse : le régime d'autodécharge des électrodes négatives est réduit, il est alors de l'ordre du tiers de celui des électrodes positives. Le régime de floating apparaît comme excédant largement le besoin de ces batteries.

Dans ce dernier cas, en effet, l'imposition d'un faible courant dont l'intensité est cinq à dix fois inférieure à celle des courants de floating traditionnel apparaît suffisante pour maintenir l'état de charge de la batterie. Plus précisément (cf. Figure 111) :

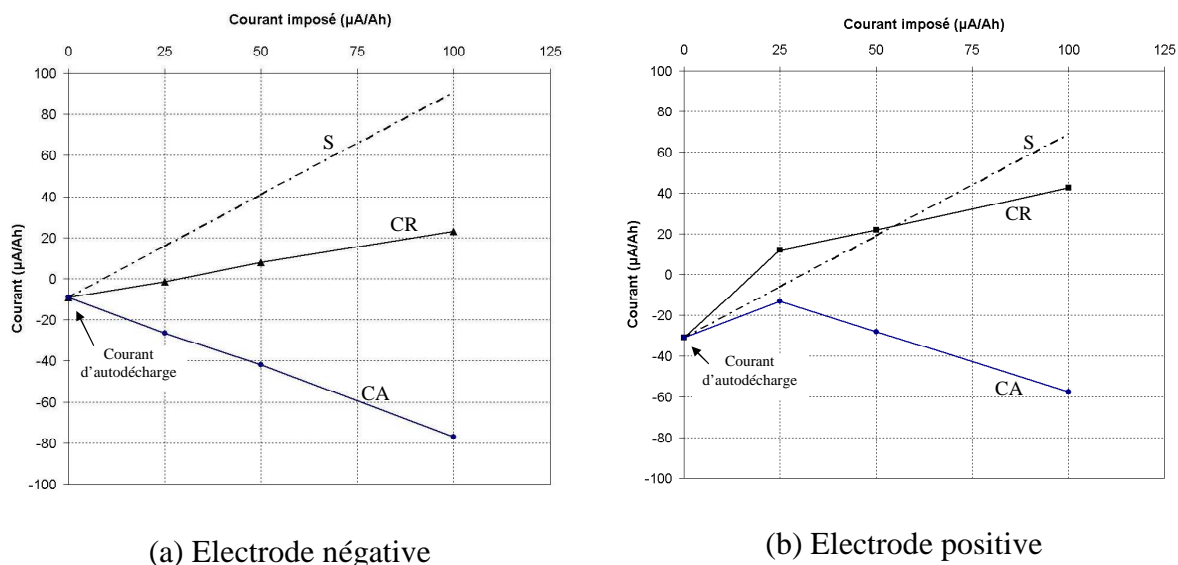


Figure 111 : Bilans de courant en fonction de faible courant imposé : (a) Électrode négative, (b) Électrode positive. (S) : la somme du courant d'autodécharge en circuit ouvert et du faible courant imposé. (CR) : le courant résultant calculé à partir de l'évolution des taux de sulfate. (CA) : courant de décharge associé aux réactions secondaires responsables de l'autodécharge. Il est égal à la différence entre le courant résultant et le courant imposé,  $CA = CR - \text{faible courant imposé}$ .

- L'électrode négative voit son état de charge stabilisé avec un courant dont l'intensité est triple de celle de son autodécharge constatée en circuit ouvert. On peut évoquer ici un pseudo rendement de l'ordre de 30%.
- Le cas de l'électrode positive est apparu plus surprenant : 25  $\mu\text{A/Ah}$  de courant de charge y compense 31  $\mu\text{A/Ah}$  de courant d'autodécharge et de plus complète la charge à un régime de 12  $\mu\text{A/Ah}$ . Le pseudo rendement évoqué ci-dessus apparaît ici supérieur à 100%,  $(31 + 12)/25 = 172\%$ . Autrement dit l'effet observé au-delà d'une compensation de l'autodécharge correspond à une diminution du régime des réactions secondaires responsables de l'autodécharge.

La compréhension de ce dernier résultat passe par l'analyse des mécanismes de l'autodécharge des électrodes positives. Cette autodécharge est la conséquence de deux réactions lentes mais inéluctables, car largement hors de leur potentiel d'équilibre. Il s'agit d'une part de la production d'oxygène gazeux par l'électrolyse de l'eau, d'autre part de la corrosion de l'alliage de plomb constituant le collecteur – grille – de l'électrode positive. Le potentiel de l'électrode positive au repos est supérieur aux potentiels d'équilibre de ces réactions respectivement, de plus de 400 mV et de plus de 2 V. La réaction de dégagement d'oxygène gazeux, pilotée par l'étape de transfert de charge, ne peut répondre, à une augmentation de tension, que par une augmentation de son régime. Elle ne peut donc pas être la cause de la diminution de l'autodécharge.

Il n'en va pas de même pour la réaction de corrosion. En circuit ouvert, en effet, le potentiel mixte qui résulte de la coexistence des réactions d'autodécharge et de la réaction principale de charge/décharge fait que l'état stable du matériau d'électrode est le sulfate de plomb. Le faible courant de charge imposé déplace le potentiel d'équilibre de la réaction principale de charge/décharge : l'état stable du matériau d'électrode est alors le dioxyde de plomb. Cette différence fait que la couche de monoxyde de plomb présente à l'interface grille/matériaux d'électrode est alors stable et protège l'alliage de grille. Il s'agit donc d'un phénomène de type passivation, et le faible courant imposé, au-delà d'une fonction de compensation de l'autodécharge, assure également une fonction de type protection anodique de la grille. L'évaluation de l'effet notable qui en résulte, ainsi que la faible surtension (2 mV) associée, nous mènent à confirmer l'existence d'un minimum de corrosion, mais à considérer que la surtension positive associée à ce minimum est plus faible que celles précédemment publiées.

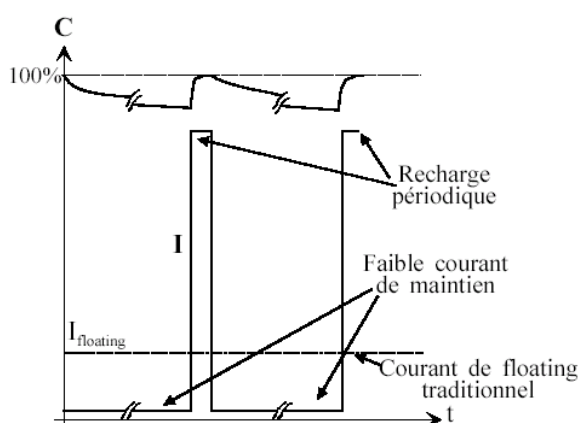


Figure 112 : Le principe de la nouvelle méthode de maintien en charge avec faibles courants imposés et charges périodiques.

La nouvelle méthode de maintien en charge que nous avons développée à partir de ces résultats consiste à maintenir la batterie sous faible courant imposé et à pratiquer périodiquement, par exemple tous les trois mois, une charge de complément ou rattrapage. Cette charge est

destinée, dans les cas où les faibles courants ne compensent que partiellement l'autodécharge, à ramener périodiquement la batterie à un état de charge maximum.

Dans le cas des batteries sans antimoine, ces charges périodiques pourraient s'avérer non nécessaires. Les batteries à recombinaison, dites batteries étanches, constituent l'essentiel des batteries stationnaires sans antimoine. Leur utilisation reste aujourd'hui freinée par leur manque de fiabilité et leur durée de vie réduite en floating. Pour s'affranchir des problèmes de fiabilité, nous avons combiné la méthode des faibles courants avec une architecture de batterie que nous appelons «Multibat Stationnaire», à trois branches parallèles gérées de façon individuelle, telle que présente Figure 113. La défaillance d'un élément n'entraîne pas la perte de la fonction secours. Seule la branche comportant l'élément défaillant est affectée, soit un tiers de la capacité disponible. Par ailleurs, les défaillances sont détectées par mesure de capacité périodique (aujourd'hui tous les 6 mois), par décharge complète d'une branche parmi les trois.

La durée de vie des batteries étanches devrait être améliorée de façon notable par la mise en œuvre des faibles courants. On sait en effet que corrosion de la grille positive et assèchement de l'électrode sont des causes majeures de fin de vie de ces batteries. Au-delà de la réduction de la vitesse de corrosion, une réduction de la perte d'eau est également attendue. En effet, on sait que l'eau électrolysée par surcharge est recombriquée catalytiquement sur l'électrode négative, avec une efficacité élevée, de l'ordre de 98%. Par contre, l'eau consommée pour fournir l'oxygène de la couche de corrosion est bloquée de façon irréversible. La diminution de la vitesse de corrosion doit ainsi entraîner une diminution de la consommation d'eau dans le temps et retarder ainsi une éventuelle défaillance par assèchement.

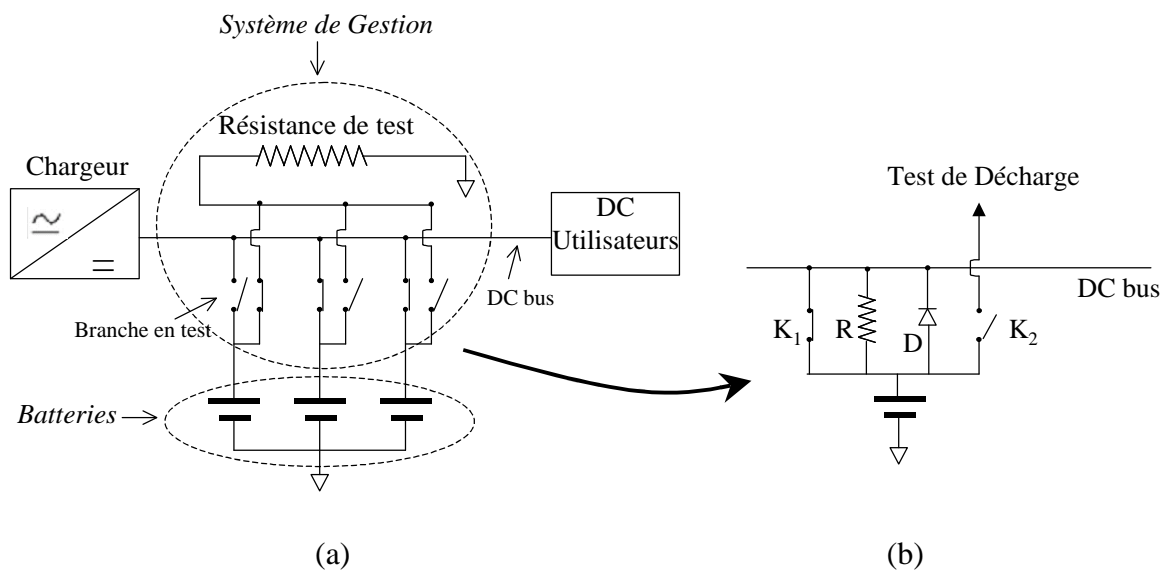


Figure 113 : (a) Schéma simplifié de système « Multibat Stationnaire ». (b) Zoom des composants électroniques d'une de trois branches de batteries utilisant la méthode de faible courant.

## CONCLUSION ET PERSPECTIVES INDUSTRIELLES

Les deux domaines sur lesquels ont porté notre étude peuvent apparaître disjoints, opposés. Il s'agissait en effet de gérer, pour la charge rapide, des courants « extrêmement forts », et pour le maintien en charge des batteries de secours, des courants « extrêmement faibles ». En fait, un fort point commun les lie : il s'agit, dans les deux cas, de gérer un équilibre entre les réactions principales de charge/décharge et les réactions secondaires de production d'hydrogène et d'oxygène par électrolyse de l'eau.

Nous avons abordé ce travail de thèse sur l'accumulateur au plomb avec quelques interrogations sur l'intérêt d'étudier un système aussi mature et dont le fonctionnement est sans doute bien connu.

Nous avons découvert un domaine complexe, vivant, et nous y sommes immergés avec difficulté mais passion. Si nous pensons maintenant en maîtriser quelques aspects, nous devons reconnaître que des questions sans réponse à ce jour se sont accumulées tout au long de notre étude. Nous espérons cependant avoir contribué modestement, à la connaissance du fonctionnement de cette batterie et à la façon de l'utiliser. Nous avons eu la chance de voir quelques applications industrielles s'engager à la suite de notre travail. Elles sont principalement les suivantes :

### ***1. Charge rapide avec déstratification précoce***

La charge rapide des batteries au plomb ouvertes mettant en œuvre la technique de déstratification précoce a été conçue et réalisée avec, comme premier objectif, la charge de batteries de stockage associées aux réseaux de distribution électrique. Il s'agit de stocker, la nuit, pendant une période de 4 heures, de l'énergie électrique produite de façon excédentaire et donc à faible coût, et de la restituer pendant les pointes de consommation de la journée. Ce projet en cours de recherche et développement financé par l'ANR, a initié plusieurs projets d'application mettant en œuvre cette technique.

Une industrialisation de la technique de déstratification précoce est engagée par IES-Synergy, constructeur français de chargeurs industriels. Implanté en option sur un chargeur opérant traditionnellement en 12 heures, l'algorithme de gestion de la charge permet de rendre la batterie opérationnelle en un temps de 4 à 6 heures.

Une version plus sophistiquée de l'algorithme, prenant en compte la dérivée de l'acceptance de charge, a été conçue pour gérer la charge rapide des batteries au plomb ouvertes à des régimes hors normes de l'ordre de l'heure. L'application visée est une charge méridienne, permettant d'augmenter l'autonomie quotidienne d'un bus électrique. Des essais sont envisagés prochainement dans le cadre d'un projet de transports électriques urbains.

### ***2. Multibat et faibles courants***

L'architecture de batterie à trois branches parallèles gérées individuellement (Multibat Stationnaire) associée à la mise en œuvre de faibles courants imposés, est en cours d'expérimentation, en vraie grandeur, dans six postes-sources du réseau EDF. Ces postes sont situées dans la région parisienne et le sud de la France.

Plus récemment, la Direction de la Production Hydraulique a décidé d'adopter cette nouvelle technologie pour des batteries de secours assurant la sécurité des ouvrages de production hydraulique. Vingt systèmes seront réalisés et installés au cours du deuxième semestre 2009.

LEAD ACID BATTERIES IN EXTREME CONDITIONS: ACCELERATED CHARGE, MAINTAINING THE CHARGE WITH  
IMPOSED LOW CURRENT, POLARITY INVERSIONS  
INTRODUCING NON-CONVENTIONAL CHARGE METHODS

**Abstract**

Three main applications of lead acid batteries are starting, lighting and ignition batteries, motive batteries and stationary batteries. Increasing attention to the global climate change and the sustainable development open new applications for the energy storage using lead acid batteries: electric transport, renewable energies such as photovoltaic and wind, grid storage, quality and emergency supplies. In some cases, new applications need new charge algorithms. Various studies were conducted with lead acid batteries in extreme conditions: accelerated charge for vented batteries, maintaining the charge with imposed low current for stationary batteries and deep discharge with polarity inversion. A new charge method for accelerated and fast charges of flooded lead acid batteries was developed. A new method of maintaining the charge with imposed low currents and periodical charges was tested on different technologies of lead acid batteries. It has the advantages of reducing drastically corrosion, of limiting water loss due to corrosion and the need of periodical charges.

**Keys words**

Lead acid batteries, fast charges, stratification, self-discharge, float charge, intermittent charge, corrosion, deep discharge, polarity inversion.

---

ETUDE DU COMPORTEMENT DE BATTERIES AU PLOMB EN CONDITIONS EXTREMES :  
CHARGE RAPIDE, MAINTIEN EN CHARGE PAR FAIBLE COURANT IMPOSE, INVERSIONS DE  
POLARITEINTRODUCTION DE PROCEDES DE CHARGE ATYPIQUES

**Résumé**

Les trois grands domaines d'application de batteries au plomb sont les batteries de démarrage, les batteries de traction et les batteries stationnaires. Les évolutions des marchés, notamment celui de l'énergie, ouvrent de nouvelles applications de stockage par accumulateur au plomb: transports électriques, énergies renouvelables dont éolien et photovoltaïque, stockage réseau, qualité, secours. Dans la plupart des cas, les contraintes de l'application mènent à revoir profondément les algorithmes de charge. Nous avons mené différentes études sur les batteries au plomb dans des conditions extrêmes: charge rapide pour batteries ouvertes, maintien en charge pour batteries stationnaires, décharge profonde avec inversion de polarité. À partir de ces travaux, un nouvel algorithme de charge rapide avec une phase de déstratification précoce a été mis au point. De plus, une nouvelle méthode de maintien en charge par faible courant imposé a été testée sur différentes technologies de batteries au plomb. Elle montre plusieurs avantages en termes de réduction importante de la corrosion, de diminution de la perte d'eau due à la corrosion et de besoin de charges périodiques.

**Mots clés**

Batteries au plomb, charges rapides, stratification, auto-décharge, floating, charge intermittente, corrosion, décharge profond, inversion de polarité.

---

LABORATORIES / LABORATOIRES

EDF R&D – Electrical Equipment Laboratory  
Batteries and Energy Management  
Avenue des Renardières - Ecuelles  
77818 Moret sur Loing Cedex - France

Laboratoire d'Electrotechnique de Montpellier  
Institut Electronique du Sud  
Université Montpellier II – 860 rue st Priest  
34090 Montpellier - France